UNIVERSIDAD COMPLUTENSE DE MADRID

FACULTAD DE FARMACIA

Departamento de Farmacología

TESIS DOCTORAL

Potencial terapéutico de diterpenos en inflamación y cardioprotección

MEMORIA PARA OPTAR AL GRADO DE DOCTOR

PRESENTADA POR

Irene Cuadrado Berrocal

Directores

Beatriz de las Heras Polo
Lisardo Boscá Gomar

Madrid, 2014

UNIVERSIDAD COMPLUTENSE DE MADRID

FACULTAD DE FARMACIA

Departamento de Farmacología

POTENCIAL TERAPÉUTICO DE DITERPENOS EN INFLAMACIÓN Y CARDIOPROTECCIÓN

MEMORIA PARA OPTAR AL GRADO DE DOCTOR CON MENCIÓN EUROPEA PRESENTADA POR

Irene Cuadrado Berrocal

Bajo la dirección de los doctores

Beatriz de las Heras Polo

Lisardo Boscá Gomar

Madrid, 2013

Beatriz de las Heras Polo, Profesora Titular de la Universidad Complutense de Madrid y **Lisardo Boscá Gomar,** Profesor de Investigación del Consejo Superior de Investigaciones Científicas (CSIC),

CERTIFICAN:

Que la presente Tesis Doctoral presentada por **Dña. Irene Cuadrado Berrocal**, titulada: "Potencial terapéutico de diterpenos en inflamación y cardioprotección", ha sido realizada bajo nuestra dirección y asesoramiento.

Revisado el presente trabajo, expresan su conformidad para la presentación del mismo considerando que reúne los requisitos necesarios para ser juzgada por el Tribunal correspondiente.

Madrid a 26 de Septiembre de 2013

Fdo. Beatriz de las Heras Polo

Fdo. Lisardo Boscá Gomar

COMPLUTENSE UNIVERSITY OF MADRID

FACULTY OF PHARMACY

Department of Pharmacology

TERAPEUTIC POTENTIAL OF DITERPENES ON INFLAMMATION AND CARDIOPROTECTION

Submitted to the Faculty of Pharmacy in partial fulfillment of the requirements for the Degree of DOCTOR OF PHILOSOPHY in Pharmacology with European Mention at the Complutense University of Madrid

by

Irene Cuadrado Berrocal

Madrid, 2013

A mis padres

A mi hermana Marta

A Juan

AGRADECIMIENTOS

Unos años realizando la Tesis sirven para muchas cosas. No sólo aprendes técnicas y manejo de laboratorio, sino que aprendes a desarrollarte como persona gracias a todos los contratiempos que vas superando. Todo este camino andado que está llegando a su fin lo he podido hacer (y disfrutar) porque me he rodeado de gente estupenda que me han ayudado y apoyado en todo momento.

En primer lugar quiero agradecer a la directora del Departamento de Farmacología, la Dra. Paulina Bermejo y a todos los que integran este departamento por acogerme y hacer tan agradable cada día de laboratorio. Especialmente agradezco a la Dra. Beatriz de las Heras por dirigir este trabajo depositando toda su confianza en mí y en nuestra investigación.

Agradezco al Dr. Lisardo Boscá por aceptar dirigir esta Tesis junto con Beatriz y por transmitirnos tu optimismo y tu serenidad. Gracias a los dos por implicaros en este trabajo con tesón y por compartir vuestros conocimientos conmigo.

A todos los que han formado parte del M5 durante estos cinco años: a Natalia y a Pilar, porque llegué y os tocó enseñarme las entrañas de un laboratorio. Lo hicisteis tan bien que me terminé quedando! A Izaskun por los grandes momentos que vivimos juntas y por conseguir sacarme todas las sonrisas del mundo. A Juan Carlos, por acompañarme en esta última etapa, quizá la más importante. Hacemos buen equipo, y lo sabes. También agradecer a Conchi, Hodei, Sandrita y Fernanda, que aunque estuvieron poco tiempo, dejaron huella.

A todos mis compañeros y amigos del Departamento: María, Laura, Miguel, Catia, Patricia, Adil, Adriana, MªÁngeles, Karim, Ricardo, Vanesa, Alba, Andrea, Elena, Ana, Carlos, Tarek I, Tarek II, Ahmed, Raúl…Con muchos de ellos he ido a la par haciendo la Tesis, otros son ya doctores, pero con todos he podido compartir muy buenos momentos dentro y fuera del laboratorio. He aprendido mucho con vosotros, y entre todos algún día comprenderemos los misterios del western blot. A todos los profesores y personal administrativo del

Departamento por brindarme vuestra ayuda cuando la he necesitado. A Jesús, Rosa y a Nieves, os agradezco la disposición y el cariño que siempre mostráis, que me ha facilitado mucho las horas de trabajo.

Quería agradecer a mis amigos de la facultad, en primer lugar a Paula y a Ricardo, porque estamos juntos desde el primer año de carrera cuando nos encontramos compartiendo una taquilla y aún nos seguimos complementando. Sois maravillosos. En segundo lugar a los que decidieron ser doctores y seguimos compartiendo experiencias, congresos y muchas risas: a Pedro, María Areche, Anita y Carmen.

Quisiera agradecer el apoyo de todo el equipo del B11 en el IIB: Paloma, María F., María P., María J., Vero, Patricia, Noelia, Gema… muchas gracias por acogerme como una más en vuestro laboratorio, por enseñarme nuevas técnicas y ayudarme tanto con los animales. Por otra parte agradecer a Mariví su amabilidad e inestimable dedicación, gracias a la cual ha sido posible realizar la parte final de este trabajo. Además quiero agradecer a la Dr. Sonsoles Hortelano por tus recomendaciones y tu amabilidad en todo momento.

A mis amigas de la farmacia, muy especialmente a Noelia y Alicia. Gracias por cubrirme cuando llegaba tarde y por entender que la culpa era de los experimentos! Con vosotras es genial trabajar. También quiero agradecer a la familia Wey por vuestra amistad y los buenos momentos que pasamos juntos para olvidar una semana dura trabajo. A Chris, Rubén y Alfredo, nunca pensé que unas clases de alemán iban a dar para tanto! (mejor en el pasaje que en clase….). Muchas gracias por ayudarme con los problemas informáticos.

My special appreciation goes to Dr. Vidal-Puig, from the Institute of Metabolic Sciences at the University of Cambridge, and to his entire group, for accepting me to do a scientific stay and for the affection and welcome received from them. I am grateful to all my colleagues and friends for their support and friendship during my stay. Thank you for making me feel at home while in Cambridge.

Mostrar mi más sincero agradecimiento a Sergio por ayudarme desde el primer momento y por descubrirme aquel sitio fabuloso de noodles. Muchas gracias por tus consejos y por escucharme.

De forma muy especial quiero agradecer a mi familia el cariño recibido, especialmente a mis abuelos, a los cuatro, porque de alguna manera estáis siempre conmigo. A Jesús, por su empeño en aprender lo que es un cardiomiocito. A mis padres y a mi hermana Marta, a los que adoro, por preocuparos y por confiar en mí y por vuestro incondicional amor; os dedico esta Tesis porque sois los pilares de mi vida. A Juan, por estar a mi lado en todo momento y porque consigues darme toda la paz que necesito. Este tiempo de esfuerzo y agobios lo habéis compartido conmigo, y gracias a vosotros ha sido un camino más fácil.

ÍNDICE

Índice

Índice

ABREVIATURAS

Abreviaturas

COX: Ciclooxigenasa

ECV: Enfermedades cardiovasculares

ERK: Quinasa regulada por señales extracelulares (extracelular-signal regulated kinase)

GGPP: Geranil geranil pirofosfato

I/R: Isquemia/Reperfusión

IAM: Infarto Agudo de Miocardio

IAP: Proteína Inhibidora de la Apoptosis (Inhibitor of Apoptosis Protein)

IFN: Interferón

IL: Interleuquina

IκB: Proteínas inhibitorias κB

JNK: Quinasa del N-terminal de c-Jun (c-Jun-N-terminal kinase)

LOX: Lipooxigenasa

LPS: Lipopolisacárido

LT: Leucotrieno

MAPK: Proteína quinasa activada por mitógenos (Mitogen-Activated Protein Kinases)

MyD88: Proteína 88 de respuesta primaria de diferenciación mieloide (Myeloid Differentiation primary-response protein 88)

NF-κB: Factor nuclear κB

NK: Célula Natural Killer

NO: Óxido nítrico

NOS: Óxido nítrico sintasa

PAMPs: Patrones Moleculares Asociados a Patógenos (Pathogen-Associated Molecular Patterns)

PGs: Prostaglandinas

PI3K: Fosfoinositol 3 quinasa (phosphoinositide 3-kinase)

PTPM: Poro de transición de permeabilidad mitocondrial

RISK: Reperfusion Injury Signalling Kinases

RNIs: Especies reactivas de nitrógeno (Reactive Nitrogen Intermediate)

ROIs: Especies reactivas de oxígeno (Reactive Oxygen Intermediate)

SAFE: Survivor Activating Factor Enhancement

STAT: Activador de la transcripción (Signal Transducer and Activator of Transcription)

TAK-1: Quinasa 1 activada por TGF-β (TGF-β-Activated Kinase-1)

TGF-β: Factor de crecimiento transformante β

Abreviaturas

TIR: Receptores Toll/Interleuquina 1 (dominio) (Toll/IL-1 receptor)

TIRAP: Proteína adaptadora que contiene dominio TIR (TIR domain-containing Adaptor Protein)

TLR: Receptores tipo Toll (Toll-like receptors)

TNF-α: Factor de Necrosis Tumoral-α

TRAF: Factor asociado al receptor de TNF (TNF Receptor Associated Factor)

TRIF: Proteína adaptadora con el dominio TIR que induce IFN-β (TIR-domain-containing adaptor protein-inducing IFN-β)

ENGLISH SUMMARY

English Summary

1. Introduction

Bioactive natural compounds can be considered very promising molecules for the development of new therapeutic agents. Terpenes are plant-derived secondary metabolites formed from five carbon isoprene units with great therapeutic potential. In particular, diterpenes represent a large group of terpenes with a wide range of biological activities such as anti-inflammatory, anti-bacterial, hypotensive, cardioprotective, cytoprotective, etc.

The innate immune system constitutes a first-line host defense mechanism that is found in all species mediated by different cells, as macrophages. Inflammation is one of the first responses of the immune system to harmful stimuli, such as pathogens, physical injury or damaged cells that ultimately lead to the restoration of a normal tissue structure and function. Macrophages play a key role in the inflammatory response and serve as an essential interface between innate and adaptive immunity. Toll-like receptors (TLRs) initiate innate immune responses leading to the activation of inflammatory pathways. On sensing the presence of pathogens through TLRs and other receptors, macrophages are stimulated to secrete a battery of cytokines that recruit effectors cells into the infected area. Thus, stimulation of TLR4 by lipopolysaccharide (LPS) triggers the recruitment of the cytoplasmic adaptor protein MyD88 and subsequently culminates in the activation of downstream signaling pathways as the transcription factor nuclear factor-κB (NF-κB) pathway. Activation of NF-κB leads to the upregulation of pro-inflammatory enzymes and cytokines such as nitric oxide synthase-2 (NOS-2), cyclooxygenase-2 (COX-2), interleukins (IL-1β and IL-6) and tumor necrosis factor-α (TNF-α). NF-κB activation is controlled by the IKK complex, which induces the phosphorylation and degradation of IκB inhibitor proteins, allowing the nuclear translocation of this transcription factor. Hence, NF-κB is a relevant target for the development of anti-inflammatory agents.

Increasing scientific evidence support the involvement of inflammation as a critical component of cardiovascular diseases such as acute myocardial infarction, which is the major cause of morbidity and mortality worldwide. To date, research is focused on novel interventions directed to efficiently protect

the heart from myocardial ischemia/reperfusion (I/R) injury and to reduce the infarct size. Results from both experimental and clinical trials indicate that inflammatory mediators are involved in the pathogenesis of cardiovascular diseases contributing to cardiac remodeling and peripheral vascular disturbances.

Myocardial ischemia is a condition in which lack of blood flow to the cardiac muscle occurs resulting in deficient oxygen and nutrient supply to the heart. The restoration of blood flow to an organ or tissue is termed reperfusion. Paradoxically, although myocardial reperfusion is essential for myocardial salvage, it can itself induce myocardial injury and cardiomyocyte death, a phenomenon termed “myocardial ischemia and reperfusion injury”. Ischemia-reperfusion (I/R) injury is also referred as the damage to cardiac tissue when blood supply returns after a period of ischemia.

During I/R three mechanisms of cardiomyocytes death namely apoptosis, necrosis and autophagy are involved. Massive cell death takes place during the first few minutes of reperfusion. A therapeutic approach in the treatment of I/R is the search for cardioprotective agents which may be administered at the time of reperfusion, to attenuate myocardial damage. Although several studies have assessed the cardioprotective potential of different drugs (e.g. Cyclosporine A) with promising results in animals, their use as adjunctive therapy has not achieved a successful translation into the clinical setting.

Many molecular and biochemical pathways responsible for cardioprotection have been elucidated and have provided targets for pharmacological interventions and therapeutic strategies. A cardioprotective strategy is the activation of the Reperfusion Injury Salvage Kinase (RISK) pathway, which includes activation of kinases as PI3K/Akt and extracellular regulated kinase (ERK 1/2) at the time of reperfusion. An alternative protective pathway termed the Survivor Activating Factor Enhancement (SAFE) is initiated by TNF-α and involves the activation of Janus kinase (JAK) and signal transducer and activator of transcription 3 (STAT-3). Related to the inflammatory response, TLR4 is located in the heart and plays an important role in mediating I/R injury. Relevant signaling pathways, such as ERK 1/2

pathways, interacting with the TLR4 signaling pathway are also causes of myocardial I/R injury. These different pathways activate a series of downstream transcriptional factors, produced a large quantity of inflammatory cytokines, and initiate the inflammatory response. Finally, AMPK signaling, which orchestrates the regulation of energy pathways is rapidly activated during ischemia, as part of an innate survival cardiac mechanism.

2. Aim

The main objective proposed in this thesis was to evaluate the potential therapeutic activity of diterpenes labdane and kaurane as anti-inflammatory and cardioprotective agents.

3. Results

Two series of diterpenes were evaluated as anti-inflammatory agents and the mechanism of action of these compounds was investigated using LPS-induced inflammatory responses in macrophages. Firstly, the effects of a series of 63 *ent*-kaurane derivatives on NO release were evaluated. Thirteen of the tested compounds were able to inhibit NO production with an IC_{50} in the range 2-10 μM. The results demonstrated that compounds **9, 10, 17, 28, 37, 48, 55, 61** and **62** were not cytotoxic at concentrations up to 25 μM. Compounds **28, 55** and **62** were selected for further evaluation. These compounds potently inhibited the protein expression of NOS-2, exerting their inhibitory effects at the transcriptional level, as shown by quantitative PCR analysis.

One of the most important regulators of the inflammatory response is the transcription factor NF-κB. Degradation of cytosolic IκBα protein in LPS-activated macrophages was impaired in macrophages pretreated with compounds **28, 55** and **62**. The results obtained suggest that inhibition of NF-κB activation might be a mechanism involved in the anti-inflammatory effects of these kaurane derivatives. Also, a downregulation in the levels of some proinflammatory cytokines after treatment with kaurane derivatives was also observed.

Secondly, a series of labdane diterpenes was also evaluated. The labdanolic acid methyl ester (LAME) showed anti-inflammatory activity by inhibition of the release of several pro-inflammatory mediators (NO, PGE_2, IL-6, TNF-α and IP-10) in peritoneal macrophages. Cell viability was not affected by LAME and consequently the inhibitory effects of LAME were not due to cytotoxicity.

LAME potently inhibited the expression of NOS-2 and COX-2 enzymes. NF-κB was also involved in the anti-inflammatory mechanism of LAME as this compound impaired IκB protein degradation. When MAPK activation was evaluated, the phosphorylation of ERK 1/2 and JNK were almost completely abolished by pre-incubation with LAME. The fact that the active compound inhibited both the MAPK and NF-κB pathways indicates that its site of action is at a level upstream of the IKK/MAPKKs branching point in the LPS signal transduction pathway. Kinetic analysis performed after stimulation with LPS revealed a time-dependent phosphorylation of TAK-1, which was significantly inhibited by treatment with this compound. The *in vivo* effects of LAME were confirmed in an LPS-induced sepsis mouse model. The results obtained showed that LAME significantly improved animal survival rate and decreased circulating cytokines levels (TNF-α and IL-6) compared to untreated mice, protecting endotoxemic mice from death.

Previous studies by our group demonstrated the cytoprotective and anti-inflammatory properties of three labdane diterpenes derived from hispanolone (T1, T2 and T3), which led us to evaluate them as a possible pharmacological approach for cardioprotection to ameliorate I/R injury.

Apoptosis is involved in cardiomyocyte loss after ischemia. Our data showed a significant protection exerted by diterpenes T1 and T2 on early apoptotic signaling in cardiomyocytes (H9c2 and isolated rat cardiomyocytes) exposed to anoxia/reoxygenation (A/R). A significant reduction of Bax accumulation and up-regulation of the antiapoptotic proteins xIAP, Bcl-2 were observed. In agreement with these data, the activi ty of caspase-3 was significantly decreased after treatment, mainly with T1.

In addition, analysis of cell survival signaling pathways showed that diterpenes T1 and T2 added after A/R increased phospho-AKT and phospho-ERK 1/2 levels. These cardioprotective effects were lost when AKT activity was pharmacologically inhibited. Moreover, the labdane-induced cardioprotection involves activation of AMPK, suggesting a role for energy homeostasis in their mechanism of action. Thus, the mechanism involved activation of specific survival signals (PI3K/AKT pathways, ERK1/2 and AMPK) and inhibition of apoptosis.

Finally, we evaluated the protective effects of the active diterpene T1 in two rat experimental models of I/R, [Langendorff-perfused heart and a myocardial infarction after left anterior descending coronary artery (LAD) occlusion]. In both models, T1 showed an anti-apoptotic profile preventing cardiomyocytes death. T1 also increased the levels of pro-survival proteins (AKT, PDK1 and AMPK). Cardiac function after myocardial infarction was significantly improved when T1 was intravenously administered at early reperfusion, as evidenced by hemodynamic recovery and decreased myocardial infarct size.

4. **Conclusions**

I. Kaurane and labdane diterpenes exerted anti-inflammatory effects in macrophages. These compounds inhibited NF-κB activation and thus, the expression of classic inflammatory genes regulated by this transcription factor. Kaurane diterpenes **28**, **55** and **62** and labdane labdanolic acid methyl ester (**LAME**) were the most active compound.The diterpene LAME remained its effectiveness as anti-inflammatory agent in a LPS-induced sepsis mouse model. Treatment with LAME increased animal survival rate and reduced circulatory levels of cytokines IL-6 and TNF-α in diterpene-treated animals.

II. Labdane diterpenes derived from hispanolone (**T1** and **T2**) exerted cytoprotective effects in cardiomyocytes subjected to anoxia/reperfusion injury. These compounds showed an

antiapoptotic profile. They also increased the levels of key proteins involved in cell survival.

III. Diterpene **T1** showed cardioprotective activity in animal models of ischemia/reperfusion (I/R) injury through activation of specific survival pathways (PI3K/AKT). In addition, T1 improved cardiac function and reduced infarct size in a myocardial infarction rat model, when administered at the onset of reperfusion.

IV. Labdane diterpenes are emerging as potential agents for treatment of inflammation-based diseases.

OBJETIVOS GENERALES

Objetivos generales

El **objetivo** de esta Tesis Doctoral ha sido la evaluación del potencial antiinflamatorio y cardioprotector de diterpenos de tipo labdano y kaurano.

Los **objetivos específicos** propuestos para el desarrollo de este trabajo han sido los siguientes:

- Evaluar la actividad antiinflamatoria de nuevos diterpenos con estructuras de tipo kaurano y labdano.
- Determinar las dianas moleculares de actuación de estos compuestos y caracterizar su potencial actividad en modelos de inflamación *in vivo*.
- Estudiar la actividad cardioprotectora de diterpenos labdánicos.
- Evaluar los efectos de los diterpenos activos en modelos animales de patologías cardiacas (daño por isquemia/reperfusión).

INTRODUCCIÓN

1. LOS DERIVADOS DE PRODUCTOS NATURALES COMO FUENTE DE NUEVOS AGENTES BIOACTIVOS.

Los productos naturales aislados de plantas, microorganismos y animales, así como sus derivados semisintéticos, han desempeñado un papel destacado en la obtención de nuevos fármacos, contribuyendo al descubrimiento de nuevas moléculas de interés terapéutico (Lourenco *et al.*, 2012). A pesar de las ventajas que los productos naturales han ofrecido a la terapéutica en el pasado, su uso se limitó durante algún tiempo por el desarrollo de la Química Combinatoria y el "Screening de alto rendimiento" que permitía estudiar un gran número de moléculas en un tiempo relativamente corto. (Harvey, 2008). Afortunadamente, en las últimas décadas ha resurgido el interés por los productos naturales, conscientes del valor de la diversidad estructural que nos aporta la naturaleza, lo que ha estimulado la búsqueda de nuevos compuestos con actividades biológicas diversas (Harvey *et al.*, 2010; Mishra *et al.*, 2011).

En la terapéutica actual existen un gran número de fármacos de origen natural. Las nuevas técnicas de aislamiento y screening han fomentado estrategias de búsqueda basadas en el descubrimiento de moléculas a partir de productos naturales, en base a conocimientos de etnofarmacología, obteniéndose compuestos muy eficaces en el tratamiento de diversas enfermedades. Ejemplos representativos son los taxanos como el taxol y sus derivados el docetaxel o más recientemente el ortataxel, con mayor especificidad tumoral (Ojima *et al.*, 2012). La digoxina, quinina o artemisina, ácido salicílico, codeína, atropina, efedrina o la morfina son otros ejemplos de fármacos obtenidos de origen natural (Gilani *et al.*, 2005; Wells, 2011).

Por todo ello, la naturaleza es considerada como una fuente destacada de obtención compuestos para uso terapéutico, ya que proporciona una gran cantidad de moléculas farmacológicamente activas que sirven de base para el diseño de nuevos fármacos en distintas áreas terapéuticas (Mishra *et al.*, 2011; Newman *et al.*, 2012; Vasanthi *et al.*, 2012).

1.1 Terpenos.

Los terpenos constituyen uno de los grupos de compuestos naturales más destacados por su valor terapéutico. Desde el punto de vista químico, son

metabolitos secundarios que derivan de una vía biosintética común que se origina a partir del ácido mevalónico y se encuentran en diversos organismos (hongos, plantas, organismos marinos, etc.) en diferente proporción (Huang *et al.*, 2012; Wagner *et al.*, 2003). La vía parte del acetato y sigue a través del mevalonato y sus productos de condensación (Wagner *et al.*, 2003). La unidad biosintética elemental de los compuestos resultantes no es el ácido mevalónico (C_6), sino un derivado de éste, el isopentenil pirofosfato (IPP) (**C_5**) o isopreno activo (2-metil-1,3-butadieno).

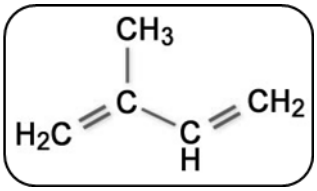

Molécula de Isopreno

Por fosforilación y descarboxilación deriva a isopentenil pirofosfato (IPP) y por isomerización esteroespecífica a dimetilalil pirofosfato (DMAPP), con gran reactividad.. La condensación mediante unión “cabeza-cola” de estos dos últimos compuestos origina el geranil pirofosfato (GPP) (**C_{10}**), precursor de *monoterpenos*. La adición al GPP de nuevas unidades de IPP origina moléculas de farnesil pirofosfato (FPP) (**C_{15}**), geranil geranil pirofosfato (GGPP) (**C_{20}**) y geranil farnesil pirofosfato (GFPP) (**C_{25}**) precursores de *sesquiterpenos*, *diterpenos* y *sesteterpenos*, respectivamente. Los *triterpenos* (**C_{30}**) y *tetraterpenos* (**C_{40}**) provienen del escualeno y del fitoeno, quienes a su vez provienen de la unión “cola-cola” de dos moléculas de FPP y dos moléculas de GGPP, respectivamente (Marco, 2006).

- **Diterpenos**

Como se ha mencionado anteriormente, el geranilgeranil pirofosfato (GGPP) es el precursor de los diterpenos, que normalmente son sólidos cristalinos, contienen cuatro unidades de isopreno (C_{20}) y mayoritariamente se han aislado en especies de las familias *Asteraceae* y *Lamiaceae* (Peters, 2010). Atendiendo a su estructura química se pueden clasificar en lineales o cíclicos. Diterpenos lineales y monocíclicos incluyen el fitol, que forma la cadena lipófila

de la clorofila y la vitamina A o retinol, respectivamente (Wagner *et al.*, 2003). Dependiendo de cómo se pliegue el GGPP, el sistema bicíclico que se forma inicialmente tendrá una configuración diferente de los estereocentros creados y dará lugar a diferentes esqueletos (Ruiz, 2002).

Tabla 1: Clasificación de los diterpenos cíclicos.

Diterpenos cíclicos
Diterpenos bicíclicos: labdanos y clerodanos
Diterpenos tricíclicos: pimaranos, isopimaranos, abietanos, cassanos y rosanos
Diterpenos tetracíclicos: kauranos, atisiranos, beyeranos y giberelinas
Diterpenos pentacíclicos: traquilobanos
Diterpenos macrocíclicos: cembranos, casbanos o taxanos
Diterpenos mixtos: vibsano o briarano

El interés farmacológico de los productos naturales de naturaleza terpénica ha ido en aumento en los últimos años. Diversos estudios han destacado las distintas actividades biológicas, que incluyen propiedades antiinflamatorias, antibacterianas, antivirales, antifúngicas, citotóxicas, antitumorales, cardioprotectoras, etc. (Chinou, 2005; de las Heras *et al.*, 2009; de las Heras *et al.*, 2003; Dong *et al.*, 2011; Ojha *et al.*, 2012; Salminen *et al.*, 2008).

Entre los diterpenos bicíclicos destacan los diterpenos de **tipo labdano** con un amplio espectro de actividades biológicas como agentes cardioprotectores, citotóxicos o antiinflamatorios (Chinou, 2005; de las Heras *et al.*, 1999; Lee *et al.*, 2011). Numerosos derivados de tipo labdano actúan inhibiendo la vía de activación de NF-κB. Uno de estos compuestos es el andalusol, aislado de *Sideritis foetens,* que ejerce actividad antiinflamatoria tanto en modelos *in vitro* e *in vivo* inhibiendo la expresión de la enzima óxido nítrico sintasa-2 (NOS-2) posiblemente al inhibir la activación de IKK e impedir que NF-κB se transloque al núcleo (de las Heras *et al.*, 1999).

El andrografólido y sus derivados, aislados de *Andrographis paniculata,* han sido descritos como agentes antiinflamatorios, antidiabéticos, antimaláricos, cardioprotectores o hepatoprotectores (Jayakumar *et al.*, 2013). El andrografólido y sus derivados reducen la producción de mediadores proinflamatorios, probablemente a través de la inhibición de la vía de señalización NF-κB (Lee *et al.*, 2011; Lim *et al.*, 2012; Zhu *et al.*, 2013). Además, algunos de sus derivados han mostrado ser potentes agentes cardioprotectores, en un modelo de isquemia/reperfusión en corazón aislado (Awang *et al.*, 2012).

La hispanolona es un diterpeno labdánico aislado de la *Ballota hispanica* (Labietae). Estudios químicos han permitido realizar transformaciones con el fin de obtener moléculas más activas como agentes antiinflamatorios, antitumorales y cardioprotectores. Estos compuestos disminuyen la liberación de mediadores proinflamatorios como el óxido nítrico (NO), prostaglandina E_2 (PGE_2) así como del factor de necrosis tumoral-α (TNF-α) en macrófagos estimulados con el LPS lo que sugiere que su actividad antiinflamatoria está al menos parcialmente, mediada por la inhibición de NF-κB. Además de los efectos producidos *in vitro*, la hispanolona y algunos de sus derivados han sido evaluados en modelos de inflamación *in vivo* siendo capaces de reducir el edema de oreja inducido por el éster de forbol TPA (Giron *et al.*, 2008). Recientemente también se ha descrito el potencial antitumoral de nuevos derivados de la hispanolona que son capaces de inducir apoptosis en distintas líneas celulares tumorales, a través de la vía de receptores de muerte. Además estos derivados de hispanolona inhiben el crecimiento tumoral en modelos animales (Traves *et al.*, 2012a). Por otra parte, distintos derivados de la hispanolona han sido descritos como agentes cardioprotectores al inducir las vías de supervivencia, protegiendo al corazón frente a un daño isquémico (Cuadrado *et al.*, 2011).

Los diterpenos tetracíclicos de **tipo kaurano** son probablemente uno de los grupos más estudiados por sus diversas actividades biológicas como agentes antimicrobianos, moduladores de la apoptosis, inhibidores de la fagocitosis o neuroprotectores. Diterpenos como el foliol y linearol, aislados de la especie *Sideritis linearifolia*, han demostrado actividad antiinflamatoria inhibiendo la

expresión de la enzima NOS-2 a través del bloqueo del factor de transcripción NF-κB (Castrillo *et al.*, 2001). Kemebacetal, excisanin o isodojaponin, aislados de la especie *Isodon Japonicus* (Hong *et al.*, 2008), o crotoquininas derivados de las hojas de *Croton Tonkinensis* (familia Euphorbiaceae) también son potentes inhibidores de la liberación de NO mediante la inhibición del factor NF-κB (Kuo *et al.*, 2013). La oridonina es un diterpeno kaurano con actividad antiinflamatoria y antitumoral. Los mecanismos de acción de este compuesto incluyen la modulación de las proteínas MAPK, inhibición de NF-κB y la inducción de la apoptosis y autofagia en células tumorales (Tian *et al.*, 2013). También se han descrito diterpenos kaurano como potentes agentes neuroprotectores, probablemente por sus propiedades antioxidantes a través de la vía de señalización del factor nuclear de transcripción eritroide-2 (Nrf-2) (Gonzalez-Burgos *et al.*, 2013).

1.2 Diterpenos objeto de estudio.

En esta Tesis Doctoral se ha realizado el estudio farmacológico de dos series químicas de diterpenos de tipo kaurano y labdano. En primer lugar, se ha evaluado la actividad antiinflamatoria de una serie de 63 diterpenos de tipo kaurano derivados del ácido kaurenóico (**artículo 1**) y de una serie química de 9 diterpenos de tipo labdano derivados del labdaneidol (**artículo 2**). La segunda parte de la Tesis ha versado sobre la actividad cardioprotectora de una serie de 11 diterpenos de tipo labdano derivados de la hispanolona (**artículos 3 y 4**).

La serie de diterpenos de tipo kaurano y de diterpenos labdánicos derivados del labdaneidol, fueron suministrados por la Dra. Ana Estévez Braun del Instituto Universitario de Bio-Orgánica “Antonio González”, (Universidad de la Laguna, Tenerife, España).

Los diterpenos de tipo labdano derivados de hispanolona fueron suministrados por el Dr. Benjamín Rodríguez del Instituto de Química Orgánica del Consejo Superior de Investigaciones Científicas (CSIC, Madrid, España).

2. LA INFLAMACIÓN

La respuesta inmune es el mecanismo principal por el cual un organismo se defiende frente a posibles patógenos. La defensa del individuo dependerá de

su capacidad para identificar e inducir una respuesta adecuada para eliminar el agente dañino. Los dos mecanismos específicos de respuesta inmunitaria son la respuesta innata y la respuesta adaptativa (Hoffmann *et al.*, 2013). La **inmunidad innata** constituye la primeras línea de defensa del organismo mediada por distintos tipos celulares como los macrófagos y encargados de degradar los patógenos mediante el reconocimiento de moléculas específicas asociadas con el patógeno (PAMPs) a través de receptores transmembrana conocidos como "Toll-like receptors" (TLRs), al mismo tiempo que sintetizan mediadores inflamatorios (Schnare *et al.*, 2001). Además, estas células son las encargadas de presentar los antígenos a los linfocitos T, dando lugar a la **respuesta inmune adaptativa**. Gracias a la variedad de receptores presentes en los linfocitos T y B, la respuesta inmune adaptativa se caracteriza por la gran especificidad que presenta frente antígenos de agentes patógenos (Takeda *et al.*, 2001).

La inflamación es una de las primeras respuestas del sistema inmune que tiene como objetivo eliminar los agentes nocivos y reparar el daño tisular ocasionado. El término inflamación proviene del latín *inflammatio*, que significa hacer fuego o encender. En el siglo I d.C el médico romano Celso definió por primera vez los signos generales de la inflamación como los "cuatro puntos cardinales de la inflamación": calor, rubor, edema (hinchazón) y dolor (Serhan *et al.*, 2008). Estos signos clínicos derivan de los fenómenos fisiológicos, celulares y humorales que se desencadenan en cualquier tejido en respuesta a un daño como traumatismo físico, infección por patógenos, isquemia, radiaciones o incluso daño autoinmune. Todos ellos van a provocar una agresión sobre las células del huésped poniendo en marcha una cascada de eventos moleculares, celulares y vasculares con una finalidad defensiva que constituyen la respuesta inflamatoria.

A nivel local se inicia con la producción y liberación de diversos mediadores como son los lípidos bioactivos, citoquinas y quimioquinas, radicales de nitrógeno (RNIs) y de oxígeno (ROIs). A nivel sistémico se produce un incremento de la síntesis de proteínas de fase aguda, producidas por el hígado. Esto conlleva eventos vasculares tempranos de vasodilatación, con acumulación celular en el foco inflamatorio que se manifiesta como un eritema

o **calor y rubor**. Además, aumenta la adhesión de leucocitos a las paredes de los vasos sanguíneos de la zona y se incrementa la permeabilidad capilar lo que favorece la extravasación de leucocitos, principalmente neutrófilos y monocitos, al torrente circulatorio, facilitando la salida de proteínas plasmáticas. Como consecuencia del desequilibrio osmótico se produce el **edema** o hinchazón que se debe tanto a la acción directa de quininas (como la bradiquinina) como a la acción indirecta de las anafilotoxinas que median la liberación de histamina y leucotrienos. El **dolor** es consecuencia de la liberación de estos mediadores y el aumento de la presión local sobre las terminaciones nerviosas (Sherwood *et al.*, 2004).

La inflamación puede ser aguda y crónica en función de su duración. La inflamación **aguda** tiene una evolución relativamente breve y sus principales características son el aumento del flujo sanguíneo debido a la vasodilatación, el exudado de proteínas y fluido plasmático por el aumento de la permeabilidad capilar y la migración de células inflamatorias al foco inflamatorio. Por otra parte, la inflamación **crónica** presenta una duración mayor y se caracteriza por la presencia de linfocitos y macrófagos, así como por la proliferación de vasos sanguíneos y tejido conjuntivo.

Durante el proceso inflamatorio participan distintos tipos de células, algunas se encuentran de forma permanente en los tejidos (células endoteliales de vasos sanguíneos, mastocitos y macrófagos) y otras migran al área inflamada desde el torrente circulatorio (plaquetas y leucocitos).

En un principio, la inflamación es una respuesta beneficiosa y fisiológica para el organismo ya que provoca una serie de cambios a nivel sistémico que activan la capacidad de la respuesta inmune innata para suprimir la infección. Esta respuesta finaliza con la eliminación del agente dañino y la recuperación de la función y estructura del tejido dañado (**resolución de la inflamación**). Sin embargo, en caso de infecciones graves o si esta inflamación persiste puede llegar a ser perjudicial para el individuo (Barreiro *et al.*, 2010; Nathan, 2002). Por ello es fundamental regular y controlar los procesos de resolución de la inflamación. Se han identificado varios derivados lipídicos biactivos que se sintetizan en la fase de resolución, actuando a nivel local. Entre ellos destacan las **resolvinas, protectinas** y **lipoxinas** (Schwab *et al.*, 2007;

Schwab *et al.*, 2006).

2.1 Las citoquinas como mediadores de la respuesta inflamatoria.

La citoquinas son proteínas de bajo peso molecular implicadas en la regulación de la respuesta inmune innata y adaptativa y en la hematopoyesis. Además, actúan como moduladores inflamatorios participando tanto en la inflamación aguda como crónica. Las células endoteliales, los macrófagos (inmunidad innata) y los linfocitos T (inmunidad adaptativa) son los tipos celulares que mayor cantidad de citoquinas liberan (Dinarello, 2000). Generalmente actúan de forma sinérgica entre ellas o junto a otros estímulos pudiendo inducir la síntesis de otras citoquinas.

Las principales citoquinas proinflamatorias incluyen las interleuquinas (**IL-1, IL-6)** y **TNF-α** producidas principalmente por macrófagos. Las citoquinas IL-1 y TNF-α actúan conjuntamente en el foco inflamatorio estimulando la expresión de enzimas proinflamatorias como la ciclooxigenasa-2 (COX-2) y la óxido nítrico sintasa-2 (NOS-2), responsables de la producción de PGs y NO, respectivamente. Además actúan como agentes quimiotácticos e inducen la expresión de moléculas de adhesión (ICAM-1, VCAM-1 y selectina E) (Barreiro *et al.*, 2010; Dinarello, 2011; Moser *et al.*, 2004). El **IFN-γ** también es una citoquina proinflamatoria (también llamada linfoquina) sintetizada por los macrófagos, linfocitos T activados y células Natural Killer (NK) desempeñando un importante papel en los mecanismos de defensa al inducir la producción de NO y aumentar la actividad del TNF-α.

Sin embargo, existe otro grupo de citoquinas capaces de inhibir la expresión de genes inflamatorios o impedir la acción de las citoquinas proinflamatorias. Entre las principales citoquinas antiinflamatorias destacan las IL-4, IL-6, IL-10, IL-13 y el factor de crecimiento transformante-β (TGF-β). La IL-6 es una citoquina pleiotrópica que en función del entorno actuará como anti o proinflamatoria con un amplio espectro de actividades en la regulación inmune, hematopoyesis, inflamación y oncogénesis (Hirano, 2010). Cuando esta citoquina actúa como antiinflamatoria disminuye la liberación de IL-1, TNF-α e IFN-γ y potencia la síntesis de las citoquinas antiinflamatorias IL-10 y TGF-β

(Kishimoto, 2010). Por otra parte la IL-10 es una citoquina esencial para la regulación de la respuesta inmune y el mantenimiento de la homeostasis tisular. Es sintetizada mayoritariamente por los linfocitos T, monocitos, macrófagos y células dendríticas. Su función principal es inhibir la síntesis de IFN-γ e IL-2 pero además bloquea la translocación al núcleo del factor de transcripción NF-κB (Iyer *et al.*, 2012).

Las quimioquinas como Cxcl5, Cxcl9 o Ccl17, son citoquinas liberadas principalmente por macrófagos, células endoteliales, linfocitos T, fibroblastos y monocitos cuya función principal es controlar la adhesión y quimiotaxis, es decir, la atracción y activación de leucocitos polimorfonucleares, monocitos y linfocitos hacia el tejido inflamado (Moser *et al.*, 2004).

2.2 TLRs y receptores de citoquinas proinflamatorias.

Se ha descrito la similitud en los genes implicados en *Drosophila*, muy similares a los presentes en mamíferos. En primer lugar se identificó la proteína transmembrana *Toll* de *Drosophila* como receptor frente a las infecciones por hongos. Más adelante se describió el homólogo de la proteína Toll en humanos (hToll) con capacidad para inducir la producción de citoquinas proinflamatorias. Se trataba del Receptor-4 Toll-Like (Hoffmann, 2003).

Se han descrito 11 receptores TLRs en mamíferos, presentando cada uno de ellos ciertas homologías entre humanos y ratones (Figura 1). Son glicoproteínas transmembrana de tipo I con una estructura trimodular que presentan un dominio extracelular N-terminal rico en residuos de leucina (LRRs). El extremo C-terminal del dominio citoplasmático intracelular se conoce como dominio *Toll/IL-1 receptor* (TIR) por su homología con el receptor de IL-1. Por ello, el grupo de receptores de IL-1 (IL-1R) y el grupo de TLRs forman parte de la superfamilia TIR (Fekonja *et al.*, 2012; Kawai *et al.*, 2006)

Durante la activación del sistema inmune innato y posterior respuesta inflamatoria, tanto TLRs como IL-1R señalizan de manera similar por su dominio citoplasmático TIR, caracterizado por la presencia de tres regiones de gran homología fundamentales para la activación de diversas vías de

señalización como la vía del factor de transcripción NF-κB (Takeda *et al.*, 2004; Vezzani *et al.*, 2011).

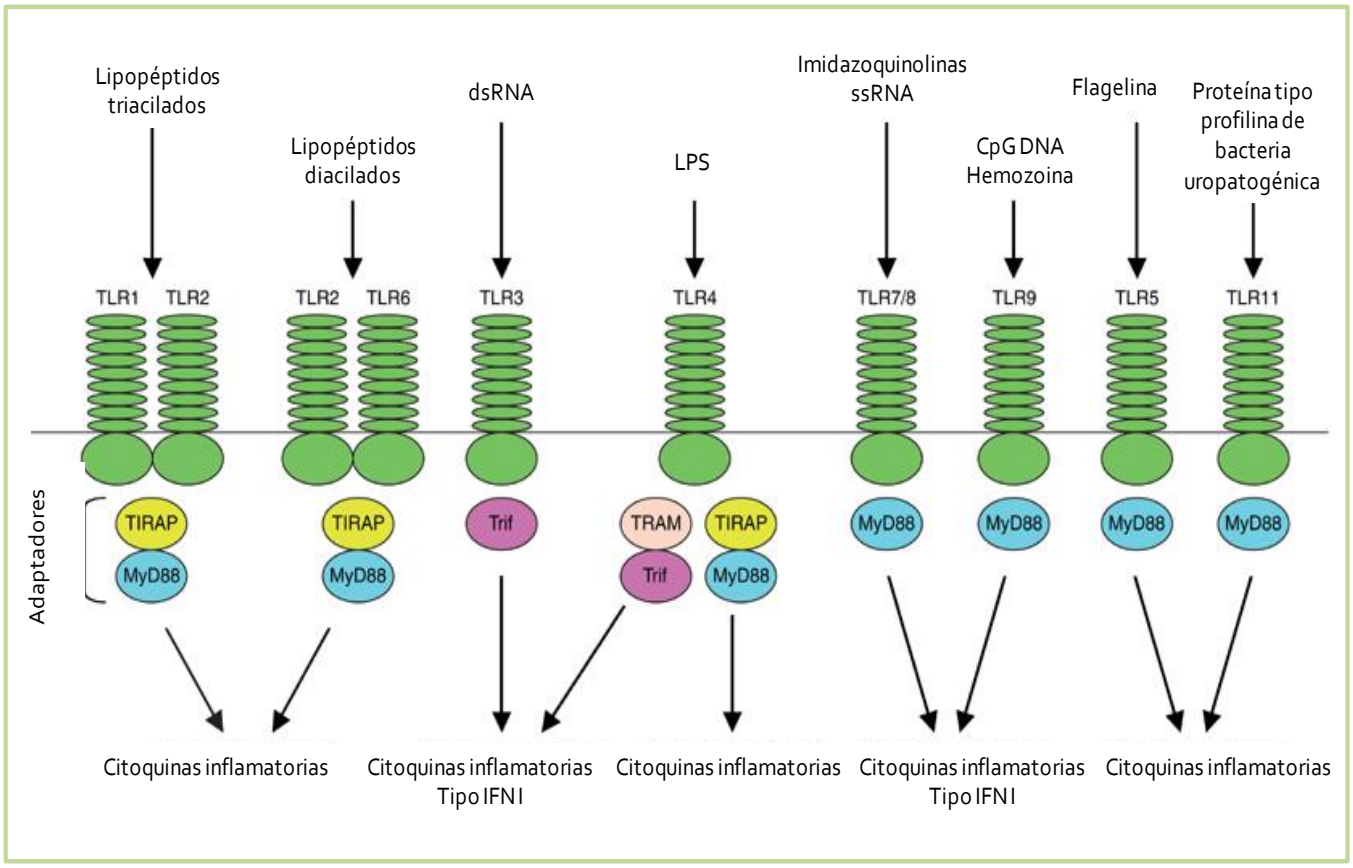

Figura 1. Respuestas mediadas por los distintos tipos de TLRs (adaptado de Kawai y Akira, 2006).

2.2.1 Vías de señalización mediadas por TLRs.

Diversos tipos celulares, incluidos los macrófagos, inician la primera línea de defensa frente a una infección o inflamación a través de la activación de receptores TLRs al unirse con distintas moléculas como lipoproteínas o PAMPs (*Pathogen-Associated Molecular Patterns).* Esta compleja cascada de señalización comienza con la dimerización de los receptores lo que permitirá la interacción con unas proteínas adaptadoras intracelulares que contienen dominios TIR: MyD88 (*myeloid differentiation factor 88*), TIRAP (*TIR domain-containing adapter protein*), TRIF (*TIR-domain-containing adaptor protein-inducing IFN*β) y TRAM (*TRIF-related adapter molecule*) que van a determinar

la especificidad de las diferentes vías de señalización mediadas por los TLRs (Kawai *et al.*, 2006).

Se han descrito dos vías de señalización en TLRs. La vía de señalización **clásica o dependiente de MyD88** que comienza tras la activación de TLR1, TLR2, TLR4, TLR5, TLR7, TLR9 y TLR10 y la vía **independiente de MyD88**, tras la activación de TLR3 y TLR4 (Vandenbon *et al.*, 2012) (Figura 2).

2.2.1.1 Vía dependiente de MyD88.

Todos los TLRs, excepto TLR3, señalizan a través de MyD88 por contener el dominio TIR. MyD88 se une a proteínas IRAK (*IL-1 receptor associated kinase*), que se activan por autofosforilación favoreciendo su asociación a TRAF6. Se forma el complejo IRAK-TRAF6 que se libera del receptor e interacciona en la membrana plasmática con la quinasa TAK-1 (*Transforming growth factor* β*-activated kinase-1*), produciendo su activación (Keating *et al.*, 2007). La proteína TAK-1 puede activar al complejo IKK permitiendo la fosforilación en los residuos de serina de los inhibidores IκB que serán degradados por el proteasoma 26S. De esta forma, el heterodímero NFκB p50/p65 va a quedar libre para migrar al núcleo. Por otra parte, TAK-1 puede fosforilar y activar a las proteínas MAP quinasas (MAPK) y posteriormente a la proteína activadora-1 (AP-1) participando en el mismo proceso de transcripción en el núcleo, coordinando la inducción de genes que codifican para numerosos mediadores inflamatorios (Kawai *et al.*, 2006).

2.2.1.2 Vía independiente de MyD88

Se ha descrito que el LPS también puede inducir la activación de NF-κB y MAPK en macrófagos y células dendríticas deficientes de MyD88. En este caso son los receptores TLR3 y TLR4 los que pueden activar una vía dependiente de TRIF.

A través de esta vía se va a activar NF-κB y MAPK, en este caso mediante la unión de las moléculas adaptadoras TRAM/TRIF con TRAF6 que conlleva la activación de TAK-1. Por otra parte se va a activar IRF3 (*interferon regulatory*

factor 3); para ello, IRF3 es fosforilado por TKB1 e IKKε, favoreciendo la dimerización de IRF3 y su translocación al núcleo para activar la transcripción de los genes que codifican para IP-10 e IFN tipo 1: IFNβ e IFNα (Kawai *et al.*, 2006; Takeda *et al.*, 2001). La figura 2 muestra las dos vías de activación del receptor TLR4 (vía dependiente e independiente de MyD88) durante el proceso inflamatorio.

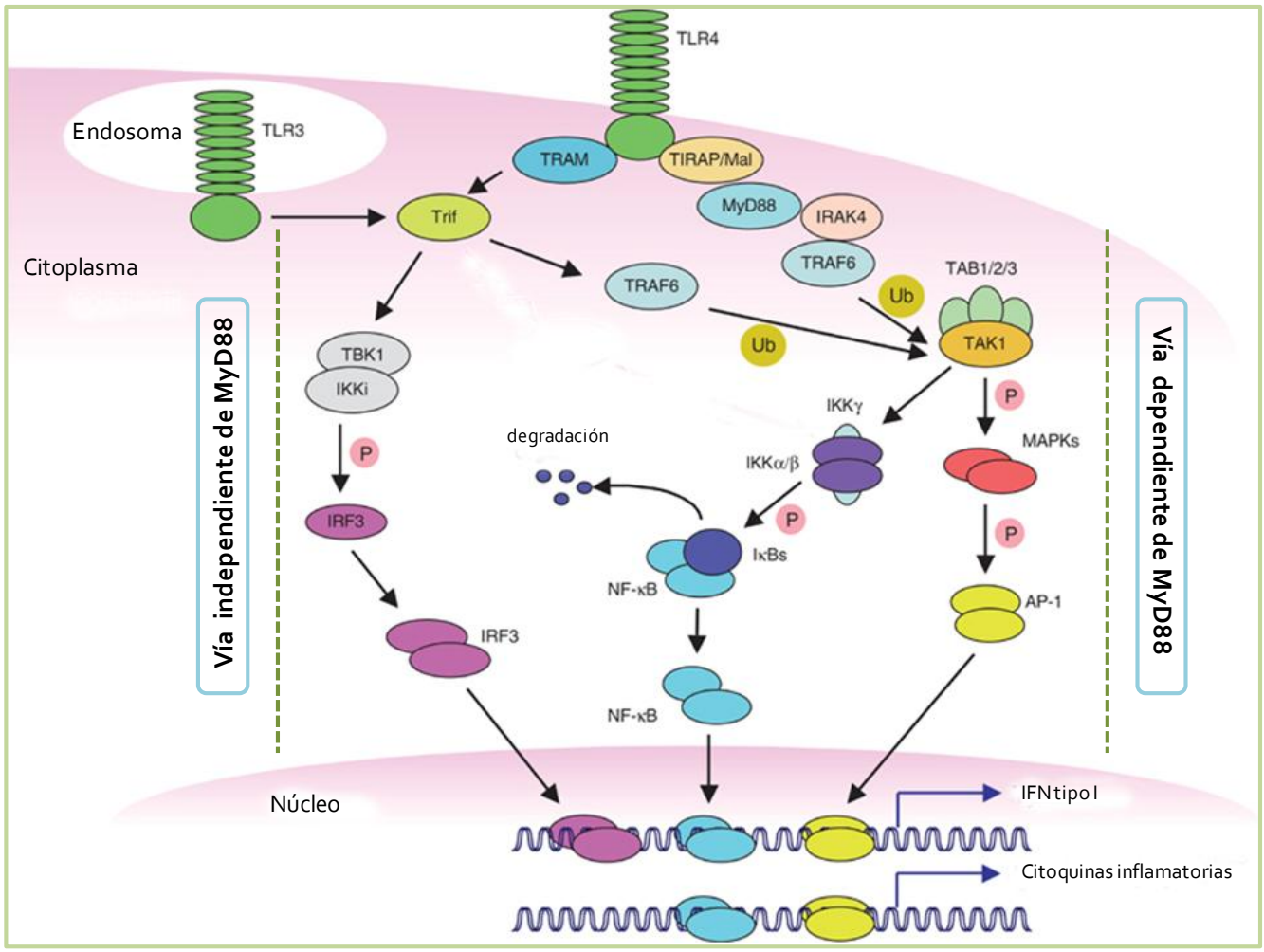

Figura 2. Vías de señalización mediadas por TLR4: vía dependiente de MyD88 y vía dependiente de TRIF (adaptado de Kawai y Akira, 2006).

El macrófago presenta con gran variedad de receptores de membrana para llevar a cabo sus funciones. Además de los receptores TLRs e IL-1R responsables del reconocimiento de antígenos, cabe destacar el papel de otros

receptores de citoquinas proinflamatorias como los miembros de la familia de TNF.

Los receptores de membrana descritos para los miembros de la familia TNF se agrupan dentro de los **TNF-R** que incluyen TNF-RI, TNF-RII, el receptor de linfotoxina β (LT-βR), Fas, CD40 y el ligando de OX-40 entre muchos otros. Todos ellos se caracterizan porque sus dominios extracelulares de unión a ligandos presentan gran homología y contienen cisteínas. Las respuestas específicas a las citoquinas van a depender tanto del receptor como del tipo celular, siendo el lipopolisacárido LPS el estímulo más potente para la inducción de TNF-α en macrófagos (Croft *et al.*, 2012). La unión de los miembros de TNF con sus respectivos receptores va a desencadenar diversas acciones como la diferenciación y supervivencia celular, producción de citoquinas inflamatorias y, al igual que los receptores TLR, también van a contribuir a la activación de los factores de transcripción AP-1 y NF-κB. Por el contrario, algunos de los miembros de estos receptores, como Fas y TNF-RI, originan señales que inducen la muerte celular por apoptosis (Croft *et al.*, 2013; Chu, 2013).

2.3 El factor de transcripción NF-κB en la respuesta inflamatoria.

Uno de los principales factores de transcripción implicados en la regulación de la respuesta inflamatoria es el factor NF-κB. La activación de este factor es necesaria para el desarrollo de la respuesta inmune al inducir la expresión de genes de primera defensa frente a microorganismos. Además, NF-κB ejerce un papel importante en el desarrollo de la inmunidad adaptativa ya que interviene en la proliferación, activación y producción de citoquinas por linfocitos T y B (Beinke *et al.*, 2004; Roman-Blas *et al.*, 2006; Vallabhapurapu *et al.*, 2009).

En condiciones basales, NF-κB está presente en el citoplasma de forma inactiva unido a las proteínas inhibitorias κB (IκB). La familia de proteínas IκB se caracteriza por la presencia de unas secuencias de repetición de anquirina y está compuesta por siete miembros: IκBα, IκBβ, IκBε, IκBγ, IκBζ, IκBns y Bcl3 (B-cell lymphoma 3). Las proteínas IκBα, β y ε se localizan en el citoplasma unidas a distintas unidades de NF-κB. IκBγ se transcribe en la región C-

terminal de p105 y también aparece en el citoplasma junto a p100, que actúa como inhibidor de NF-κB. Estas cuatro proteínas se degradan tras ser fosforiladas, lo cual no ocurre con el resto de miembros (IκBζ, IκBns y Bcl3) que se localizan principalmente en el núcleo (Calzado *et al.*, 2007; Carmody *et al.*, 2007; Hayden *et al.*, 2012).

Se han descrito varias vías de activación del factor de transcripción NF-κB. La activación clásica comienza en respuesta a diferentes señales extracelulares como son las citoquinas proinflamatorias (TNF-α e IL-1), mitógenos, el LPS o por activación del receptor de células T. En esta vía las proteínas IκBα son fosforiladas por las proteínas IκB quinasas o complejo IKKs, formado por dos subunidades catalíticas (IKKα e IKKβ) y una reguladora (IKKγ, también llamada NEMO). Tras esta fosforilación se lleva a cabo la poliubiquitinación de IκB y su posterior degradación por la subunidad 26S del proteasoma. Como consecuencia de la degradación de IκB, el complejo p65/p50 se transloca al núcleo donde va a regular la transcripción de numerosos genes proinflamatorios, como aquellos que codifican para citoquinas, receptores implicados en la adhesión y migración leucocitaria y enzimas que producen mediadores inflamatorios secundarios como COX-2 y NOS-2 (Li *et al.*, 2002; Xie *et al.*, 1994).

2.4 El macrófago en la respuesta inflamatoria.

En el proceso inflamatorio participan diferentes tipos de células efectoras que varían a medida que evoluciona la respuesta inflamatoria. Uno de los tipos celulares directamente implicado desde el inicio hasta la resolución de la inflamación es el macrófago.

Los macrófagos son células especializadas que forman parte del sistema inmune con un papel esencial en la respuesta primaria a patógenos, así como en el mantenimiento de la homeostasis tisular, inflamación e inmunidad. Derivan de las células madre hematopoyéticas de la médula ósea, que tras diferenciarse en monocitos migran desde el torrente circulatorio a diferentes tejidos y órganos diferenciándose en macrófagos, específicos de cada tejido (Auffray *et al.*, 2009; Gordon *et al.*, 2005). Los macrófagos permanecen inactivos en los tejidos pero pueden activarse a través de los receptores TLRs,

al reconocer estímulos como el LPS, citoquinas o secuencias de reducido tamaño en los patógenos llamados PAMPs desencadenando así la respuesta inmunitaria (Fujiwara *et al.*, 2005).

Diversas funciones han sido atribuidas a los macrófagos durante el proceso inflamatorio. Una vez activados pueden actuar como células fagocíticas, como células secretoras de distintos mediadores, como célula presentadora de antígenos y finalmente, como célula reparadora de los tejidos dañados durante el proceso inflamatorio. Los macrófagos son células dinámicas que junto a los monocitos circulantes pertenecen al sistema fagocítico mononuclear cuya principal función es la **fagocitosis**, eliminando microorganismos invasores, células extrañas y tejidos muertos (Brown *et al.*, 2012; Nathan, 2008). Por otra parte, los macrófagos también son **células secretoras** de mediadores como las citoquinas (IL-1, IL-6, TNF-α) y quimioquinas, que promueven la respuesta inflamatoria ya que estimulan la fagocitosis, activan a los linfocitos T, estimulan la hematopoyesis, etc. (Classen *et al.*, 2009; Mills, 2001). Estas células, una vez activadas, además de secretar factores quimiotácticos, producen mediadores proinflamatorios y citotóxicos, como son las ROIs y RNIs.

Otra de las funciones fundamentales del macrófago activado es su **capacidad presentadora de antígenos**. Tras la fagocitosis, los macrófagos degradan las proteínas y procesan los antígenos para presentarlos en los complejos mayores de histocompatibilidad (MHC) permitiendo que los linfocitos T puedan reconocer estos compuestos como extraños. Por su capacidad destructiva, los macrófagos guiarán el curso de la respuesta inflamatoria e intervienen en la síntesis y reparación del tejido dañado durante el proceso inflamatorio, participando de forma activa en la **resolución de la inflamación** (Laskin *et al.*, 2001).

- Polarización de los macrófagos.

Se ha descrito una heterogeneidad fenotípica en el macrófago dependiendo del grado de diferenciación, distribución tisular y respuesta a estímulos endógenos y exógenos (Hristodorov *et al.*, 2012). Los macrófagos tienen capacidad para modificar su perfil funcional en respuesta a una variedad de estímulos y polarizarse en distintos fenotipos. Recientemente ha surgido el concepto de polarización de los macrófagos y haciendo referencia a la

dicotomía Th1/Th2, se han propuesto dos subtipos de macrófagos según sean activados por la vía clásica (M1) o activación alternativa (M2) (Traves *et al.*, 2012b). Los diferentes modos de polarización de los macrófagos van a depender del entorno y del daño que se haya producido (Figura 3).

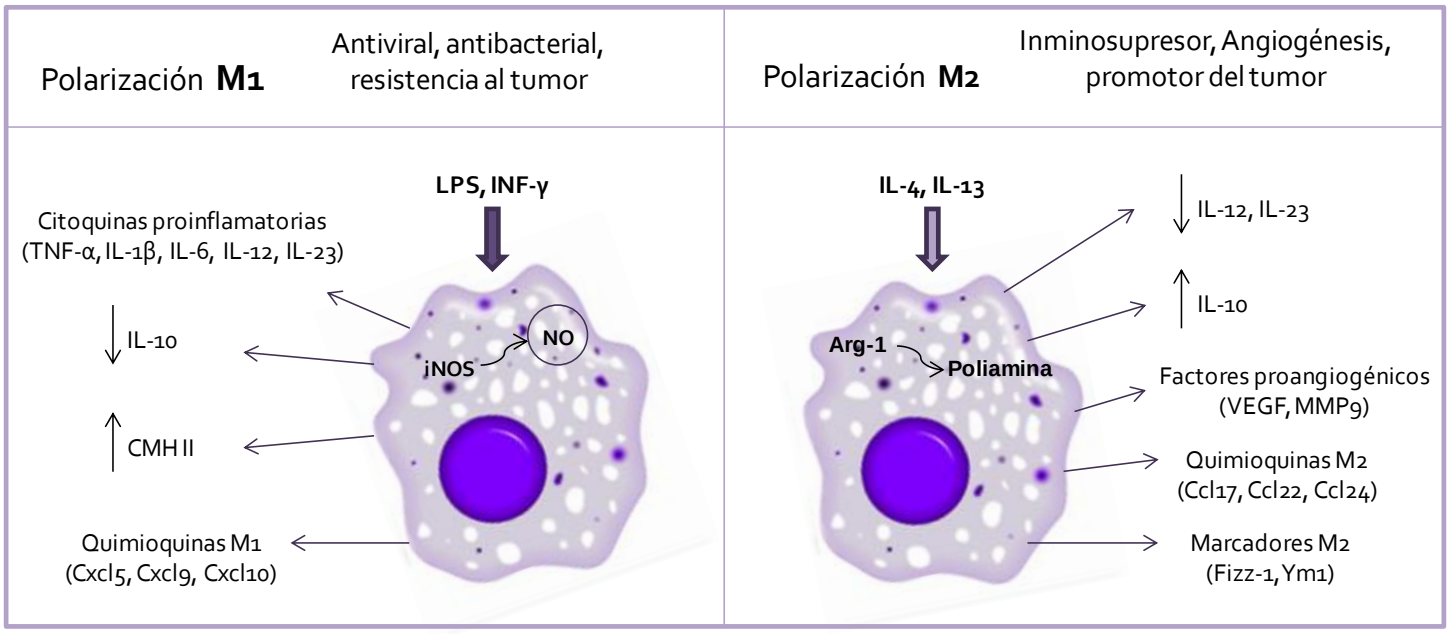

Figura 3. **Esquema simplificado de la polarización de los macrófagos M1 y M2** (adaptado de Través et al. 2012b).

La **activación clásica** es fundamental para el inicio y mantenimiento del proceso inflamatorio así como en la respuesta frente a patógenos y respuesta inmune (Traves *et al.*, 2012b). Ésta hace referencia a los macrófagos **M1** que se activan tras la interacción con el receptor TLR4 de IFN-γ sólo o en cooperación con estímulos como LPS o lipoproteínas, reconocidos como PAMPs. El origen de IFN-γ puede ser tanto de células del sistema inmune innato como del sistema inmune adaptativo. Inicialmente tras un estímulo de estrés o la presencia de un patógeno, las células NK, como parte de la inmunidad innata, producirán IFN-γ polarizando a los macrófagos a M1. Este grupo de macrófagos activados de forma clásica, produce cantidades elevadas de citoquinas proinflamatorias como TNF-α, interleuquinas (IL-1, IL-23 o IL-12), quimioquinas proinflamatorias como Cxcl9 o Cxcl10, promoviendo la respuesta

inmune Th1 (linfocitos T helper 1) y amplificando su polarización con aportes continuos de IFN-γ a partir de estos linfocitos T (Hristodorov *et al.*, 2012). Además, estas células ejercen actividad antiproliferativa y citotóxica al adquirir una capacidad fagocítica elevada y por su capacidad de secretar RNIs y ROIs como NO y aniones superóxido (Hasko *et al.*, 2012). Por último, los M1 expresan mayores niveles de antígenos del MHC tipos I y II (Mantovani *et al.*, 2004).

En el otro extremo se encuentran los macrófagos de **activación alternativa** (macrófagos **M2)** con escasa capacidad presentadora de antígenos. La polarización M2 supone una disminución de la expresión de IL-12 y IL-23 modulando y aumentando los niveles de la citoquina antiinflamatoria IL-10. Además liberan quimioquinas como Ccl17 y factores proangiogénicos (VEGF, MMP9). Finalmente se caracterizan por la expresión de genes implicados en el remodelado tisular, como Fizz-1 (*Found in Inflammatory Zone 1*) y YM1 (*chitinase 3-like 3*) (Raes *et al.*, 2002a; Raes *et al.*, 2002b)

Se han descrito varias subpoblaciones (M2a, b y c), entre ellas M2a interviene en la cicatrización de heridas y remodelado tisular tras la estimulación de IL-4 o IL-13, activando la vía STAT6 (*Signal Transducer and Activator of Transcription 6*). Esta activación desempeña un papel esencial en la diferenciación de las células Th2, producción de quimioquinas y de inmunoglobulina E (IgE) (Mosser *et al.*, 2008). Por otra parte, las subpoblaciones M2b y M2c participan en la modulación de la respuesta inmune tras la unión de complejos inmunes con los ligandos de TLR y ligandos del receptor de IL-1 (IL1R) o de IL-10, respectivamente (Gordon *et al.*, 2010; Hristodorov *et al.*, 2012; Mantovani *et al.*, 2004).

2.5 Otros mediadores implicados en la inflamación.

En el desarrollo del proceso inflamatorio se ha descrito la participación de distintos mediadores proinflamatorios entre los que se incluyen mediadores solubles, como las citoquinas y quimioquinas comentados anteriormente, así como distintos **lípidos bioactivos** como los eicosanoides, prostanoides, resolvinas, protectinas y lipoxinas).

En la fase inicial de la inflamación los neutrófilos liberan *eicosanoides* formados a partir del ácido araquidónico (AA) de las membranas celulares, que es sustrato de diferentes enzimas como las del sistema citocromo P-450 o las lipoxigenasas (LOXs) y ciclooxigenasas (COX) responsables de la síntesis de leucotrienos (LTs) y prostaglandinas (PGs), respectivamente (Smith *et al.*, 2011)

La COX es una enzima bifuncional que participa en el proceso inflamatorio catalizando el primer paso en la biosíntesis de prostanoides, las prostaglandinas activas (PGD_2, PGE_2, $PGF_{2\alpha}$), prostaciclina (PGI_2) y al TXA_2. De las dos isoformas de esta enzima, COX-1 y COX-2, la expresión de esta última puede ser inducida de una forma rápida en distintos tipos celulares como los macrófagos en respuesta a diferentes estímulos proinflamatorios (Simon, 1999; Smith *et al.*, 2011). Una de las **prostaglandinas** más destacada como mediador en el proceso inflamatorio, así como en el dolor, es la PGE_2. La PGE_2 ejerce su función a través de su interacción con diferentes subtipos de receptores específicos de tipo receptores acoplados a proteínas G (receptores EP 1-4) (Kawabata, 2011).

La lesión tisular que acompaña al proceso inflamatorio agudo provoca la liberación de mediadores como las PGs y los LTs. Más recientemente se ha descrito la participación de otros mediadores lipídicos antiinflamatorios y pro-resolutivos como las resolvinas, protectinas y lipoxinas en la resolución de la inflamación (Kohli *et al.*, 2009) (Figura 4).

Las *lipoxinas* (LXA_4, LXB_4) son lípidos bioactivos que se forman a partir del metabolismo del AA por acción de las enzimas LOXs y cuya actividad principal es bloquear la entrada de los neutrófilos al foco inflamatorio (Serhan *et al.*, 2008; Weylandt *et al.*, 2012).

Las *resolvinas* (D-resolvinas, E-resolvinas) al igual que *protectinas* se forman a partir de los ácidos grasos omega-3. Las E-resolvinas derivan del ácido eicosapentaenoico (EPA) y las D-resolvinas, protectinas y las maresinas, recientemente descritas, derivan del ácido docosahexaenoico (DHA). Los ácidos grasos omega-3, así como sus derivados, actúan de forma específica como lípidos antiinflamatorios al inhibir la producción de PGs y LTs y favoreciendo la resolución de la inflamación. Entre sus acciones se encuentra

la inhibición de la migración de los neutrófilos favoreciendo la fagocitosis de células apoptóticas por los macrófagos y el bloqueo de la activación de la vía NF-κB de ciertas citoquinas proinflamatorias (Lee *et al.*, 2012; Weylandt *et al.*, 2012).

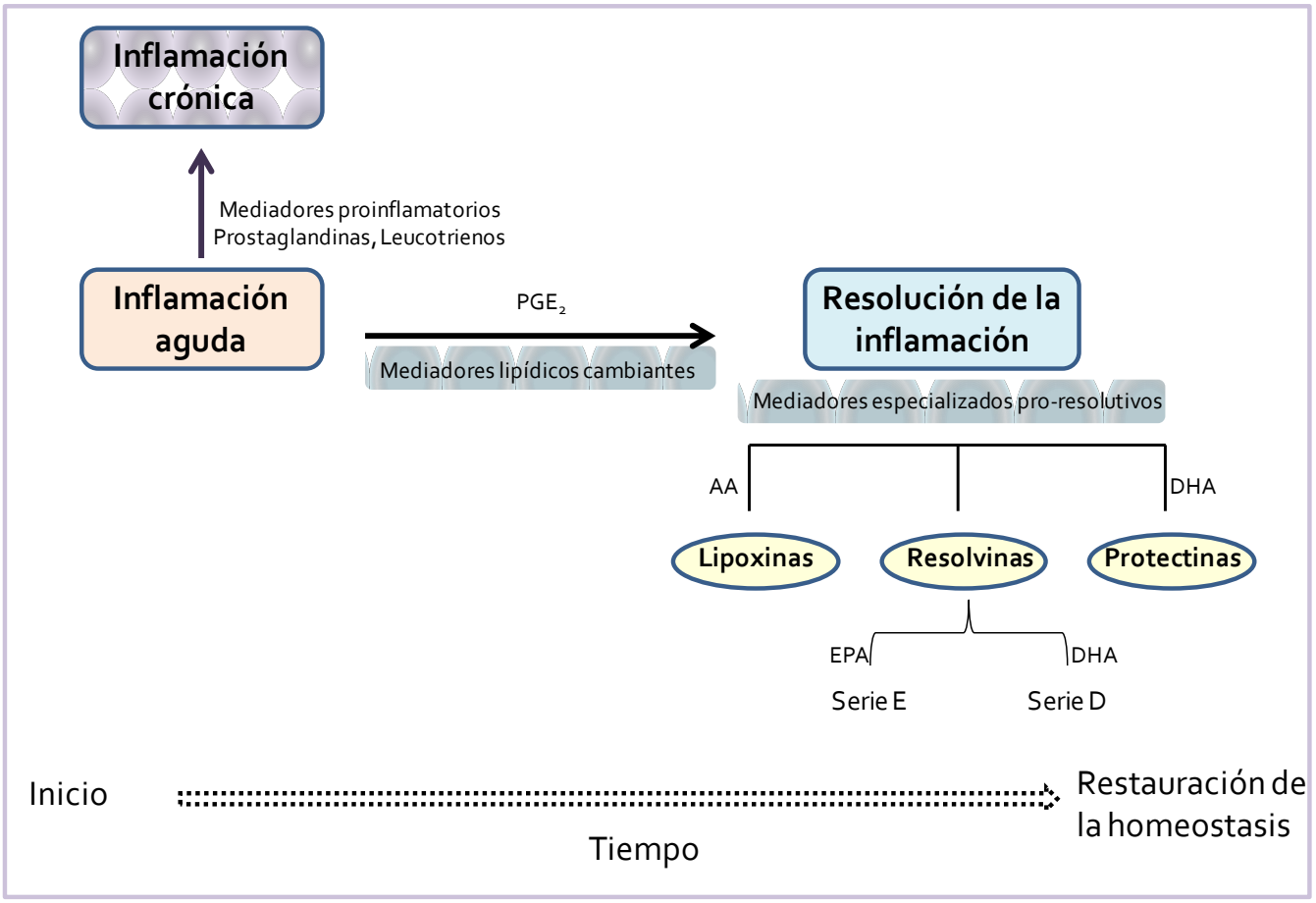

Figura 4: Mediadores lipídicos implicados en la resolución de la inflamación

Los macrófagos también generan **especies intermediarias de oxígeno y de nitrógeno** (ROIs y RNIs) como NO, H_2O_2 y O_2^-, mediadores con gran capacidad de oxidación, nitración, halogenación y desaminación de los lípidos, proteínas, ácidos nucleicos, etc. siendo responsables del daño celular y en la lesión tisular (Nagata, 2005).

El NO es uno de los RNI más destacados cuya producción está catalizada por la enzima NOS a partir del aminoácido L-arginina (Knowles *et al.*, 1994). Existen dos isoformas constitutivas de esta enzima que están presentes en condiciones fisiológicas en el endotelio vascular y cardiomiocitos (eNOS o NOS-3) y neuronas (nNOS o NOS-1) y su actividad es dependiente de Ca^{2+}. Además, la isoenzima inducible e independiente de Ca^{2+} (iNOS o NOS-2) se expresa en diversos tipos celulares, entre ellos los macrófagos, en respuesta a estímulos patológicos. El NO tiene propiedades tanto pro como antiapoptóticas dependiendo de la concentración de este mediador. Las isoformas constitutivas (eNOS y nNOS) generan pequeñas cantidades de NO (en el rango picomolar) con efectos antiapoptóticos o protectores en las células, mientras que la síntesis a partir de NOS-2 es aproximadamente mil veces mayor y conlleva a la muerte celular (Taylor *et al.*, 2003). Esta isoforma se regula a nivel transcripcional ya que el gen que codifica para NOS-2 contiene lugares de unión específicos para factores de transcripción como NF-κB.

El mediador NO participa en la regulación de la vía de la COX y viceversa. Sin embargo, los mecanismos por los que el NO regula la producción de PGs, no han sido perfectamente establecidos (Salvemini *et al.*, 2013). La interacción de ambas vías se puede producir a distintos niveles y diversos estudios han demostrado que tanto el NO como donadores exógenos de este gas, son capaces de inducir la actividad COX. Actualmente, se han propuesto varios mecanismo post-transduccionales que explicarían la síntesis de las PGs mediada por NO. Por una parte, el NO y el anión superóxido pueden producirse simultáneamente, reaccionando entre sí para formar peroxinitrito actuando sobre la COX. Otro posible mecanismo sería la S-nitrosilación directa de las enzimas COX (Kim, 2011).

3. EL DAÑO CARDIACO

3.1 Enfermedades cardiovasculares.

A pesar de los grandes avances en la terapia cardiovascular de los últimos años, las enfermedades cardiovasculares (ECV) siguen siendo una de las principales causas de muerte e incapacidad, con predicciones epidemiológicas que apuntan a que su morbimortalidad superará a la del cáncer y las

enfermedades infecciosas en los próximos años en todos los países del mundo. De acuerdo con los datos aportados por la Sociedad Europea de Cardiología, la OMS ha estimado que cada año fallecen 3.8 millones de hombres y 3.4 millones de mujeres a causa de las ECV. Además, se estima que en 2020 el número de fallecimientos por esta causa se duplique (Hausenloy *et al.*, 2013a).

El corazón es un órgano muy susceptible a los procesos de estrés con una capacidad regenerativa limitada. Las expresiones clínicas más frecuentes de las ECV son, entre otras, la insuficiencia cardiaca, isquemia/reperfusión (I/R) e infarto agudo de miocardio (IAM) (Whelan *et al.*, 2010). Además, en los últimos años se ha descrito el papel que la respuesta inmune innata desempeña en la patogénesis de numerosos procesos cardiovasculares como la aterosclerosis, el daño por I/R, miocarditis viral, etc., patologías en las que se ha descrito un componente inflamatorio subyacente (Mann, 2011).

3.2 Isquemia/reperfusión (I/R).

La falta de flujo sanguíneo hacia el corazón provoca un desequilibrio entre el aporte y la demanda de oxígeno y nutrientes, denominado **isquemia**. Si la isquemia es limitada en el tiempo, es tratada de forma rápida o se resuelve de forma espontánea, los cardiomiocitos no sufren daño. Sin embargo, una isquemia prolongada más de 20 minutos puede desencadenar un IAM. En este caso, el tamaño del área infartada depende fundamentalmente de la duración de la isquemia y de la sensibilidad de los miocitos. Otros factores implicados en la muerte celular son la circulación colateral hacia la zona isquémica, la existencia o no de oclusión coronaria, la demanda de oxígeno y nutrientes, así como la capacidad del miocardio de activa vías de supervivencia frente al daño (Thygesen *et al.*, 2012).

La **reperfusión** (restauración del flujo sanguíneo de forma rápida y temprana), es el tratamiento de elección tras un periodo de isquemia, pero paradójicamente, desencadena la muerte celular, en particular de aquellas que sobrevivieron al periodo isquémico aumentando por tanto, el daño cardiaco (Ruiz-Meana *et al.*, 2009). En su conjunto, este fenómeno se denomina daño por I/R, descrito por Kloner et al (1974), observándose un aumento del área

infartada durante el periodo de reperfusión (Kloner *et al.*, 1974). Por ello, la prevención del daño por reperfusión podría ser el objetivo estudios dirigidos a mejorar la supervivencia del paciente tras un evento de IAM.

3.2.1 Mecanismos implicados en la muerte de los cardiomiocitos.

Distintos tipos de muerte celular como la apoptosis, necrosis y autofagia han sido descritos en el daño por I/R (Whelan *et al.*, 2010).

3.2.1.1 Necrosis

La muerte celular por necrosis tiene lugar mayoritariamente durante los primeros minutos de la reperfusión, provocando cambios morfológicos y bioquímicos que afectan a la mitocondria y a la membrana plasmática. La lesión mitocondrial priva a la célula de energía para el mantenimiento de la homeostasis, mientras que la lesión de la membrana plasmática altera su capacidad osmorreguladora, produciéndose edema de la célula y orgánulos que finalmente se rompen, perdiéndose la integridad de la membrana. En la muerte por necrosis se han caracterizado distintos mecanismos como la liberación ROS, la sobrecarga de Ca^{2+} y apertura de los poros de transición de permeabilidad mitocondrial (PTPM), entre otros (Chiong *et al.*, 2011).

Como consecuencia de la ruptura de la célula otros tipos celulares, como las plaquetas, fibroblastos y neutrófilos son atraídos al foco necrótico, contribuyendo así al daño por reperfusión y desencadenando una respuesta inflamatoria (Eltzschig *et al.*, 2011). Se ha observado que los pacientes con infarto de miocardio tienen un incremento en el número de plaquetas activas circulantes que van a condicionar la función endotelial y la contractilidad del miocardio (Barrabes *et al.*, 2007).

3.2.1.2 Apoptosis

La apoptosis es un tipo de muerte celular programada con un papel esencial en el desarrollo y mantenimiento de la homeostasis tisular (Gottlieb, 2011; Green, 2000). Este proceso requiere cantidades altas de energía y conlleva cambios morfológicos que incluyen la alteración del citoesqueleto y la envoltura nuclear, la fragmentación del ADN y la formación de cuerpos apoptóticos que serán rápidamente eliminados por células fagocíticas, fundamentalmente por

los macrófagos, evitando que se produzca una reacción inflamatoria (Silva, 2010).

La apoptosis contribuye a la muerte celular asociada al daño por I/R. Se han descrito dos vías principales por las que se puede desencadenar el proceso apoptótico en cardiomiocitos: la vía intrínseca o mitocondrial y la vía extrínseca o de receptores de muerte. Ambas vías convergen en la activación de un conjunto de enzimas cisteinil-aspartato proteasas, denominadas caspasas.

Vía intrínseca o mitocondrial

El órgano principal de esta vía es la mitocondria. Los cardiomiocitos expresan varias proteínas de la familia Bcl-2, tanto antiapoptóticas (Bcl-2, Mcl-1 o Bcl-XL) como proapoptóticas (Bax, Bak, Bad o Bid), que regulan la permeabilización de la membrana mitocondrial y la liberación del citocromo *c* y otras proteínas al citosol (Scarabelli *et al.*, 2006). La sobreexpresión de Bcl-2 en cardiomiocitos, así como niveles bajos de Bax reduce sustancialmente el tamaño del infarto y la muerte por apoptosis tras un episodio de I/R.

En respuesta a I/R, las proteínas Bax y Bak forman poros en la membrana externa mitocondrial a través de los cuales las proteínas citocromo *c* o la adaptadora Apaf-1 (*Apoptotic Protease Activating Factor-1*) llegan al citoplasma. El citocromo *c*, se va a unir al dATP y al Apaf-1 formando así el complejo apoptosoma, lo cual implica la activación de la caspasa 9 o iniciadora que a su vez activa las caspasas efectoras como la 3, 6 y 7 (Bratton *et al.*, 2010; Chiong *et al.*, 2011).

Además, se ha descrito la implicación de las proteínas reguladoras Smac/DIABLO y Omi/HtrA2 localizadas en la mitocondria, cuya acción es inhibir la acción de las proteínas inhibidoras de la apoptosis, denominadas IAP, entre las que se encuentra XIAP (*X-linked inhibitor of apoptosis protein*), uno de los reguladores endógenos de la apoptosis mejor caracterizados e importante en los cardiomiocitos. Tras un estímulo apoptótico como la I/R, Smac/DIABLO y Omi/HtrA2 se translocan al citosol donde degradan a XIAP desencadenando la activación de las caspasas. Los cardiomiocitos presentan una resistencia elevada a la apoptosis, ya que en condiciones normales tienen actividad

reducida de la proteína Apaf-1 y caspasas y expresión elevada de proteínas XIAP (Chiong *et al.*, 2011; Wang *et al.*, 2012)

Factores independientes de caspasa liberados desde la mitocondria durante el proceso de I/R como son AIF (*Apoptosis inducing factor*) y el Endo-G (*Endonuclease-G*) que migran al núcleo provocando la fragmentación del ADN durante la apoptosis también han sido implicados. Por ello, la inhibición de la liberación de estos factores muestra un claro efecto cardioprotector (Chiong *et al.*, 2011; Portt *et al.*, 2011).

Vía extrínseca o de receptores de muerte

La vía extrínseca se inicia en la membrana plasmática a través de los receptores de muerte (TNFR1, FAS/CD95, TRAIL (*TNF-related apoptosis-inducing ligand*) y finaliza con la activación de las caspasas (Bratton *et al.*, 2010). Tanto FAS como TNFR1 se expresan en cardiomiocitos y han sido implicados en patologías cardiovasculares (Kubota *et al.*, 1997).

Moléculas adaptadoras como FADD (*Fas-associated Death Domain*) actúan de nexo entre los receptores de muerte y las caspasas iniciadoras, concretamente la pro-caspasa 8. La unión de estas proteínas forma el llamado complejo de señalización de muerte denominado DISC (*Death-Inducing Signaling Complex*), activando finalmente la caspasa-3 (Portt *et al.*, 2011). Esta vía puede ser activada también por la vía intrínseca tras la proteólisis de Bid en tBid que ocurre por un lado al interaccionar tBid con Bax en la mitocondria (Figura 5).

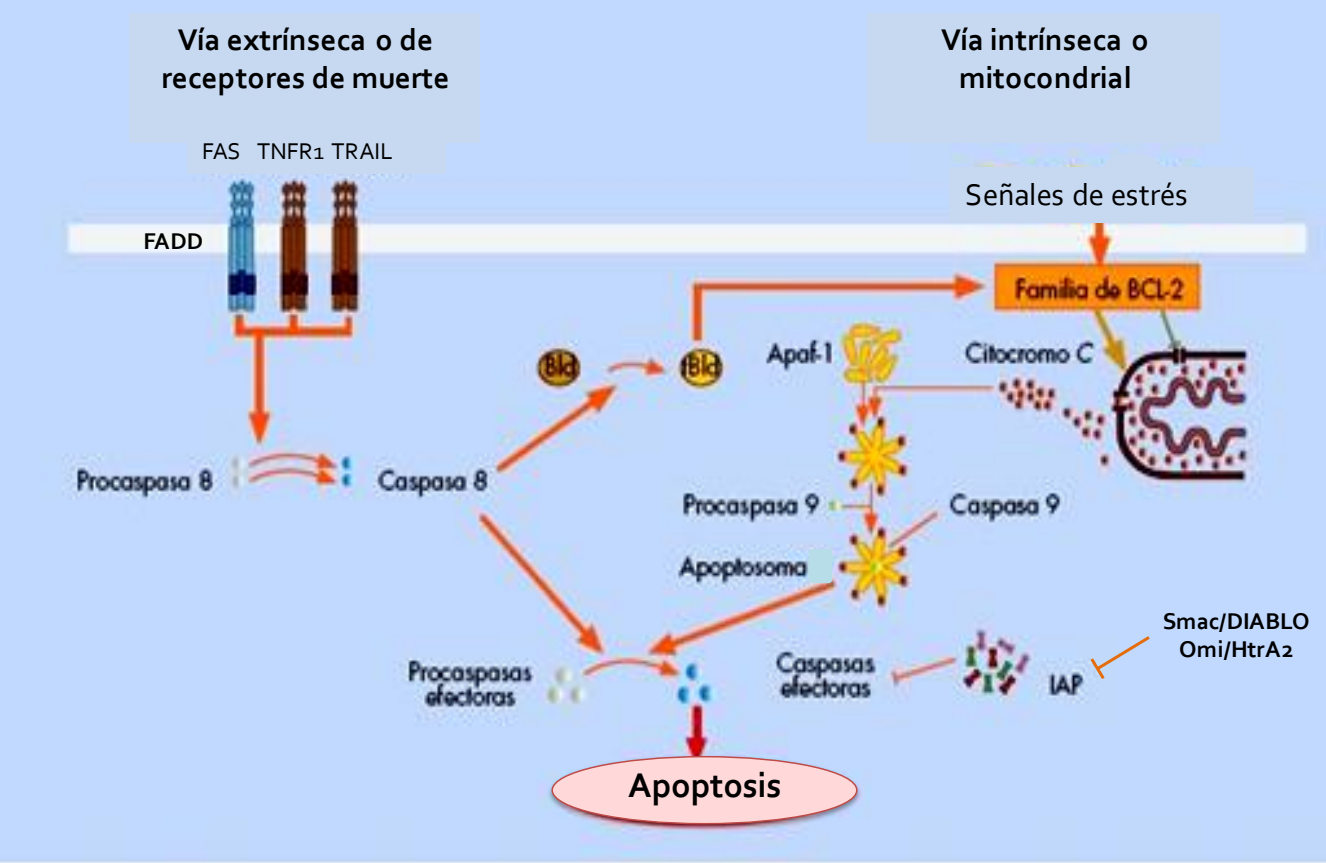

Figura 5. Vías extrínseca e intrínseca de muerte por apoptosis en cardiomiocitos.

3.2.1.3 Autofagia

La autofagia es una vía catabólica implicada en la degradación de proteínas y orgánulos celulares dañados, que son englobados por una estructura denominada autofagosoma. Diversos estudios han descrito un aumento del número de autofagosomas en el corazón expuesto a daño por I/R, lo que pone de manifiesto que este estímulo puede inducir muerte por autofagia (Gustafsson *et al.*, 2009; Hamacher-Brady *et al.*, 2006). Sin embargo, no se ha establecido el mecanismo por el que la autofagia podría contribuir a la cardioprotección.

La autofagia es otro mecanismo de muerte que se ha descrito (Matsui *et al.*, 2007) en los cardiomiocitos y existen estudios que evidencian que este proceso está aumentado en distintas patologías como la hipertrofia cardiaca, cardiomiopatía, así como durante el daño por I/R (Matsui *et al.*, 2007). En este

último caso puede tener un comportamiento dual en función de los estímulos que induzcan su activación y el papel que desempeña continúa siendo objeto de estudio respecto a si la autofagia contribuye a la cardioprotección (Wei *et al.*, 2013) o si por el contrario la autofagia inducida por señales como la activación de AMPK (*AMP-activated protein kinase*) por ROS o sobrecarga de Ca^{2+} intracelular entre otros durante la I/R es perjudicial para la célula (Gustafsson *et al.*, 2009).

En cardiomiocitos, apoptosis y autofagia son procesos interrelacionados entre sí, concretamente en el momento de la apertura del PTPM. Además, se ha descrito la interacción de la proteína Beclina 1 y las proteínas antiapoptóticas de la familia Bcl-2 (Bcl-XL y Bcl-2) (Matsui *et al.*, 2007).

3.3 I/R e Inflamación.

Como ya se ha descrito anteriormente, la inflamación es un componente destacado en la patogénesis del daño cardiaco por I/R. En la fase isquémica inicial se produce la inducción de estrés oxidativo que contribuye a la disfunción endotelial aumentando la permeabilidad y liberación de citoquinas proinflamatorias que conlleva a la activación e infiltración de leucocitos, exacerbando el daño miocárdico y produciendo muerte celular (Marchant *et al.*, 2012). Venkatachalam y colaboradores han descrito cómo la inhibición de la adhesión de los neutrófilos y neutralización de la liberación de distintos mediadores inflamatorios (como la IL-18) atenúa el daño miocárdico en I/R (Venkatachalam *et al.*, 2009).

Se ha descrito la participación de los receptores TLRs en el sistema cardiovascular. Estos receptores, además de reconocer los PAMPs son capaces de reconocer otros ligandos moleculares endógenos denominados DAMPs (*Damage-Associated Molecular Partterns*) que se liberan durante el daño celular o muerte como en el caso de células necróticas, proteínas de la matriz extracelular y proteínas de choque térmico (HSP). La unión de estas moléculas con los TLRs provoca una respuesta inflamatoria en las células activando NF-κB con la posterior liberación de citoquinas y mediadores inflamatorios (TNF-α, IL-1β, IL-6 y NO) (Mann, 2011). Por todo ello, es evidente que la activación de los TLRs contribuye al desarrollo y progresión de las

enfermedades cardiovasculares. Se ha descrito la expresión de al menos seis receptores de la familia TLR: TLR2, TLR3, TLR4, TLR5, TLR7 y TLR9 en cardiomiocitos murinos, siendo TLR2 y TLR4 los más estudiados (Chao, 2009; Feng *et al.*, 2011).

La presencia de este componente inflamatorio se ha puesto en manifiesto en ratones modificados genéticamente, deficientes de TLR4, sometidos a isquemia por oclusión temporal de la arteria coronaria descendente izquierda en los que se observa menor inflamación, en particular una menor infiltración de neutrófilos y reducción de estrés oxidativo, además de mostrar menor tamaño del infarto (Oyama *et al.*, 2004). Por otra parte, la administración de antagonistas del receptor TLR4 como el *eritoran*, se asocia con una reducción significativa del área infartada (Shimamoto *et al.*, 2006).

La señalización de los TLRs converge en la activación del factor de transcripción NF-κB cuya función en el daño por I/R ha sido descrita. A semejanza de la implicación de los TLRs implicados en la inflamación, la inhibición de NF-κB se ha traducido en una reducción de la disfunción contráctil en los cardiomiocitos (Hofmann *et al.*, 2011).

Al igual que se ha sugerido durante la inflamación, en situaciones de daño por I/R también existe un incremento en la liberación de AA catalizada por la enzima FLA_2 y que posteriormente será metabolizado por las enzimas LOX, COX y citocromo P450 (CYP) como precursor de lípidos bioactivos como la PGE_2. La $iFLA_2\beta$ es la que predomina en el miocardio, regulada por las alteraciones en las concentraciones de Ca^{2+} y por el equilibrio bioenergético en los cardiomiocitos (Jenkins *et al.*, 2009; Mancuso *et al.*, 2003).

Uno de los mediadores lipídicos más destacados en la patogénesis de las enfermedades cardiovasculares es la prostaglandina E_2 (PGE_2) cuya liberación se incrementa para adaptar al miocardio isquémico durante la I/R a través de los receptores acoplados a proteína G (EP1, 2, 3 y 4). En el desarrollo de I/R los macrófagos activados migran hacia el miocardio donde liberan citoquinas (TNF-α o IL-β6), quimioquinas (proteína quimioatrayente de monocitos, MCP-1) y otros mediadores de la inflamación (Suzuki *et al.*, 2011). En esta situación, la PGE_2 muestra un efecto cardioprotector al atenuar la actividad de las células inflamatorias en el corazón, aunque los mecanismos de acción están aún en

estudio. Por ello, estimulando selectivamente los receptores EP en el miocardio con fármacos agonistas, se puede conseguir reducir el daño producido por la reperfusión en el miocardio isquémico (Hishikari *et al.*, 2009).

3.4 Cardioprotección.

Como ya se ha comentado anteriormente, la supervivencia de las células tras un periodo de isquemia depende entre otros factores de la duración de la isquemia a la que han estado sometidos. La reperfusión coronaria ha sido aceptada como la terapia estándar para el tratamiento del infarto agudo de miocardio (Kloner, 2011).

Paradójicamente esta terapia no garantiza que las células isquémicas sobrevivan, habiéndose descrito que aunque la reperfusión restaura el flujo sanguíneo, oxígeno y nutrientes al músculo cardiaco la propia restauración del flujo, fenómeno conocido como “daño por reperfusión”, desencadena la muerte celular. La reperfusión se acompaña de complicaciones como la disminución de la función contráctil y la aparición de arritmias, además de agravar la muerte de los cardiomiocitos por apoptosis, necrosis o autofagia de los cardiomiocitos previamente dañados (Piper *et al.*, 2009; Sanz-Rosa *et al.*, 2012).

La búsqueda de agentes cardioprotectores que mejoren la función del miocardio, que disminuyan la aparición de arritmias, capaces de retrasar el inicio de la muerte celular y en general, que eviten la progresión del infarto durante un daño por I/R, es un área de intensa investigación. En las últimas décadas se han evaluado numerosas moléculas capaces de reducir en distinta medida el daño por I/R en modelos animales; sin embargo, los intentos por trasladar estos resultados a la práctica clínica en la mayoría de los casos han sido infructuosos (Downey *et al.*, 2009).

El corazón posee una gran capacidad de adaptación endógena, denominada “condicionamiento”, para tolerar los efectos del daño agudo originado por un estímulo de I/R y este punto es objeto de estudio de nuevas estrategias mecánicas y farmacológicas (Kloner, 2011). Se han descrito dos mecanismos cardioprotectores endógenos en el miocardio: pre y postcondicionamiento isquémico. El **precondicionamiento isquémico (PreC)** es una respuesta adaptativa en la cual la exposición a breves episodios de I/R incrementa

significativamente la capacidad del corazón de resistir a un daño isquémico inmediatamente posterior (Moreu-Burgos *et al.*, 2007).

Por otra parte, ciclos cortos de I/R aplicados tras un periodo largo de isquemia y en el momento de la reperfusión también confieren un efecto cardioprotector en el miocardio isquémico; fenómeno denominado **postcondicionamiento isquémico (PostC)**. Esta técnica de cardioprotección se describió por primera vez en 2003 cuando Zhao y colaboradores (Zhao *et al.*, 2003) comprobaron que la aplicación de ciclos de 30 segundos de I/R al inicio de la reperfusión después de 60 minutos de isquemia, conseguían reducir el tamaño del infarto en un 40% en un modelo canino, mostrando resultados, en este aspecto, similares al PreC. El descubrimiento de ambos procesos ha permitido desarrollar nuevas estrategias de cardioprotección basadas en el conocimiento de los mecanismos moleculares y celulares implicados en el daño y supervivencia celular durante la I/R.

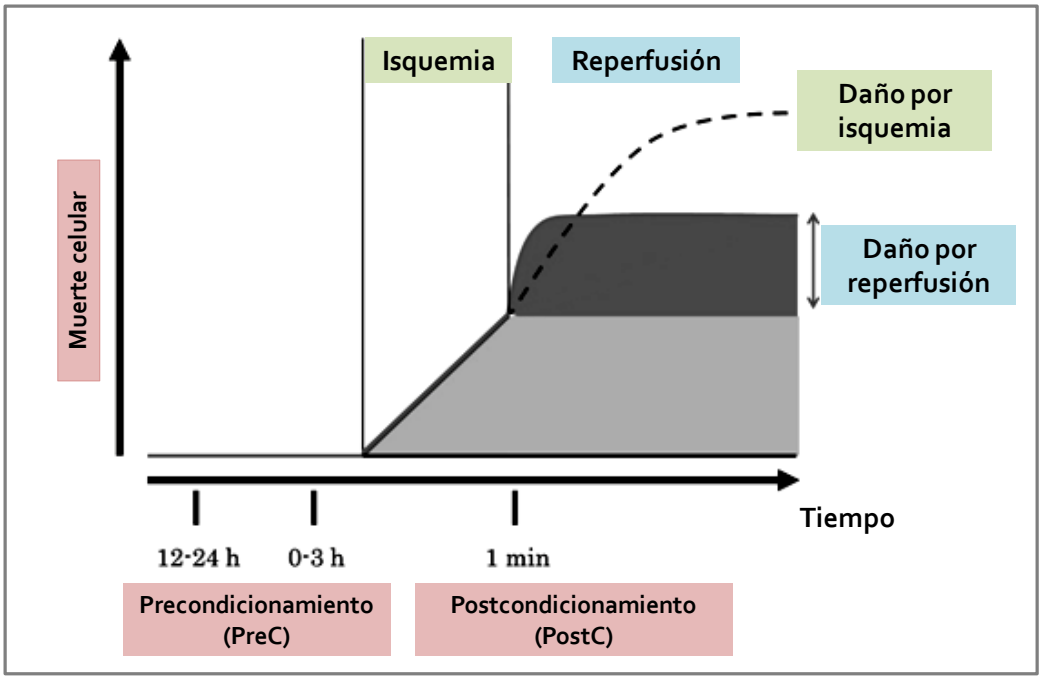

Figura 6. Cronograma del desarrollo del daño por isquemia/reperfusión (I/R) en el miocardio. En una primera fase (isquemia) la muerte celular en las áreas de riesgo isquémico aumenta proporcionalmente al tiempo que esté sin reperfundir. Paradójicamente la reperfusión que sobreviene induce mayor daño en el miocardio en una etapa temprana (área negra).

Tratamientos farmacológicos en el PostC pueden reducir el daño producido por la reperfusión (área gris) (adaptado de Minamino, T. 2012).

3.4.1 Mecanismos implicados en cardioprotección.

Los mecanismos de cardioprotección descritos hasta el momento afectan a distintas dianas como vías de señalización intracelular, funciones de orgánulos intracelulares como el retículo sarcoplásmico y la mitocondria, así como el control de la homeostasis celular (Ferdinandy *et al.*, 2007; Hausenloy *et al.*, 2013a).

3.4.1.1 Vía RISK (Reperfusion Injury Signaling Kinases)

Esta vía, descrita en el PreC y PostC, está integrada por una cascada de varias proteínas quinasas. Se ha demostrado que la activación por fármacos en el comienzo de la reperfusión, de distintas proteínas quinasas implicadas en la supervivencia celular consigue reducir notablemente el tamaño del infarto del miocardio.

La estimulación de receptores acoplados a proteína G (RAPG) por ligandos endógenos como los autacoides (adenosina, bradiquinina y opioides), así como el efecto de factores de crecimiento, citoquinas, el péptido natriurético, etc., pueden iniciar la activación de diferentes vías de protección celular. Existen evidencias de que la activación de receptores de adenosina A2 y A3, del receptor de bradiquinina B2 y de los receptores opioides durante la isquemia y en la reperfusión, es fundamental para proporcionar protección a través de la vía RISK (Hausenloy *et al.*, 2004; Kin *et al.*, 2005). Tras demostrar que la naloxona, antagonista no específico del receptor opiode, era capaz de suprimir la protección proporcionada por el PostC en modelos animales, se investigó el efecto que supone en este punto la presencia de antagonistas farmacológicos de los receptores opioides tipo δ, κ y μ (Zatta *et al.*, 2008).

La vía RISK está formada por las vías de supervivencia celular PI3K (*Phosphatidylinositide 3-kinase*)/AKT y MAPK (*Mitogen-Activated Protein Kinases*) extracelular p42/p44 (ERK 1/2), que al ser activadas en el momento de la reperfusión, confieren cardioprotección. En primer lugar la vía de PI3K es activada mediante la unión de diferentes factores de crecimiento y citoquinas a sus respectivos receptores en la superficie celular

(Wymann *et al.*, 2005). Como consecuencia, se genera una señalización en cascada que llega hasta el núcleo. Entre las proteínas activadas por esta vía, la serina/treonina quinasa, AKT, es la mejor caracterizada, cuya activación está implicada en la supervivencia celular, concretamente al conferir cardioprotección frente un daño por I/R (Datta *et al.*, 1996). Entre las dianas directas de esta proteína se incluyen las caspasas 3 y 9 o los miembros de la superfamilia Bcl-2, sobre las que actúa impidiendo la señalización apoptótica (Stiles, 2009).

Por otra parte, la familia de proteínas serina/treonina quinasas, MAPK, participan en vías de transducción implicadas en procesos de proliferación y diferenciación celular. En los cardiomiocitos, la subfamilia ERK es probablemente la mejor caracterizada. Estas proteínas se activan en respuesta a factores de crecimiento y mitógenos que a través de receptores acoplados a proteína G activan MEK que posteriormente activa ERK1/2 (Yeh *et al.*, 2013). Se consideran proteínas antiapoptóticas ya que su activación forma parte de los mecanismos de cardioprotección descritos en la vía RISK evitando la apoptosis de los cardiomiocitos en la reperfusión (Ravingerova *et al.*, 2003).

La activación de la vía RISK conlleva a la inactivación de una nueva quinasa GSK-3β (Glycogen Synthase Kinase), implicada en diferentes funciones celulares como el metabolismo del glucógeno y la supervivencia celular (Heusch, 2009). Por otra parte, recientemente se ha descrito que PI3K está relacionada con la vía de la eNOS donde el NO tiene al menos dos dianas de actuación en la mitocondria: los canales de potasio dependientes de ATP (mK_{ATP}) y el PTPM (Frohlich *et al.*, 2013). Esta vía de señalización es una de las dianas más importantes en el desarrollo de nuevos fármacos cardioprotectores (Figura 7).

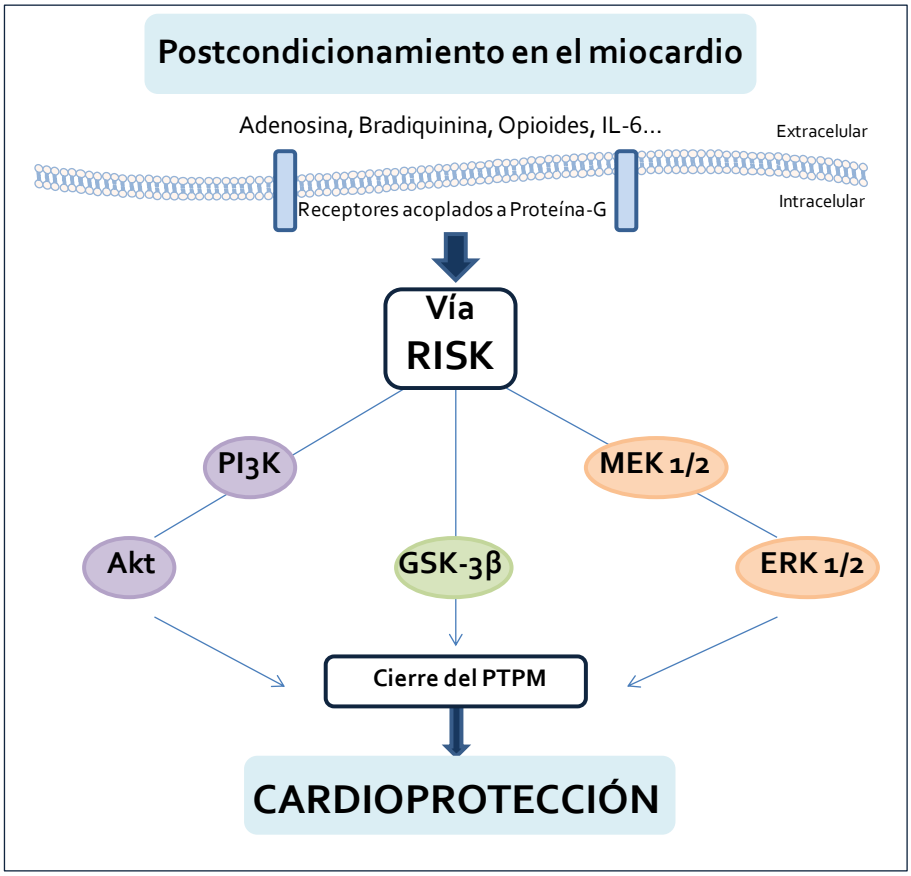

Figura 7. Señalización a través de la vía RISK, implicada en la cardioprotección durante el postcondicionamiento en el miocardio.

3.4.1.2 Vía SAFE (Survivor Activating Factor Enhancement)

La activación de la vía SAFE, por citoquinas como TNF-α y la posterior activación de la vía de JAK/STAT, también confieren protección en un evento de PostC. Esta vía puede activarse en solitario o en paralelo a la vía RISK al comienzo de la reperfusión (Lecour, 2009; Minamino, 2012). Concretamente, TNF-α es una citoquina que contribuye a la disfunción miocárdica en la I/R y a la muerte celular por apoptosis. Su efecto es diferente en función de dos variables: de la concentración a la que se libere (a bajas concentraciones es cardioprotector pero a altas es dañino) y a cuál de sus dos receptores se une (su unión al receptor TNFR 1 parece tener efecto negativo mientras que si se une al receptor TNFR2 resulta cardioprotector) (Lacerda *et al.*, 2009). En conjunto estos factores potencian y/o complementan el efecto producido durante la vía RISK, pero mecanísticamente no existe una relación clara entre

las vías RISK y SAFE, aunque se cree que todas las cascadas implicadas pueden converger a nivel mitocondrial como punto final (Heusch, 2009; Lecour, 2009) (Figura 8).

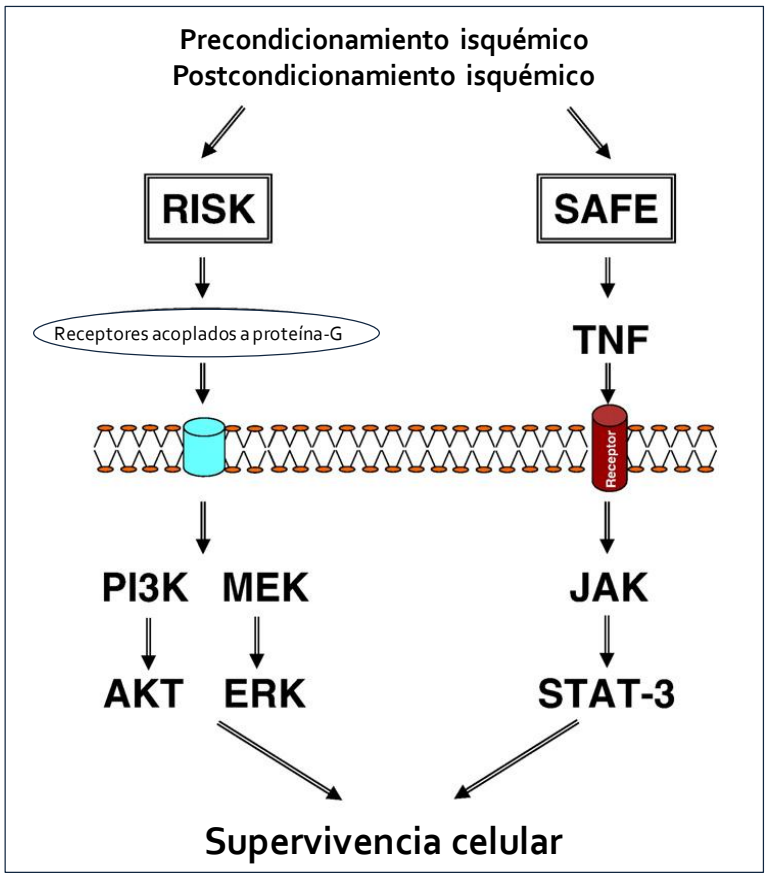

Figura 8. La activación de las vías de señalización RISK y SAFE confieren cardioprotección frente el daño por I/R (adaptado de Lecour S, 2009).

3.4.1.3 AMPK (AMP-Activated Protein Kinase)

A nivel celular es una de las vías implicadas en la terapia para evitar el daño por I/R. AMPK es una proteína que se activa en respuesta a estímulos metabólicos como el estrés oxidativo e hiperosmótico, la hipoxia o la isquemia. A nivel molecular, AMPK es una proteína heterotrimérica formada por una subunidad catalítica α y dos subunidades reguladoras, β y γ (Lage *et al.*, 2008). Además, se ha descrito el efecto protector de la activación de AMPK en el miocardio durante la I/R (Morrison *et al.*, 2011). El mecanismo por el cual confiere cardioprotección es ralentizar todo el metabolismo energético del

miocardio y todos sus procesos celulares, protegiéndolo así del daño en el momento de la reperfusión y por tanto, reducir el tamaño del infarto.

La activación farmacológica de esta vía es considerada como una estrategia terapéutica en el tratamiento de las enfermedades cardiovasculares. La primera molécula identificada como activador del AMPK fue el nucleósido 5-aminoimidazol-4 carboxiamida-1-β-D-ribofuranósido (AICAR) que aumenta la actividad de AMPK en numerosos tejidos, incluyendo el corazón (Zaha *et al.*, 2012).

3.4.1.4 Otros mecanismos implicados en cardioprotección

Los efectos de las vías de señalización ya mencionadas repercuten a nivel mitocondrial en la inhibición del poro de transmisión mitocondrial así como en la apertura del canal de potasio dependiente de ATP. Como ya se ha descrito en los mecanismos de muerte de los cardiomiocitos, la apertura del **PTPM** es una de las dianas más importantes en cardioprotección. Varios estudios lo ponen de manifiesto usando inhibidores de PI3K como LY294002 o la worthmanina en el comienzo de la reperfusión lo que sugiere que la inhibición de la apertura del PTPM es mediada por la vía PI3K/AKT durante el PostC (Bopassa *et al.*, 2006). Recientemente se ha descrito el efecto del ácido epoxieicosatrienoico (EET) que induce cardioprotección mediando la apertura del PTPM por la activación de los canales de potasio dependientes de ATP mitocondriales así como de los canales de potasio activados por Ca^{2+} y activación de las vías de señalización PI3K/AKT y ERK 1/2 (Gross *et al.*, 2013).

Por otra parte es de gran interés la búsqueda de compuestos capaces de reducir los niveles de **Ca^{2+} intracelular** para prevenir la apertura del PTPM y la hipercontractura de los cardiomiocitos, evitando así, la muerte celular. Se han obtenido resultados favorables con la inhibición farmacológica en modelos animales en cuanto a la reducción del tamaño del infarto, sin embargo, en la práctica clínica han sido desfavorables (Frohlich *et al.*, 2013).

La **proteína quinasa G** (PKG) es un mediador fundamental en el proceso de cardioprotección y se activa en el PostC a través de la cascada RISK por mediación de AKT y vía eNOS. Posteriormente se activa **PKC** que resulta en la

sensibilización del receptor de adenosina A2B o en la inhibición de la apertura del PTPM (Murphy, 2004).

Durante la isquemia y principalmente durante la reperfusión, la elevada producción de **ROS** se asocia con un mayor daño cardiaco. El hecho de que los ROS participen de forma dual y opuesta en el contexto de la cardioprotección es paradójico ya que se requieren ciertos niveles de ROS para generar respuestas fisiológicas de supervivencia como mediadores de las vías de señalización y proliferación celular (Halliwell, 2013). Esto podría explicarse por diferencias en la compartimentalización (citosólicos o mitocondriales), momento de su producción (en la isquemia o en la reperfusión) y en la cantidad y tipos de ROS liberados. Existen compuestos que han resultado satisfactorios en modelos animales, como es el caso de la *stobadina* (derivado de piridoindol), que ha mostrado una gran capacidad antioxidante con propiedades protectoras en un modelo de Langendorff en rata (Broskova *et al.*, 2011; Chouchani *et al.*, 2013).

RESULTADOS

Capítulo 1

Synthesis and anti-inflammatory activity of ent-kaurene derivatives

European Journal of Medicinal Chemistry**.** 46(4):1291-305 (2011)

Synthesis and anti-inflammatory activity of *ent*-kaurene derivatives.

Idaira Hueso-Falcón*, **Irene Cuadrado***, Florencia Cidre, Juan M. Amaro-Luis, Ángel G. Ravelo, Ana Estevez-Braun, Beatriz de las Heras, Sonsoles Hortelano

*equal contribution

European Journal of Medicinal Chemistry. 46(4):1291-305 (2011)

Los objetivos de este trabajo han sido la descripción de la síntesis y el estudio de la potencial actividad antiinflamatoria de una serie de 63 compuestos diterpénicos con estructura *ent*-kaurano, derivados del ácido kaurenoico. Inicialmente, se determinó la capacidad de los diterpenos objeto de estudio como inhibidores de la liberación de NO, uno de los principales mediadores del proceso inflamatorio. De los 63 diterpenos evaluados, trece (**9, 10, 11, 12, 14, 17, 23, 28, 37, 48, 55, 61** y **62**) fueron capaces de inhibir la producción de NO con un valor de IC_{50} en el rango 2-10 μM. La evaluación de la viabilidad celular en la línea de macrófagos RAW 267.4 en presencia de concentraciones crecientes de los compuestos confirmó los diterpenos **11**, **12**, **14** y **23** produjeron una disminución significativa de la viabilidad celular, mientras que los compuestos **9, 10, 17, 28, 37, 48, 55, 61** y **62** no mostraron toxicidad.

Los diterpenos activos (**28**, **55** y **62**) inhibieron significativamente la expresión de la enzima proinflamatoria NOS-2 a nivel transcripcional. Los efectos antiinflamatorios observados estaban mediados por la inhibición de la activación del factor de transcripción NF-κB implicado en el proceso inflamatorio. Además, estos diterpenos producían una disminución significativa de la liberación de otros mediadores inflamatorios como las citoquinas IL-6, IL-1α, TNF-α e IFN-γ en macrófagos estimulados con LPS.

Los datos de este estudio ponen de manifiesto el potencial antiinflamatorio de los diterpenos kauranos.

European Journal of Medicinal Chemistry 46 (2011) 1291–1305

Contents lists available at ScienceDirect

European Journal of Medicinal Chemistry

journal homepage: http://www.elsevier.com/locate/ejmech

Original article

Synthesis and anti-inflammatory activity of *ent*-kaurene derivatives

Idaira Hueso-Falcón [a,b,1], Irene Cuadrado [c,1], Florencia Cidre [d], Juan M. Amaro-Luis [e], Ángel G. Ravelo [a,b], Ana Estevez-Braun [a,b,*], Beatriz de las Heras [c,*], Sonsoles Hortelano [d,*]

[a] *Instituto Universitario de Bio-Orgánica "Antonio González", Universidad de La Laguna, Avda. Astrofísico Fco. Sánchez 2, 38206 La Laguna, Tenerife, Spain*
[b] *Instituto Canario de Investigaciones del Cáncer (ICIC)[2], Spain*
[c] *Departamento de Farmacología, Facultad de Farmacia, Universidad Complutense, Plaza Ramón y Cajal s/n, 28040 Madrid, Spain*
[d] *Unidad de Inflamación y Cáncer, Área de Biología Celular y del Desarrollo, Centro Nacional de Microbiología, Instituto de Salud Carlos III, Ctra Majadahonda-Pozuelo, Km 2,200, 28220 Majadahonda, Madrid, Spain*
[e] *Departamento de Química, Facultad de Ciencias, Universidad de los Andes, Mérida, Venezuela*

ARTICLE INFO

Article history:
Received 9 December 2010
Received in revised form
24 January 2011
Accepted 25 January 2011
Available online 3 February 2011

Keywords:
Inflammation
Kaurenes
NO
NOS-2
NF-κB
Cytokines

ABSTRACT

A series of kaurene derivatives (**1**–**63**) were prepared and evaluated for anti-inflammatory activity. Thirteen of the tested compounds were able to inhibit NO production with an IC_{50} between 2 and 10 μM. Compounds **11**, **12**, **14** and **23** showed low percentage of cell viability, whereas compounds **9**, **10**, **17**, **28**, **37**, **48**, **55**, **61** and **62** were non-cytotoxic at the concentration up to 25 μM. Some structure–activity relationships were outlined. Compounds **28**, **55** and **62**, were selected as representative compounds and they potently inhibited the protein expression of NOS-2. We also determined that inhibition of NF-κB activation might be the mechanism involved in anti-inflammatory effects of these kaurene derivatives. As expected, cytokines IL-6, IL-1α, TNF-α and IFN-γ were downregulated in the presence of compound **28**, **55** and **62** after stimulation with LPS. These results indicate that kaurene derivatives might be used for the design of new anti-inflammatory agents.

1. Introduction

Inflammation is an adaptive response that is triggered by noxious stimuli and conditions, including infection and tissue injury. If the acute inflammatory response fails to eliminate the pathogen, the inflammatory process persists and acquires new characteristics.

Macrophages play a key role in the inflammatory response and serve as an essential interface between innate and adaptive immunity. On sensing the presence of pathogens through Toll-like (TLRs) and other receptors, macrophages are stimulated to secrete a battery of cytokines that recruit effector cells into the infected area. Thus, stimulation of TLR4 by lipopolysaccharide (LPS) triggers the recruitment of the cytoplasmic adapter protein MyD88 and subsequently culminates in the activation of downstream signaling pathways. These pathways induce the expression of various inflammatory mediators, including nitric oxide (NO), prostaglandins (PGs), chemokines and inflammatory cytokines that are well-known to be involved in the pathogenesis of inflammatory response [1–4].

One of the most important regulators of the inflammatory response is the transcription factor NF-κB. NF-κB exists mainly as a heterodimer comprised of subunits of the Rel family p50 and p65, which is normally sequestered in the cytosol as an inactive complex by association with the inhibitory proteins IκB [5]. The activation of NF-κB involves the phosphorylation of IκBs at two critical serine residues (Ser32, Ser36) *via* the IκB kinase (IKK) signalosome complex [6,7]. Once IκBs have been phosphorylated, they are ubiquitinated and degraded by 26S proteosome [8,9]. Degradation of IκB allows the NF-κB to translocate to the nucleus, where it regulates the transcription of all significant pro-inflammatory chemokines/cytokines, many angiogenic growth factors, TNF-α, inducible nitric oxide synthase (NOS-2), COX-2, ICAM-1, VCAM-1, E-selectin and pathways of cell proliferation and survival [10–12].

Abbreviations: NO, nitric oxide; NOS-2, inducible nitric oxide synthase; LPS, lipopolysaccharide; MTT, 3-(4,5-dimethylthiazol-2-yl)-2,5-diphenyltetrazolium bromide; PGs, prostaglandins; TLCK, N_{α}-Tosyl-l-lysine chloromethyl ketone hydrochloride; TLRs, Toll-like receptors.

* Corresponding authors. Tel.: +34 918223291; fax: +34 918223269.
E-mail addresses: aestebra@ull.es (A. Estevez-Braun), lasheras@farm.ucm.es (B. de las Heras), shortelano@isciii.es (S. Hortelano).

[1] Both authors contributed equally to this work.

[2] http://www.icic.es.

0223-5234/$ – see front matter © 2011 Elsevier Masson SAS. All rights reserved.
doi:10.1016/j.ejmech.2011.01.052

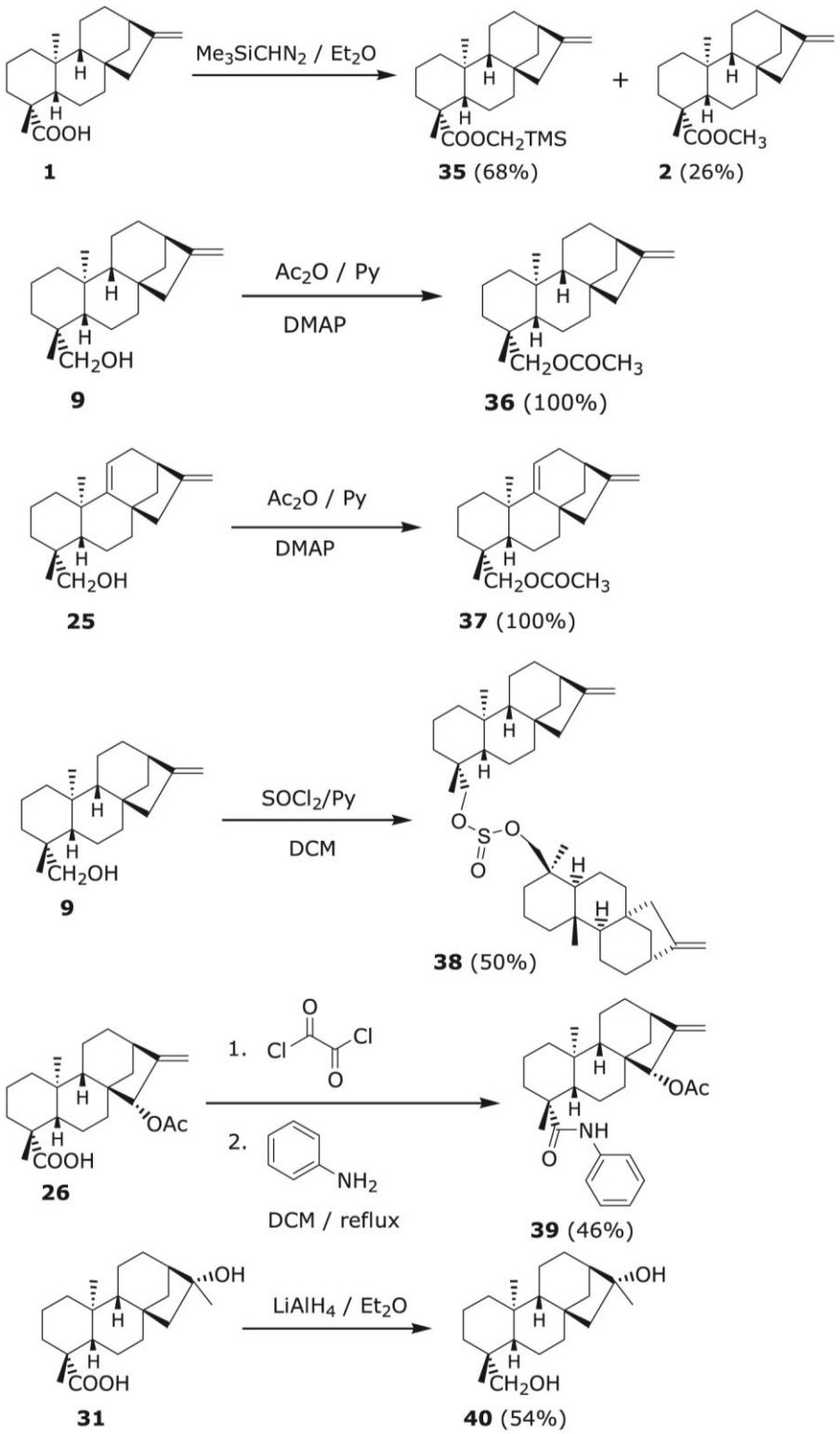

Scheme 1. Obtention of derivatives (**35**–**40**) by modifications at C-19.

double bond was reduced under hydrogenation conditions and compound **45** was consequently obtained. The spiro compounds **46** and **47** were obtained when the dihydroxyl derivative **14** was treated with 3 equiv of $SOCl_2$ and pyridine in DCM. Esterification of compound **18** with 2-furoyl chloride afforded a mixture 1.2:1 of the corresponding mono- (**48**) and di-furoate (**49**) compounds. Epoxidation of the double bonds present in compound **17** produced the epoxide isomers (**50**) and (**51**). Compounds **52**–**63** were obtained by ozonolysis of the exocyclic double bond of kaurene derivatives **2**, **8**, **10**, **12**, **30** and **35** (Scheme 3). With compound **2** and **30** only the expected ketones (**52**) and (**59**) were obtained. The treatment of compound **8** in dry DCM under N_2

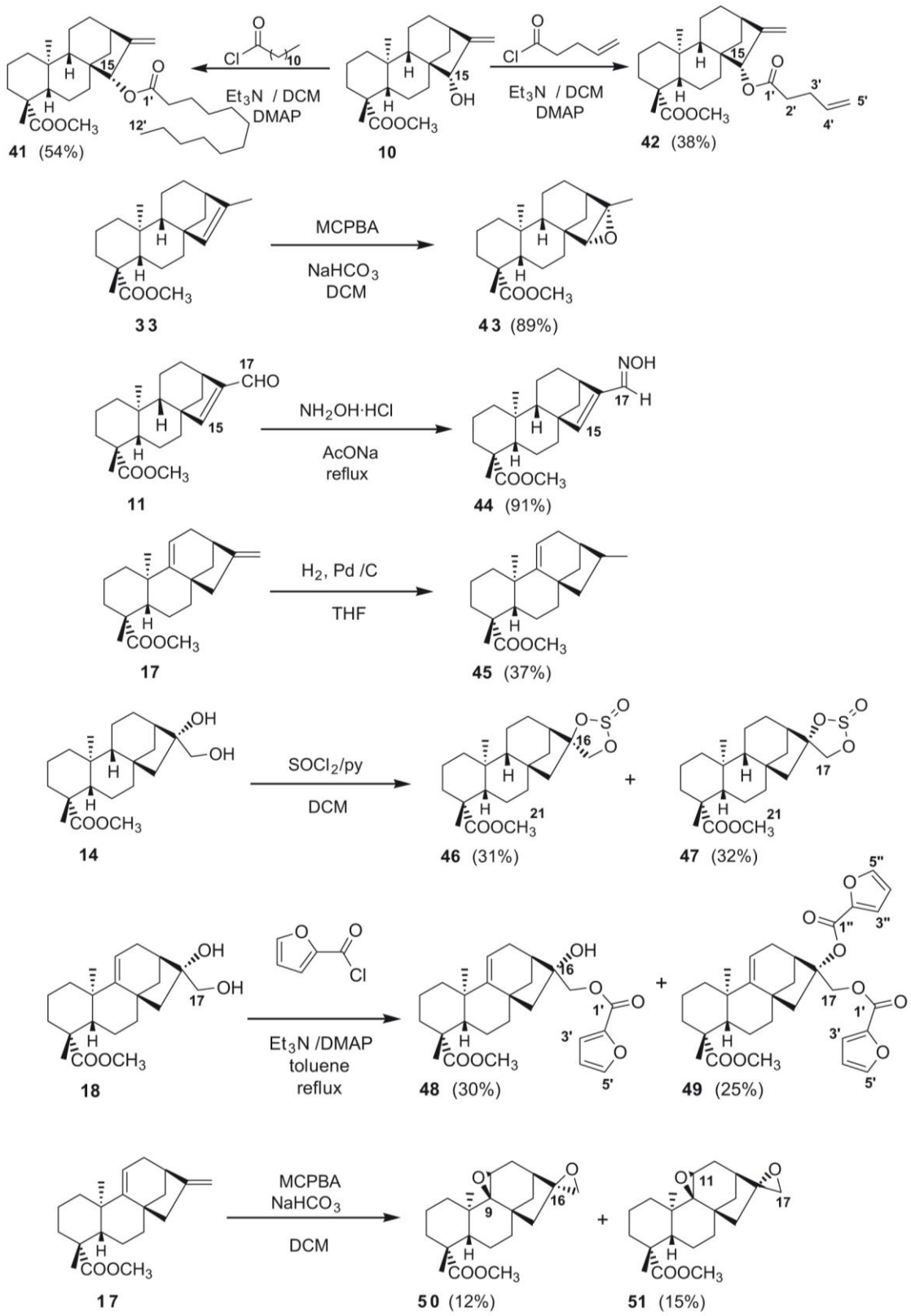

Scheme 2. Obtention of derivatives (**41**–**51**) by ring C and D modifications.

atmosphere at −78° with O_3 for 30 s and then, with 2.7 equiv of Me_2S yielded after purification three compounds **53** (54%), **54** (21%) and **55** (20%). The structures of **54** and **55** were ratified by the correlations detected in the HMBC spectrum. A plausible explanation to the formation of the lactone moiety is based on a Baeyer–Villiger oxidation on the carbonyl compound formed in the ozonolysis. Other tentative formation is shown in Scheme 4 according to the result published by Schank et al. [18].

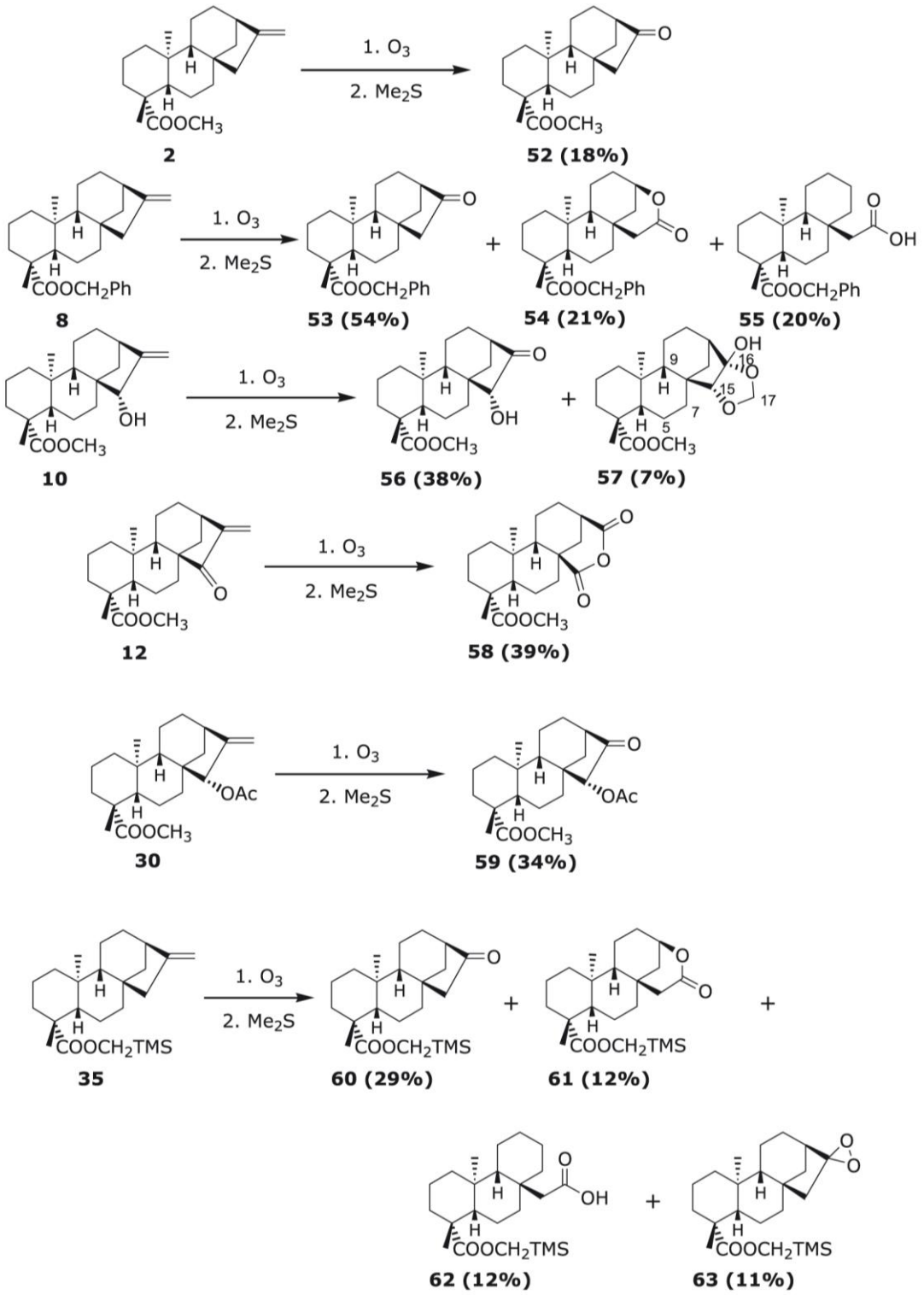

Scheme 3. Derivatives (**52**–**63**) obtained by ozonolysis.

Derivative **55** apparently is formed by opening of the corresponding lactone but **55** does not possess the corresponding hydroxyl group at C-16. In the ozonolysis of compound **10** furthermore of the carbonyl derivative **56** another unexpected derivative **57** was obtained in low yield (7%). Its structure was determined on the basis of the following HMBC correlations H-17/C-15, C-16 and H-7/C-15. The orientation of the hydrogen H-15 and the methylendioxy moiety was established by the NOE effects detected between H-15 and the hydrogens H-5 and H-9. When the α,β-unsaturated carbonyl compound (**12**) was ozonized only the anhydride **58** was obtained in 39% yield. Finally four compounds **60**–**62** were obtained from the reductive ozonolysis of **35**. The isolation of compound **63** having a dioxirane moiety supports the proposed mechanism illustrated in Scheme 4.

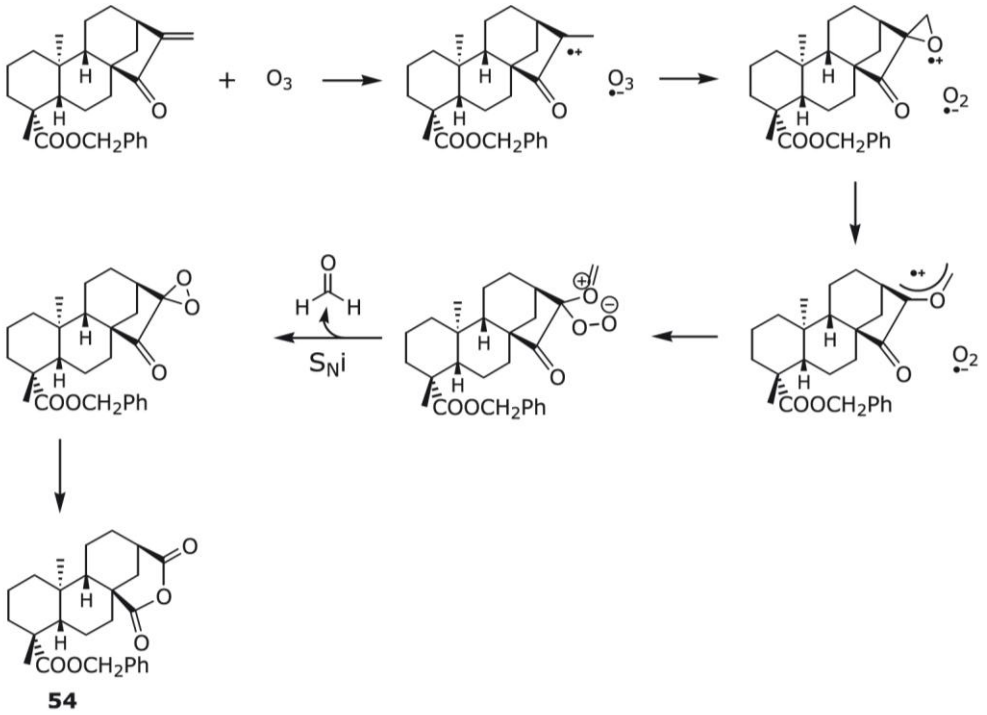

Scheme 4. Plausible formation of compound **54**.

3. Results and discussion

3.1. Lipopolysaccahride (LPS)-induced NO production

To evaluate whether kaurene derivatives (**1**–**63**) regulate inflammatory response, we investigated the anti-inflammatory effects and underlying mechanisms of action of these derivatives using LPS-induced inflammatory responses. In murine RAW 264.7 macrophage cells treatment with LPS induces NOS-2 and NO release. NO production can be detected by measuring the accumulation of nitrite with the Griess method [19]. RAW 264.7 cells were pre-incubated with a range of concentrations (1–25 μM) of compounds (Table 1) or the vehicle solution dimethyl sulfoxide (DMSO) for 15 min before their stimulation with LPS (250 ng/ml). Thirteen of the tested compounds were able to inhibit NO production with an IC_{50} between 2 and 10 μM (Table 1). To discard that the inhibitory effect on NO release was due to cytotoxicity, we analyzed the percentage of cell viability by MTT (3-(4,5-dimethylthiazol-2-yl)-2,5-diphenyltetrazolium bromide) assays. Compounds **11**, **12**, **14** and **23** showed low percentage of cell viability, whereas compounds **9**, **10**, **17**, **28**, **37**, **48**, **55**, **61** and **62** were non-cytotoxic at the concentration up to 25 μM.

From the obtained results some structure–activity relationships can be established. The higher inhibitory activities were exerted by compounds **10**, **12**, **14**, **17**, **28**, **55**, **61** and **62**. We observed two different behaviors depending on the existence or not of the double bond at C-9–C-11. In the series of kaurenoic acid (**1**), without the mentioned double bond, only good activities were achieved with the introduction of different groups at D ring. Thus, the introduction of a hydroxyl or a carbonyl group at C-15 led to an increased activity (compare **2** vs **10** and **12**). Compound (**12**) resulted be cytotoxic but similar NO inhibitory activity was obtained with compound **28** having a carboxylic acid instead of the methyl ester and a 95% of cell viability. The replacement of the exocyclic double bond at C-16–C-17 by epoxy (compounds **4** and **5**), aldehyde (compound **6**), or oxime (compound **7**) function did not produce an improved activity. The esterification of the hydroxyl group at C-15 of compound **10** with different acylation agents yielded inactive compounds (compare **10** vs **30** and **41**).

In the series of grandiflorenic acid (**16**) with a double bond at C-9–C-11, the methyl ester **17** presented an IC_{50} of 5 μM, and the importance of the mentioned double bond for the activity is evident when we compared the activity of **17** vs **2**. The selective hydrogenation of compound **17** afforded the inactive compound **45**, which indicated that the exocyclic double bond plays an important role for the activity. The replacement of the two double bonds by epoxides yielded the inactive compounds **50** and **51**. Respect to the nature of the substituents at C-19 the methyl ester (**17**) resulted to be more active than the carboxylic acid (**16**) and the hydroxyl derivative (**25**). The introduction of different groups at the ring D led to derivatives less active and more cytotoxic (compare **17** vs **19** and **23**). The tricyclic acids **55** and **62** obtained by ozonolisis showed good inhibitory activity with an IC_{50} of 7 μM. With respect to the unexpected lactones **54** and **61** formed also by ozonolisis, only **61** showed inhibitory effect on NO release which indicated the importance of the nature of esters at C-4.

In summary, these results indicate that compounds **10**, **17**, **28**, **55**, **61** and **62** can be pointed as the most active derivatives, exerting their anti-inflammatory activity in a dose dependent manner (Fig. 2).

3.2. Compounds *28*, *55* and *62* inhibit NOS-2 protein and mRNA expression

Although the six compounds exert inhibitory effects on NO release with similar IC_{50} values, we selected compounds **28**, **55** and **62** for further evaluation as they showed a more potent inhibition at higher concentrations (Fig. 2). In order to discard cytotoxicity of these compounds, we measured cell viability with MTT assay. As we can observe in Fig. 3, none of them was toxic. To further analyze the signaling pathways modulated by compounds **28**, **55** and **62**, we studied the activation of the pro-inflammatory gene NOS-2.

Table 1
IC_{50} values (μM) of compounds **1**–**63** on NO inhibition and cell viability.

Compound	NO inhibition	Cell viability (%)
1	>25 ± 1.2	70
2	25 ± 2.3	90
3	>25 ± 1.7	72
4	>25 ± 4.6	90
5	>25 ± 3.1	66
6	>25 ± 1.8	90
7	>25 ± 1.2	25
8	>25 ± 3.5	46
9	10 ± 1.1	80
10	5 ± 0.7	97
11	5 ± 1.1	76
12	4 ± 0.4	32
13	20 ± 1.4	97
14	5 ± 1.2	69
15	>25 ± 2.2	90
16	15 ± 1.9	90
17	5 ± 1.3	100
18	>25 ± 6.2	35
19	>25 ± 4.2	67
20	25 ± 1.7	18
21	>25 ± 1.9	30
22	>25 ± 2.3	50
23	10 ± 1.9	50
24	>25 ± 1.3	23
25	>25 ± 6.9	50
26	>25 ± 1.5	58
27	>25 ± 2.6	100
28	2.5 ± 0.3	95
29	>25 ± 4.6	48
30	>25 ± 3.5	40
31	Not tested	Not tested
32	25 ± 3.7	52
33	>25 ± 5.5	100
34	>25 ± 1.2	82
35	>25 ± 3.7	95
36	12 ± 2.5	99
37	10 ± 2.6	90
38	>25 ± 1.5	99
39	>25 ± 2.8	85
40	>25 ± 1.3	95
41	>25 ± 4.7	95
42	Not tested	Not tested
43	14 ± 3.5	95
44	>25 ± 3.2	99
45	>25 ± 0.5	95
46	17 ± 3.5	95
47	>25 ± 4.1	60
48	10 ± 0.5	99
49	Not tested	Not tested
50	>25 ± 1.3	99
51	Not tested	Not tested
52	>25 ± 1.2	98
53	12 ± 0.7	95
54	>25 ± 1.9	50
55	7 ± 0.6	95
56	>25 ± 2.8	95
57	Not tested	Not tested
58	>25 ± 2.5	95
59	>25 ± 3.8	99
60	Not tested	Not tested
61	5 ± 1.1	95
62	7 ± 0.9	95
63	Not tested	Not tested

IC_{50} values refer to the concentration needed to inhibit 50% of NO release after LPS stimulation in the presence of the compounds.
RAW 264.7 cells were treated with the compounds in a range of concentrations of 1–25 μM in the presence of LPS (250 ng/ml) for 24 h. Supernatants were analyzed for NO release by the Griess reaction and cell viability was determined by MTT assay. IC_{50} values are means ± SD of three independent experiments carried out by triplicate.

Macrophages were pre-incubated with derivatives and stimulated with LPS for 24 h. All compounds potently inhibited the protein expression of NOS-2 (Fig. 4A). Inhibitory effects were exerted at the transcriptional level as revealed analysis of NOS-2 mRNA by quantitative PCR (Fig. 4B).

3.3. Anti-inflammatory effects of derivatives *28*, *55* and *62* are mediated by NF-κB inhibition

An important transcription factor in the regulation of inflammation is NF-κB. The binding of LPS to TLR4 on macrophages activates NF-κB leading to the upregulation of pro-inflammatory enzymes and cytokines such as NOS-2, COX-2, IL-1β, TNF-α, MCP-1 and IL-6. Thus, NF-κB signaling and pathways that regulate its activity have become a focus for intense drug development and application screening [20,21]. To investigate the mechanism of action of kaurene derivatives on macrophage function, we examined the effect of compounds **28**, **55** and **62** on the levels of cytosolic IκBα protein in LPS-activated macrophages. As we can observe in Fig. 5, degradation of IκBα was impaired in activated cells pretreated with compounds **28**, **55** and **62**. These results suggest that inhibition of NF-κB activation might be the mechanism involved in anti-inflammatory effects of these kaurene derivatives.

Inhibition of NF-κB activation can occur by different mechanisms including (a) inhibiting the activation of IKK complex, (b) targeting the proteasomal degradation of IκBs or (c) interfering the translocation of NF-κB to the nucleus, or the binding of NF-κB to DNA. Nevertheless, the most effective and selective approach for the inhibition of NF-κB activation is provided by inhibitors of the IKK activity [20,21]. Since, we have previously described that several kaurane diterpenes such as foliol and linearol specifically targeting IKK kinase activity [22], we cannot rule out this mechanism for the anti-inflammatory effects of compounds **28**, **55** and **62**. Nonetheless, further experiments must be accomplished to determine the degree of specificity on NF-κB inhibition of our compounds.

3.4. Kaurene derivatives inhibit cytokine release

Macrophage activation is also associated with the release of several pro-inflammatory cytokines and chemokines. In order to explore whether other inflammatory mediators such as cytokines were affected by treatment with kaurene derivatives, we analyzed levels of IL-6, IL-1α, TNF-α and IFN-γ. As expected, all cytokines were downregulated in the presence of compound **28**, **55** and **62** after stimulation with LPS (Fig. 6). Interestingly, similar results have been described for several IKK inhibitors that inhibit TNF-α production upon LPS stimulation in murine models [20]. The most potent inhibition was observed on IL-6 production; a pro-inflammatory cytokine which is known to increase dramatically in response to inflammation and brain injury, and it has been described to play a key role in pathologies such as rheumatoid arthritis. There are several binding sites for a number of transcription factors in the 5′ region of the IL-6 gene, including NF-κB, CREB, NF-IL-6, and AP-1 box. Our results have shown that compounds **28**, **55** and **62** antagonized the increase of IL-6 induced by LPS, indicating that NF-κB activation is the only transcription factor involved on IL-6 release. These data are according with recent studies on the IL-6 promoter that demonstrate that IL-6 induction by several transcription factors occurs in a highly stimulus-specific or cell-specific manner. Thus, NF-κB has been shown to regulate the induced transcription of IL-6 in murine macrophages [23].

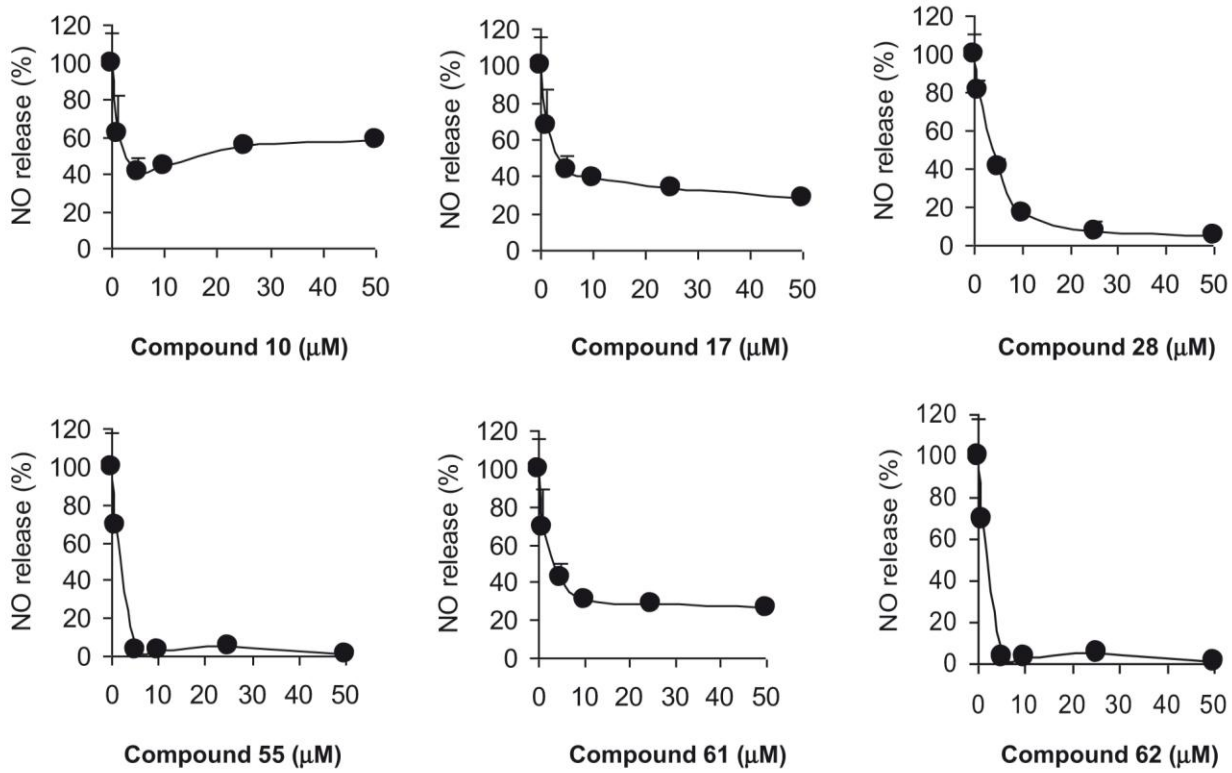

Fig. 2. Dose-dependent effects of compounds **10**, **17**, **28**, **55**, **61** and **62** on NO release. RAW 264.7 cells were pre-treated with diterpenoids (1, 5, 10, 25 and 50 μM) for 15 min and then stimulated with 250 ng/ml LPS for 24 h. The accumulation of nitrite in the culture medium was measured with the Griess reagent. Experiments were carried out in triplicate and the results are the means ± S.D. of three different experiments.

4. Conclusion

In an attempt to discover novel anti-inflammatory agents, a series of kaurene derivatives were synthesized and evaluated for their ability to suppress NO production in LPS-stimulated RAW 264.7 macrophages. Thirteen compounds were especially potent inhibitors of NO release, although the anti-inflammatory effects of compounds **11**, **12**, **14** and **23** were attributable to their cytotoxicity as assessed by MTT assay. Three of these analogs, compounds **28**, **55** and **62** showed the most potent anti-inflammatory effect. The existence of a carboxylic acid seems to play an important role for NO inhibitory activity and cell survival, since it is present in the three mentioned active compounds. The good activity of tricyclic derivatives **55** and **62** obtained by ozonolysis demonstrates that the presence of the ring D can further enhance the activity. In the tetracyclic series the combination of methyl ester at C-19/hydroxyl group at C-15 or carboxylic acid at C-19/carbonyl group at C-15 led to an increase in the anti-inflammatory activity. Compounds **28**, **55** and **62** also demonstrated significant inhibitory effects on IκBα degradation. Therefore, the activity of these compounds may be at least in part due to its NF-κB inhibitory activity. In addition to the inhibitory effects on NO production, compounds **28**, **55** and **62** were able to inhibit several cytokines involved in the inflammatory response after LPS stimulation such as IL-6, IL-1β, TNF-α and IFN-γ.

In summary, we have identified three novel compounds with potential anti-inflammatory properties that might be use for the future development of a new class of anti-inflammatory agents.

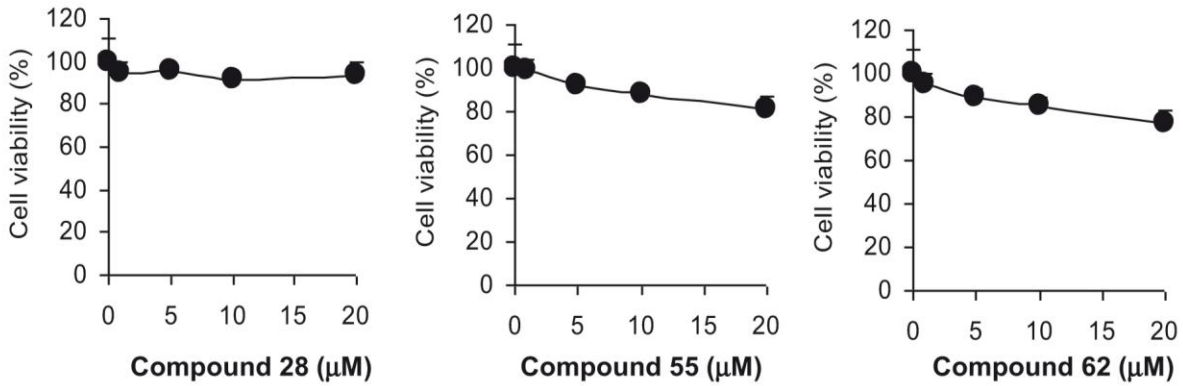

Fig. 3. Cell viability of compounds **28**, **55** and **62**. RAW 264.7 cells were pre-treated with diterpenoids (1, 5, 10, 25 and 50 μM) for 15 min and then stimulated with 250 ng/ml LPS for 24 h. Cell viability was determined by the MTT assay. Experiments were carried out in triplicate and the results are the means ± S.D. of three different experiments.

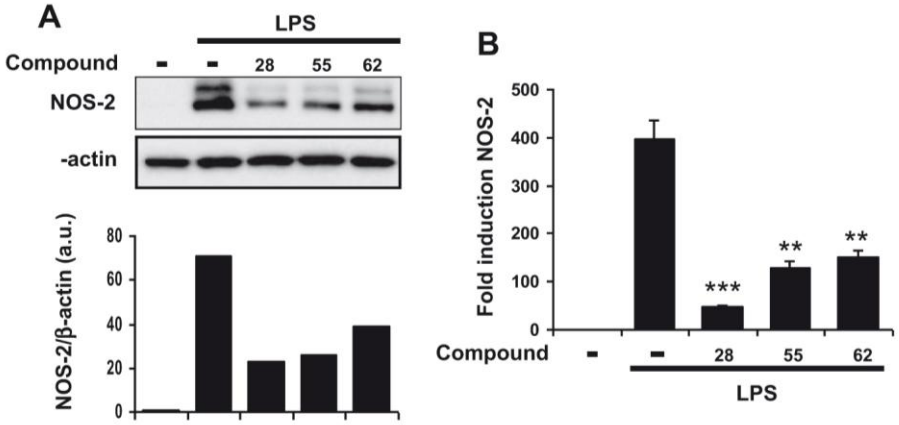

Fig. 4. Compounds **28**, **55** and **62** inhibit NOS-2 expression. A) Macrophages were pre-incubated for 15 min with compounds **28**, **55** and **62** (5 μM) followed by stimulation with 250 ng/ml LPS for 24 h. NOS-2 protein was detected by Western blot. β-Actin content was used as a loading control. Results show a representative experiment of three. B) Macrophages were pre-incubated as in A and stimulated with 250 ng/ml LPS for 4 h. Relative expression of NOS-2 mRNA was determined by real-time quantitative PCR. Results show the means ± S.D. of three independent experiments carried out in triplicate. $^{**}p < 0.01$, $^{***}p < 0.001$ vs LPS.

5. Experimental

5.1. Chemistry

All solvents and reagents were purified by standard techniques reported in Perrin, D.D.; Amarego, W.L.F. Purification of Laboratory Chemicals, 3rd edition, Pergamon Press, Oxford, 1988 or used as supplied from commercial sources as appropriate. Reactions were monitored by TLC (on silica gel POLYGRAM SIL G/UV_{254} foils). Purification by column flash-chromatography used Merk Kiesel 60-H (0.063–0.2 mm) as adsorbent and different mixtures of hexanes–ethylacetate as eluent. Pre-coated TLC plates SIL G-100 UV_{254} (Machery-Nagel) were used for preparative-TLC purification. ^{1}H NMR spectra were recorded in $CDCl_3$ or C_6D_6 at 300 or 400 MHz, using a Bruker AMX300 or Bruker AMX400 instruments. For ^{1}H spectra, chemical shifts are given in parts per million (ppm) and are referenced to the residual solvent peak. The following abbreviations are used: s, singlet; d, doublet; t, triplet; q, quartet; m, multiplet; br, broad. Proton assignments and stereochemistry are supported by ^{1}H–^{1}H COSY and ROESY where necessary. Data are reported in the following manner: chemical shift (multiplicity, coupling constant if appropriate, integration). Coupling constants (J) are given in Hertz (Hz) to the nearest 0.5 Hz. ^{13}C NMR spectra were recorded at 75 and 100 MHz using a Bruker AMX300 or Bruker AMX400 instruments. Carbon spectra assignments are supported by DEPT-135 spectra, ^{13}C–^{1}H (HMQC) and ^{13}C–^{1}H (HMBC) correlations where necessary. Chemical shifts are quoted in ppm and are referenced to the appropriate residual solvent peak. MS and HRMS were recorded on a VG Micromass ZAB-2F. IR spectra were taken on a Bruker IFS28/55 spectrophotometer. Kaurenoic acid (**1**), grandiflorenic acid (**16**), 15α-acetoxy kaurenoic acid (**26**) and 16α-hydroxy kaurenoic acid (**31**) were used as starting material to synthesize the diterpenes. These diterpenes were isolated from *Espeletia chardonii* using the habitual previously described methodology [24–28].

5.1.1. Preparation of compound **35**

To 489.5 mg of compound **1** (1.621 mmol) dissolved in Et_2O was added 1 ml of 2 M solution of Me_2SiCHN_2 in Et_2O. The reaction mixture was stirred at room temperature for 15 h. Then the solvent was removed and the residue was purified by chromatotron using hexanes/toluene (40%) to afford 30.1 mg of compound **2** (26%) as an amorphous white solid and 424.9 mg of compound **35** (68%) as yellow oil. ^{1}H NMR (300 MHz, $CDCl_3$) δ: 4.79 (1H, s, H-17a), 4.74 (1H, s, H-17b), 3.75 (1H, d, $J = 14$ Hz, H-21a), 3.57 (1H, d, $J = 14$ Hz, H-21b), 2.63 (1H, s, H-13), 2.03 (2H, s, H-15), 1.15 (3H, s, H-18), 0.80 (3H, s, H-20), 0.09 (9H, s, Si($\underline{C}H_3$)$_3$), 2.18–0.79 (18H, m). ^{13}C NMR (75 MHz, $CDCl_3$) δ: 178.1 (s, $\underline{C}$-19), 155.4 (s, C-16), 102.8 (t, C-17), 56.8 (d, C-5), 56.6 (t, C-21), 54.8 (d, C-9), 48.7 (t, C-15), 43.9 (s, C-8), 43.7 (s, C-4), 43.5 (d, C-13), 41.1 (t, C-7), 40.5 (t, C-1), 39.3 (t, C-14), 39.2 (s, C-10), 38.0 (t, C-3), 32.8 (t, C-12), 28.7 (q, C-18), 21.8 (t, C-6), 18.9 (t, C-2), 18.1 (t, C-11), 15.2 (q, C-20), −3.13 (q, Si($\underline{C}H_3$)$_3$). EIMS m/z (%): 388 ([M]$^+$, 92); 373 (95); 345 (29); 285 (28); 257 (100); 241 (34); 123 (52); 121 (26); 109 (33); 107 (25); 105 (27); 97 (23); 91 (30); 81 (38); 79 (23); 73 (42); 59 (35); 55 (29). HREIMS: 388.2794 (calcd for $C_{24}H_{40}O_2Si$ [M]$^+$ 388.2798). IR ν_{max}: 2931, 2853, 1722, 1462, 1250, 1227, 1147, 860 cm^{-1}. UV (EtOH) λ_{max} (log ϵ): 202.0 (3.55) nm. $[\alpha]_D^{20}$: −68.42 (c 0.9, $CHCl_3$).

5.1.2. Preparation of compound **36**

8.7 mg (0.030 mmol) of compound **9** dissolved in the minimum amount of pyridine were treated with an excess of Ac_2O (6.1 μl, 3 equiv) in the presence of catalytic amount of DMAP. The reaction mixture was stirred for 24 h, after elimination of solvent, compound **36** (7.1 mg, 100%) was obtained as an amorphous white solid. ^{1}H NMR (300 MHz, $CDCl_3$) δ: 4.79 (1H, s, H-17a), 4.73 (1H, s,

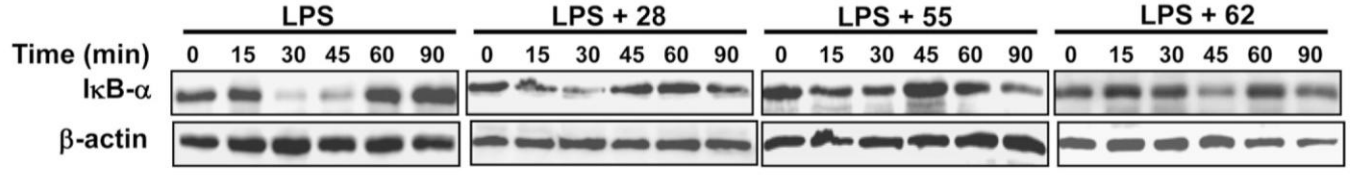

Fig. 5. Kaurene derivatives inhibit NF-κB activity. Macrophages were pre-treated for 15 min with kaurene derivatives (5 μM) and then activated for the indicated times with 250 ng/ml LPS. The levels of IκBα were determined by Western blot. β-Actin was used as a loading control. Results show a representative experiment of three.

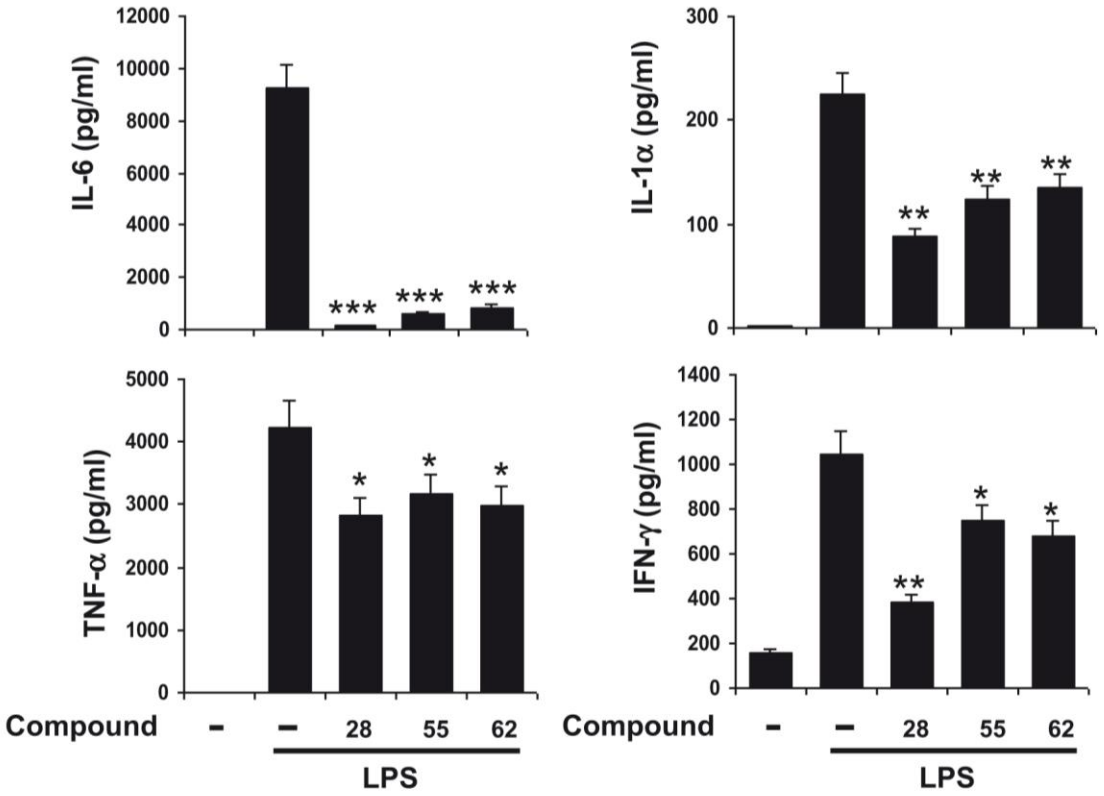

Fig. 6. Cytokine release is inhibited by kaurene derivatives. Macrophages were treated or untreated with compound **28**, **55** and **62** (5 μM) for 15 min followed by stimulation for 24 h with LPS 250 ng/ml. Production of IL-6, IL-1α, TNF-α and IFN-γ was determined in supernatant by ELISA. Results show the means ± S.D. of three independent experiments carried out in triplicate. $^{*}p < 0.05$, $^{**}p < 0.01$, $^{***}p < 0.001$ vs LPS.

H-17b), 4.21 (1H, d, $J = 11$ Hz, H-19a), 3.87 (1H, d, $J = 11$ Hz, H-19b), 2.63 (1H, s, H-13), 2.04 (3H, s, $OCOCH_3$), 1.02 (3H, s, H-18), 0.93 (3H, s, H-20), 1.96–0.73 (20H, m). ^{13}C NMR (75 MHz, $CDCl_3$): 171.2 (s, $OCOCH_3$), 155.6 (s, C-16), 102.7 (t, C-17), 66.9 (t, C-19), 56.5 (d, C-5), 55.9 (d, C-9), 48.8 (t, C-15), 43.9 (s, C-8), 43.7 (d, C-13), 41.3 (t, C-7), 40.1 (t, C-1), 39.4 (t, C-14), 38.9 (s, C-4), 36.8 (s, C-10), 36.1 (t, C-3), 32.9 (t, C-12), 27.3 (q, C-18), 20.8 (q, $OCOCH_3$), 20.2 (t, C-6), 18.0 (t, C-2), 18.0 (t, C-11), 17.8 (q, C-20). EIMS *m/z* (%): 330 ($[M]^+$, 45); 315 (23); 270 (26); 257 (63); 255 (54); 227 (44); 167 (30); 149 (100); 147 (32); 145 (30); 135 (49); 133 (30); 123 (90); 121 (39); 109 (52); 107 (46); 105 (51); 95 (45); 93 (52); 91 (66); 81 (72); 79 (48); 67 (39); 57 (37); 55 (58). HREIMS: 330.2542 (calcd for $C_{22}H_{34}O_2$ $[M]^+$ 330.2559). IR ν_{max}: 2927, 2855, 1740, 1448, 1370, 1239, 1032, 873 cm^{-1}. UV (EtOH) λ_{max} (log ϵ): 202.0 (3.58) nm. $[\alpha]_D^{20}$: −40.13 (c 0.8, $CHCl_3$).

5.1.3. Preparation of compound *37*

Following the same procedure described above, 8.7 mg (0.030 mmol) of compound **25** were treated with 8.63 μl of Ac_2O (3 equiv) to yield quantitatively 10.0 mg of compound **37** as amorphous white solid. ^{1}H NMR (300 MHz, $CDCl_3$): 5.19 (1H, s, H-11), 4.91 (1H, s, H-17a), 4.78 (1H, s, H-17b), 4.30 (1H, d, $J = 10.9$ Hz, H-19a), 4.07 (1H, d, $J = 10.9$ Hz, H-19b), 2.73 (1H, s, H-13), 2.64 (1H, d, $J = 15.6$ Hz, H-15a), 2.17 (1H, d, $J = 15.6$ Hz, H-15b), 2.05 (3H, s, $OCOCH_3$), 1.07 (3H, s, H-18), 0.93 (3H, s, H-20), 2.41–0.90 (15H, m). ^{13}C NMR (75 MHz, $CDCl_3$): 171.2 (s, $OCOCH_3$), 158.4 (s, C-9), 156.8 (s, C-16), 113.6 (d, C-11), 105.0 (t, C-17), 66.1 (t, C-19), 50.3 (t, C-15), 45.2 (d, C-5), 44.5 (t, C-14), 41.9 (s, C-4), 41.0 (d, C-13), 39.8 (t, C-1), 37.8 (s, C-8), 37.5 (t, C-3), 37.1 (s, C-10), 35.9 (t, C-12), 29.1 (t, C-7), 26.2 (q, C-18), 25.2 (q, C-20), 20.8 (q, $OCOCH_3$), 18.5 (t, C-2), 17.6 (t, C-6). EIMS *m/z* (%): 328 ($[M]^+$, 78); 313 (96); 255 (44); 253 (100); 185 (25); 183 (27); 173 (29); 159 (29); 147 (43); 143 (27); 129 (27); 117 (29); 105 (47); 95 (22); 93 (28); 91 (54); 81 (33); 55 (44). HREIMS: 328.2405 (calcd for $C_{22}H_{32}O_2$ $[M]^+$ 328.2402). IR ν_{max}: 2930, 2868, 1738, 1659, 1460, 1373, 1240, 1032, 983 cm^{-1}. UV (EtOH) λ_{max} (log ϵ): 202.0 (3.55) y 243.0 (3.11) nm. $[\alpha]_D^{20}$: +22.59 (c 1.1, $CHCl_3$).

5.1.4. Preparation of compound *38*

To 16.7 mg of compound **9** (0.058 mmol) dissolved in 5 ml of dry CH_2Cl_2 were added 4.69 μl of pyridine (1 equiv) and 4.22 μl of $SOCl_2$ (1 equiv) under N_2 atmosphere. The reaction mixture was stirred at room temperature for 4 h, until disappearance of the starting material (4 h). Then H_2O was poured and the mixture was extracted several times with CH_2Cl_2. The organic phases were collected and dried over anhydrous $MgSO_4$, then were filtered, concentrated and purified by preparative-TLC using hexanes/AcOEt (9.5:0.5). 9.1 mg of compound **38** (50%) were obtained. ^{1}H NMR (300 MHz, $CDCl_3$) δ: 4.80 (2H, s, H-17a, H-17′a), 4.74 (2H, s, H-17b, H-17′b), 4.15 (1H, d, $J = 9.9$ Hz, H-19a ó H-19′a), 4.01 (1H, d, $J = 9.9$ Hz, H-19a ó H-19′a), 3.77 (1H, d, $J = 9.9$ Hz, H-19b ó H-19′b), 3.63 (1H, d, $J = 9.9$ Hz, H-19b ó H-19′b), 2.64 (2H, s, H-13, H-13′), 1.03 (3H, s, H-18, H-18′), 0.98 (6H, s, H-20, H-20′), 2.31–0.73 (41H, m). ^{13}C NMR (75 MHz, $CDCl_3$) δ: 158.2 (s, C-9, C-9′), 156.6 (s, C-16, C-16′), 113.7 (d, C-11, C-11′), 105.1 (t, C-17, C-17′), 64.0 (t, C-19 ó C-19′), 63.6 (t, C-19 ó C-19′), 50.3 (t, C-15, C-15′), 45.3 (d, C-5 ó C-5′), 45.2 (d, C-5 ó C-5′), 44.5 (t, C-14, C-14′), 41.9 (s, C-8, C-8′), 41.0 (d, C-13, C-13′), 39.7 (t, C-1, C-1′), 37.8 (s, C-10, C-10′), 37.5 (t, C-12, C-12′), 37.4 (s, C-4 ó C-4′), 37.4 (s, C-4 ó C-4′), 35.5 (t, C-3 ó C-3′), 35.4 (t, C-3 ó C-3′), 29.1 (t, C-7, C-7′), 26.3 (q, C-18 ó C-18′), 26.2 (q, C-18 ó C-18′), 25.2 (q, C-20, C-20′), 18.4 (t, C-2 ó C-2′), 18.3 (t, C-2 ó C-2′), 17.6 (t, C-6, C-6′). EIMS *m/z* (%): 622 ($[M]^+$, 5); 287 (79); 271 (54); 270 (50); 257 (79); 175 (23); 161 (63); 147 (47); 123 (47); 111 (100); 106 (37); 105 (64); 95 (49); 94 (59); 93 (43); 91 (38); 81 (61); 55 (35). HREIMS: 622.4421 (calcd

for $C_{40}H_{62}O_3S$ $[M]^+$ 622.4420). IR ν_{max}: 2932, 2868, 1461, 1189, 972, 925, 874, 756 cm^{-1}. UV (EtOH) λ_{max} (log ϵ): 201.6 (3.29) nm. $[\alpha]_D^{20}$: +46.75 (c 0.8, $CHCl_3$).

*5.1.5. Preparation of compound **39***

To a solution of 33.5 mg of **26** (0.093 mmol) in dry DCM (5 ml) at 0 °C were added 21.2 μl of oxalyl chloride (2 equiv) and one drop of DMF. The reaction mixture was stirred for 26 h, then 4.5 equiv of aniline were added and the reaction was left for 75 h at room temperature. The solvent was removed and the residue was purified by TC-preparative using hexanes/AcOEt (30%) to yield 18.8 mg of compound **39** (46%) as a yellow oil. ^1H NMR (300 MHz, $CDCl_3$) δ: 7.47 (2H, d, J = 7.5 Hz, H-2′, H-6′), 7.32 (2H, t, J = 7.5 Hz, H-3′, H-5′), 7.10 (1H, t, J = 7.5 Hz, H-4′), 5.26 (1H, s, H-15), 5.09 (2H, s, H-17), 2.77 (1H, s, H-13), 2.08 (3H, s, $OCOCH_3$), 1.27 (3H, s, H-18), 0.90 (3H, s, H-20), 2.19–0.85 (19H, m). ^{13}C NMR (75 MHz, $CDCl_3$) δ: 174.8 (s, C-19), 170.9 (s, $OCOCH_3$), 155.0 (s, C-16), 137.7 (s, C-1′), 128.8 (d, C-3′, C-5′), 124.0 (d, C-4′), 120.0 (d, C-2′, C-6′), 109.8 (t, C-17), 82.7 (d, C-15), 56.9 (d, C-5), 52.6 (d, C-9), 47.2 (s, C-8), 44.3 (s, C-4), 42.2 (d, C-13), 40.6 (t, C-1), 39.6 (s, C-10), 38.0 (t, C-3), 36.8 (t, C-7), 34.7 (t, C-14), 32.3 (t, C-12), 29.5 (q, C-18), 21.2 (t, C-6), 21.1 (q, $OCOCH_3$), 19.0 (t, C-2), 18.2 (t, C-11), 15.8 (q, C-20). EIMS m/z (%): 435 ($[M]^+$, 25); 375 (12); 256 (21); 255 (100); 185 (11); 173 (28); 162 (17); 159 (15); 123 (15); 109 (12); 105 (11); 95 (11); 93 (87); 91 (12); 81 (17); 55 (12). HREIMS: 435.2754 (calcd for $C_{28}H_{37}NO_3$ $[M]^+$ 435.2773). IR ν_{max}: 3398, 2932, 2866, 1729, 1667, 1597, 1521, 1435, 1370, 1307, 1243, 1022, 752, 693 cm^{-1}. UV (EtOH) λ_{max} (log ϵ): 202.4 (4.03) y 241.6 (3.68) nm. $[\alpha]_D^{20}$: −96.80 (c 1.0, $CHCl_3$).

*5.1.6. Preparation of compound **40***

To 13.3 mg of compound **31** dissolved in dry THF were added 6.3 mg of $LiAlH_4$ (4 equiv) under N_2 atmosphere. The reaction mixture was stirred for six days. Then it was treated with a saturated solution of dipotassium salt of L(+)-tartaric acid and extracted several times with AcOEt. The organic layers were separated, dried over anhydrous $MgSO_4$ and concentrated. The residue was purified by preparative-TLC using hexanes/AcOEt 40% to yield 6.9 mg of compound **40** (54%) as an amorphous white solid. ^1H NMR (300 MHz, $CDCl_3$) δ: 3.73 (1H, d, J = 10.9 Hz, H-19a), 3.44 (1H, d, J = 10.9 Hz, H-19b), 1.35 (3H, s, H-17), 1.01 (3H, s, H-18), 0.95 (3H, s, H-20), 1.90–0.73 (23H, m). ^{13}C NMR (75 MHz, $CDCl_3$) δ: 79.1 (s, C-16), 65.3 (t, C-19), 57.6 (t, C-15), 56.7 (d, C-5), 56.5 (d, C-9), 48.7 (d, C-13), 45.0 (s, C-8), 42.2 (t, C-7), 40.2 (t, C-1), 39.0 (s, C-4), 38.4 (s, C-10), 37.3 (t, C-3), 35.4 (t, C-14), 26.8 (q, C-17), 26.5 (t, C-12), 24.2 (q, C-18), 20.4 (t, C-6), 18.0 (q, C-20), 18.0 (t, C-2), 17.8 (t, C-11). EIMS m/z (%): 306 ($[M]^+$, 1); 302 (15); 288 (17); 275 (25); 258 (30); 257 (100); 161 (19); 147 (21); 135 (26); 123 (52); 121 (28); 109 (36); 107 (28); 105 (38); 95 (32); 94 (41); 91 (30); 81 (34); 79 (26); 55 (23). HREIMS: 306.2563 (calcd for $C_{20}H_{34}O_2$ $[M]^+$ 306.2559). IR ν_{max}: 3365, 2926, 2864, 2850, 1697, 1447, 1122, 1030, 1010, 756, 462 cm^{-1}. $[\alpha]_D^{20}$: −25.94 (c 0.7, $CHCl_3$).

*5.1.7. Preparation of compound **41***

To a solution of 10.7 mg of compound **10** (0.032 mmol) in dry DCM were added 11.2 μl of lauroyl chloride (1.5 equiv), 13.5 μl of Et_3N (3 equiv) and catalytic amount of DMAP. The reaction mixture was stirred for 48 h under N_2 atmosphere. Then the solvent was removed and the crude was purified by preparative-TLC using hexanes/AcOEt 10% to yield 9.0 mg of compound **41** (54%) as a yellow oil. ^1H NMR (300 MHz, $CDCl_3$) δ: 5.25 (1H, s, H-17a), 5.07 (1H, s, H-17b), 5.07 (1H, s, H-15), 3.63 (3H, s, H-21), 2.77 (1H, s, H-13), 1.25 (20H, sa, H-2′-11′), 1.16 (3H, s, H-18), 0.89 (3H, m, H-12′), 0.82 (3H, s, H-20), 2.33–0.85 (18H, m). ^{13}C NMR (75 MHz, $CDCl_3$) δ: 177.9 (s, C-19), 173.9 (s, C-1′), 155.3 (s, C-16), 109.6 (t, C-17), 82.4 (d, C-15), 56.3 (d, C-5), 52.6 (d, C-9), 50.9 (q, C-21), 47.2 (s, C-8), 43.5 (s, C-4), 42.2 (d, C-13), 40.3 (t, C-1), 39.4 (s, C-10), 37.7 (t, C-3), 37.0 (t, C-7), 34.5 (t, C-14), 32.4 (t, C-12), 31.7 (t, C-2′), 29.4 (t, C-3′), 29.3 (t, C-4′, C-5′), 29.1 (t, C-6′), 29.0 (t, C-7′, C-8′), 28.9 (t, C-9′), 28.4 (t, C-10′), 24.9 (q, C-18), 22.4 (t, C-11′), 20.6 (t, C-6), 18.8 (t, C-2), 18.1 (t, C-11), 15.4 (q, C-20), 13.9 (q, C-12′). EIMS m/z (%): 514 ($[M]^+$, 9); 332 (42); 315 (30); 314 (100); 299 (66); 273 (14); 255 (74); 254 (37); 239 (35); 183 (29); 147 (22); 121 (28); 107 (24); 71 (22); 57 (45); 55 (32). HREIMS: 514.4027 (calcd for $C_{33}H_{54}O_4$ $[M]^+$ 514.4022). IR ν_{max}: 2927, 2855, 1729, 1463, 1233, 1189, 1154 cm^{-1}. UV (EtOH) λ_{max} (log ϵ): 202.0 (3.41) nm. $[\alpha]_D^{20}$: −39.67 (c 0.9, $CHCl_3$).

*5.1.8. Preparation of compound **42***

To a solution of 9.4 mg (0.028 mmol) of compound **10** in 4 ml of dry DCM were added 10 μl of Et_3N (2.5 equiv), 10 μl of 4-pentenoyl chloride (3.2 equiv) and catalytic amount of DMAP. The reaction mixture was stirred for 42 h under N_2 atmosphere. Then the solvent was eliminated and the crude was purified by TLC using hexanes/AcOEt 10% to yield 4.5 mg of compound **42** (38%) as an amorphous white solid. ^1H NMR (300 MHz, $CDCl_3$) δ: 5.84 (1H, m, H-4′), 5.27 (1H, s, H-17a), 5.08 (3H, sa, H-17b, H-15, H-5′a), 5.01 (1H, dd, J = 1.6 y 11.8 Hz, H-5′b), 3.64 (3H, s, H-21), 2.78 (1H, s, H-13), 2.41 (4H, m, H-2′, H-3′), 1.16 (3H, s, H-18), 0.83 (3H, s, H-20), 2.19–0.78 (18H, m). ^{13}C NMR (75 MHz, $CDCl_3$) δ: 178.2 (s, C-19), 172.9 (s, C-1′), 155.3 (s, C-16), 136.5 (d, C-4′), 115.2 (t, C-5′), 109.7 (t, C-17), 82.7 (d, C-15), 56.4 (d, C-5), 52.6 (d, C-9), 51.0 (q, C-21), 47.2 (s, C-8), 43.8 (s, C-4), 42.2 (d, C-13), 40.6 (t, C-1), 39.4 (s, C-10), 38.0 (t, C-3), 37.0 (t, C-2′), 34.9 (t, C-3′), 33.6 (t, C-7), 32.4 (t, C-14), 28.8 (t, C-12), 28.4 (q, C-18), 20.7 (t, C-6), 19.1 (t, C-2), 18.1 (t, C-11), 15.2 (q, C-20). EIMS m/z (%): 414 ($[M]^+$, 14); 332 (34); 315 (28); 314 (94); 299 (68); 255 (91); 254 (41); 239 (58); 211 (20); 147 (24); 121 (39); 109 (23); 107 (33); 105 (30); 93 (24); 91 (37); 83 (49); 81 (25); 79 (23); 55 (100). HREIMS: 414.2773 (calcd for $C_{26}H_{38}O_4$ $[M]^+$ 414.2770). IR ν_{max}: 2929, 2855, 1727, 1458, 1232, 1155, 992, 908, 773 cm^{-1}. UV (EtOH) λ_{max} (log ϵ): 201.6 (3.51) nm. $[\alpha]_D^{20}$: −41.11 (c 0.4, $CHCl_3$).

*5.1.9. Preparation of compound **43***

To 26.7 mg of compound **33** (0.225 mmol) dissolved in dry DCM were added 42.3 mg (2 equiv) of MCPBA and 31.8 mg of $NaHCO_3$ (4.5 equiv). The reaction mixture was left to room temperature for 4 h, then the organic phase was separated and treated with a saturated solution of sodium thiosulfate. The organic phase was separated again and dried over anhydrous magnesium sulfate, the mixture was filtered, the solvent was removed under reduced pressure and the crude was purified by preparative-TLC using hexanes/AcOEt 20% to yield 25.1 mg of compound **43** (89%) as an amorphous white solid.

^1H NMR (300 MHz, $CDCl_3$) δ: 3.62 (3H, s, H-21), 2.64 (1H, s, H-15), 1.41 (3H, s, H-17), 1.16 (3H, s, H-18), 0.80 (3H, s, H-20), 2.18–0.83 (19H, m). ^{13}C NMR (75 MHz, $CDCl_3$): 177.7 (s, C-19), 67.8 (d, C-15), 61.1 (s, C-16), 56.5 (d, C-5), 50.9 (q, C-21), 49.3 (d, C-9), 43.6 (s, C-8), 43.5 (s, C-4), 40.6 (t, C-1), 39.0 (s, C-10), 38.8 (d, C-13), 37.8 (t, C-3), 35.5 (t, C-7), 31.9 (t, C-14), 28.5 (q, C-18), 26.7 (t, C-12), 20.4 (t, C-6), 18.8 (t, C-2), 18.0 (t, C-11), 14.9 (q, C-20), 14.4 (q, C-17). EIMS m/z (%): 332 ($[M]^+$, 63); 317 (25); 314 (11); 289 (28); 273 (76); 257 (45); 255 (23); 173 (18); 159 (23); 149 (23); 147 (26); 135 (64); 133 (33); 123 (53); 121 (100); 109 (49); 107 (76); 105 (39); 95 (43); 93 (45); 91 (48); 81 (50); 79 (45); 67 (33); 55 (47). HREIMS: 332.2343 (calcd for $C_{21}H_{32}O_3$ $[M]^+$ 332.2351). IR ν_{max}: 2947, 2848, 1724, 1446, 1232, 1194, 1153, 986, 845, 771 cm^{-1}. UV (EtOH) λ_{max} (log ϵ): 201.8 (2.91) nm. $[\alpha]_D^{20}$: −45.88 (c 1.0, $CHCl_3$).

*5.1.10. Preparation of compound **44***

To a solution of 19.8 mg of hydroxylamine hydrochloride (7.2 mg, 3 equiv) and 19.8 mg sodium acetate (3.2 equiv) in 0.4 ml of H_2O, 29.8 mg of aldehyde **11** in 3 ml of EtOH was added. The

reaction mixture was stirred under reflux for 23 h. Then the EtOH was removed, and the residue was extracted with DCM (3 × 10 ml). The organic phases were collected and dried over anhydrous $MgSO_4$, filtered and concentrated. The residue was purified by preparative-TLC using hexanes/AcOEt (4:1) and 23.5 mg of compound **44** (91%) were obtained as an amorphous yellow solid. ^{1}H NMR (300 MHz, $CDCl_3$) δ: 7.85 (1H, s, H-17), 5.82 (1H, s, H-15), 3.64 (3H, s, H-21), 2.94 (1H, d, J = 3 Hz, H-13), 1.17 (3H, s, H-18), 0.86 (3H, s, H-20), 2.18–0.76 (19H, m). ^{13}C NMR (75 MHz, $CDCl_3$) δ: 177.8 (s, C-19), 147.3 (d, C-17), 147.0 (d, C-15), 139.4 (s, C-16), 56.4 (d, C-5), 51.0 (q, C-21), 49.7 (s, C-8), 46.4 (d, C-9), 43.6 (s, C-4), 43.0 (t, C-7), 40.5 (t, C-1), 39.6 (d, C-13), 39.5 (s, C-10), 38.5 (t, C-14), 37.8 (t, C-3), 28.5 (q, C-18), 24.8 (t, C-12), 20.4 (t, C-6), 18.8 (t, C-2), 18.6 (t, C-11), 15.0 (q, C-20). EIMS m/z (%): 345 ([M]$^+$, 18); 330 (11); 329 (51); 328 (100); 312 (32); 268 (79); 267 (54); 252 (35); 162 (21); 123 (66); 121 (29); 117 (24); 109 (47); 108 (24); 107 (36); 91 (35); 81 (38); 79 (29); 67 (32); 55 (40). HREIMS: 345.2301 (calcd for $C_{21}H_{31}NO_3$ [M]$^+$ 345.2304). IR ν_{max}: 3421, 3286, 2939, 2851, 1723, 1464, 1446, 1233, 1191, 1159, 970, 950, 738 cm^{-1}. UV (EtOH) λ_{max} (log ϵ): 248.4 (3.83) nm. $[\alpha]_D^{20}$: −107.94 (c 1.0, $CHCl_3$).

5.1.11. Preparation of compound **45**

72.6 mg (0.231 mmol) of compound **17** dissolved in 4 ml of dry THF were hydrogenated in the presence of catalytic amount of Pd/C 10%. The reaction mixture was stirred for 1 h until disappearance of the starting material. After elimination of solvent the resulting residue was purified by preparative-TLC using hexanes/AcOEt (20%) to yield 27.1 mg of compound **45** (37%) as a white amorphous solid. ^{1}H NMR (300 MHz, $CDCl_3$) δ: 5.18 (1H, t, J = 3 Hz, H-11), 3.64 (3H, s, H-21), 1.16 (3H, s, H-18), 1.00 (3H, d, J = 8 Hz, H-17), 0.89 (3H, s, H-20), 2.41–1.04 (19H, m). ^{13}C NMR (75 MHz, $CDCl_3$) δ: 177.9 (s, C-19), 158.1 (s, C-9), 114.8 (d, C-11), 51.0 (q, C-21), 49.7 (t, C-15), 46.5 (d, C-5), 45.8 (t, C-14), 44.6 (s, C-4), 42.2 (s, C-8), 41.0 (t, C-1), 38.3 (s, C-10), 38.2 (t, C-3), 37.5 (d, C-13), 36.8 (d, C-16), 30.1 (t, C-12), 29.6 (t, C-7), 27.9 (q, C-18), 23.1 (q, C-20), 20.1 (t, C-2), 18.6 (q, C-17), 18.4 (t, C-6). EIMS m/z (%): 316 ([M]$^+$, 38); 301 (77); 271 (41); 257 (49); 241 (100); 197 (63); 159 (36); 134 (40); 121 (53); 109 (94); 107 (62); 95 (53); 93 (46); 91 (98); 81 (54); 79 (37); 57 (47); 55 (55). HREIMS: 316.2390 (calcd for $C_{21}H_{32}O_2$ [M]$^+$ 316.2402). IR ν_{max}: 2933, 2867, 1723, 1460, 1376, 1220, 1149, 978, 757 cm^{-1}. $[\alpha]_D^{20}$: +37.33 (c 0.9, $CHCl_3$).

5.1.12. Preparation of compounds **46** and **47**

To 33.8 mg of compound **14** (0.097 mmol) dissolved in 5 ml of dry CH_2Cl_2 were added 23.5 μl of pyridine (3 equiv) and 21.1 μl of $SOCl_2$ (3 equiv) under N_2 atmosphere. The reaction mixture was stirred at room temperature for 1 h, until disappearance of the starting material (4 h). Then H_2O was poured and the mixture was extracted several times with CH_2Cl_2. The separated organic phases were dried over anhydrous $MgSO_4$, filtered and concentrated. The residue was purified by preparative-TLC using toluene to yield 11.8 mg of compound **46** (31%) and 12.2 mg of compound **47** (32%) as amorphous white solids. Compound **46**: ^{1}H NMR (300 MHz, $CDCl_3$) δ: 4.58 (1H, d, J = 8.7 Hz, H-17a), 4.42 (1H, d, J = 8.7 Hz, H-17b), 3.63 (3H, s, H-21), 2.28 (1H, d, J = 15.2 Hz, H-15a), 2.16 (1H, d, J = 15 Hz, H-14a), 2.14 (1H, s, H-13), 1.16 (3H, s, H-18), 0.81 (3H, s, H-20), 2.05–0.74 (18H, m). ^{13}C NMR (75 MHz, $CDCl_3$) δ: 177.7 (s, C-19), 98.9 (s, C-16), 69.7 (t, C-17), 56.5 (d, C-5), 54.7 (d, C-9), 53.1 (t, C-15), 51.0 (q, C-21), 44.9 (d, C-13), 44.6 (s, C-8), 43.5 (s, C-4), 40.7 (t, C-7), 40.3 (t, C-1), 39.1 (s, C-10), 37.8 (t, C-3), 37.7 (t, C-14), 28.4 (q, C-18), 26.8 (t, C-12), 21.7 (t, C-6), 18.8 (t, C-2), 18.1 (t, C-11), 15.2 (q, C-20). EIMS m/z (%): 396 ([M]$^+$, 9); 364 (14); 337 (100); 336 (35); 315 (67); 314 (37); 273 (60); 255 (59); 147 (34); 135 (23); 123 (67); 121 (90); 109 (59); 107 (50); 105 (30); 95 (35); 93 (37); 91 (42); 81 (41); 79 (39); 67 (33); 55 (39). HREIMS: 396.1966 (calcd for $C_{21}H_{32}O_5S$ [M]$^+$ 396.1970). IR ν_{max}: 2946, 2875, 1727, 1467, 1212, 1161, 962, 819, 762, 681 cm^{-1}. $[\alpha]_D^{20}$: −64.49 (c 1.2, $CHCl_3$). Compound **47**: ^{1}H RMN (300 MHz, $CDCl_3$) δ: 4.71 (1H, d, J = 8.6 Hz, H-17a), 4.33 (1H, d, J = 8.6 Hz, H-17b), 3.64 (3H, s, H-21), 2.60 (1H, s, H-13), 1.16 (3H, s, H-18), 0.81 (3H, s, H-20), 2.29–0.72 (20H, m). ^{13}C NMR (75 MHz, $CDCl_3$) δ: 177.7 (s, C-19), 98.6 (s, C-16), 71.1 (t, C-17), 56.5 (d, C-5), 55.3 (t, C-15), 54.8 (d, C-9), 51.0 (q, C-21), 46.1 (d, C-13), 44.5 (s, C-8), 43.5 (s, C-4), 40.9 (t, C-7), 40.4 (t, C-1), 39.1 (s, C-10), 38.0 (t, C-3), 37.7 (t, C-14), 28.4 (q, C-18), 26.6 (t, C-12), 21.7 (t, C-6), 18.8 (t, C-2), 18.8 (t, C-11), 15.3 (q, C-20). EIMS m/z (%): 396 ([M]$^+$, 4); 337 (100); 315 (37); 273 (49); 255 (20); 123 (43); 121 (45); 109 (37); 107 (29); 95 (23); 91 (24); 81 (27); 79 (23); 55 (24). HREIMS: 396.1988 (calcd for $C_{21}H_{32}O_5S$ [M]$^+$ 396.1970). IR ν_{max}: 2948, 2875, 1726, 1467, 1209, 1161, 963, 822, 685 cm^{-1}. $[\alpha]_D^{20}$: −44.84 (c 1.2, $CHCl_3$).

5.1.13. Preparation of compounds **48** and **49**

To 9.3 mg of compound **18** (0.027 mmol) dissolved in 3 ml of toluene were added 8.5 μl of 2-furoyl (3 equiv), Et_3N (15 μl, 4 equiv) and catalytic amount of DMAP. The reaction mixture was stirred under reflux for 18 h. The solvent was removed and the residue was purified by preparative-TLC using hexanes/AcOEt 40%, to yield 10.0 mg of compound **48** (30%) and 3.6 mg of compound **49** (25%) as amorphous white solids. **49** resulted be unstable and decomposes with the time. Compound **48**: ^{1}H NMR (300 MHz, $CDCl_3$) δ: 7.59 (1H, d, J = 1.0 Hz, H-5′), 7.21 (1H, d, J = 3.5 Hz, H-3′), 6.53 (1H, dd, J = 1.0, 3.5 Hz, H-4′), 5.16 (1H, s, H-11), 4.33 (1H, d, J = 11.3 Hz, H-17a), 4.27 (1H, d, J = 11.3 Hz, H-17b), 3.65 (3H, s, H-21), 1.17 (3H, s, H-18), 0.90 (3H, s, H-20), 2.48–0.83 (16H, m). ^{13}C NMR (75 MHz, $CDCl_3$) δ: 177.7 (s, C-19), 158.5 (s, C-9), 157.4 (s, C-1′), 146.3 (d, C-5′), 144.1 (s, C-2′), 118.1 (d, C-11), 113.3 (d, C-3′), 111.7 (d, C-4′), 82.6 (s, C-16), 70.3 (t, C-17), 54.7 (t, C-15), 51.1 (q, C-21), 46.4 (d, C-5), 44.6 (d, C-13), 44.6 (s, C-4), 42.7 (s, C-8), 42.6 (t, C-14), 40.7 (t, C-1), 38.4 (s, C-10), 38.1 (t, C-3), 30.2 (t, C-12), 29.6 (t, C-7), 27.9 (q, C-18), 23.1 (q, C-20), 19.9 (t, C-2), 18.2 (t, C-6). EIMS m/z (%): 424 ([M$^+$ − 18] 12); 312 (67); 297 (36); 273 (25); 271 (17); 255 (23); 253 (37); 237 (43); 213 (26); 197 (34); 173 (20); 172 (25); 157 (23); 145 (27); 144 (26); 143 (27); 131 (40); 129 (25); 117 (26); 112 (33); 109 (26); 107 (19); 105 (39); 95 (100); 91 (50); 81 (18); 79 (19); 55 (29). HREIMS: 424.2264 (calcd for $C_{26}H_{32}O_5$ ([M]$^+$ − 18) 424.2250). IR ν_{max}: 3501, 2931, 2858, 1720, 1469, 1397, 1297, 1226, 1179, 1151, 1122, 971, 762 cm^{-1}. UV (EtOH) λ_{max} (log ϵ): 202.0 (3.51) y 251.0 (3.60) nm. $[\alpha]_D^{20}$: +7.60 (c 0.5, $CHCl_3$). Compound **49**: ^{1}H NMR (300 MHz, $CDCl_3$) δ: 7.55 (2H, s, H-5′, H-5″), 7.12 (1H, d, J = 3.4 Hz, H-3′ ó H-3″), 7.08 (1H, d, J = 3.4 Hz, H-3′ ó H-3″), 6.47 (2H, m, H-4′, H-4″), 5.28 (1H, J = 12.3 Hz, H-17a), 5.23 (1H, s, H-11), 4.37 (1H, d, J = 12.3 Hz, H-17b), 3.64 (3H, s, H-21), 2.77 (1H, s, H-13), 1.17 (3H, s, H-18), 0.91 (3H, s, H-20), 2.48–0.83 (17H, m). ^{13}C NMR (75 MHz, $CDCl_3$): 177.7 (s, C-19), 158.0 (s, C-9), 157.0 (s, C-1′, C-1″), 146.2 (d, C-5′ ó C-5″), 145.9 (d, C-5′ ó C-5″), 145.1 (s, C-2′ ó C-2″), 144.1 (s, C-2′ ó C-2″), 117.8 (d, C-11), 117.8, 117.4 y 113.8 (4C, d, C-3′, C-3″, C-4′, C-4″), 93.2 (s, C-16), 65.6 (t, C-17), 53.6 (t, C-15), 51.1 (q, C-21), 46.2 (d, C-5), 44.6 (s, C-4), 42.7 (t, C-14), 42.4 (d, C-13), 42.3 (s, C-8), 40.7 (t, C-1), 38.4 (s, C-10), 38.0 (t, C-3), 29.9 (t, C-12), 29.5 (t, C-7), 27.8 (q, C-18), 23.2 (q, C-20), 19.9 (t, C-2), 18.1 (t, C-6). EIMS m/z (%): 424 ([M]$^+$ − 112($C_5H_4O_3$), 7); 312 (44); 297 (30); 253 (16); 237 (24); 197 (16); 145 (15); 111 (23); 105 (18); 97 (11); 95 (100); 91 (21); 57 (21); 55 (24). HREIMS: 424.2262 (calcd for $C_{26}H_{32}O_5$ ([M]$^+$ − 112 ($C_5H_4O_3$)) 424.2250).

5.1.14. Epoxidation of compound **17** to obtain compounds **50** and **51**

To 70.7 mg of compound **17** (0.225 mmol) dissolved in 15 ml of dry DCM were added 222.6 mg (4 equiv) of MCPBA and 153.3 mg of $NaHCO_3$ (8.1 equiv). The reaction mixture was left to room temperature for 4 h, then the organic phase was separated and treated with a saturated solution of sodium thiosulfate. The organic

phase was separated again and dried over anhydrous magnesium sulfate, the mixture was filtered, the solvent was removed under reduced pressure and the crude was purified by preparative-TLC using hexanes/AcOEt 20% to yield 9.4 mg of compound **50** (12%) and 11.6 mg of compound **51** (15%) as amorphous white solids. Compound **50**: ^{1}H NMR (300 MHz, $CDCl_3$) δ: 3.63 (3H, s, H-21), 3.08 (1H, dd, J = 3.7, 9.8 Hz, H-11), 2.83 (1H, d, J = 5.4 Hz, H-17a), 2.79 (1H, d, J = 5.2 Hz, H-17b), 1.19 (3H, s, H-18), 0.65 (3H, s, H-20), 2.27–0.85 (18H, m). ^{13}C NMR (100 MHz, $CDCl_3$) δ: 177.7 (s, C-19), 69.1 (s, C-9), 66.0 (s, C-16), 54.7 (t, C-17), 53.9 (d, C-11), 51.1 (q, C-21), 48.5 (d, C-5), 46.0 (t, C-15), 44.0 (s, C-4), 42.1 (s, C-8), 39.3 (t, C-1), 39.0 (t, C-3), 37.9 (s, C-10), 37.6 (t, C-14), 36.0 (d, C-13), 31.9 (t, C-12), 28.4 (q, C-18), 26.6 (t, C-7), 19.6 (t, C-2), 18.9 (t, C-6), 14.6 (q, C-20). EIMS m/z (%): 346 ([M]$^+$, 10); 330 (8); 287 (19); 286 (13); 258 (19); 257 (12); 173 (23); 150 (26); 149 (100); 147 (27); 136 (70); 135 (57); 133 (27); 123 (71); 122 (74); 121 (60); 109 (49); 107 (65); 105 (53); 95 (39); 93 (46); 91 (55); 81 (41); 79 (42); 67 (32); 55 (56). HREIMS: 346.2137 (calcd for $C_{21}H_{30}O_4$ [M]$^+$ 346.2144). IR ν_{max}: 2929, 2855, 1722, 1458, 1226, 1148, 1036, 983, 893, 757 cm^{-1}. UV (EtOH) λ_{max} (log ϵ): 201.2 (3.10) nm. $[\alpha]_D^{20}$: −0.64 (c 0.47, $CHCl_3$). Compound **51**: ^{1}H NMR (300 MHz, $CDCl_3$) δ: 3.64 (3H, s, H-21), 3.07 (1H, d, J = 3.4 Hz, H-11), 2.85 (1H, d, J = 4.5 Hz, H-17a), 2.80 (1H, d, J = 4.5 Hz, H-17b), 2.23 (1H, d, J = 13.5 Hz, H-15a), 1.21 (3H, s, H-18), 0.67 (3H, s, H-20), 2.10–0.98 (17H, m). ^{13}C NMR (75 MHz, $CDCl_3$) δ: 177.7 (s, C-19), 69.6 (s, C-9), 68.8 (s, C-16), 53.5 (d, C-11), 51.1 (q, C-21), 50.5 (t, C-17), 48.5 (d, C-5), 45.4 (t, C-14), 44.1 (s, C-4), 43.2 (s, C-8), 39.3 (t, C-1), 38.7 (t, C-3), 38.7 (d, C-13), 37.9 (s, C-10), 37.7 (t, C-12), 29.5 (t, C-7), 28.9 (t, C-15), 28.4 (q, C-18), 19.6 (t, C-2), 18.8 (t, C-6), 14.8 (q, C-20). EIMS m/z (%): 346 ([M]$^+$, 49); 328 (35); 317 (37); 288 (72); 269 (32); 257 (35); 253 (53); 225 (40); 211 (57); 173 (71); 159 (45); 149 (79); 147 (52); 145 (51); 135 (57); 133 (54); 129 (43); 121 (86); 118 (78); 109 (61); 107 (84); 105 (96); 95 (53); 93 (60); 91 (100); 81 (60); 79 (67); 67 (48); 55 (81). HREIMS: 346.2144 (calcd for $C_{21}H_{30}O_4$ [M]$^+$ 346.2144). IR ν_{max}: 2926, 2855, 1722, 1459, 1383, 1226, 1147, 1038, 981, 775 cm^{-1}. UV (EtOH) λ_{max} (log ϵ): 201.0 (2.95) nm. $[\alpha]_D^{20}$: −6.92 (c 0.5, $CHCl_3$).

5.1.15. Preparation of compound **52**

A solution of 24.4 mg of compound **2** (0.077 mmol) in 30 ml of dry CH_2Cl_2 at −78 °C was ozonized until the color of the solution changed to dark blue-gray (30 s). The reaction mixture was then quenched with 10 μl of dry Me_2S (1.76 equiv) and concentrated under vacuum. The residue was purified by preparative-TLC using hexanes/AcOEt (30%) to afford 4.3 mg of compound **52** (18%) as an amorphous white solid. ^{1}H NMR (300 MHz, $CDCl_3$) δ: 3.66 (3H, s, H-20), 2.39 (1H, s, H-13), 1.16 (3H, s, H-17), 0.88 (3H, s, H-19), 2.30–0.82 (20H, m). ^{13}C NMR (75 MHz, $CDCl_3$) δ: 222.5 (s, C-16), 177.7 (s, C-18), 56.5 (d, C-5), 54.7 (t, C-15), 53.7 (d, C-9), 51.0 (q, C-20), 47.5 (d, C-13), 43.5 (s, C-4), 42.2 (s, C-8), 40.8 (t, C-7), 40.4 (t, C-1), 39.3 (s, C-10), 37.7 (t, C-3), 37.0 (t, C-14), 29.3 (t, C-12), 28.5 (q, C-17), 20.5 (t, C-6), 18.8 (t, C-2), 18.5 (t, C-11), 15.7 (q, C-19). EIMS m/z (%): 318 ([M]$^+$, 26); 300 (4); 286 (16); 259 (100); 149 (12); 133 (10); 123 (17); 121 (23); 109 (23); 107 (19); 95 (15); 93 (12); 79 (15); 67 (12); 55 (15). HREIMS: 318.2185 (calcd for $C_{20}H_{30}O_3$ [M]$^+$ 318.2195). IR ν_{max}: 2945, 2870, 1726, 1463, 1235, 1192, 1150 cm^{-1}. $[\alpha]_D^{20}$: −67.07 (c 0.4, $CHCl_3$).

5.1.16. Preparation of compounds **53**, **54** and **55**

A solution of 19.7 mg of compound **8** (0.050 mmol) in 30 ml of dry CH_2Cl_2 at −78° C was ozonized until the color of the solution changed to dark blue-gray (30 s). The reaction mixture was then quenched with 10 μl of dry Me_2S (2.7 equiv) and concentrated under vacuum. The residue was purified by preparative-TLC using hexanes/AcOEt (20%) to afford 10.6 mg of compound **53** (54%), 4.4 mg of compound **54** (21%) and 4.2 mg (20%) of compound **55** as amorphous white solids. Compound **53**: ^{1}H NMR (300 MHz, $CDCl_3$) δ: 7.35 (5H, m, H-22–H-26), 5.14 (1H, d, J = 12.4 Hz, H-20a), 5.07 (1H, d, J = 12.4 Hz, H-20b), 2.37 (1H, s, H-13), 1.21 (3H, s, H-17), 0.82 (3H, s, H-19), 2.37–0.76 (21H, m). ^{13}C NMR (75 MHz, $CDCl_3$) δ: 222.6 (s, C-16), 176.9 (s, C-18), 135.9 (s, C-21), 128.3 (d, C-23, C-25), 128.0 (d, C-22, C-26), 127.9 (d, C-24), 68.8 (t, C-20), 56.7 (d, C-5), 54.7 (t, C-15), 53.7 (d, C-9), 47.5 (d, C-13), 43.7 (s, C-8), 42.2 (s, C-4), 40.8 (t, C-7), 40.4 (t, C-1), 39.4 (s, C-10), 37.7 (t, C-3), 36.9 (t, C-14), 29.2 (t, C-12), 28.6 (q, C-17), 20.6 (t, C-6), 18.8 (t, C-2), 18.5 (t, C-11), 15.8 (q, C-19). IEMS m/z (%): 394 ([M]$^+$, 14); 303 (30); 285 (11); 259 (15); 257 (22); 149 (15); 121 (11); 109 (12); 107 (13); 95 (12); 93 (11); 91 (100); 81 (14); 79 (12); 55 (13). HREIMS: 394.2522 (calcd for $C_{26}H_{34}O_3$ [M]$^+$ 394.2508). IR ν_{max}: 2947, 2872, 1723, 1455, 1232, 1146, 752, 699 cm^{-1}. UV (EtOH) λ_{max} (log ϵ): 202.0 (3.53) nm. $[\alpha]_D^{20}$: −40.19 (c 1.1, $CHCl_3$). Compound **54**: ^{1}H NMR (300 MHz, $CDCl_3$) δ: 7.36 (5H, m, H-22–H-26), 5.14 (1H, d, J = 12.4 Hz, H-20a), 5.06 (1H, d, J = 12.4 Hz, H-20b), 4.76 (1H, sa, H-13), 2.25 (2H, m, H-15), 1.21 (3H, s, H-17), 0.76 (3H, s, H-19), 2.27–0.80 (18H, m). ^{13}C NMR (75 MHz, $CDCl_3$) δ: 176.8 (s, C-18), 172.1 (s, C-16), 135.7 (s, C-21), 128.3 (d, C-23, C-25), 128.0 (d, C-22, C-26), 127.9 (d, C-24), 75.6 (d, C-13), 65.9 (t, C-20), 56.6 (d, C-5), 52.8 (d, C-9), 47.9 (t, C-15), 43.6 (s, C-4), 42.8 (t, C-7), 40.9 (t, C-1), 39.2 (s, C-10), 37.5 (t, C-3), 33.6 (s, C-8), 32.8 (t, C-14), 28.6 (q, C-17), 28.5 (t, C-12), 19.8 (t, C-6), 18.9 (t, C-2), 16.1 (t, C-11), 16.0 (q, C-19). IEMS m/z (%): 410 ([M]$^+$, 4); 319 (16); 273 (17); 259 (11); 121 (8); 107 (10); 91 (100); 81 (11); 55 (10). HREIMS: 410.2458 (calcd for $C_{26}H_{34}O_4$ [M]$^+$ 410.2457). IR ν_{max}: 2951, 2930, 1725, 1458, 1227, 1143, 996, 697 cm^{-1}. UV (EtOH) λ_{max} (log ϵ): 207.6 (3.43) nm. $[\alpha]_D^{20}$: −61.00 (c 0.4, $CHCl_3$). Compound **55**: ^{1}H NMR (300 MHz, $CDCl_3$) δ: 7.34 (5H, m, H-22–H-26), 5.15 (1H, d, J = 12.4 Hz, H-20a), 5.04 (1H, d, J = 12.4 Hz, H-20b), 2.72 (1H, d, J = 13.0 Hz, H-15a), 2.18 (1H, d, J = 13.0 Hz, H-15b), 1.20 (3H, s, H-17), 0.83 (3H, s, H-19), 2.54–0.65 (21H, m). ^{13}C NMR (75 MHz, $CDCl_3$) δ: 177.2 (s, C-18), 176.9 (s, C-16), 135.9 (s, C-21), 128.2 (d, C-23, C-25), 127.9 (d, C-22, C-26), 127.8 (d, C-24), 65.8 (t, C-20), 56.9 (d, C-5), 50.9 (d, C-9), 44.9 (t, C-15), 43.6 (s, C-4), 41.8 (t, C-7), 40.7 (t, C-1), 39.5 (s, C-10), 37.6 (t, C-3), 36.7 (s, C-8), 30.3 (t, C-12, C-14), 28.7 (q, C-17), 21.8 (t, C-6 ó C-13), 20.3 (t, C-6 ó C-13), 19.7 (t, C-2), 19.1 (t, C-11), 18.1 (q, C-19). EIMS m/z (%): 412 ([M]$^+$, 1); 394 (2); 352 (21); 303 (10); 277 (16); 275 (21); 261 (14); 135 (10); 121 (10); 109 (14); 107 (15); 95 (13); 91 (100); 81 (14); 55 (8). HREIMS: 412.2628 (calcd for $C_{26}H_{36}O_4$ [M]$^+$ 412.2614). IR ν_{max}: 2934, 2870, 1721, 1461, 1225, 1140, 698 cm^{-1}. UV (EtOH) λ_{max} (log ϵ): 205.4 (3.52) nm. $[\alpha]_D^{20}$: −40.19 (c 1.1, $CHCl_3$).

5.1.17. Preparation of compounds **56** and **57**

A solution of 44.0 mg of compound **10** (0.133 mmol) in 30 μl of dry CH_2Cl_2 at −78° C was ozonized until the color of the solution changed to dark blue-gray (2 min). The reaction mixture was then quenched with 20 μl of dry Me_2S (2.0 equiv) and concentrated under vacuum. The residue was purified by preparative-TLC using hexanes/AcOEt (15%) to afford 16.8 mg of compound **56** (38%) and 3.2 mg of compound **57** (7%) as amorphous white solids. Compound **56**: ^{1}H NMR (300 MHz, $CDCl_3$) δ: 3.65 (3H, s, H-20), 3.63 (1H, s, H-15), 3.35 (1H, d, J = 1.92 Hz, H-13), 1.20 (3H, s, H-17), 0.90 (3H, s, H-19), 2.52–0.82 (19H, m). ^{13}C NMR (75 MHz, $CDCl_3$) δ: 221.8 (s, C-16), 177.7 (s, C-18), 80.8 (d, C-15), 56.5 (d, C-5), 53.5 (d, C-9), 51.0 (q, C-20), 46.4 (d, C-13), 44.7 (s, C-8), 43.5 (s, C-4), 40.4 (t, C-1), 39.4 (s, C-10), 37.7 (t, C-3), 33.9 (t, C-7), 33.6 (t, C-14), 29.4 (t, C-12), 28.5 (q, C-17), 19.7 (t, C-6), 18.8 (t, C-2), 18.8 (t, C-11), 16.0 (q, C-19). EIMS m/z (%): 334 ([M]$^+$, 96); 319 (10); 302 (18); 291 (15); 274 (100); 259 (23); 247 (17); 215 (16); 175 (11); 147 (17); 135 (22); 123 (47); 121 (82); 109 (55); 107 (53); 95 (37); 93 (35); 81 (44); 79 (35); 55 (44); 53 (12). HREIMS: 334.2153 (calcd for $C_{20}H_{30}O_4$ [M]$^+$ 334.2144). IR ν_{max}: 3467, 2934, 2854, 1725, 1464, 1234, 1155, 1002, 736 cm^{-1}. $[\alpha]_D^{20}$: −23.91 (c 0.2, $CHCl_3$). Compound **57**: ^{1}H NMR (300 MHz,

$CDCl_3$) δ: 5.08 (1H, s, H-17a), 5.02 (1H, s, H-17b), 3.66 (1H, s, OH), 3.64 (3H, s, H-21), 3.64 (1H, s, H-15), 1.18 (3H, s, H-18), 0.84 (3H, s, H-20), 2.20–0.87 (19H, m). ^{13}C NMR (75 MHz, $CDCl_3$) δ: 177.9 (s, C-19), 111.5 (s, C-16), 93.9 (t, C-17), 93.7 (d, C-15), 56.6 (d, C-5), 52.6 (d, C-9), 51.0 (q, C-21), 45.7 (s, C-8), 43.5 (s, C-4), 42.1 (d, C-13), 40.3 (t, C-1), 39.2 (s, C-10), 37.8 (t, C-3), 34.8 (t, C-7), 34.5 (t, C-12), 28.5 (q, C-18), 25.7 (t, C-14), 20.4 (t, C-6), 18.8 (t, C-2), 17.9 (t, C-11), 15.2 (q, C-20). EIMS *m/z* (%): 364 ([M]$^+$, 1); 334 (84); 274 (97); 259 (29); 247 (19); 149 (22); 133 (29); 123 (57); 121 (100); 109 (66); 107 (66); 105 (34); 95 (48); 93 (45); 91 (48); 81 (56); 79 (46); 67 (43); 55 (62). HREIMS: 364.2252 (calcd for $C_{21}H_{32}O_5$ [M]$^+$ 364.2250). IR ν_{max}: 3439, 2943, 2854, 1724, 1464, 1234, 1159, 1097, 1064, 1002, 977 cm^{-1}. UV (EtOH) λ_{max} (log ϵ): 202.0 (3.23) nm. $[\alpha]_D^{20}$: −24.48 (c 0.3, $CHCl_3$).

5.1.18. Preparation of compound **58**

A solution of 40.0 mg of compound **12** (0.121 mmol) in dry CH_2Cl_2 at −78° C was ozonized until the color of the solution changed to dark blue-gray (2 h). The reaction mixture was then quenched with 20 μl of dry Me_2S (2.2 equiv) and concentrated under vacuum. The residue was purified by preparative-TLC using hexanes/AcOEt (40%) to afford 16.3 mg of compound **58** (39%) as an amorphous white solid. ^{1}H NMR (300 MHz, $CDCl_3$) δ: 3.65 (3H, s, H-20), 2.75 (1H, s, H-13), 1.16 (3H, s, H-17), 0.86 (3H, s, H-19), 2.43–0.77 (18H, m). ^{13}C NMR (75 MHz, $CDCl_3$) δ: 184.7 (s, C-15), 182.3 (s, C-16), 177.8 (s, C-18), 55.6 (d, C-5), 51.1 (q, C-20), 44.9 (d, C-9), 44.1 (s, C-8), 43.4 (s, C-4), 41.4 (t, C-7), 39.1 (t, C-1), 38.6 (s, C-10), 37.6 (t, C-3), 36.9 (d, C-13), 31.3 (t, C-14), 28.5 (q, C-17), 21.8 (t, C-12), 19.6 (t, C-6), 19.0 (t, C-2), 18.4 (t, C-11), 17.5 (q, C-19). EIMS *m/z* (%): 348 ([M]$^+$, 15); 330 (6); 276 (36); 261 (38); 217 (60); 180 (34); 135 (33); 121 (100); 109 (60); 107 (50); 93 (43); 91 (41); 81 (42); 79 (59); 67 (39); 55 (52). HREIMS: 348.1925 (calcd for $C_{20}H_{28}O_5$ [M]$^+$ 348.1937). IR ν_{max}: 2948, 2875, 1712, 1457, 1239, 1151, 755 cm^{-1}. $[\alpha]_D^{20}$: −21.43 (c 0.6, $CHCl_3$).

5.1.19. Preparation of compound **59**

A solution of 32.5 mg of compound **30** (0.087 mmol) in dry CH_2Cl_2 at −78° C was ozonized until the colour of the solution changed to dark blue-gray (2 h). The reaction mixture was then quenched with 15 μl of dry Me_2S (2.3 equiv) and concentrated under vacuum. The residue was purified by preparative-TLC using Hexanes/AcOEt (20%) to afford 11.1 mg of compound **59** (34%) as an amorphous white solid. ^{1}H NMR (300 MHz, $CDCl_3$) δ: 4.80 (1H, d, J = 1.89 Hz, H-15), 3.65 (3H, s, H-20), 2.56 (1H, s, H-13), 2.10 (3H, s, $OCOCH_3$), 1.17 (3H, s, H-17), 0.89 (3H, s, H-19), 2.27–0.82 (18H, m). ^{13}C NMR (75 MHz, $CDCl_3$) δ: 217.5 (s, C-16), 177.6 (s, C-18), 169.9 (s, $O\underline{C}OCH_3$), 80.3 (d, C-15), 56.2 (d, C-5), 53.1 (d, C-9), 51.1 (q, C-20), 46.8 (d, C-13), 44.5 (s, C-8), 43.5 (s, C-4), 40.2 (t, C-1), 39.4 (s, C-10), 37.6 (t, C-3), 34.6 (t, C-7), 33.8 (t, C-14), 29.4 (t, C-12), 28.4 (q, C-17), 20.4 (q, $OCO\underline{C}H_3$), 19.6 (t, C-6), 18.7 (t, C-2, C-11), 15.9 (q, C-19). EIMS *m/z* (%): 376 ([M]$^+$, 51); 361 (29); 335 (21); 334 (100); 317 (29); 316 (43); 275 (42); 274 (65); 257 (36); 256 (27); 123 (26); 121 (67); 109 (34); 107 (34); 105 (22); 95 (29); 93 (25); 91 (26); 81 (34); 79 (28); 67 (24); 55 (32). HREIMS 376.2235 (calcd for $C_{22}H_{32}O_5$ [M]$^+$ 376.2250). IR ν_{max}: 3487, 2947, 2870, 1754, 1725, 1464, 1371, 1232, 1155, 1023, 756 cm^{-1}. UV (EtOH) λ_{max} (log ϵ): 200.6 (2.55) nm. $[\alpha]_D^{20}$: −11.39 (c 1.1, $CHCl_3$).

5.1.20. Preparation of compounds **60–63**

A solution of 77.3 mg of compound **35** (0.199 mmol) in 25 ml of dry CH_2Cl_2 at −78° C was ozonized until the colour of the solution changed to dark blue-gray (30 s). The reaction mixture was then quenched with 30 μl of dry Me_2S (2 equiv) and concentrated under vacuum. The residue was purified by preparative-TLC using hexanes/AcOEt (20%) to afford 22.3 mg of compound **60** (29%), 9.8 mg of compound **61** (12%), 9.5 mg (20%) of compound **62** and 9.3 mg of compound **63** as yellow oils. Compound **60**: ^{1}H NMR (300 MHz, $CDCl_3$) δ: 3.74 (1H, dd, J = 4.0, 14.2 Hz, H-20a), 3.59 (1H, dd, J = 4.0, 14.2 Hz, H-20b), 2.39 (1H, s, H-13), 1.17 (3H, s, H-17), 0.86 (3H, s, H-19), 0.10 (9H, s, $Si(CH_3)_3$), 2.28–0.80 (20H, m). ^{13}C NMR (75 MHz, $CDCl_3$) δ: 222.5 (s, C-16), 178.1 (s, C-18), 56.8 (t, C-20), 56.7 (d, C-5), 54.7 (t, C-15), 53.6 (d, C-9), 47.5 (d, C-13), 43.8 (s, C-8), 42.2 (s, C-4), 40.8 (t, C-7), 40.5 (t, C-1), 39.3 (s, C-10), 37.8 (t, C-3), 37.0 (t, C-14), 29.2 (t, C-12), 28.7 (q, C-17), 20.7 (t, C-6), 18.8 (t, C-2), 18.5 (t, C-11), 15.7 (q, C-19), −3.1 (q, $Si(\underline{C}H_3)_3$). EIMS *m/z* (%): 390 ([M]$^+$, 47); 375 (100); 287 (15); 259 (82); 199 (19); 163 (20); 123 (33); 121 (24); 109 (34); 107 (32); 105 (21); 97 (34); 95 (41); 93 (33); 91 (32); 81 (52); 79 (38); 73 (61); 67 (35); 59 (49); 55 (59). HREIMS: 390.2586 (calcd for $C_{23}H_{38}O_3Si$ [M]$^+$ 390.2590). IR ν_{max}: 2951, 2871, 1741, 1720, 1249, 1147, 858 cm^{-1}. UV (EtOH) λ_{max} (log ϵ): 201.2 (2.75) nm. $[\alpha]_D^{20}$: −44.06 (c 1.0, $CHCl_3$).

Compound **61**: ^{1}H NMR (300 MHz, $CDCl_3$) δ: 4.79 (1H, s, H-13), 3.76 (1H, d, J = 14 Hz, H-20a), 3.59 (1H, d, J = 14 Hz, H-20b), 1.18 (3H, s, H-17), 0.84 (3H, s, H-19), 0.10 (9H, s, $Si(CH_3)_3$), 2.24–0.84 (20H, m). ^{13}C NMR (75 MHz, $CDCl_3$) δ: 178.0 (s, C-18), 172.1 (s, C-16), 75.6 (d, C-13), 56.9 (t, C-20), 56.6 (d, C-5), 52.9 (d, C-9), 47.9 (t, C-15), 43.6 (s, C-4), 42.8 (t, C-7), 40.9 (t, C-1), 39.2 (s, C-10), 37.6 (t, C-3), 33.7 (s, C-8), 32.8 (t, C-14), 28.8 (q, C-17), 28.8 (t, C-12), 19.9 (t, C-6), 18.9 (t, C-2), 16.2 (t, C-11), 16.0 (q, C-19), −3.1 (q, $Si(\underline{C}H_3)_3$). EIMS *m/z* (%): 406 ([M]$^+$, 27); 391 (100); 303 (36); 275 (45); 215 (27); 193 (22); 121 (20); 107 (22); 95 (31); 81 (24); 73 (33); 59 (23); 55 (26). HREIMS: 406.2556 (calcd for $C_{23}H_{38}O_4Si$ [M]$^+$ 406.2539). IR ν_{max}: 2954, 2874, 1724, 1223, 1146, 858 cm^{-1}. UV (EtOH) λ_{max} (log ϵ): 201.4 (2.79) nm. $[\alpha]_D^{20}$: −58.37 (c 0.9, $CHCl_3$). Compound **62**: ^{1}H NMR (300 MHz, $CDCl_3$) δ: 3.76 (1H, d, J = 14 Hz, H-20a), 3.76 (1H, d, J = 14 Hz, H-20b), 2.75 (1H, d, J = 12.8 Hz, H-15a), 2.17 (1H, d, J = 12.8 Hz, H-15b), 1.17 (3H, s, H-17), 0.87 (3H, s, H-19), 0.10 (9H, s, $Si(CH_3)_3$), 2.22–0.69 (19H, m). ^{13}C NMR (75 MHz, $CDCl_3$) δ: 178.4 (s, C-16), 177.6 (s, C-18), 56.8 (d, C-5), 56.8 (t, C-20), 51.0 (d, C-9), 45.0 (t, C-15), 43.7 (s, C-4), 41.9 (t, C-7), 40.7 (t, C-1), 39.5 (s, C-10), 37.8 (t, C-3), 36.8 (s, C-8), 30.3 (t, C-14, C-12), 28.8 (q, C-17), 21.9 (t, C-6 or C-13), 20.3 (t, C-6 or C-13), 19.8 (t, C-2), 19.1 (t, C-11), 18.1 (q, C-19), −3.1 (q, $Si(\underline{C}H_3)_3$). EIMS *m/z* (%): 408 ([M]$^+$, 9); 393 (51); 349 (41); 305 (19); 277 (100); 245 (21); 217 (79); 173 (14); 147 (21); 135 (40); 123 (27); 121 (33); 109 (52); 107 (28); 95 (38); 93 (24); 81 (37); 79 (20); 73 (36); 67 (22); 59 (32); 55 (28). HREIMS: 408.2679 (calcd for $C_{23}H_{40}O_4Si$ [M]$^+$ 408.2696). IR ν_{max}: 2952, 2872, 1703, 1250, 1141, 858, 757 cm^{-1}. UV (EtOH) λ_{max} (log ϵ): 201.8 (2.89) nm. $[\alpha]_D^{20}$: −34.11 (c 0.9, $CHCl_3$). Compound **63**: ^{1}H NMR (300 MHz, $CDCl_3$) δ: 3.75 (1H, d, J = 14.2 Hz, H-20a), 3.57 (1H, d, J = 14.2 Hz, H-20b), 3.10 (1H, s, H-13), 1.15 (3H, s, H-17), 0.83 (3H, s, H-19), 0.10 (9H, s, $Si(CH_3)_3$), 2.32–0.79 (20H, m). ^{13}C NMR (75 MHz, $CDCl_3$) δ: 178.1 (s, C-18), 117.5 (s, C-16), 56.7 (t, C-20), 56.5 (d, C-13), 54.9 (d, C-5), 50.4 (t, C-15), 43.8 (s, C-4), 42.8 (s, C-8), 41.0 (t, C-7), 40.4 (t, C-1), 39.5 (s, C-10), 39.3 (d, C-9), 37.9 (t, C-3), 36.9 (t, C-14), 28.7 (q, C-17), 25.6 (t, C-12), 21.5 (t, C-6), 18.8 (t, C-2), 17.8 (t, C-11), 15.1 (q, C-19), −3.1 (q, $Si(\underline{C}H_3)_3$). EIMS *m/z* (%): 406 ([M]$^+$, 8); 391 (76); 375 (35); 347 (40); 303 (20); 275 (44); 259 (33); 231 (21); 215 (60); 199 (30); 157 (30); 149 (29); 135 (54); 133 (41); 123 (46); 121 (74); 109 (62); 107 (73); 105 (39); 95 (67); 93 (55); 91 (50); 81 (87); 79 (51); 73 (100); 67 (45); 59 (67); 55 (63). HREIMS: 406.2545 (calcd for $C_{23}H_{38}O_4Si$ [M]$^+$ 406.2539). IR ν_{max}: 2950, 2850, 1721, 1250, 1154, 857, 757 cm^{-1}. UV (EtOH) λ_{max} (log ϵ): 201.4 (3.04) nm. $[\alpha]_D^{20}$: −63.23 (c 0.9, $CHCl_3$).

5.2. Cell culture

The murine macrophage cell line RAW 264.7 was maintained in RPMI 1640 medium supplemented with 10% FCS, L-glutamine and antibiotics, as previously described [29].

5.3. Determination of NO synthesis

NO release was determined with Griess reagent as previously described [30]. Briefly, NO release was determined spectrophotometrically by the accumulation of nitrite in the medium. The absorbance at 548 nm was compared with a standard of $NaNO_2$.

5.4. MTT assay for cell viability

RAW 264.7 cells were plated at a density of 10^5 cells/well in 96-well plates. To determine the appropriate concentration not toxic to cells, cells were incubated in the presence of different concentrations of derivatives for 24 h, before they were then reacted with MTT (3-[4,5-dimethylthiazol-2-yl]-2,5-diphenyl tetrazolium bromide) at 37 °C for 4 h. The reaction product, formazan, was extracted with dimethyl sulfoxide (DMSO) and the absorbance was read at 540 nm. Assays were performed in triplicate, and results are expressed as the percent reduction in cell viability compared to untreated control cultures for at least three independent experiments.

5.5. Preparation of cytosolic and nuclear extracts

Cells were washed twice with ice-cold buffer A (10 mM Hepes, pH 7.9; 1 mM EDTA, 1 mM EGTA, 10 mM KCl, 1 mM DTT, 0.5 mM PMSF, 2 μg/ml aprotinin, 10 μg/ml leupeptin, 2 μg/ml TLCK (N_α-Tosyl-L-lysine chloromethyl ketone hydrochloride), 5 mM NaF, 1 mM $NaV0_4$, 10 mM Na_2MoO_4) containing 120 mM NaCl and scraped off the plate. Cells were lysed at 4 °C with 0.2 ml of buffer A supplemented with 0.5% Nonidet P-40 and under continuous shaking. After centrifugation of the cell lysate the supernatant was stored at −80 °C (cytosolic extract) and the pellets were resuspended in 50 μl of buffer A supplemented with 20% glycerol-0.4 M KCl and gently shaken for 30 min at 4 °C. Protein content was assayed using the Bio-Rad protein reagent. All cell fractionation steps were carried out at 4 °C.

5.6. Western blot analysis

Western blot of cell extracts were prepared and incubated with anti-NOS-2, anti-IκBα and anti-β-actin (Santa Cruz Biotechnology). Blots were developed by ECL according to the manufacturer's instructions (GE Healthcare). β-Actin was used as a loading control.

5.7. RNA analysis and quantitative PCR

Total RNA was isolated from cells using TRIzol reagent (Invitrogen) according to the manufacturer's instruction. Quantitative PCR (SYBRgreen) analysis was performed with an ABI 7700 sequence detector as described [30]. Each sample was run in duplicate, and all samples were analyzed in parallel for the expression of the housekeeping gene 36B4 (acidic ribosomal phosphoprotein P0), used as an endogenous control to normalize the expression level of target genes. Fold induction was determined from average replicate values. Primer sequences are available on request.

5.8. Assay of cytokines

Cytokine production in the cell culture was measured with ELISA kits from R&D systems according to the manufacturer's instructions.

5.9. Statistical analysis

The data shown are the mean ± S.D. Statistical significance was estimated with Student's t test for unpaired observations using the InStart program (GraphPad Software). Values of $^*p < 0.05$ were considered significant.

Acknowledgments

This work was supported by grants PI08.0070 from FIS, MPY 1410/09 from ISCIII and Fundación Mutua Madrileña to S.H., by a Santander-Complutense grant to S.H. and B. de las H. We also thank the financial support from the Spanish MICINN (SAF2009-13296-C02-01) and ICIC (Instituto Canario de Investigación del Cáncer) to A.E.B. IHF thanks MICINN for a predoctoral fellowship. We thank Sandra Herranz for her excellent technical assistance.

Appendix. Supplementary data

Supplementary data related to this article can be found online at doi:10.1016/j.ejmech.2011.01.052.

References

[1] D.J. Berg, J. Zhang, J.V. Weinstock, H.F. Ismail, K.A. Earle, H. Alila, R. Pamukcu, S. Moore, R.G. Lynch, Gastroenterology 123 (2002) 1527–1542.
[2] J.W. Rose, K.E. Hill, H.E. Watt, N.G. Carlson, J. Neuroimmunol. 149 (2004) 40–49.
[3] P.F. Gomez, M.H. Pillinger, M. Attur, N. Marjanovic, M. Dave, J. Park, C.O. Bingham III, H. Al Mussawir, S.B. Abramson, J. Immunol. 175 (2005) 6924–6930.
[4] K.H. Kwon, A. Murakami, R. Hayashi, H. Ohigashi, Biochem. Biophys. Res. Commun. 337 (2005) 647–654.
[5] P.A. Baeuerle, Cell 95 (1998) 729–731.
[6] K. Brown, S. Gerstberger, L. Carlson, G. Franzoso, U. Siebenlist, Science 267 (1995) 1485–1488.
[7] M.A. O'Connell, B.L. Bennett, F. Mercurio, A.M. Manning, N. Mackman, J. Biol. Chem. 273 (1998) 30410–30414.
[8] J. DiDonato, F. Mercurio, C. Rosette, J. Wu-Li, H. Suyang, S. Ghosh, M. Karin, Mol. Cell Biol. 16 (1996) 1295–1304.
[9] I. Sanchez-Perez, S.A. Benitah, M. Martinez-Gomariz, J.C. Lacal, R. Perona, Mol. Biol. Cell. 13 (2002) 2933–2945.
[10] Y. Kim, S.M. Fischer, J. Biol. Chem. 273 (1998) 27686–27694.
[11] S. Ghosh, M. Karin, Cell 109 (S81–S96) (2002).
[12] M. Karin, Nature 441 (2006) 431–436.
[13] M.L. Handel, Inflamm. Res. 46 (1997) 282–286.
[14] I. Tegeder, E. Niederberger, E. Israr, H. Guhring, K. Bruce, C. Euchenhofer, S. Grosch, G. Geisslinger, FASEB J. 15 (2001) 2–3.
[15] H.M. Gao, J.S. Hong, Trends Immunol. 29 (2008) 357–365.
[16] A. Klegeris, P.L. McGeer, Curr. Alzheimer Res. 2 (2005) 355–365.
[17] I. Hueso-Falcon, N. Giron, P. Velasco, J.M. Amaro-Luis, A.G. Ravelo, B. de las Heras, S. Hortelano, A. Estevez-Braun, Bioorg. Med. Chem. 18 (2010) 1724–1735.
[18] K. Schank, H. Beck, S. Pistorius, Helv. Chim. Acta 87 (2004) 2025–2049.
[19] L.C. Green, D.A. Wagner, J. Glogowski, P.L. Skipper, J.S. Wishnok, S.R. Tannenbaum, Anal. Biochem. 126 (1982) 131–138.
[20] S. Uwe, Biochem. Pharmacol. 75 (2008) 1567–1579.
[21] B. de las Heras, S. Hortelano, Inflamm. Allergy Drug Targets 8 (2009) 28–39.
[22] A. Castrillo, B. de las Heras, S. Hortelano, B. Rodriguez, A. Villar, L. Bosca, J. Biol. Chem. 276 (2001) 15854–15860.
[23] B.-C. Chen, C.-C. Liao, M.-J. Hsu, Y.-T. Liao, C.-C. Lin, J.-R. Sheu, C.-H. Lin, J. Immunol. 177 (2006) 681–693.
[24] R.D. Torrenegra, A. Tellez, N. Alba, G. Garcia, Rev. Colomb. Quim. 23 (1994) 29–35.
[25] A. Usubillaga, J. De Hernandez, N. Perez, M. Kiriakidis, Phytochemistry 12 (1973) 2999.
[26] A. Usubillaga, A. Morales, Phytochemistry 11 (1972) 1856–1857.
[27] J. Cuatrecasas, Phytologia 35 (1976) 43–61.
[28] A. Usubillaga, M. Romero, R. Aparicio, Acta Hortic. 597 (2003) 129–130.
[29] N. Girón, P.G. Traves, B. Rodriguez, R. Lopez-Fontal, L. Bosca, S. Hortelano, B. de las Heras, Toxicol. Appl. Pharmacol. 228 (2008) 179–189.
[30] M. Zeini, P.G. Traves, R. Lopez-Fontal, C. Pantoja, A. Matheu, M. Serrano, L. Bosca, S. Hortelano, J. Immunol. 177 (2006) 3327–3336.

Capítulo 2

Labdanolic acid methyl ester (LAME) exerts anti-inflammatory effects through inhibition of TAK-1 activation.

Toxicology and Applied Pharmacology. 258(1):109-17 (2012)

Labdanolic acid methyl ester (LAME) exerts anti-inflammatory effects through inhibition of TAK-1 activation.

Irene Cuadrado, Florencia Cidre, Sandra Herranz, Ana Estévez-Braun, Beatriz de las Heras and Sonsoles Hortelano.

Toxicology and Applied Pharmacology. 258(1):109-17 (2012)

El objetivo de este trabajo de investigación fue el estudio del mecanismo de acción del diterpeno labdánico LAME (éster metílico del ácido labdanólico) como agente antiinflamatorio, analizando las vías de señalización implicadas.

El estudio de la viabilidad celular en macrófagos peritoneales de ratón mediante ensayo MTT y citometría de flujo, mostró que el compuesto LAME (1-100μM) no presentaba toxicidad celular. Los efectos antiinflamatorios previos de este compuesto, fueron confirmados por la disminución significativa de los niveles de las enzimas NOS-2 y COX-2, con reducción de la expresión génica a nivel transcripcional en presencia de LAME. Además, el tratamiento con LAME inhibía la fosforilación de IκBα, así como la translocación al núcleo de la subunidad p65. Estos datos, confirmados mediante microscopía confocal, demostraron la actividad inhibidora de LAME en la vía de activación de este factor de transcripción.

El tratamiento de las células con LAME inhibió la vía de las proteínas MAPKs, en concreto la expresión de las proteínas ERK y JNK. La fosforilación de la quinasa TAK-1, enzima común a las vías de activación de NF-κB y MAPKs, también estaba inhibida en presencia de este compuesto.

La actividad antiinflamatoria de este diterpeno fue confirmada en un modelo de sepsis en ratón inducido por LPS. El tratamiento con LAME aumentó la supervivencia de los animales, lo que sugería su acción protectora frente a la muerte por sepsis. Asimismo, LAME producía una reducción significativa de los niveles séricos de las citoquinas TNF-α e IL-6.

La escasa toxicidad mostrada por LAME, junto a su eficacia antiinflamatoria indicaban el potencial uso de este compuesto en el tratamiento de procesos inflamatorios.

Toxicology and Applied Pharmacology 258 (2012) 109–117

Contents lists available at SciVerse ScienceDirect

Toxicology and Applied Pharmacology

journal homepage: www.elsevier.com/locate/ytaap

Labdanolic acid methyl ester (LAME) exerts anti-inflammatory effects through inhibition of TAK-1 activation

Irene Cuadrado [a,1], Florencia Cidre [b,1], Sandra Herranz [b], Ana Estevez-Braun [c,d,2], Beatriz de las Heras [a,*], Sonsoles Hortelano [b,**]

[a] Departamento de Farmacología, Facultad de Farmacia, Universidad Complutense, Plaza Ramón y Cajal s/n, 28040 Madrid, Spain
[b] Unidad de Inflamación y Cáncer. Área de Biología Celular y Desarrollo. Centro Nacional de Microbiología, Instituto de Salud Carlos III, Madrid, Spain
[c] Instituto Universitario de Bio-Orgánica "Antonio González". Universidad de La Laguna. Avda. Astrofísico Fco. Sánchez 2. 38206. La Laguna, Tenerife, Spain
[d] Instituto Canario de Investigaciones del Cáncer (ICIC), Spain

ARTICLE INFO

Article history:
Received 18 July 2011
Revised 10 October 2011
Accepted 11 October 2011
Available online 21 October 2011

Keywords:
NOS-2
Inflammation
Labdanes
Prostaglandin E_2
Lipopolysaccharide

ABSTRACT

Labdane derivatives obtained from the diterpenoid labdanediol suppressed NO and PGE_2 production in LPS-stimulated RAW 264.7 macrophages. However, mechanisms involved in these inhibitory effects are not elucidated. In this study, we investigated the signaling pathways involved in the anti-inflammatory effects of labdanolic acid methyl ester (LAME) in peritoneal macrophages and examined its therapeutic effect in a mouse endotoxic shock model. LAME reduced the production of NO and PGE_2 in LPS-activated macrophages. This effect involved the inhibition of NOS-2 and COX-2 gene expression, acting at the transcription level. Examination of the effects of the diterpene on NF-κB signaling showed that LAME inhibits the phosphorylation of IκBα and IκBβ, preventing their degradation and the nuclear translocation of the NF-κB p65 subunit. Moreover, inhibition of MAPK signaling was also observed. A further experiment revealed that LAME inhibited the phosphorylation of transforming growth factor-β (TGF-β)-activated kinase 1 (TAK1), an upstream signaling molecule required for IKK and mitogen-activated protein kinases (MAPKs) activation. Inflammatory cytokines such as IL-6, TNF-α and IP-10 were downregulated in the presence of this compound after stimulation with LPS. Additionally, LAME also improved survival in a mouse model of endotoxemia and reduced the circulatory levels of cytokines (IL-6, TNF-α). In conclusion, these results indicate that labdane diterpene LAME significantly attenuates the pro-inflammatory response induced by LPS both *in vivo* and *in vitro*.

Introduction

Innate immunity constitutes the first-line of host defense in multicellular organisms. Early recognition of microbial products by the innate immune system is a strict requirement for the production of an effective inflammatory response.

Many host cell types, including macrophages, initiate the first line of defense against infection by sensing specific microbial pathogen-associated molecular patterns (PAMPs) through Toll-like receptors (TLRs). Upon ligand binding, TLRs activate complex signaling networks that induce the production of proinflammatory cytokines, the acquisition of a phagocytotic phenotype, and the initiation of subsequent innate effector mechanisms that can enhance host anti-tumor responses (Schnare et al., 2001). Different TLRs sense and transmit signals by detecting different pathogen components. For example, TLR2, TLR3, TLR4, and TLR9 are respectively activated by lipoproteins/peptidoglycans (Takeuchi et al., 1999), viral RNA, lipopolysaccharide (LPS) (Poltorak et al., 1998), and bacterial DNA (Hemmi et al., 2000). Activated TLR ligands initiate a plethora of signaling cascades via specific adaptor proteins such as myeloid differentiation primary response gene 88 (MyD88), MyD88-adapter-like (MAL, also known as Toll-interleukin 1 receptor [TIR] domain-containing adapter protein [TIRAP]), TIR-domain-containing adapter-inducing interferon-β (TRIF) and TRIF-related adaptor molecule (TRAM) (Takeda et al., 2003). All TLRs except TLR3 recruit the adaptor molecule MyD88

Abbreviations: IKK, IκB kinases; IRAK, IL-1 receptor-associated kinase; LAME, Labdanolic acid methyl ester; LPS, lipopolysaccharide; MAL, MyD88-adapter-like; MAPK, mitogen-activated protein kinase; MTT, 3-(4,5-dimethylthiazol-2-yl)-2,5-diphenyltetrazolium bromide; MyD88, myeloid differentiation primary response gene 88; NO, nitric oxide; NOS-2, nitric oxide synthase; PAMPs, pathogen-associated molecular patterns; PGE_2, prostaglandin E_2; TLCK, N_α-Tosyl-L-lysine chloromethyl ketone hydrochloride; TLRs, Toll-like receptors; TAK1, Transforming growth factor-β (TGF-β)-activated kinase 1; TRAF6, TNF receptor-associated factor 6; TRAM, TRIF-related adaptor molecule; TRIF, TIR-domain-containing adapter-inducing interferon-β.

* Corresponding author. Fax: +34 91 8223269.
** Correspondence to: S. Hortelano, Unidad de Inflamación y Cáncer, Área de Biología Celular y del Desarrollo, Centro Nacional de Microbiología, Instituto de Salud Carlos III, Ctra Majadahonda-Pozuelo, Km 2,200, 28220 Majadahonda, Madrid, Spain. Fax: +34 91 8223269.
E-mail addresses: lasheras@farm.ucm.es (B. de las Heras), shortelano@isciii.es (S. Hortelano).
[1] Contributed equally to this work.
[2] http://www.icic.es.

0041-008X/$ – see front matter © 2011 Elsevier Inc. All rights reserved.
doi:10.1016/j.taap.2011.10.013

through the TIR domain, triggering the so-called MyD88-dependent pathway. TLR3 activates a MyD88 independent pathway that signals through TRIF, while TLR4 signals through the MyD88 and the TRIF pathways.

MyD88 molecules recruit IL-1 receptor-associated kinase (IRAK)-4 and facilitate IRAK-4-mediated phosphorylation of IRAK-1. Phosphorylation and degradation of IRAK1 induce ubiquitination of TNF receptor-associated factor (TRAF) 6 (Kawai and Akira, 2006) that activates the transforming growth factor β-activated kinase-1 (TAK1) kinase complex, resulting in activation of MAPKs and IκB kinases (IKK) (Keating et al., 2007; Takaesu et al., 2001).

These signaling pathways in turn activate a variety of transcription factors that include NF-κB (p50/p65) and AP-1 (c-Fos/c-Jun) (Lee and Kim, 2007) which coordinate the induction of many gene-encoding inflammatory mediators, including nitric oxide (NO), prostaglandins (PGs), chemokines and cytokines (Gomez et al., 2005).

These signals are essential for the classical outcome of TLR activation: the orchestration of host innate and adaptive immune responses. However, a persistent activation of the TLR-mediated intracellular signal transduction pathway in monocytes/macrophages, characterized by the excessive release of proinflammatory cytokines, may lead to the development of numerous pathologies. Thus, suppression and/or inhibition of the above-mentioned signaling molecules may have great potential for preventing and treating of inflammation-associated diseases.

Bioactive natural products can be considered very promising starting points for the development of new therapeutic agents. These compounds have been widely used in the treatment of infection and inflammatory diseases for thousands of years, having a dominant role in the discovery of leads for the development of new therapeutic agents (Butler and Newman, 2008). The transcription factor NF-κB has been shown to be a target for therapeutic intervention to treat numerous inflammatory diseases (Zuany-Amorim et al., 2002). In this context, natural products as diterpenes are potent inhibitors of NF-κB (de las Heras and Hortelano, 2009). The labdane diterpenes andalusol and hispanolone derivatives (Chinou, 2005; de Las Heras et al., 1999; Girón et al., 2008), hedychilactones A–C from *Hedychium coronarium* (Matsuda et al., 2002) and andrographolide from *Andrographis paniculata* (Xia et al., 2004) are representative examples. Interestingly, we have recently described that derivatives from the diterpene labdanediol suppressed some inflammatory responses as NO and PGE_2 production in LPS-stimulated RAW 264.7 macrophages (Girón et al., 2010), but mechanisms involved in these inhibitory effects are not elucidated. In the present study we analyzed the signaling pathways involved in the anti-inflammatory actions of LAME (*labdanolic acid methyl ester*), the most active of these labdane derivatives, and evaluated its protective effects in a mouse model of endotoxic shock.

Material and methods

Materials. Ultrapure 0111:B4 LPS from *Escherichia coli* was from InvivoGen (San Diego, CA). SYBR Green/Fluorescein qPCR master mix was from SABiosciences (Frederick, MD). TRIzol reagent was from Invitrogen (Carlsbad, CA). Difco thioglycollate broth was from Becton-Dickinson (Franklin Lakes, NJ). Antibodies to total MAPKs, total TAK-1 and phosphorylated forms (p-TAK-1, p38, JNK-SAPK and ERK) were from Cell Signaling Technology (Beverly, MA). Anti-NOS-2, anti-IκBα, anti-p65, and anti-β-actin were from Santa Cruz Biotechnology (Santa Cruz, CA); anti-COX-2 from Cayman Chemical (Ann Arbor, MI), and anti-PSF from Sigma (St. Louis, MO). Western blot reagents (polyvinylidene difluoride membranes and ECL kit) were from GE Healthcare (Pittsburgh, PA).

Preparation of the labdanolic acid methyl ester (LAME) compound. LAME was prepared from labdanolic acid as previously described (Girón et al., 2010). Stock solutions were prepared in dimethylsulfoxide (DMSO) and further diluted in culture medium. Chemical structure of LAME is shown in Fig. 1A.

Animals. All procedures involving animals were carried out according to European Union guidelines and the Declaration of Helsinki principles for the handling and use of laboratory animals. Additionally, experimental protocols were approved by the 'Ethics Committee for

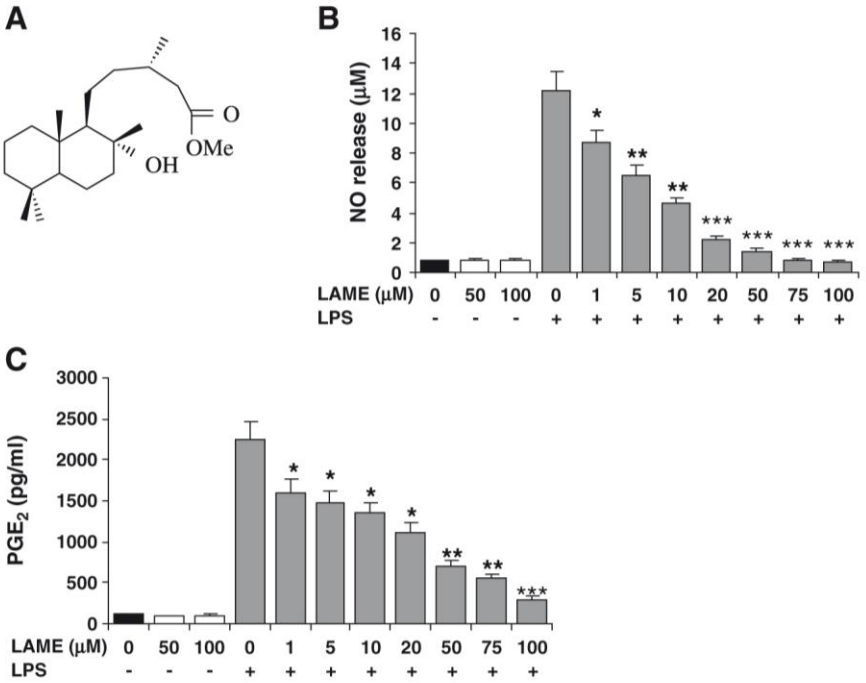

Fig. 1. *Dose-dependent inhibitory effect of LAME on NO and PGE_2 release.* (A) Chemical structure of LAME. (B) Peritoneal macrophages were incubated with LAME (50 and 100 μM) for 24 h or were pre-incubated for 30 min with different concentrations of LAME (1, 5, 10, 20, 50, 75 and 100 μM) followed by stimulation with 200 ng/ml LPS for 24 h. The accumulation of nitrite in the culture medium was measured with the Griess reagent. (C) Peritoneal macrophages were incubated as in B and PGE_2 release was measured with ELISA. Experiments were carried out in triplicate and results show the mean ± S.D. of five independent experiments. *P<0.05, **P<0.01, ***P<0.001, with respect to the LPS condition.

Animal Experimentation' of the Instituto de Salud Carlos III (ISCIII), which followed National (normative 1201/2005) and International recommendations (normative 609/86 from EU). Balb/c mice free of pathogens (6–8 weeks old) were bred in our animal facility and supplied with food and water *ad libitum* and exposed to a 12 h light–dark cycle.

Preparation of elicited peritoneal macrophages. Murine peritoneal macrophages were obtained from thioglycolate-injected mice as previously described (Zeini et al., 2006). Cells were seeded at $1\times10^6/cm^2$ in RPMI 1640 containing 10% FBS and 2% penicillin/streptomycin antibiotics. Non-adherent cells were removed 2 h after seeding by extensive washing with medium.

Determination of NO synthesis. NO was measured by the Griess reaction as previously described (Hueso-Falcón et al., 2011). Briefly, NO release was determined spectrophotometrically as the accumulation of nitrite in the medium. Absorbance at 548 nm was compared with standard $NaNO_2$ solutions.

Assay of PGE_2 release. Levels of PGE_2 in the culture media were quantified per duplicate using EIA kits (R&D Systems, Minneapolis, MN. USA).

MTT assay for cell viability. Macrophages were plated at a density of 10^5 cells/well in 96-well plates. To determine the appropriate non-toxic concentrations to cells, cells were incubated in the presence of different concentrations of LAME for 24 h, before they reacted with MTT (3-[4,5-dimethylthiazol-2-yl]-2,5-diphenyl tetrazolium bromide) at 37 °C for 4 h. The reaction product, formazan, was extracted with dimethyl sulphoxide (DMSO) and the absorbance was read at 540 nm. Assays were performed in triplicate, and results are expressed as the percent reduction in cell viability compared to untreated control cultures for at least three independent experiments.

Flow cytometry analysis of apoptosis. After treatment with the appropriate stimuli, cells were stained with 0.005% (w/v) propidium iodide (PI) and annexin-V and immediately analyzed in a FACSCanto II flow cytometer (Becton Dickinson) according to a previously described protocol (Hortelano et al., 2002).

Preparation of cytosolic and nuclear extracts. Cells were washed twice with ice-cold buffer A [10 mM Hepes, pH 7.9; 1 mM EDTA, 1 mM EGTA, 10 mM KCl, 1 mM DTT, 0.5 mM PMSF] containing 120 mM NaCl and protease inhibitor cocktail (Sigma) and scraped off the plate. Cells were lysed at 4 °C with 0.2 ml buffer A supplemented with 0.5% Nonidet P-40 and under continuous shaking. After centrifugation, the supernatant was stored at −80 °C (cytosolic extract) and the pellets were resuspended in 50 µl of buffer A supplemented with 20% glycerol-0.4 M KCl and gently shaken for 30 min at 4 °C. Nuclear protein extracts were obtained by centrifugation at 13 000×*g* for 15 min, and the supernatant was stored at −80 °C. Protein content was assayed with the Bio-Rad protein reagent. All cell fractionation steps were carried out at 4 °C.

Western blot analysis. Equal amounts of protein lysates extracted from macrophages were separated by SDS-PAGE and transferred onto PVDF membranes (Millipore, MA, US). Blots on the membranes were blocked in 5% BSA and probed with the antibodies to total MAPKs, total TAK-1 and phosphorylated forms of TAK-1, p38, JNK-SAPK and ERK (Cell Signaling Technology), with anti-NOS-2, anti-IκBα, anti-IκBβ, anti-p65, anti-β-actin (Santa Cruz Biotechnology), anti-COX-2 (Cayman Chemical), and anti-PSF (Sigma). The blots were then incubated with secondary goat anti-mouse or-rabbit IgG antibodies (Cell Signaling) and developed with ECL according to the manufacturer's instructions (GE Healthcare). β-actin was used as a loading control for whole-cell and cytosolic extracts, and anti-PSF was used as a loading control for nuclear extracts. After treatment with 100 mM β-mercaptoethanol, 2% SDS in TBS and heating at 60 °C for 30 min, blots were sequentially re-probed with antibodies.

RNA analysis and quantitative PCR. Total RNA was isolated from cells and mouse tissues with Trizol reagent (Invitrogen). Quantitative PCR (SYBRgreen) analysis was performed with an ABI7700 sequence analyzer as described (Girón et al., 2008). Each sample was run in duplicate, and all samples were analyzed in parallel for the expression of the housekeeping gene 36B4 (acidic ribosomal phosphoprotein P0), which was used as an endogenous control for normalization of the expression level of target genes. Fold induction was determined from mean replicate values. Primer sequences are available on request.

Confocal microscopy. Peritoneal macrophages were grown on coverslips, were pretreated for 30 min with LAME and then activated for 30 min with LPS. After washing the covers twice with PBS, the cells were fixed for 2 min with methanol at −20 °C, blocked for 60 min with 3% BSA at room temperature, and incubated for 60 min with 1:100 anti-IκBα or anti-IκBβ antibodies. After three washes with ice-cold PBS, samples were incubated for 60 min with a Cy3 conjugated secondary antibody (1:300) against rabbit IgG (GE Healthcare). Nuclei were revealed by staining with Hoechst 42 (1:1000). Cells were viewed on a MRC-1024 confocal microscope (Bio-Rad), and the fluorescence was measured and electronically evaluated. Laser sharp software (Bio-Rad) was used to determine the relative intensity of the fluorescence per pixel and the percentage of cytosolic and nuclear localization.

Cytokine assay. Cytokine production by cultured macrophages was quantified by enzyme-linked immunosorbent assay (ELISA) kits from R&D systems according to the manufacturer's instructions.

LPS-induced endotoxic shock and measurement of TNF-α and IL-6 levels. Twenty mice were randomly divided into two groups (10 mice per group). The two groups of mice were injected *i.p.* with DMSO (control) or LAME (20 mg/kg). One hour after LAME administration, control and LAME-administered mice were injected *i.p.* with 10 mg/kg of LPS. Survival of both groups was monitored for 7 days. At 90 min after injection of LPS, blood was collected by submandibular bleeding to evaluate the changes in the serum levels of TNF-α and IL-6. This time point was chosen, as 90 min of endotoxemic results in a maximal increase in the serum levels of TNF-α in this species (De Kimpe et al., 1995). The blood sample was centrifuged (3300×*g* for 3 min) to separate serum. The content of TNF-α and IL-6 in serum samples (50 µl) was determined by enzyme-linked immunosorbent assay (ELISA) (R&D Systems, Minneapolis, MN, USA) according to the manufacturers' instructions.

Statistical analysis. Data shown are means ± SD of five separate experiments. Significant differences were established by one-way ANOVA, using the GraphPad Instat program (GraphPad Software V2.03). The Kaplan–Meier method was used to compare the differences in mortality rates between groups. $P<0.05$ was accepted as statistically significant.

Results

LAME inhibits NO and PGE_2 release in LPS-stimulated macrophages

To determine the effect of LAME (Fig. 1A) in relevant inflammatory mediators such as NO and PGE_2, peritoneal macrophages were pretreated with LAME for 30 min and subsequently incubated with LPS for 24 h. Nitrite accumulation in the culture medium was inhibited dose-dependently by LAME (46% and 81% inhibition with 10 and

20 μM, respectively) (Fig. 1B). Similar results were obtained for PGE_2 release (50% and 69% inhibition with 10 and 20 μM, respectively) (Fig. 1C). On the other hand, LAME was not able to induce NO release or PGE_2 production in resting cells.

To confirm that the inhibitory effects of LAME were not due to cytotoxicity, we analyzed the percentage of cell viability by apoptosis and MTT assay. Cell viability was not affected by any dose of LAME as we can observe in Fig. 2A and B. The DMSO concentration (<0.01%) used as LAME vehicle had no effect on nitrite production or viability.

LAME inhibits the induction of NOS-2 and COX-2 at the transcriptional level

To further analyze the signaling pathways modulated by LAME, we studied whether the inhibitory effects on the pro-inflammatory mediators PGE_2 and NO were related to NOS-2 and COX-2 enzyme modulation, as markers of the activation process. In unstimulated peritoneal macrophages, levels of NOS-2 and COX-2 proteins were undetectable. As Fig. 3A shows, LAME potently inhibited the expression of NOS-2, showing also inhibitory effects on COX-2. Moreover, analysis of NOS-2 and COX-2 mRNA by quantitative PCR revealed that this compound inhibited LPS-induced expression, once again showing greater activity on NOS-2 induction (Fig. 3B).

Anti-inflammatory effects of LAME are mediated by NF-κB inhibition

Activation of NF-κB is a key step in the onset of the inflammatory response. To investigate the mechanism of action of LAME on macrophage function, we examined its effects on the levels of cytosolic IκBα protein in LPS-activated macrophages. Phosphorylation of IκBα was impaired in activated cells pretreated with LAME. This effect was accompanied by inhibition of IκBα degradation and a reduced accumulation of the NF-κB p65 subunit in the nucleus after LPS stimulation

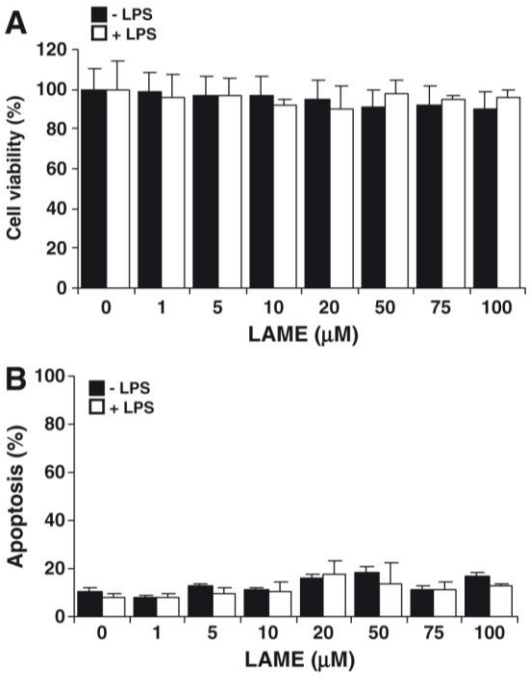

Fig. 2. *Effects of LAME on cell viability.* Peritoneal macrophages were incubated with different concentrations of LAME (1, 5, 10, 20, 50, 75 and 100 μM) in the presence or absence of 200 ng/ml LPS for 24 h. (A) Cell viability was determined by the MTT assay. (B) Apoptosis was analyzed by flow cytometry after PI and annexin-V labeling. Experiments were carried out in triplicate and results show the mean ± S.D. of five independent experiments.

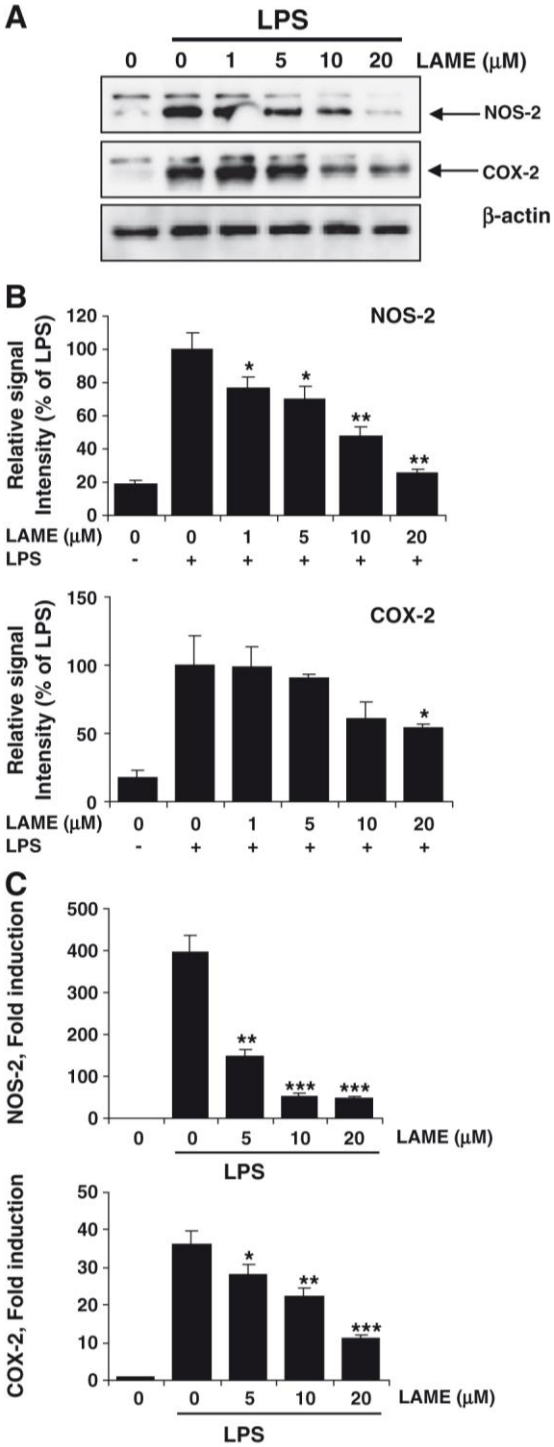

Fig. 3. *NOS-2 and COX-2 expression is inhibited by LAME.* (A) Macrophages were pre-incubated for 30 min with LAME (1, 5, 10 and 20 μM) followed by stimulation with 200 ng/ml LPS for 24 h. NOS-2 and COX-2 proteins were detected by Western blot. β-actin content was used as a loading control. Western blot shows a representative experiment of three. (B) Densitometry analysis of NOS-2 and COX-2 expression was performed. Results show the mean ± S.D. of five independent experiments of Western Blot and are expressed as the percentage of relative signal intensity with respect to the LPS condition. *P<0.05, **P<0.01, with respect to the LPS condition. (C) Macrophages were pre-incubated for 30 min with LAME (5, 10, and 20 μM) followed by stimulation with 200 ng/ml LPS for 4 h. Relative expression of NOS-2 and COX-2 was determined by quantitative PCR. Results show the mean ± S.D. of five independent experiments. *P<0.05, **P<0.01, ***P<0.001 with respect to the LPS condition.

(Fig. 4A). The subcellular localization of IκBα and IκBβ in activated macrophages (30 min) was also analyzed by confocal microscopy, further confirming impaired degradation after incubation with LAME (Fig. 4B).

Effects of LAME on MAPK activation

Proteins of the NF-κB family are important target molecules of MAPKs, which mediate signal transduction from the cell surface to the nucleus (Janssen-Heininger et al., 2000; Schulze-Osthoff et al., 1997). We therefore examined the activation state of the distinct MAPK pathways to assess their potential involvement in the inhibitory actions of LAME. Treatment of macrophages with LPS induced a marked increase in the amounts of phosphorylated ERK and JNK (p-ERK and p-JNK) which was almost completely blocked by pre-incubation of cells with LAME, while the total protein expression of each kinase remained constant (Fig. 5). In contrast, the level of p–p38 was slighted affected.

LAME Inhibits LPS-induced inflammation at the TAK1

The fact that LAME inhibits both the MAPK and NF-κB pathways indicates that the site of action of LAME is at a level upstream of the IKK/MAPKKs branching point in the LPS signal transduction pathway. In the TLR/MyD88-signaling pathway, activated IRAK1 interacts with TRAF6, which in turn leads to the activation of TAK1-mediated NF-κB and MAPK (Keating et al., 2007; Takaesu et al., 2001). Therefore, we examined whether LAME suppressed LPS-induced NF-κB activation through the inhibition of TAK1. As shown in Fig. 6, kinetic analysis (0–60 min) following stimulation with LPS revealed time-dependent phosphorylation of TAK1, however treatment with LAME significantly inhibited the phosphorylation of TAK-1.

LAME inhibits cytokine release

In order to explore whether other inflammatory mediators such as cytokines were affected by treatment with LAME, we analyzed levels of IL-6, TNF-α and IP-10. As expected, all cytokines were downregulated

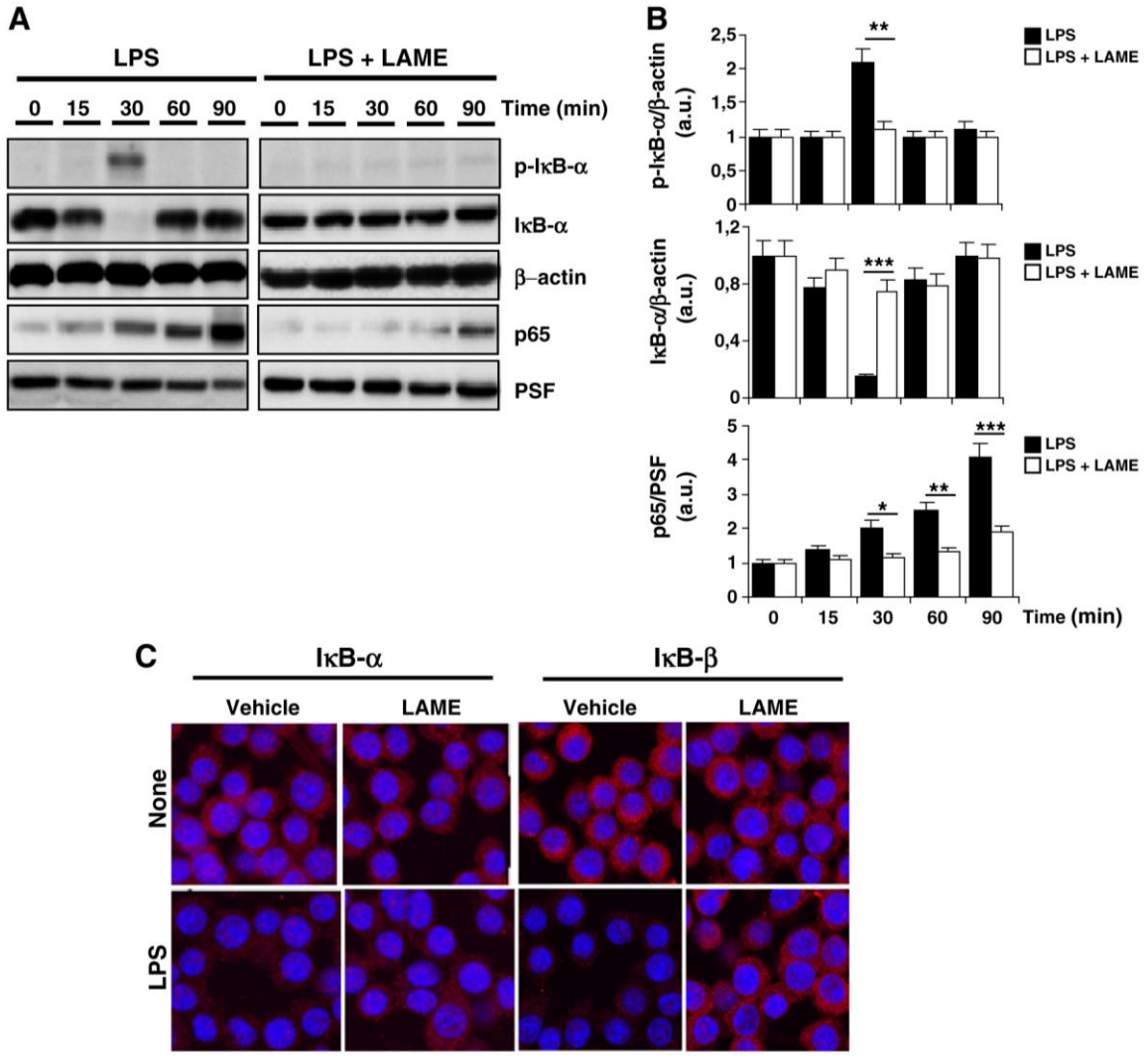

Fig. 4. *LAME inhibits NF-κB activities.* (A) Macrophages were pre-treated for 30 min with LAME (10 μM) and then activated for the indicated times (15, 30, 60 and 90 min) with 200 ng/ml LPS. The levels of p-IκBα, IκBα (cytosolic extracts) and p65 (nuclear extracts) were determined by Western blot. β-actin was used as a loading control for cytosolic extracts, and anti-PSF was used as a loading control for nuclear extracts. A representative experiment of three is shown. (B) Densitometry analysis shows the mean ± S.D. of three independent experiments of Western Blot. *P<0.05, **P<0.01, ***P<0.001. (C) Macrophages were pretreated for 30 min with LAME (10 μM) and then activated for 30 min with 200 ng/ml LPS. Fixed cells were probed with anti-IκBα and anti-IκBβ antibodies and stained with Cy3-labeled anti-rabbit IgG (red). Hoescht 42 stained nuclei are shown in blue. Cells were viewed on a MRC-1024 confocal microscope (Bio-Rad), and the fluorescence was measured and electronically evaluated. Laser sharp software (Bio-Rad) was used to determine the relative intensity of the fluorescence per pixel and the percentage of cytosolic and nuclear localization.

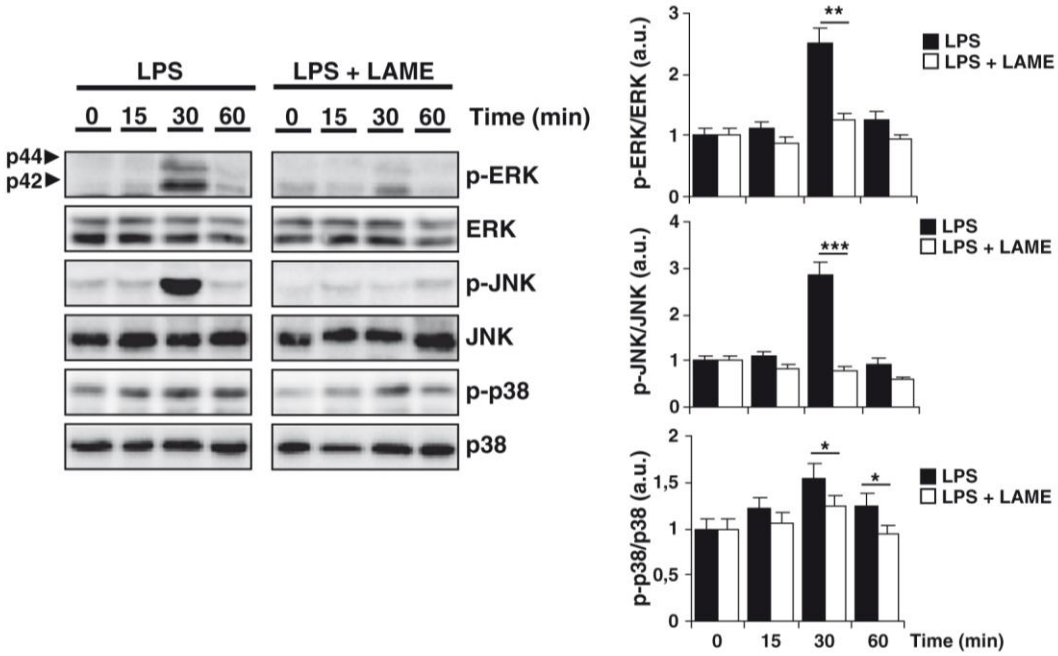

Fig. 5. *Regulation of MAPK activities by LAME.* Macrophages were pre-treated for 30 min with LAME (10 μM) and then activated for the indicated times with 200 ng/ml LPS. Levels of phospho- and total MAPKs were determined by Western blot. Representative experiments are shown of three performed. Densitometry analysis shows the mean ± S.D. of three independent experiments of Western Blot. *P<0.05, **P<0.01 and ***P<0.001.

at the protein and mRNA level in the presence of LAME after stimulation with LPS (Fig. 7).

LAME administration improves survival and attenuates the inflammatory response in endotoxemic animals

To further confirm activity of LAME *in vivo*, mice were injected with LPS in the presence or absence of LAME. The results showed that LAME significantly improved survival rate compared to untreated mice (67.50% vs 0%) (Fig. 8A), suggesting that LAME protects sepsis mice from death. Furthermore, improved survival was associated with decreased circulating cytokine levels (TNF-α and IL-6) in LAME-treated mice compared with untreated mice (Fig. 8B). These results demonstrate that LAME not only decreases the release of pro-inflammatory cytokines *in vitro* but also has the same inhibitory effect *in vivo*.

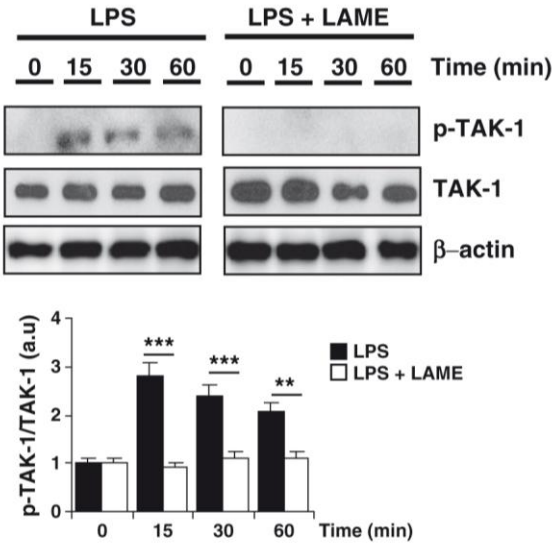

Fig. 6. *LAME inhibits TAK-1 phosphorylation.* Macrophages were pre-treated for 30 min with LAME (10 μM) and then activated for the indicated times with 200 ng/ml LPS. Levels of phospho- and total TAK-1 were determined by Western blot. β-actin content was used as a loading control. Representative experiments are shown of three performed. Densitometry analysis shows the mean ± S.D. of three independent experiments of Western Blot. **P<0.01 and ***P<0.001.

Discussion

Macrophages play a key role in the inflammatory response and serve as an essential interface between innate and adaptive immunity. On sensing the presence of pathogens through TLRs and other receptors, macrophages are stimulated to secrete a battery of cytokines that recruit effector cells into the infected area. Among TLRs, TLR4 has a dominant role in various inflammatory diseases (Zuany-Amorim et al., 2002). Stimulation of TLR4 by LPS triggers the recruitment of the cytoplasmic adaptor protein MyD88 and the activation of TAK1, which subsequently activates downstream signaling pathways such as the NF-κB and MAPKs pathways. These pathways induce the expression of various inflammatory mediators, including NO, PGs, chemokines and inflammatory cytokines that are well-known to be involved in the pathogenesis of inflammatory response (Gomez et al., 2005).

Based on these assumptions, modulation of LPS-induced TLR4 signaling or regulation of cytokine production may constitute a therapeutic strategy in many inflammatory diseases, such as bronchitis, gastritis, inflammatory bowel disease, multiple sclerosis, rheumatoid arthritis and sepsis.

The search for natural products with anti-inflammatory activity has increased enormously in recent years. Terpenoids have been identified as having a broad spectrum of biological activities, including antibacterial, antiviral, anti-inflammatory, cytotoxic, anti-tumor, etc (Castrillo et al., 2001; de Las Heras et al., 1999, 2001, 2003; Fernandez et al., 2001a, 2001b; Navarro et al., 1997, 2000, 2001; Pang et al., 1996; Xia et al., 2004). Among them, labdanes, members of the bicyclic diterpenoid group, have been identified as anti-inflammatory compounds (Chinou, 2005), through inhibition of transcription factor NF-κB signaling pathway. The molecular cascade of signaling events involved in NF-κB activation, provides several steps

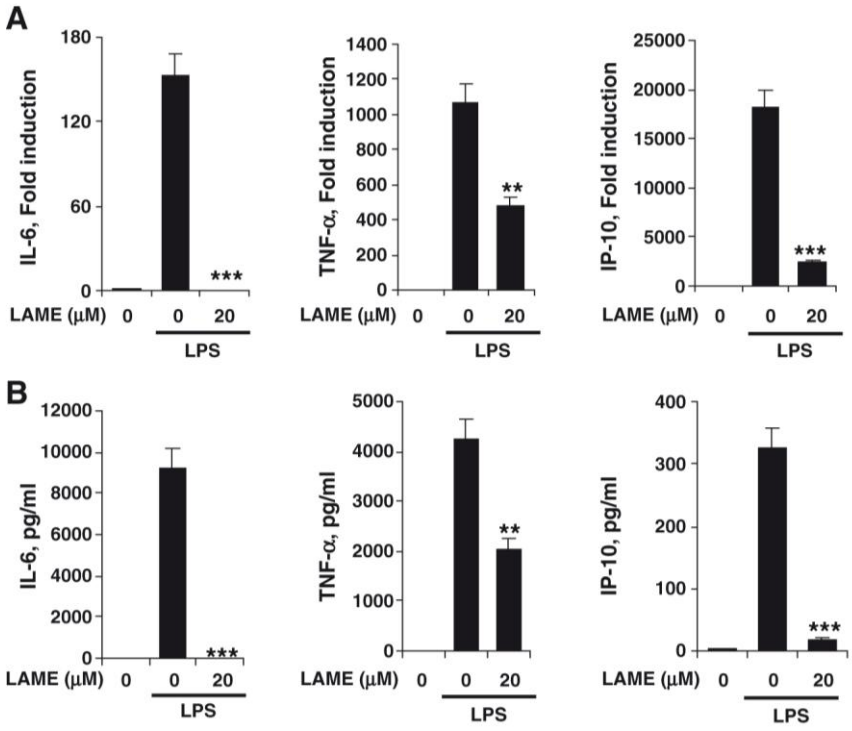

Fig. 7. *Cytokine release is inhibited by LAME.* (A) Macrophages were treated or untreated with LAME (10 μM) for 30 min followed by stimulation for 4 h with LPS 200 ng/ml. mRNA levels of IL-6, TNF-α and IP-10 were determined by quantitative PCR. (B) Macrophages were treated or untreated with LAME (10μM) for 30 min followed by stimulation for 24 h with LPS 200 ng/ml. Production of IL-6, TNF-α and IP-10 was determined in supernatant by ELISA. Results show the mean ± S.D. of three independent experiments carried out in triplicate. *P<0.05, **P<0.01, ***P<0.001 vs. LPS.

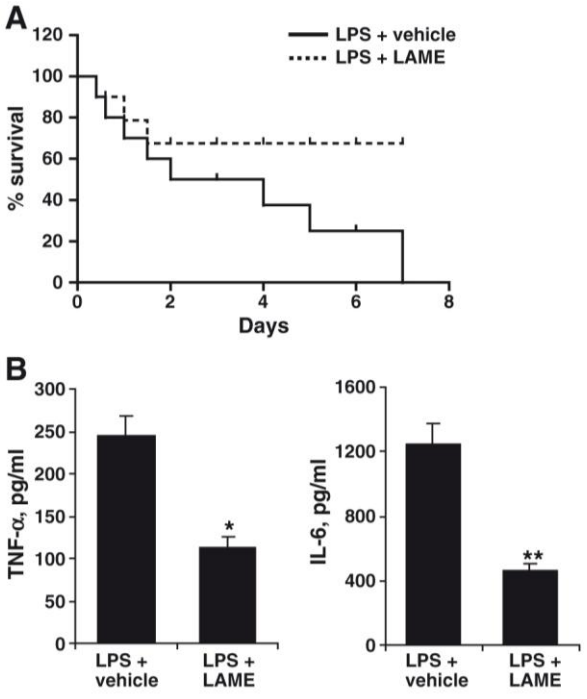

Fig. 8. *LAME increased the survival rate and reduced circulatory levels of IL-6 and TNF-α in a LPS-endotoxemic model.* Mice 8 weeks old, were injected i.p. with 10 mg/kg LPS (n = 10) or 10 mg/kg LPS and LAME 20 mg/kg (n = 10). Mice survival was monitored at intervals of 12 h for 7 days. (A) The overall difference in survival rate between the groups with and without LAME was significant (P<0.01). (B) Serum levels of TNF-α and IL-6 were assayed with ELISA kits. Results are expressed as mean ± SD. *P<0.05 and ** P<0.01.

for specific inhibition of NF-κB activity. In unstimulated cells, NF-κB is sequestered in the cytoplasm by association with the inhibitory proteins IκB (Hayden and Ghosh, 2004). In response to an extracellular signal (e.g., inflammatory cytokines, mitogens, bacterial products, or oxidative stress), IκB is phosphorylated by IκB kinases (IKKs) at specific serine residues. The phosphorylation is followed by Lys48-linked (UbK48) polyubiquitination of IκB, which marks the protein for degradation by the 26S proteasome (Ghosh and Karin, 2002). Degradation of IκB allows the NF-κB to translocate to the nucleus, where it binds to the promoter region of various genes. Thus, inhibition of NF-κB activation can occur by different mechanisms including (a) inhibiting the activation of IKK complex, (b) targeting the proteasomal degradation of or (c) interfering the translocation of NF-κB to the nucleus, or the binding of NF-κB to DNA. Nevertheless, the most effective and selective approach for the inhibition of NF-κB activation is provided by inhibitors of the IKK activity (Bremner and Heinrich, 2002; Karin et al., 2004). In this context, several labdanes-type diterpenes such as andalusol and hispanolone derivatives have been reported specifically targeting the IKK kinase activity (de Las Heras et al., 1999; Girón et al., 2008). In the present study, we have extended the analysis of the biological activities of labdane diterpenes by evaluating the effects of LAME, on LPS-induced inflammation *in vitro* and *in vivo*, in an attempt to explore the mechanisms involved in its anti-inflammatory effects. We have shown that LAME inhibits the production of NO and PGE_2 in LPS-stimulated macrophages and that this inhibitory effect is not mediated by cytotoxic effects on macrophages. Inhibition of NO and PGE_2 production was accompanied by concentration-dependent decreases in the expression of NOS-2 and COX-2 protein and mRNA, indicating that the impaired release of NO and PGE_2 can be attributed to inhibition of NOS-2 and COX-2 expression at the transcriptional level.

On the other hand, cytokines like TNF-α and IL-6 have been reported to be pro-inflammatory *in vitro* and *in vivo*, thus TNF-α

elicits a number of physiological effects that include septic shock, inflammation, cachexia, and cell death and is known to be crucial for the induction of NO synthesis in IFN-γ and/or LPS-stimulated macrophages. Similarly, IL-6 is an endogenous mediator of LPS-induced fever. Our findings show that LAME efficiently inhibited cytokine release (TNF-α, IL-6 and IP-10) by LPS-stimulated macrophages.

Overproduction and release of inflammatory mediators (NO and PGs) and cytokines (TNF-α, and IL-6) are mediated by the activation of inducible transcription factors, such as NF-κB (Karin and Ben Neriah, 2000).

In the present study, we found that LAME inhibits LPS-induced IκBα phosphorylation and degradation, and p65 nuclear translocation, indicating that its anti-inflammatory actions are at least partially mediated by inhibition of NF-κB-dependent gene transcription.

In addition to NF-κB activation, the stimulation of macrophage TLR4 receptor rapidly leads to the activation of different MAPK cascades, which ultimately results in the activation of p38, ERK and JNK. Our data shows that LAME inhibits ERK and JNK phosphorylation/activation indicating that the beneficial effect of this compound is mediated by different pathways.

Suppression of phosphorylation events for NF-κB and MAPK strongly suggested that the target of LAME could be activated at an earlier time in response to LPS. TAK1, a well-characterized MAPK kinase kinase family member, has emerged as a key regulator of signal transduction cascades leading to the activation of the transcription factors NF-κB and AP-1. Accumulating evidence suggests that the activation of TAK1 in response to different stimuli TNF-α, IL-1β, IL-18, RANKL, osmotic stress, TLR and BCR and upon Ag stimulation (Shim et al., 2005; Wald et al., 2001; Wang et al., 2001) is a common signal for activating downstream targets such as IKK and MAPK (Chen et al., 2006; Cuevas et al., 2007). Thus, this kinase may represent a novel site for pharmacological intervention in a number of inflammatory conditions. LAME prevented LPS-induced TAK-1 phosphorylation, suggesting that this compound inhibited LPS-induced inflammation by interference with this kinase.

In addition to these *in vitro* data, LAME also showed anti-inflammatory activity *in vivo*. In animals treated with LPS and LAME, circulating levels of the pro-inflammatory cytokines IL-6 and TNF-α were all significantly reduced in comparison to LPS-treated animals. Moreover, LAME treatment increased survival in sepsis mice.

In summary, our data demonstrate that LAME has potent anti-inflammatory activity in macrophages, as indicated by transcriptional inhibition of NOS-2 and COX-2 expression and activity and impaired cytokine release. These effects are mediated by the inhibition of TAK-1 activation, thereby resulting in the blockade of downstream IKK and MAPKs signaling transduction pathways. The possible regulatory mechanism of repression of LPS-induced inflammation by LAME is summarized in Fig. 9. Finally, the low cytotoxicity of LAME and its effectiveness as anti-inflammatory agent *in vivo* indicate that LAME has potential use in the treatment of inflammatory diseases, and could have therapeutic potential for reducing inflammatory responses during sepsis or for allergic cutaneous disorders such as allergic contact dermatitis and atopic dermatitis.

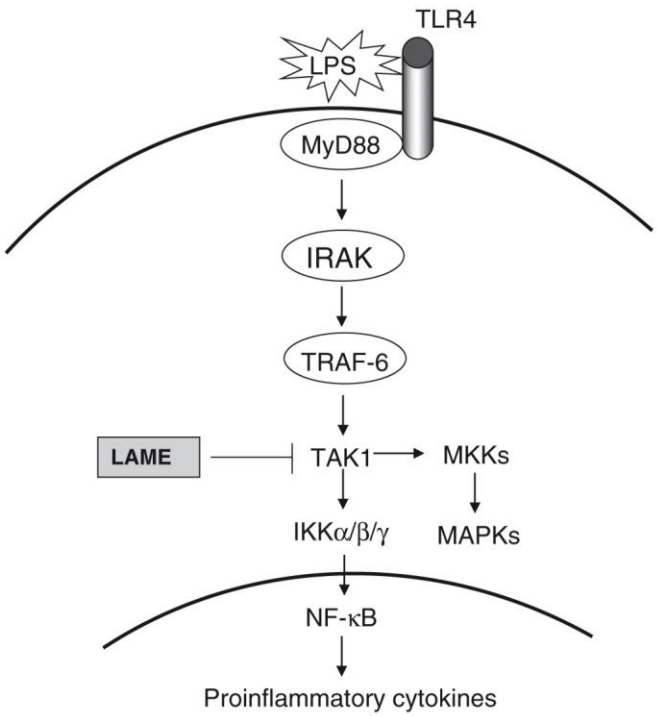

Fig. 9. *A proposed model for the anti-inflammatory effects of LAME.* Upon LPS stimulation, TLR4 triggers the recruitment of the cytoplasmic adaptor protein MyD88 and the activation of TAK1, which subsequently activates downstream signaling pathways such as the NF-κB and MAPKs pathways. These pathways induce the expression of various inflammatory mediators, including NO, PGs, chemokines and inflammatory cytokines that are well-known to be involved in the pathogenesis of inflammatory response. LAME inhibits TAK-1 activation, resulting in blocking downstream IKK and MAPKs signaling transduction and decreasing the release of inflammatory mediators.

Conflict of interest

The authors disclose any potential conflict of interest.

Acknowledgments

This work was supported by grants PI08.0070 from FIS, MPY 1410/09 from ISCIII and Fundación Mutua Madrileña to S.H, by a Santander-Complutense grant to S.H. and B. de las H. We also thank the financial support from the Spanish MICINN (SAF2009-13296-C02-01) and ICIC (Instituto Canario de Investigación del Cáncer) to AEB.

References

Bremner, P., Heinrich, M., 2002. Natural products as targeted modulators of the nuclear factor-kappaB pathway. J. Pharm. Pharmacol. 54, 453–472.
Butler, M.S., Newman, D.J., 2008. Mother Nature's gifts to diseases of man: the impact of natural products on anti-infective, anticholestemics and anticancer drug discovery. Prog. Drug Res 65, 1,3–1,44.
Castrillo, A., de las Heras, B., Hortelano, S., Rodriguez, B., Villar, A., Bosca, L., 2001. Inhibition of the nuclear factor kappa B (NF-kappa B) pathway by tetracyclic kaurene diterpenes in macrophages. Specific effects on NF-kappa B-inducing kinase activity and on the coordinate activation of ERK and p38 MAPK. J. Biol. Chem. 276, 15854–15860.
Chen, Z.J., Bhoj, V., Seth, R.B., 2006. Ubiquitin, TAK1 and IKK: is there a connection? Cell Death Differ. 13, 687–692.
Chinou, I., 2005. Labdanes of natural origin-biological activities (1981–2004). Curr. Med. Chem. 12, 1295–1317.
Cuevas, B.D., Abell, A.N., Johnson, G.L., 2007. Role of mitogen-activated protein kinase kinase kinases in signal integration. Oncogene 26, 3159–3171.
De Kimpe, S.J., Hunter, M.L., Bryant, C.E., Thiemermann, C., Vane, J.R., 1995. Delayed circulatory failure due to the induction of nitric oxide synthase by lipoteichoic acid from *Staphylococcus aureus* in anaesthetized rats. Br. J. Pharmacol. 114, 1317–1323.
de las Heras, B., Hortelano, S., 2009. Molecular basis of the anti-inflammatory effects of terpenoids. Inflamm. Allergy Drug Targets 8, 28–39.
de las Heras, B., Navarro, A., Diaz-Guerra, M.J., Bermejo, P., Castrillo, A., Bosca, L., Villar, A., 1999. Inhibition of NOS-2 expression in macrophages through the inactivation of NF-kappaB by andalusol. Br. J. Pharmacol. 128, 605–612.
de las Heras, B., Abad, M.J., Silvan, A.M., Pascual, R., Bermejo, P., Rodriguez, B., Villar, A.M., 2001. Effects of six diterpenes on macrophage eicosanoid biosynthesis. Life Sci. 70, 269–278.
de las Heras, B., Rodriguez, B., Bosca, L., Villar, A.M., 2003. Terpenoids: sources, structure elucidation and therapeutic potential in inflammation. Curr. Top. Med. Chem. 3, 171–185.
Fernandez, M.A., de las Heras, B., Garcia, M.D., Saenz, M.T., Villar, A., 2001a. New insights into the mechanism of action of the anti-inflammatory triterpene lupeol. J. Pharm. Pharmacol. 53, 1533–1539.
Fernandez, M.A., Tornos, M.P., Garcia, M.D., de las Heras, H.B., Villar, A.M., Saenz, M.T., 2001b. Anti-inflammatory activity of abietic acid, a diterpene isolated from *Pimenta racemosa* var. grissea. J. Pharm. Pharmacol. 53, 867–872.
Ghosh, S., Karin, M., 2002. Missing pieces in the NF-kappaB puzzle. Cell 109 (Suppl), S81–S96.
Girón, N., Traves, P.G., Rodriguez, B., Lopez-Fontal, R., Bosca, L., Hortelano, S., de las Heras, H.B., 2008. Suppression of inflammatory responses by labdane-type diterpenoids. Toxicol. Appl. Pharmacol. 228, 179–189.

Girón, N., Perez-Sacau, E., Lopez-Fontal, R., Amaro-Luis, J.M., Hortelano, S., Estevez-Braun, A., de las Heras, H.B., 2010. Evaluation of labdane derivatives as potential anti-inflammatory agents. Eur. J. Med. Chem. 45, 3155–3161.
Gomez, P.F., Pillinger, M.H., Attur, M., Marjanovic, N., Dave, M., Park, J., Bingham III, C.O., Al Mussawir, H., Abramson, S.B., 2005. Resolution of inflammation: prostaglandin E2 dissociates nuclear trafficking of individual NF-kappaB subunits (p65, p50) in stimulated rheumatoid synovial fibroblasts. J. Immunol. 175, 6924–6930.
Hayden, M.S., Ghosh, S., 2004. Signaling to NF-kappaB. Genes Dev. 18, 2195–2224.
Hemmi, H., Takeuchi, O., Kawai, T., Kaisho, T., Sato, S., Sanjo, H., Matsumoto, M., Hoshino, K., Wagner, H., Takeda, K., Akira, S., 2000. A Toll-like receptor recognizes bacterial DNA. Nature 408, 740–745.
Hortelano, S., Zeini, M., Castrillo, A., Alvarez, A.M., Bosca, L., 2002. Induction of apoptosis by nitric oxide in macrophages is independent of apoptotic volume decrease. Cell Death Differ. 9, 643–650.
Hueso-Falcón, I., Cuadrado, I., Cidre, F., Amaro-Luis, J.M., Ravelo, A.G., Estevez-Braun, A., de las Heras, B., Hortelano, S., 2011. Synthesis and anti-inflammatory activity of ent-kaurene derivatives. Eur. J. Med. Chem. 46, 1291–1305.
Janssen-Heininger, Y.M., Poynter, M.E., Baeuerle, P.A., 2000. Recent advances towards understanding redox mechanisms in the activation of nuclear factor kappaB. Free Radic. Biol. Med. 28, 1317–1327.
Karin, M., Ben Neriah, Y., 2000. Phosphorylation meets ubiquitination: the control of NF-[kappa]B activity. Annu. Rev. Immunol. 18, 621–663.
Karin, M., Yamamoto, Y., Wang, Q.M., 2004. The IKK NF-kappa B system: a treasure trove for drug development. Nat. Rev. Drug Discov. 3, 17–26.
Kawai, T., Akira, S., 2006. TLR signaling. Cell Death Differ. 13, 816–825.
Keating, S.E., Maloney, G.M., Moran, E.M., Bowie, A.G., 2007. IRAK-2 participates in multiple toll-like receptor signaling pathways to NF-κB via activation of TRAF6 ubiquitination. J. Biol. Chem. 282, 33435–33443.
Lee, M.S., Kim, Y.J., 2007. Signaling pathways downstream of pattern-recognition receptors and their cross talk. Annu. Rev. Biochem. 76, 447–480.
Matsuda, H., Morikawa, T., Sakamoto, Y., Toguchida, I., Yoshikawa, M., 2002. Labdane-type diterpenes with inhibitory effects on increase in vascular permeability and nitric oxide production from Hedychium coronarium. Bioorg. Med. Chem. 10, 2527–2534.
Navarro, A., de las Heras, B., Villar, A.M., 1997. Andalusol, a diterpenoid with anti-inflammatory activity from Siderits foetens Clemen. Z. Naturforsch. C 52, 844–849.
Navarro, A., de las Heras, B., Villar, A., 2000. Immunomodulating properties of the diterpene andalusol. Planta Med. 66, 289–291.
Navarro, A., de las Heras, B., Villar, A., 2001. Anti-inflammatory and immunomodulating properties of a sterol fraction from Sideritis foetens Clem. Biol. Pharm. Bull. 24, 470–473.
Pang, L., de las Heras, B., Hoult, J.R., 1996. A novel diterpenoid labdane from *Sideritis javalambrensis* inhibits eicosanoid generation from stimulated macrophages but enhances arachidonate release. Biochem. Pharmacol. 51, 863–868.
Poltorak, A., He, X., Smirnova, I., Liu, M.Y., Van Huffel, C., Du, X., Birdwell, D., Alejos, E., Silva, M., Galanos, C., Freudenberg, M., Ricciardi-Castagnoli, P., Layton, B., Beutler, B., 1998. Defective LPS signaling in C3H/HeJ and C57BL/10ScCr mice: mutations in Tlr4 gene. Science 282, 2085–2088.
Schnare, M., Barton, G.M., Holt, A.C., Takeda, K., Akira, S., Medzhitov, R., 2001. Toll-like receptors control activation of adaptive immune responses. Nat. Immunol. 2, 947–950.
Schulze-Osthoff, K., Ferrari, D., Riehemann, K., Wesselborg, S., 1997. Regulation of NF-kappa B activation by MAP kinase cascades. Immunobiology 198, 35–49.
Shim, J.H., Xiao, C., Paschal, A.E., Bailey, S.T., Rao, P., Hayden, M.S., Lee, K.Y., Bussey, C., Steckel, M., Tanaka, N., Yamada, G., Akira, S., Matsumoto, K., Ghosh, S., 2005. TAK1, but not TAB1 or TAB2, plays an essential role in multiple signaling pathways in vivo. Genes Dev. 19, 2668–2681.
Takaesu, G., Ninomiya-Tsuji, J., Kishida, S., Li, X., Stark, G.R., Matsumoto, K., 2001. Interleukin-1 (IL-1) receptor-associated kinase leads to activation of TAK1 by inducing TAB2 translocation in the IL-1 signaling pathway. Mol. Cell. Biol. 21, 2475–2484.
Takeda, K., Kaisho, T., Akira, S., 2003. Toll-like receptors. Annu. Rev. Immunol. 21, 335–376.
Takeuchi, O., Hoshino, K., Kawai, T., Sanjo, H., Takada, H., Ogawa, T., Takeda, K., Akira, S., 1999. Differential roles of TLR2 and TLR4 in recognition of gram-negative and gram-positive bacterial cell wall components. Immunity 11, 443–451.
Wald, D., Commane, M., Stark, G.R., Li, X., 2001. IRAK and TAK1 are required for IL-18-mediated signaling. Eur. J. Immunol. 31, 3747–3754.
Wang, C., Deng, L., Hong, M., Akkaraju, G.R., Inoue, J., Chen, Z.J., 2001. TAK1 is a ubiquitin-dependent kinase of MKK and IKK. Nature 412, 346–351.
Xia, Y.F., Ye, B.Q., Li, Y.D., Wang, J.G., He, X.J., Lin, X., Yao, X., Ma, D., Slungaard, A., Hebbel, R.P., Key, N.S., Geng, J.G., 2004. Andrographolide attenuates inflammation by inhibition of NF-kappa B activation through covalent modification of reduced cysteine 62 of p50. J. Immunol. 173, 4207–4217.
Zeini, M., Traves, P.G., Lopez-Fontal, R., Pantoja, C., Matheu, A., Serrano, M., Bosca, L., Hortelano, S., 2006. Specific contribution of p19(ARF) to nitric oxide-dependent apoptosis. J. Immunol. 177, 3327–3336.
Zuany-Amorim, C., Hastewell, J., Walker, C., 2002. Toll-like receptors as potential therapeutic targets for multiple diseases. Nat. Rev. Drug Discov. 1, 797–807.

Capítulo 3

Labdane diterpenes protect against anoxia/reperfusion injury in cardiomyocytes: involvement of Akt activation.

***Cell Death and Disease**,* doi: 10.1038cddis.2011 (2011)

Labdane diterpenes protect against anoxia/reperfusion injury in cardiomyocytes: involvement of AKT activation.

Irene Cuadrado, María Fernández-Velasco, Lisardo Boscá and Beatriz de las Heras

***Cell Death and Disease**,* doi: 10.1038cddis.2011 (2011)

Este estudio tuvo como objetivo evaluar el efecto cardioprotector de tres derivados del diterpeno labdánico hispanolona (**T1**: dehidrohispanolona, **T2**: 8,9-dehidrohispanolona 15,16-lactol y **T3**: 14,15,16-trisnor-13,9α-hispanolida) en un modelo de anoxia/reoxigenación (A/R) en cardiomiocitos, estudiando los mecanismos moleculares implicados.

Los diterpenos **T1** y **T2** mostraron actividad cardioprotectora frente al estímulo A/R, tanto en la línea celular H9c2 como en cardiomiocitos aislados de rata. En ambos modelos, estos diterpenos, especialmente **T1**, ejercieron una acción protectora frente a la muerte por apoptosis en células sometidas a daño por A/R, evidenciada por la disminución del porcentaje de células apoptóticas y caspasa-3 positivas. Además, el tratamiento con **T1** y **T2** mostró un perfil antiapoptótico al reducir el cociente Bcl-2/Bax y aumentar la expresión de proteínas como xIAP o Hsp70.

El efecto cardioprotector estaba mediado por un aumento de proteínas implicadas en vías de supervivencia (AKT y ERK 1/2), así como por la activación de AMPK, proteína implicada en la homeostasis energética.

Estos resultados muestran el efecto cardioprotector de estos compuestos, no descrito hasta el momento, lo que abre nuevas posibilidades al estudio de los diterpenos de tipo labdano como potenciales agentes en enfermedades cardiovasculares.

Citation: Cell Death and Disease (2011) 2, e229; doi:10.1038/cddis.2011.113

www.nature.com/cddis

Labdane diterpenes protect against anoxia/reperfusion injury in cardiomyocytes: involvement of AKT activation

I Cuadrado[1], M Fernández-Velasco[2], L Boscá*[,2] and B de las Heras*[,1]

Several labdane diterpenes exert anti-inflammatory and cytoprotective actions; therefore, we have investigated whether these molecules protect cardiomyocytes in an anoxia/reperfusion (A/R) model, establishing the molecular mechanisms involved in the process. The cardioprotective activity of three diterpenes (T1, T2 and T3) was studied in the H9c2 cell line and in isolated rat cardiomyocyte subjected to A/R injury. In both cases, treatment with diterpenes T1 and T2 protected from A/R-induced apoptosis, as deduced by a decrease in the percentage of apoptotic and caspase-3 active positive cells, a decrease in the Bcl-2/Bax ratio and an increase in the expression of antiapoptotic proteins. Analysis of cell survival signaling pathways showed that diterpenes T1 and T2 added after A/R increased phospho-AKT and phospho-ERK 1/2 levels. These cardioprotective effects were lost when AKT activity was pharmacologically inhibited. Moreover, the labdane-induced cardioprotection involves activation of AMPK, suggesting a role for energy homeostasis in their mechanism of action. Labdane diterpenes (T1 and T2) also exerted cardioprotective effects against A/R-induced injury in isolated cardiomyocytes and the mechanisms involved activation of specific survival signals (PI3K/AKT pathways, ERK1/2 and AMPK) and inhibition of apoptosis.
Cell Death and Disease (2011) **2,** e229; doi:10.1038/cddis.2011.113; published online 10 November 2011
Subject Category: Experimental Medicine

Cardiac injury due to ischemia (anoxia)/reperfusion (I(A)/R) is caused by two main mechanisms, apoptosis and necrosis, the latter being accelerated by reperfusion.[1–5] Knowledge of molecular mechanisms involved in A/R reveals that cardioprotection is afforded by activation during reperfusion of the anti-apoptotic and prosurvival kinase signaling cascades PI3K-AKT and p42/p44 extracellular signal-regulated kinases (ERK1/2).[6,7] Early activation of ERK1/2 inhibits procaspase processing and induces the expression of proteins of the anti-apoptotic Bcl-2 family (Bcl-2 and Bcl-xL). Thus, therapeutic strategies that target and attenuate reperfusion-induced injury may provide novel pharmacological agents, which can be used in current early reperfusion maneuvring, the established standard therapy for acute myocardial infarction. As no drugs to reduce reperfusion injury are currently available for clinical use,[8] it is interesting to search for new interventions administered at the time of reperfusion.

Bioactive natural products can be considered as very promising molecules for the development of new therapeutic agents and terpenes, which constitute one of the groups with great therapeutic potential.[9–12] In particular, diterpenes have shown a broad spectrum of biological activities (antibacterial, antiviral, anti-inflammatory, cytotoxic, antitumour, etc), regulating inflammation and the innate immune response.[13–17] Our previous findings on the anti-inflammatory and cytoprotective effects of diterpenes[9,10,14] prompted us to evaluate a possible therapeutic intervention for cardioprotection (to ameliorate A/R injury). In the present study, we have analyzed targets relevant to the reperfusion injury in an A/R model in cardiomyocytes in order to explore the mechanisms involved in the cardioprotective potential of three labdane diterpenes (Figure 1a). Our data show that two of these diterpenes (T1 and T2) exert significant cardioprotection against A/R injury through inhibition of apoptosis and activation of survival pathways.

Results

The labdane diterpenes T1 and T2 protected H9c2 cells from A/R-induced apoptosis. We first examined the viability of H9c2 cells after treatment with diterpenes (0–100 μM), using an MTT assay. As seen in Figure 2a, these diterpenes did not significantly affect cell viability at concentrations below 20 μM, and this dose was selected as the maximal concentration for the subsequent studies. Initial experiments using the experimental protocol shown in

[1]Departamento de Farmacología, Facultad de Farmacia, Universidad Complutense de Madrid, Madrid, Spain and [2]Instituto de Investigaciones Biomédicas 'Alberto Sols' (CSIC-UAM), Madrid, Spain
*Corresponding authors: L Boscá, Instituto de Investigaciones Biomédicas 'Alberto Sols' (CSIC-UAM), Arturo Duperier 4, 28029 Madrid, Spain. Tel: +34 9149 72747; Fax: +34 9158 54401; E-mail: lbosca@iib.uam.es
or B de las Heras, Departamento de Farmacología, Facultad de Farmacia, Universidad Complutense de Madrid, Plaza Ramón y Cajal s/n, 28040 Madrid, Spain. Tel: +34 9139 42276; Fax: +34 9139 41726; E-mail: lasheras@farm.ucm.es
Keywords: labdane diterpenes; apoptosis; AKT; ERK; AMPK; cardioprotection
Abbreviations: A/R, anoxia/reperfusion; AMPK, AMP-kinase; DMSO, dimethyl sulfoxide; ATCC, American Type Culture Collection; ERK, extracellular signal regulated-kinase; JNK, c-Jun N-terminal kinase; LDH, lactate dehydrogenase; MAPK, mitogen-activated protein kinase; PI3K, phosphatidylinositol 3-kinase; qRT-PCR, quantitative real-time (RT) polymerase chain reaction (PCR); SDS-PAGE, sodium dodecyl sulphate polyacrylamide gel electophoresis; T1, (dehydroisohispanolone); T2, (8,9-dehydrohispanolone 15,16-lactol); T3, (14,15,16-trisnor-13,9α-hispanolide)
Received 28.7.11; revised 21.9.11; accepted 04.10.11; Edited by RA Knight

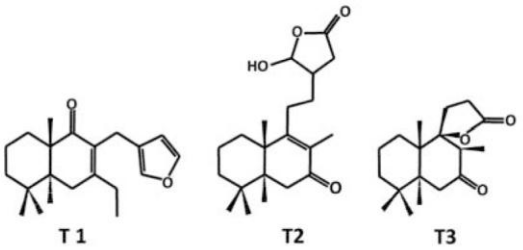

Figure 1 Chemical structure of the labdane diterpenes. Chemical structures of the labdane diterpenes derived from the hispanolone (T1, T2 and T3)

Figure 2b were designed to determine the time course in the loss of cell viability after A/R-dependent injury (Figure 2c). A/R caused a marked increase of LDH activity in the culture medium, an index of myocyte injury (Figure 2d). Addition of diterpenes T1 and to a lesser extent of T2 at 20 μM for 4 h and 6 h during reoxygenation, significantly reduced the levels of LDH released in response to A/R, whereas T3 was inactive. Figure 2e shows the dose-dependent protection exerted by T1 and T2 at 6 h after reoxygenation and Figure 2f shows the loss of protection when the diterpenes were added late after reoxygenation.

The number of apoptotic cells, which were detected as TUNEL-positive nuclei, significantly decreased in cardiomyocytes exposed to A/R and incubated with T1 during reoxygenation (6 h), and to a lesser but significant extent with T2 (Figure 2g, left). Agreement was observed between the TUNEL data and the percentage of cells with active caspase-3 as determined by the CaspGlow assay (Figure 2g, right). Quantitative analysis of these data is shown in Figure 2h. Similar data were obtained when the effects of the diterpenes T1 and T2 on caspase-3 activity and protein content were determined using specific caspase substrates and antibodies (Figures 2I and J).

T1 and T2 modulated early signaling favoring an antiapoptotic response after A/R challenge. We next studied the effects of the diterpenes on proteins involved in survival and apoptotic pathways. In this analysis, expression of proapoptotic proteins such as Bax was markedly increased 6 h after A/R, but remained unchanged in cells treated with T1 and T2. In contrast, anti-apoptotic proteins (Bcl-2 and Bcl-xL) exhibited lesser regulation. Moreover, the levels of Hsp70 and the inhibitory protein xIAP also increased after treatment of cells with diterpenes for 6 h after A/R (Figure 3a). The Bax/Bcl-2 ratio increased in H9c2 cells after A/R compared with normoxic cells, and this increase was significantly impaired by treatment with T1 and T2 (Figure 3a), all these data suggesting that these compounds favor an antiapoptotic profile.

AKT and ERK activation are involved in the protective effects of T1 and T2. Previous results led us to investigate early signaling involved in apoptosis regulation, in particular AKT and MAPKs activities, and the energetic metabolism modulated through AMPK. An initial analysis revealed that both diterpenes induced a time-dependent increase (up to 1 h) in the levels of phospho-AKT in cells incubated with T1 and T2 (Figure 3b). Moreover, addition of T1 and T2 after A/R also induced phosphorylation of AKT (both in S473 and T308), an effect suppressed by pretreatment with a PI3K inhibitor (LY294002) and/or AKT inhibitor (Figure 3c). Interestingly, inhibition of the PI3K pathway attenuated the effects of T1 on A/R-induced upregulation of Bax and on the active caspase-3 levels. Inhibition of AKT suppressed the protective effects exerted by T1 (Figure 3c). In addition, measurement of caspase-3 activity and cell viability confirmed the relevance of the AKT and to a lesser extent of the PI3 K pathways in mediating the effects of T1 after A/R (Figure 3d). MAPKs have been reported to modulate apoptosis in the heart.[18,19] We therefore examined the activation state of the distinct MAPK pathways to assess their potential involvement in the cardioprotective actions of the diterpenes. A significant basal phosphorylation of ERK1/2 was observed in H9c2 cells exposed to A/R. However, incubation of cells with T1 and T2 resulted in a marked activation of ERK phosphorylation after A/R, whereas the total protein expression of this kinase remained constant. In contrast, the levels of phospho-p38 were unaffected. As seen in Figure 3e, phospho-JNK was not modulated at the times of sampling. To point out, from an energetic aspect, phospho-AMPK levels were enhanced by diterpenes after A/R.

When other stimuli apart from A/R were used to induce apoptosis (H_2O_2, etoposide or staurosporine) the protective effects of diterpenes T1 and T2 were not observed (Figure 4). Minimal protection by T1 and T2 was found against H_2O_2, but not against etoposide and staurosporine, suggesting a specific protection against A/R injury by these diterpenes.

T1 and T2 protected primary cultures of rat cardiomyocyte against A/R injury. To confirm the cardioprotective effects of diterpenes T1 and T2 observed in H9c2 cells, we moved to primary cultures of rat cardiomyocytes subjected to A/R, following the same protocol as above. Addition of T1 and T2 significantly protected cardiomyocytes against A/R-induced injury, as deduced by the decrease in the release of LDH to the culture medium; again, T3 showed a weak activity (Figure 5a). Treatment with T1 and T2 also impaired pro-caspase-3 processing after A/R (Figure 5b). Expression of Bax following A/R was also attenuated in cells treated with diterpenes, whereas Bcl-2 and xIAP levels remained unaffected (Figure 5b).

The cardioprotective effects exerted by diterpenes in H9c2 cells involved an increase of phosphorylated AKT, ERK1/2 and AMPK levels that were confirmed in isolated cardiomyocytes (Figures 5c and d). Phospho-p38 levels were moderately increased after A/R regardless of the presence of the diterpenes and phospho-JNK remained dephosphorylated. (Figure 5d).

Discussion

Protection of the heart from I(A)/R injury still represents a great challenge in the search for new pharmacological agents.[20–22] Myocardial ischemia is due to blockage of the blood flow in the myocardium, leading to a significant change in the energy balance including depletion of ATP. A

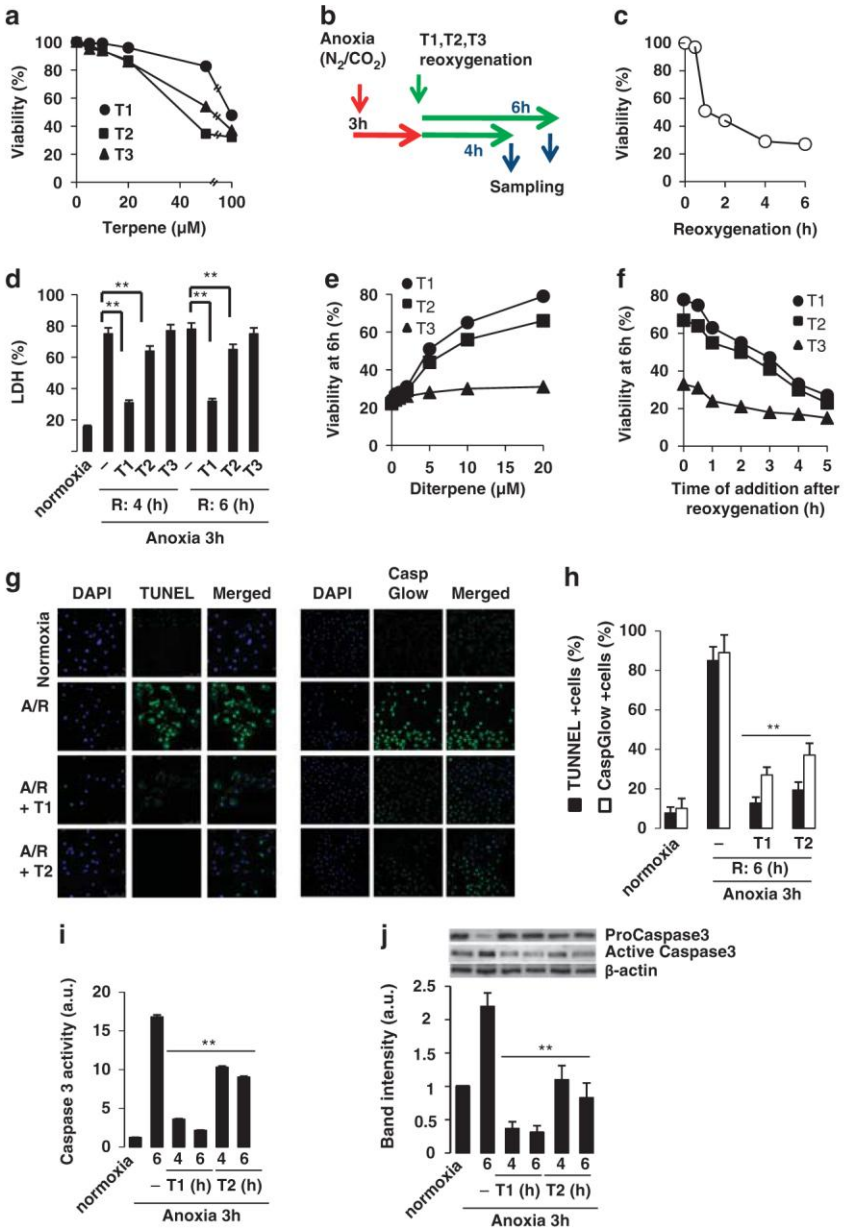

Figure 2 Labdane diterpenes protect H9c2 cells from A/R-induced injury. (**a**) Viability of H9c2 cells incubated for 24 h with diterpenes (0–100 μM), measured by the MTT assay. (**b**) Schematic diagram of the experimental protocol (T: diterpenes). (**c**) Time-dependent effect of reoxygenation on cell viability (MTT assay). (**d**) LDH release after A/R (4–6 h). Diterpenes were added prior reoxygenation. 100% LDH activity was achieved after addition of 0.5% Triton X-100 to the cell culture. $^{**}P<0.01$ treatments *versus* Triton X-100. (**e**) Dose-dependent effect of diterpenes on cell viability at 6 h after A/R. (**f**) Effect of delayed-addition of diterpenes after A/R. Cell viability was determined by the MTT assay at 6 h after reoxygenation and expressed as cell viability (%) *versus* normoxic cells. (**g**) TUNEL positive cells (*left*) and caspase active positive cells (*right*) expressed as percentage of total cells in diterpene-treated cells *versus* non-treated cells. $^{**}P<0.01$ compared *versus* A/R in the absence of diterpene. (**h**) *In situ* evaluation of caspase-3 activation. The percentage of caspase-3 positive cells was determined by fluorescence microscopy using the CaspGlow staining kit. (**i**) Caspase-3 activity and (**j**) protein levels of pro-caspase-3 and active caspase-3 were determined in cytosolic extracts from cells after A/R and treated with diterpenes T1 and T2. Lane charge was normalized with β-actin. Western blots were performed in triplicate. Results show the mean ± S.D. of three experiments. $^{**}P<0.01$ treatments *versus* A/R in the absence of diterpene

compensatory response emerges in the cardiomyocytes from the inhibition of fatty acid oxidation to an increase in the flux toward anaerobic glycolysis.[4,5,23,24] Although the drop in ATP during ischemia inhibits several basic cell processes, including membrane sodium/potassium-ATPase, reperfusion of the myocardium triggers a rapid increase in intracellular calcium that promotes opening of the mitochondrial permeability transition pore leading to the release of proapoptotic mediators and reactive oxygen species that are key factors in cardiac dysfunction.[25] In this scenario, we have evaluated the role of labdane diterpenes, members of the bicyclic diterpenoid group, that are potent anti-inflammatory molecules in immune cells and also exhibit cell-protective effects.[13] In previous studies, we analyzed a series of labdane diterpenes, some of them showing potent anti-inflammatory activity by decreasing the release of inflammatory mediators

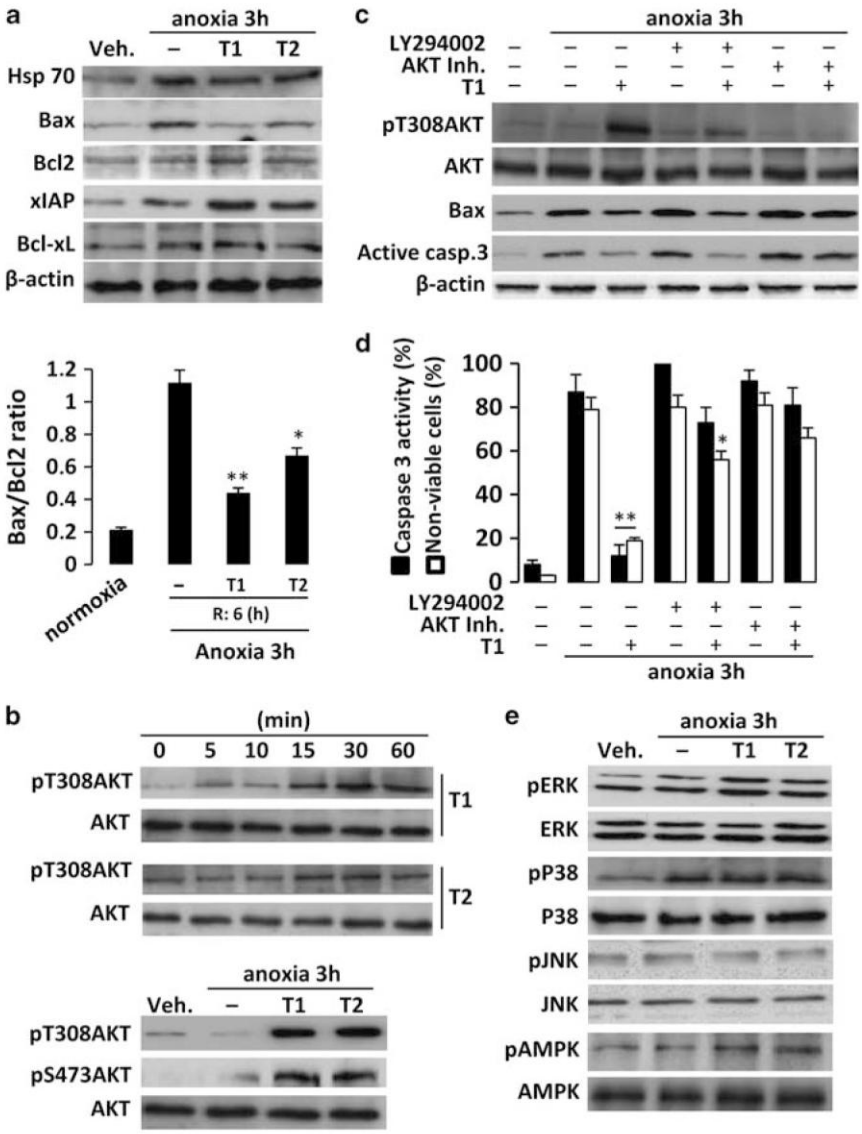

Figure 3 Diterpenes T1 and T2 promote AKT and ERK activation and favor the Bcl-2 family antiapoptotic proteins profile. (**a**) Levels of Hsp70, Bax, Bcl-2, xIAP and Bcl-xL were determined by western blot from cytosolic extracts from diterpene-treated cells. Protein loading was normalized with β-actin. The Bax/Bcl-2 ratio was determined at 6 h after reoxygenation. (**b**) Time-course of phosphorylation of AKT was determined under normoxic conditions and after A/R. Representative western blots were performed with cytosolic extracts from cells treated with T1 and T2. The samples were immunoblotted and probed with anti-phospho-T308-AKT and anti-phospho-S473-AKT antibodies or anti-AKT antibody as a loading control. (**c**) Levels of phospho-T308-AKT, Bax and caspase-3 were also determined in the presence or absence of AKT inhibitor, LY294002 and/or T1, using β-actin as a loading control. (**d**) Densitometry of caspase-3 activity levels in the presence or absence of AKT inhibitor, LY294002 and/or diterpene T1. (**e**) Regulation of MAPKs (ERK, p38, JNK) and AMPK. Results show representative blots and the mean ± S.D. out of three experiments. $^{*}P<0.05$; $^{**}P<0.01$ treatments *versus* A/R in the absence of diterpene

(NO, PGE_2, cytokines) through inhibition of NF-κB activity.[14] A selection of these diterpenes showing good chemical stability, low toxicity and potent (T2 and T3) or negligible (T3) anti-inflammatory activity have been evaluated in the present work. To our knowledge no other studies have examined the potential of labdane diterpenes for cardioprotection. There are a few that describe a protective role for natural products, such as antioxidant polyphenols,[22,26,27] and by the triterpene saponins.[28,29] In the present study, we have focused on the molecular mechanisms underlying the effects of labdanes to protect cardiomyocytes against A/R-induced injury. These diterpenes did not affect cell viability at concentrations lower than 20 μM, and T1 proved to be safe when used up to 50 μM for at least 48 h.

Cardiomyocyte loss after ischemia is mainly due to apoptosis, necrosis (when the cell is unable to support the apoptotic energetic demands), or commitment to autophagy in an attempt to rescue cell function,[21,23,30,31] all three cell-fates having an important role in the heart after I(A)/R-induced dysfunction. Indeed, prevention of the apoptosis induced by ischemia or anoxia minimizes cardiac injury**.** Our data on early apoptotic signaling after A/R shows that T1 and T2 protect against cytochrome *c* release from the mitochondria (not shown), impair Bax accumulation and upregulate the

the treatment of cardiovascular diseases, and provide useful tools for the development of chemopreventive and chemotherapeutic strategies.

Materials and Methods

Materials. Diterpenes T1 (dehydroisohispanolone), T2 (8,9-dehydrohispanolone 15,16-lactol) and T3 (14,15,16-trisnor-13,9α-hispanolide) were obtained from hispanolone as previously described.[37–39]

Dulbecco's modified Eagle's medium (DMEM) was purchased from ATCC (American Type Culture Collection). The rest of culture reagents were obtained from Invitrogen (Alcobendas, Spain). Western blot reagents were obtained (purchased)-from GE Healthcare (Buckinghamshire, UK). Antibodies were obtained (purchased) from the following suppliers: anti-ERK, anti-pERK, anti-JNK, anti-pJNK, anti-p38, anti-pp38, anti-AKT, anti-pAKT(S-473), anti-pAKT (T-308), anti-AMPK, anti-pAMPK, anti-caspase-3 (Cell Signaling Technologies, Beverly, MA, USA); anti-Hsp70 (Gen Script, Piscataway, NJ, USA); anti-Bax, anti-xIAP (BD Biosciences, San Jose, CA, USA); anti-Bcl2, anti-Bcl-xL (Santa Cruz Biotech., Santa Cruz, CA, USA). The fluorescent kit for TUNEL was from Roche (Mannheim, Germany). The CaspGLOW fluorescein active caspase-3 staining kit was obtained (purchased) from BioVision Research (San Francisco, CA, USA) and the specific fluorogenic substrate for caspase-3 was obtained (purchased) from BD Biosciences. Type II collagenase was from Worthington (Lakewood, NJ, USA). LY294002 and kinase inhibitors were obtained (purchased) from Cell Signaling.

Cell culture. H9c2 embryonic rat heart-derived cells were obtained from ATCC. The cells were cultured in DMEM with 10% fetal bovine serum (FBS), 100 U/ml penicillin, and 100 μg/ml streptomycin, and maintained in 5% CO_2 at 37 °C. When cell confluence was reached, cells were subcultured by detaching with 0.05% trypsin-EDTA and reseeding. For experiments, cells were maintained in DMEM plus 2% FBS.

Isolation of cardiac myocytes was performed as previously described.[40] Adult mate Wistar rats were heparinized (4 U/g) and anaesthetized with sodium pentobarbital (50 mg/kg). The hearts were removed and mounted on a Langerdorff-perfusion apparatus. The ascending aorta was cannulated and a retrograde perfusion was set up. The hearts were successively perfused with the following oxygenated solutions at 36 °C: (1) standard nominally Ca^{2+}-free Tyrode solution (3 min), (2) standard nominally Ca^{2+}-free Tyrode solution (15 min) containing 60 U/ml of type II collagenase. The hearts were removed from the Langerdorff apparatus, and after removal of atria, the ventricles were cut off and gently shaken for 3 min in a standard Tyrode solution containing 0.1 mM $CaCl_2$ to disperse the isolated cells. The resulting cell suspensions were filtered through a 250 μm nylon mesh and centrifuged for 4 min at 20 *g*. Finally, the cell pellets were maintained as the H9c2 cells in the presence of 0.1 mM $CaCl_2$.

Anoxia/reoxygenation (A/R) protocol. To mimic an I/R model (via anoxia in the medium), cells at 80% confluence were incubated with a glucose-free medium (previously bubbled with 95% N_2 and 5% of CO_2) for 3 h at 37 °C in a hypoxic chamber (95% N_2 and 5% CO_2). For A/R studies, the medium was then replaced by maintenance medium (DMEM with 2% FBS) during the reoxygenation period. Diterpenes (20 μM unless otherwise indicated) were then added to the cells for 4 or 6 h.

Cell viability and apoptosis assays. Cell viability was determined by the 3-[4,5-dimethylthiazol-2-yl]-2,5-diphenyl tetrazolium bromide (MTT) assay following the method described by Mossman.[41] Cells were seeded at a density of 3×10^4 cells/well in 96-well plates and were incubated with MTT (5 mg/ml) for 2 h at 37 °C. After that, the medium was removed and DMSO (100 μl) was added into each well. The optical density (OD) was determined spectrophotometrically at 540 nm.

Lactate dehydrogenase activity (LDH) was determined in the cell culture medium by measuring the conversion of pyruvate to lactate. LDH activity was analyzed spectrophotometrically at 340 nm. The activity of the LDH in the supernatants was compared with the 'total content' in cells disrupted by treatment with 0.5% Triton X-100.

Caspase-3 activity was spectrofluorometrically determined in cytosolic protein extracts using a specific substrate (Ac-DEVD-AMC) for this caspase, according to the supplier's instructions (BD Biosciences).

In vivo activation of caspase-3 in apoptotic cells was measured by fluorescence microscopy after labeling the cells with the caspase-3 inhibitor DEVD-FMK conjugated to FITC (FITC-DEVD-FMK) as a marker, following the instructions of the supplier of the CaspGLOW fluorescein active caspase-3 staining kit (BioVision Research).

For detection and quantification of apoptosis, the terminal deoxynucleotidyl transferase-mediated dUTP nick end-labeling (TUNEL) assay was performed according to the manufacturer's instructions using a commercially available kit for death detection (Roche). H9c2 cells were seeded at a density of 10^4 cells/well into sterile 8-well Chamber Slides (Falcon, Brookings, SD, USA), exposed to A/R and treated with diterpenes. After reoxygenation (6 h) cells were fixed with 4% *p*-formaldehyde for 15 min. Cells were then permeabilized in ice-cold methanol and incubated with 3% bovine serum albumin (BSA) for 30 min. Coverslips were mounted in Prolong Gold antifade reagent (Invitrogen) and examined using an Espectral Leica TCS SP25 confocal microscope (Leica, Solms, Germany). Alexa fluorescence was excited by the 488 nm line of an Argon laser 11 and emission collected through a BP filter (505–530 nm). DAPI fluorescence was excited by the Hg lamp (BP 365/12) and emissions collected through a BP filter (480–520 nm). Values of intensity fluorescence quantification were performed using the Image J software (NIH, Bethesda, MD, USA).

Protein extraction and western blot. H9c2 cells were washed twice with ice-cold Buffer A (10 mM Hepes, pH 7.9;. 1 mM EDTA, 1 mM EGTA, 10 mM KCl, 1 mM DTT, 0.5 nM PMSF, 2 μg/ml aprotinin, 10 μg/ml leupeptin, 2 μg/ml TLCK (N_α-tosyl-L-lysine chloromethyl ketone hydrochloride), 5 mM NaF, 1 mM $NaVO_4$, 10 mM Na_2MoO_4) containing 120 mM NaCl and scraped off the plate. Cells were lysed at 4 °C with 0.2 ml of buffer A supplemented with 0.5% Nonidet P-40 with continuous shaking. After centrifugation of the cell lysate the supernatant was stored at −80 °C (cytosolic cell extract).

Native cardiomyocytes were homogenized using a hand-held blender in lysis buffer containing (in mM): 50 Tris, 320 sucrose and 1 DTT, pH 7.0, plus a complete protease and phosphatase inhibitors solution. The homogenate was spun at 13 000 *g* for 10 min at 4 °C and supernatants (total cell extract) were frozen and stored at −80 °C. Protein content in both cases was assayed with the Bio-Rad protein reagent (Bio-Rad, Alcobendas, Spain).

For Western Blot equal amounts of cytosolic protein lysates were separated in 10–15% sodium dodecyl sulfate-polyacrylamide (SDS-PAGE) gel electrophoresis. The gels were blotted onto a Hybond-P membrane and incubated with the indicated antibodies. Blots were developed by ECL according to the manufacturer's instructions. β-actin was used as a loading control.

Statistical analysis. All the values are expressed as mean ± S.D. The statistical significance of differences between the means were determined with the SPSS 19 software (SPSS, Chicago, IL, USA) for Windows using a one-way analysis of variance followed by Bonferroni *post-hoc* test or Student's *t*-test, as appropriate. A *P*-value of less than 0.05 was considered to be significant.

Conflict of Interest

The authors declare no conflict of interest.

Acknowledgements. We thank Dr. Benjamín Rodriguez from the Instituto Química Orgánica, CSIC. Madrid (Spain) for kindly providing the diterpenes and Dr. Mercedes Delgado, Instituto Plurisdisciplinar, Universidad Complutense de Madrid for her technical assistance and Ms. Diana Foran, Universidad Complutense de Madrid, for her editorial assistance with the manuscript. This work was supported by grants BFU2011-24760 and PIB2010BZ-00540 from MICINN; red temática de investigación en enfermedades cardiovasculares (RECAVA, RD06/0014/0006), the Instituto de Salud Carlos III (ISCIII), MICINN & European Regional Development Fund (ERDF) 'Una manera de hacer Europa' and CIBERehd founded by Instituto de Salud Carlos III.

1. Fliss H, Gattinger D. Apoptosis in ischemic and reperfused rat myocardium. *Circ Res* 1996; **79**: 949–956.
2. Ruiz-Meana M, Garcia-Dorado D. Translational cardiovascular medicine (II). Pathophysiology of ischemia-reperfusion injury: new therapeutic options for acute myocardial infarction. *Rev Esp Cardiol* 2009; **62**: 199–209.

3. Buja LM. Myocardial ischemia and reperfusion injury. *Cardiovasc Pathol* 2005; **14**: 170–175.
4. Hausenloy DJ, Yellon DM. Preconditioning and postconditioning: underlying mechanisms and clinical application. *Atherosclerosis* 2009; **204**: 334–341.
5. Hausenloy DJ, Yellon DM. The therapeutic potential of ischemic conditioning: an update. *Nat Rev Cardiol* 2011; **6**: 12–13.
6. Zhu M, Feng J, Lucchinetti E, Fischer G, Xu L *et al.* Ischemic postconditioning protects remodeled myocardium via the PI3K-PKB/Akt reperfusion injury salvage kinase pathway. *Cardiovasc Res* 2006; **72**: 152–162.
7. Hausenloy DJ, Yellon DM. New directions for protecting the heart against ischaemia-reperfusion injury: targeting the Reperfusion Injury Salvage Kinase (RISK)-pathway. *Cardiovasc Res* 2004; **61**: 448–460.
8. Downey JM, Cohen MV. Why do we still not have cardioprotective drugs? *Circ J* 2009; **73**: 1171–1177.
9. de las Heras B, Hortelano S, Giron N, Bermejo P, Rodriguez B *et al.* Kaurane diterpenes protect against apoptosis and inhibition of phagocytosis in activated macrophages. *Br J Pharmacol* 2007; **152**: 249–255.
10. Castrillo A, de las Heras B, Hortelano S, Rodriguez B, Villar A *et al.* Inhibition of the nuclear factor κB pathway by tetracyclic kaurene diterpenes in macrophages. Specific effects on NF-κB-inducing kinase activity and on the coordinate activation of ERK and p38 MAPK. *J Biol Chem* 2001; **276**: 15854–15860.
11. de las Heras B, Hortelano S. Molecular basis of the anti-inflammatory effects of terpenoids. *Inflamm Allergy Drug Targets* 2009; **8**: 28–39.
12. Gurusamy N, Lekli I, Mukherjee S, Ray D, Ahsan MK *et al.* Cardioprotection by resveratrol: a novel mechanism via autophagy involving the mTORC2 pathway. *Cardiovasc Res* 2010; **86**: 103–112.
13. Chinou I. Labdanes of natural origin-biological activities (1981–2004). *Curr Med Chem* 2005; **12**: 1295–1317.
14. Giron N, Traves PG, Rodriguez B, Lopez-Fontal R, Bosca L *et al.* Suppression of inflammatory responses by labdane-type diterpenoids. *Toxicol Appl Pharmacol* 2008; **228**: 179–189.
15. Dong Y, Morris-Natschke SL, Lee KH. Biosynthesis, total syntheses, and antitumor activity of tanshinones and their analogs as potential therapeutic agents. *Nat Prod Rep* 2011; **28**: 529–542.
16. Navarro A, de las Heras B, Villar AM. Andalusol, a diterpenoid with anti-inflammatory activity from Siderits foetens Clemen. *Z Naturforsch C* 1997; **52**: 844–849.
17. de las Heras B, Navarro A, Diaz-Guerra MJ, Bermejo P, Castrillo A *et al.* Inhibition of NOS-2 expression in macrophages through the inactivation of NF-κB by andalusol. *Br J Pharmacol* 1999; **128**: 605–612.
18. Ren J, Zhang S, Kovacs A, Wang Y, Muslin AJ. Role of p38α MAPK in cardiac apoptosis and remodeling after myocardial infarction. *J Mol Cell Cardiol* 2005; **38**: 617–623.
19. Qi D, Hu X, Wu X, Merk M, Leng L *et al.* Cardiac macrophage migration inhibitory factor inhibits JNK pathway activation and injury during ischemia/reperfusion. *J Clin Invest* 2009; **119**: 3807–3816.
20. Mann DL. The emerging role of innate immunity in the heart and vascular system: for whom the cell tolls. *Circ Res* 2011; **108**: 1133–1145.
21. Singh SS, Kang PM. Mechanisms and Inhibitors of Apoptosis in Cardiovascular Diseases. *Curr Pharm Des* 2011; **17**: 1783–1793.
22. Zhao Y, Zhao B. Protective effect of natural antioxidants on heart against ischemia-reperfusion damage. *Curr Pharm Biotechnol* 2010; **11**: 868–874.
23. Turer AT, Hill JA. Pathogenesis of myocardial ischemia-reperfusion injury and rationale for therapy. *Am J Cardiol* 2010; **106**: 360–368.
24. Wang W, Lopaschuk GD. Metabolic therapy for the treatment of ischemic heart disease: reality and expectations. *Expert Rev Cardiovasc Ther* 2007; **5**: 1123–1134.
25. Carreira RS, Lee P, Gottlieb RA. Mitochondrial therapeutics for cardioprotection. *Curr Pharm Des* 2011; **17**: 2017–2035.
26. Thomas CJ, Ng DC, Patsikatheodorou N, Limengka Y, Lee MW *et al.* Cardioprotection from ischaemia-reperfusion injury by a novel flavonol that reduces activation of p38 MAPK. *Eur J Pharmacol* 2011; **658**: 160–167.
27. Townsend PA, Scarabelli TM, Pasini E, Gitti G, Menegazzi M *et al.* Epigallocatechin-3-gallate inhibits STAT-1 activation and protects cardiac myocytes from ischemia/reperfusion-induced apoptosis. *FASEB J* 2004; **18**: 1621–1623.
28. Tsutsumi YM, Tsutsumi R, Mawatari K, Nakaya Y, Kinoshita M *et al.* Compound K, a metabolite of ginsenosides, induces cardiac protection mediated nitric oxide via Akt/PI3K pathway. *Life Sci* 2011; **88**: 725–729.
29. Li C, Tian J, Li G, Jiang W, Xing Y *et al.* Asperosaponin VI protects cardiac myocytes from hypoxia-induced apoptosis via activation of the PI3K/Akt and CREB pathways. *Eur J Pharmacol* 2010; **649**: 100–107.
30. Matsui Y, Takagi H, Qu X, Abdellatif M, Sakoda H *et al.* Distinct roles of autophagy in the heart during ischemia and reperfusion: roles of AMP-activated protein kinase and Beclin 1 in mediating autophagy. *Circ Res* 2007; **100**: 914–922.
31. Takagi H, Matsui Y, Hirotani S, Sakoda H, Asano T *et al.* AMPK mediates autophagy during myocardial ischemia *in vivo*. *Autophagy* 2007; **3**: 405–407.
32. Wang Y. Mitogen-activated protein kinases in heart development and diseases. *Circulation* 2007; **116**: 1413–1423.
33. Kupatt C, Hinkel R, Lamparter M, von Bruhl ML, Pohl T *et al.* Retroinfusion of embryonic endothelial progenitor cells attenuates ischemia-reperfusion injury in pigs: role of phosphatidylinositol 3-kinase/AKT kinase. *Circulation* 2005; **112**: 117–122.
34. Matsui T, Tao J, del Monte F, Lee KH, Li L *et al.* Akt activation preserves cardiac function and prevents injury after transient cardiac ischemia *in vivo*. *Circulation* 2001; **104**: 330–335.
35. Wang Y, Gao E, Tao L, Lau WB, Yuan Y *et al.* AMP-activated protein kinase deficiency enhances myocardial ischemia/reperfusion injury but has minimal effect on the antioxidant/antinitrative protection of adiponectin. *Circulation* 2009; **119**: 835–844.
36. Russell 3rd RR, Li J, Coven DL, Pypaert M, Zechner C *et al.* AMP-activated protein kinase mediates ischemic glucose uptake and prevents postischemic cardiac dysfunction, apoptosis, and injury. *J Clin Invest* 2004; **114**: 495–503.
37. García-Álvarez M, Pérez-Sirvent L, Rodriguez B. Transformaciones de hispanolona I. Síntesis parcial del diterpenoide furolabdánico galeopsinas. *Anales Quím* 1981; **77**: 316–319.
38. Pérez-Sirvent L, García-Álvarez MC, Rodríguez B. Transformaciones de hispanolona II. Reacción retroaldólica de hispanolona y condensación aldólica de δ-dicetonas diterpénicas. *Anales Quím* 1981; **77**: 324–329.
39. Pérez-Sirvent L, García-Álvarez MC, Balestrieri MA, Rodríguez B. Transformaciones de hispanolona III. Reacciones del anillo B y degradación a di-homo-drimanos. *Anales Quím* 1981; **77**: 330–334.
40. Fernandez-Velasco M, Goren N, Benito G, Blanco-Rivero J, Bosca L *et al.* Regional distribution of hyperpolarization-activated current (If) and hyperpolarization-activated cyclic nucleotide-gated channel mRNA expression in ventricular cells from control and hypertrophied rat hearts. *J Physiol* 2003; **553**: 395–405.
41. Mossman T. Rapid colorimetric assay for cellular growth and survivals: application to proliferation and cytotoxicity assays. *J Immunol Methods* 1983: 55–63.

Capítulo 4

Efficient *in vivo* cardioprotection by labdane diterpenes against post-ischemic left coronary artery occlusion injury.

Efficient *in vivo* cardioprotection by labdane diterpenes against post-ischemic left coronary artery occlusion injury.

Irene Cuadrado-Berrocal, María V. Gómez-Gaviro, Yolanda Benito, Alicia Barrio, Javier Bermejo, Mª Eugenia Fernández-Santos, Pedro L. Sánchez, Francisco Fernández-Avilés, María Fernández-Velasco, Lisardo Boscá and Beatriz de las Heras.

El objetivo fue estudiar los mecanismos de cardioprotección del diterpeno activo dehidrohispanolona (**DT1**) en modelos animales: I/R en corazón perfundido de Langendorff e infarto de miocardio en rata inducido por la oclusión temporal de la arteria coronaria descendente izquierda. Con este estudio se confirmaron los efectos cardioprotectores de este diterpeno, observados previamente en cardiomiocitos.

En ambos modelos, los resultados indicaron que los efectos protectores de **DT1** frente a la apoptosis se asociaban con un aumento de la expresión de proteínas anti-apoptóticas (Bcl-xL, Bcl-2, HSP70 y xIAP), así como disminución de la activación de la proteína caspasa-3 y del porcentaje de células apoptóticas, determinado mediante TUNEL. Además, el tratamiento con **DT1** producía la activación de vías de supervivencia evidenciado por el aumento significativo de la fosforilación de las proteínas AKT, AMPK y PDK1.

Los estudios ecocardiográficos e histológicos mostraron que el tratamiento con **DT1** (5 mg/kg, i.v.) mejoraba la función cardiaca en los animales tratados, observándose una recuperación de los parámetros hemodinámicos y una reducción del área del infarto.

En resumen, los datos aportados demuestran la eficacia cardioprotectora de este diterpeno labdano en procesos de I/R cuando se administra al inicio de la reperfusión, proporcionando nuevas estrategias farmacológicas dirigidas al tratamiento del daño isquémico.

Efficient *in vivo* cardioprotection by labdane diterpenes against post-ischemic left coronary artery occlusion injury

Irene Cuadrado-Berrocal[1§], María V. Gómez-Gaviro[2§], Yolanda Benito[2], Alicia Barrio[2], Javier Bermejo[2], María Eugenia Fernández-Santos[2], Pedro L. Sánchez[2], Francisco Fernández-Avilés[2], María Fernández-Velasco[3,4], Lisardo Boscá[3,4*] and Beatriz de las Heras[1*]

[§]These authors contributed equally to this work

[1]Departamento de Farmacología, Facultad de Farmacia, Universidad Complutense de Madrid, Plaza Ramón y Cajal s/n, 28040 Madrid, Spain. [2]Servicio de Cardiología, Instituto de Investigación Sanitaria Gregorio Marañón, C/ Doctor Esquerdo 46, Madrid 28007. [3]Instituto de Investigaciones Biomédicas 'Alberto Sols' (CSIC-UAM), Arturo Duperier 4, 28029 Madrid, Spain. [4]Instituto de Investigación Hospital Universitario La PAZ, IDIPAZ, Paseo de la Castellana, 28029 Madrid, Spain

***Corresponding authors:**

Lisardo Boscá: Instituto de Investigaciones Biomédicas 'Alberto Sols' (CSIC-UAM), Arturo Duperier 4, 28029 Madrid, Spain. Tel: +34914972747 Fax: +34915854401; e-mail: lbosca@iib.uam.es

Beatriz de las Heras: Departamento de Farmacología, Facultad de Farmacia, Universidad Complutense de Madrid, Plaza Ramón y Cajal s/n, 28040 Madrid, Spain. Tel: +34913942276 Fax: +34913941726; e-mail: lasheras@ucm.es

Summary

BACKGROUND AND PURPOSE: Our previous findings indicate that labdane diterpenes exert anti-inflammatory and cytoprotective actions. This study was designed to investigate the cardioprotective effects of labdane diterpene (DT1) against cardiac ischemia/reperfusion (I/R) injury and the molecular mechanisms involved, using a complementary approach in a rat myocardial infarction model.

EXPERIMENTAL APPROACH: Myocardial infarction (MI) was induced in rats (n= 60) occluding the left anterior descending coronary artery (LAD) for 30 min followed by 72 h reperfusion. DT1 (5 mg/kg) was intravenously administered after LAD occlusion. Hearts were isolated for determination of

myocardial infarct size, histopathology and signaling pathways analysis. In addition, we investigated the possible mechanisms of cardioprotection in Langendorff-perfused model.

KEY RESULTS: Investigation of molecular pathways involved in the cardioprotection indicates that DT1 treatment attenuates myocardial injury as evidenced by increased expression of anti-apoptotic proteins and decreased caspase-3 activation and percentage of apoptotic cells. DT1 treatment promotes a significant increase in the phosphorylation state of AKT, AMPK and PDK1 and reduced phosphorylation of PKD1/2. Pharmacological inhibition of AKT following MI and prior to DT1 challenge significantly abolished the cardioprotection afforded by DT1 therapy at reperfusion, but failed to prevent PKD1/2 dephosphorylation. Cardiac function after MI was significantly improved after DT1-treatmment, as evidenced by hemodynamic recovery and decreased myocardial infarct size.

CONCLUSIONS AND IMPLICATIONS: These findings strongly demonstrate an efficient *in vivo* cardioprotection by diterpene DT1 against I/R when administered at the onset of reperfusion, opening new therapeutic strategies as adjunctive therapy for the pharmacological management of I/R injuries.

Abbreviations

I/R, ischemia/reperfusion; LAD, left anterior descending; CVD, cardiovascular diseases, IHD, ischemic heart disease; MI, myocardial infarction, DT, labdane diterpene; TUNEL, terminal deoxynucleotidyl transferase-mediated dUTP nick end-labeling; DAPI, 6-diamidino-2-phenylindole; AMPK, AMP-kinase; LDH, lactate dehydrogenase; MAPK, mitogen-activated protein kinase; PI3K, phosphatidylinositol 3-kinase; SDS-PAGE, sodium dodecyl sulphate polyacrylamide gel electrophoresis, DT1, dehydroisohispanolone; DT2, 14,15,16-trisnor-13,9α-hispanolide; HE, hematoxylin-eosin; MT, Masson Trichrome

Keywords: labdane diterpenes, ischemia/reperfusion injury, apoptosis, cardioprotection.

Introduction

Cardiovascular diseases (CVD) are, globally considered, the main cause of death in the world. The concept of CVD includes several disorders of the heart and blood vessels, being ischemic heart disease (IHD) the main problem in developed countries (Go *et al.*, 2013; Hausenloy *et al.*, 2013b). IHD occurs when a coronary artery narrows, frequently as a result of atherosclerosis, and blood supply in the heart is insufficient, resulting in angina, heart attack, or even sudden death of the patient (Frank *et al.*, 2012). When faced with ischemia, changes at the level of the failing human cardiac myocyte lead to a defect in contractile function. In addition to this, subsequent reperfusion promotes the activation of various injury responses leading to necrosis, apoptosis or autophagy (Matsui *et al.*, 2007; Singh *et al.*, 2011; Takagi *et al.*, 2007b). Indeed, ischemic heart postconditioning is one of the strategies to improve clinical outcomes in patients with coronary heart disease and it has been reported that postconditioning procedures can reduce the infarct size (Barrere-Lemaire *et al.*, 2012; Rohilla *et al.*, 2011). Myocardial infarct size, a major determinant of prognosis, can be limited by pharmacological postconditioning with cardioprotective agents (e.g. Cyclosporine A) (Hausenloy *et al.*, 2011a). However, the use of these agents as adjunctive therapy has not achieved a successful translation into the clinical setting. Novel interventions able to reduce infarct size beyond early coronary reperfusion are the matter of intense experimental and clinical research in order to reduce mortality and morbidity (Heusch, 2013; Schwartz Longacre *et al.*, 2011).

Diterpenes are compounds with a broad spectrum of biological activities (Chinou, 2005; de las Heras *et al.*, 2009; de las Heras *et al.*, 2003). We have recently reported that several diterpenes exert anti-inflammatory and cytoprotective actions (Cuadrado *et al.*, 2012; Cuadrado *et al.*, 2011; Hueso-Falcon *et al.*, 2011). In particular, labdane diterpenes exerted cardioprotective effects against I/R-induced injury in isolated cardiomyocytes and the mechanisms involved activation of specific survival signals and inhibition of death pathways (Cuadrado *et al.*, 2011). In light of this, in the present study we show a remarkable cardioprotective effect of DT1 in *in vivo* rat models of I/R when administered just before reperfusion. We provide evidence that labdane

diterpene improves cardiac function *in vivo*, exerting anti-apoptotic effects due to up-regulation of survival pathways (i.e. AKT and AMPK) in rat heart, which makes this molecule an interesting tool for future therapies.

Methods

Materials

Diterpenes DT1 (dehydroisohispanolone) and DT2 (14,15,16-trisnor-13,9α-hispanolide) were obtained and characterized from hispanolone as previously described (García-Álvarez, 1981; Pérez-Sirvent, 1981a; Pérez-Sirvent, 1981b). Culture reagents were from Life Technologies (Alcobendas, Madrid, Spain). Western blot reagents were from GE Healthcare (Buckinghamshire, UK); Immobilon-P transfer membranes and kinase inhibitors and AKT inhibitor II were from Merck-Millipore (Darmstadt, Germany). Antibodies were from the following suppliers: anti-AKT/pAKT (S473), anti-AMPK/pAMPK (T172), anti-PDK1/pPDK1 (S241), anti-PKD/pPKD (S916), and anti-Bad were from Cell signaling Tech. (Beverly, MA); anti-Hsp70 was from Gen Script (Piscataway, NJ); anti-xIAP was from BD Biosciences (San Jose, CA, USA); anti-HIF1α (R&D Systems, Sparks, NV); anti-Bcl2, anti-Bcl-xL, anti-Mcl1 and other Ab were from Santa Cruz Biotech. (Santa Cruz, CA). TUNEL fluorescent kit obtained from Roche (Mannheim, Germany) and the specific fluorogenic substrate for caspase-3 from BD Biosciences. Type II collagenase was supplied from Worthington (Lakewood, NJ). General reagents were from Sigma-Aldrich (St Louis, MO). 6-diamidino-2-phenylindole (DAPI) and Prolong Gold antifade were from BD Bioscience. Sevoflurane was from Abbott (Madrid, Spain).

Animal care

The Langendorff model was conducted following the guidelines of the Spanish Animal Care and Use Committee, according to the guidelines for ethical care of experimental animals of the European Union (2010/63/EU). This study conforms to the Guide for the Care and Use of Laboratory Animals published by the US National Institute of Health (NIH Publication No. 85–23, revised 1996). Procedures are schematically represented in Figure. 1A and were approved by the Bioethical Committee of the Consejo Superior de

Investigaciones Científicas and Autonomous University of Madrid. For myocardial infarction, a total of 60 adult male Wistar rats (5 weeks-old, body weight ~ 200-250g) were supplied by the Experimental Medicine Unit in Hospital General Universitario Gregorio Marañón, Madrid (HGUGM). The animal interventions and care were approved by the Ethical Committee of the HGUGM. The experimental procedures (represented in Figure 1A) were conducted under the "3R" policy from Russell and Burch (Rogiers, 2003).

Global ischemia/reperfusion (I/R) in Langendorff-perfused rat heart

Adult male Wistar rats were heparinized (4 units/g) and anaesthetized with sodium pentobarbital (50 mg/kg). The hearts were removed and mounted on a Langendorff-perfusion apparatus as previously described (Cuadrado *et al.*, 2011). Briefly, the ascending aorta was cannulated and a retrograde perfusion was maintained at a constant flow with different Ca^{2+}-free Tyrode solutions. For the I/R protocol, the hearts were randomly assigned to 1 of 3 experimental groups after 30 min of equilibration. In the non-ischemia group, hearts (n=7) were perfused only with Ca^{2+}-free Tyrode solution for 120 min. In the control group (n=7), ischemia was induced by perfusion with Ca^{2+}-free Tyrode solution without glucose and bubbled with N_2 (ischemic solution) for 30 min, and then reperfused with normal Ca^{2+}-free Tyrode solution for 60 min. In the treatment group (n=7), hearts were perfused with the ischemic solution and reperfused with normal Ca^{2+}-free Tyrode containing DT (20 µM) and the same procedures were repeated by using the same time intervals. The hearts were removed from the Langendorff apparatus, and after removal of atria, the left ventricle was cut into slices which were fixed in 10% formaldehyde for histopathology and TUNEL analyses. The remaining hearts were used for protein extraction.

Induction of rat myocardial infarction (MI)

For *in vivo* studies, rats were anesthetized with a mixture of O_2/sevoflurane. A small animal ventilator was used (Harvard Apparatus, Inspira, MA) with a tidal volume (Vt) of 1.65 and 85 ventilations per minute (v.p.m.). Analgesia was induced with fentanyl and buprenorphine administered intraperitoneally (i.p.). During three days after surgery, ibuprofen (20 mg/ml) was included in the drink water to provide analgesia. A left thoracotomy was performed in the intercostal space between the third and fourth ribs, followed by

a pericardiotomy. The left anterior descending coronary artery (LAD) was encircled with a 6-0 silk suture (Prolene) to form a slipknot 3.0 mm below the level of the tip of the normally positioned left atria appendage and a small piece PE-10 tube was placed-in-between for convenient release upon reperfusion. LAD occlusion was confirmed by the dramatic change in color (red to pallor) and restricted ventricular motion. After 30 min of LAD occlusion, air was expelled from the chest and reperfusion was initiated by releasing the slipknot and removing the tube, and was confirmed by the appearance of epicardial hyperemic response. An i.v. dose of DT1 (5 mg/kg) was administered by tail vein injection at the onset of reperfusion. The chest cavity was closed, sevoflurane administration was switched off and the animal was supplied with O_2 until reflexes were detected; it was placed in a cage on a heating pad until fully conscious for 72h. Animals were randomly subjected to either LAD occlusion (n=50) or sham operation (n=10). Mortality during the intervention was 26%. The survival rate in all groups after DT treatment was 100%. Immediately after surgery, animals with LAD occlusion were further assigned to one of two groups: i) MI+saline, animals treated with vehicle (normal saline containing 5% glucose + 5% DMA (dimethylacetamyde)), ii) MI+DT, animals treated with i.v. DT1 (5 mg/kg in vehicle). The sham-operated rats underwent the same surgical procedure without MI. For some determinations, two additional groups MI+AKT inhibitor (10 µM) ± DT1 were included.

Cardiac function

Cardiac function and chamber dilatation were analyzed by echocardiography using a Vevo 2100 system with a 45 MHz probe (Visualsonics, Toronto, Canada) fully blinded to the animal study group. Rats were analyzed the day before the surgery to control the basal cardiac function. Echocardiography was again performed 72h post-infarction in light anesthetized rat with 2.0% sevoflurane. M-Mode images of the left ventricle at the level of the papillary muscles were obtained, and different functional hemodynamic parameters were determined. Image acquisition and analysis were done in a blind manner. LVESV= $(7.0/(2.4+LVID;s))*LVIDs^3$; LVEDV= $(7.0/(2.4+LVID;d))*LVIDd^3$. EF= 100*(LVEDV-LVESV)/LVEDV. FS= 100*(LVIDd-LVIDs)/LVIDd.

Histological analysis and determination of infarct size

The hearts were removed immediately after sacrifice and fixed in 10% phosphate-buffered formaldehyde. The fixed tissue was then embedded in paraffin and cut in 4-µm-thick transverse cryosections. The sections were deparaffinized and stained with hematoxylin-eosin (HE) to assess the myocardial structure. Masson Trichrome (MT) staining was performed to assess cardiac fibrosis in the peri-infarct border zone area. Scar size was quantified with ImageJ (NIH, USA) using the midline method, which is the histological method that best correlates with echocardiographic measurements as previously described (Takagawa *et al.*, 2007). Briefly, the scar length was expressed as the percentage of left ventricle circumference length in which the scar occupies at least 50% of the ventricular wall thickness. For detection of interstitial fibrosis in the remote myocardium, sections were stained using the MT protocol and the amount of collagen was quantified using ImageJ.

Western blot analysis

Native cardiomyocytes and the perfused hearts were homogenized using a hand-held blender in lysis buffer containing (in mM) 50 Tris, 320 sucrose and 1 DTT, pH 7.0, plus a complete protease and phosphatase inhibitors solution. The homogenate was spun at 13,000***g*** for 15 min at 4°C and supernatants (total cell extract) were frozen and stored at -80°C. Protein content in both cases was assayed with the Bio-Rad protein reagent. For Western blot equal amounts of total protein lysates were separated in 8-15% sodium dodecyl sulfate-polyacrylamide (SDS-PAGE) gel electrophoresis. The gels were blotted onto Immobilon-P transfer membranes and incubated with the indicated antibodies. Blots were developed by ECL according to the manufacturer's instructions. GAPDH was used as loading control.

Necrosis and apoptosis assays

LDH was determined spectrophotometrically in the flow obtained after perfusion of the Langendorff heart. Caspase-3 activity was determined in total protein extracts using a specific substrate (Ac-DEVD-AMC), according to the supplier's instructions (BD Biosciences). TUNEL (terminal deoxynucleotidyl transferase-mediated dUTP nick end-labeling) staining method for detecting

apoptotic cells was used according to the manufacturer's instructions (Roche). Apoptotic index was expressed as the number of positive cells showing nuclear staining of all cardiomyocytes. Cell nuclei were counterstained with 6-diamidino-2-phenylindole (DAPI). The hearts slices were mounted in Prolong Gold antifade reagent and examined using an Espectral Leica TCS SP25 confocal microscope. Alexa fluorescence was excited by the 488 nm line of an Argon laser 11 and emission collected through a BP filter (505-530 nm). DAPI fluorescence was excited by the Hg lamp (BP 365/12) and emissions collected through a BP filter (480-520 nm). Values of intensity fluorescence quantification were performed using ImageJ.

Isolation of rat cardiomyocytes

Rat cardiomyocytes were isolated using an enzymatic technique, as previously reported(Cuadrado *et al.*, 2011). After anesthetizing the rats with sodium pentobarbital (50 mg/kg), the hearts were removed and perfused in a Langendorff-perfusion system. Briefly, the hearts were successively perfused with different oxygenated Tyrode solutions at 36°C and after perfusion the cardiomyocytes were collected and plated on slides. To mimic an I/R model, 10^5 cells/ml were incubated with a glucose-free medium (previously bubbled with 95% N_2 and 5% of CO_2) for 4h at 37°C in a hypoxic chamber (95% N_2 and 5% CO_2). DTs (20 µM) were then added to the cells up to 6 h.

Statistical analysis

All the values are expressed as mean ± SD. The statistical significance of differences between the means were determined with SPSS 19 software (SPSS Inc., Chicago, IL) for Windows using a one-way analysis of variance (ANOVA) followed by Bonferroni *post hoc* test or Student's t-test, as appropriate. A *P*-value <0.05 was considered to be significant.

Results

The labdane diterpene DT1 induces cardioprotection against anoxic injury in isolated rat cardiomyocytes

Isolated rat cardiomyocytes were exposed to anoxia for 4h followed by reoxygenation up to 6h. Labdane diterpenes (DT1-DT2) or vehicle (Figure 1B) were added at the time of reoxygenation and the phosphorylation state of AKT

and AMPK, and the percentage of TUNEL positive cells were determined at 2h and 6h after reoxygenation, respectively (Figure 1C). Protection by DT1 correlated well with the enhanced phosphorylation of AKT and AMPK, whereas DT2 failed to exhibit protection or enhancement in the phosphorylation of these proteins.

Myocardial apoptosis and necrosis in isolated rat heart submitted to I/R was attenuated after treatment with labdane diterpene DT1

Further to evaluate the cardioprotection exerted by DTs, isolated hearts mounted in a Langendorff device underwent ischemia (I) for 30 min and DTs were added when reperfusion started (R) (Figure 1A). Cell death was assessed by measurement of LDH release to the perfusate and was significantly reduced in the presence of DT1 (93% *vs.* ischemia), but only 39% when DT2 was added (Figure 2A). Heart fixation 60 min after reperfusion showed extended apoptotic areas in all regions of the myocardium (global I/R). Administration of the active DT1 significantly decreased the number of cardiac apoptotic cells detected as TUNEL-positive nuclei, compared with untreated animals following global I/R (20 ± 3% *vs.* 59.6 ± 3.6%; Figure 2B). When tissue extracts were prepared and the levels of relevant proteins involved in cytoprotection were determined (pAKT, pAMPK and pPDK1) a significant increase in these phosphoproteins was observed after DT1 treatment; however, the levels of pPKD, a kinase more involved in cellular stress (Fu *et al.*, 2011) were significantly reduced *vs.* the I/R condition (Figure 2C). In agreement with these data an increase in the expression levels of antiapoptotic proteins was evidenced (Figure 2D) at the time that the increase in caspase-3 activity observed in I/R rat hearts was markedly reduced by DT1 administration, and to a lesser extent, but statistically significant, by DT2 (Figure 2E).

In vivo administration of DT1 protects heart function after MI

These protective effects of DT1 on apoptosis were evaluated in an *in vivo* MI model induced by LAD artery occlusion. Compared to MI untreated animals, hearts from the MI+DT1 condition had significantly decreased active caspase-3 levels and activity (Figure 3AB) and a lower percentage of TUNEL positive cells (Figure 3C). A representative view of the heart sections after LAD artery occlusion stained with DAPI and for TUNEL is shown in supplementary Figure

S1A. Interestingly, pharmacological inhibition of AKT suppressed most of the inhibitory action of DT1 on caspase-3 activation and TUNEL extension suggesting that this kinase plays a key role in the cytoprotective mechanisms exerted by this labdane. We also examined the effect of DT1 on survival and apoptosis signaling pathways in the course of MI/reperfusion of the heart. Treatment of animals after LAD artery injury with DT1 induced AKT phosphorylation in S473 in whole heart compared to the corresponding untreated animals (Figure 3D). In agreement with this result phosphorylation of AMPK in T172 and PDK1 in S241 was also enhanced *vs.* the MI control group. Also, the reduced phosphorylation of PKD promoted by DT1 after MI was similar to that observed in isolated perfused hearts submitted to I/R in the Langendorff device. Regarding the balance between anti-apoptotic (Bcl-xL, Bcl-2, HSP70 and Mcl-1) and pro-apoptotic proteins (Bax and Bad), the former increased by DT1 treatment after MI, whereas the latter decreased under these conditions *vs.* the MI group (Figure 3DE).

Previous data indicated that the AKT signaling pathway plays an important role in the development of heart diseases and protects cells from apoptosis (Cuadrado *et al.*, 2011; Matsui *et al.*, 2001; Shao *et al.*, 2006; Tsutsumi *et al.*, 2011). Administration of a pharmacologic AKT inhibitor following MI and prior to DT1 challenge significantly reduced DT1-induced phosphorylation of AKT and AMPK, at the time that failed to prevent PKD1/2 dephosphorylation (Figure 3D). However, the rise in PDK1 phosphorylation in S241 induced by DT1 after MI was not abolished by the inhibition of AKT suggesting that PDK plays a minor role in the cardioprotection of heart after MI injury. Interestingly, when the HIF-1α levels were determined, DT1 enhanced the levels after MI but this effect was abolished by AKT inhibition contributing to the abrogation in the expression of HIF-1α-dependent genes. Minimal changes in the expression of most proteins regulating apoptosis were observed after AKT inhibition, suggesting that perhaps the effects of AKT on intracellular protein localization and/or modification are more relevant than the actual levels (Figure 3D).

In addition to the protein levels related to cell viability, cardiac function was also assessed by echocardiography after diterpene treatment. After 30 min

of LAD artery occlusion and 72h reperfusion, rats undergoing LAD artery ligation showed significant reduction in contractile capacity (FS: 30.6±6.9; EF: 63.4±10.1) and a marked LV enlargement *vs.* baseline. Treatment with DT1 (MI+DT1 group) prevented ventricular dilatation, as shown by LVESV and LVIDs values. Rats in the MI+DT1 group also preserved EF and FS (76.3±4.6 and 40.1±4.2, respectively) compared to MI (Figure 4A). There were no significant differences in LVIDd and LVEDV values when the MI and the MI+DT1 groups were compared (data not shown). Improved contraction of the left ventricle anterior wall was also observed in DT1+MI rats by M-Mode echocardiography (Figure S1B).

The histopathological changes in the ischemic heart tissue 3 days after reperfusion were assessed by standard H&E staining. As shown in Figure 4B, the myocardium maintained normal tissue structure and shape in the sham group and, no obvious damage was observed. However, acute MI characterized by areas of necrosis, neutrophilic inflammation and interstitial edema was observed in MI rats. The myocardial fibers were partially ruptured and lysed. Upon DT1 treatment preservation of the myocardium was observed, suggesting that DT1 markedly ameliorated the myocardial damage induced by MI.

To determine whether improved cardiac function was accompanied by changes in the size of the infarct, we sliced the heart from apex to base, stained histological sections with MT and quantified the infarct size 3 days post-infarction. As shown in Figure 4C, DT1 treatment significantly reduced infarct size, suggesting that diterpenes exert a cardioprotective effect that reduces cardiomyocyte death and, therefore, infarct size. Investigation of the myocardium remote to the infarct showed a significant decrease in interstitial fibrosis in the MI+DT1 group, indicating that DT1 prevented myocardial remodeling post-infarction.

Discussion

In the present study, we have demonstrated the efficient protection exerted by labdane diterpene DT1 on I/R injury in rat models of myocardial damage including isolated cardiomyocytes, the perfused organ and after myocardial infarction following LAD artery ligation. The protective effects of DT1 in the *in vivo* MI model involved a reduction in the infarct size and an

improvement in cardiac function. Histological evaluation of heart samples also confirmed that DTI treatment markedly ameliorated myocardial remodeling induced by MI. Indeed, the molecular mechanisms afforded by this DT appear to be conserved among the different models of I/R injury analyzed. Aside from its cardioprotective effects, both DT1 and DT2 were not toxic to normal healthy animals, as serum hepatic and renal injury markers were not affected by DT intravenous administration (not shown). To our knowledge, this is the first study to demonstrate that some labdane diterpenes are cardioprotective *in vivo*.

Diterpenes are bioactive natural products with great therapeutic potential. Diverse labdane-type diterpenes with anti-inflammatory properties have been described in the literature (Castrillo *et al.*, 2001; Cuadrado *et al.*, 2012; Chinou, 2005; de las Heras *et al.*, 1999; Giron *et al.*, 2008; Xia *et al.*, 2004). In addition, some labdane diterpenes exert cytoprotective activities, although few studies have evaluated the therapeutic potential of terpenes in cardioprotection (Cuadrado *et al.*, 2011; Tsutsumi *et al.*, 2011; Waldman *et al.*, 2013; Xu *et al.*, 2007). In the context of drug discovery, development of new compounds targeting different pathways and acting as multi-target inhibitors may provide new strategies for cardiovascular therapy (Ma *et al.*, 2010).

Apoptosis and necrosis are involved in cardiomyocyte loss after ischemia (Turer *et al.*, 2010). Investigations in cultured cardiomyocytes clearly demonstrated that both diterpenes significantly reduced apoptosis and necrosis, with DT1 exerting a major protection. When we focused on the apoptosis pathway using the rat models, we observed an up-regulation of anti-apoptotic proteins of the Bcl-2 family and reduction of caspase-3 activation, being the protective effects of DTI also confirmed by TUNEL.

A large number of studies have shown that the survival kinases PI3K/AKT play a critical role in the protection afforded by postconditioning in healthy myocardium (Hausenloy *et al.*, 2005; Mozaffari *et al.*, 2010). AKT has been reported as a cardioprotective enzyme that inhibits apoptosis and preserves cardiac function in clinically relevant cardiac disease models (Matsui *et al.*, 2003). In the context of I/R injury, AMPK, which orchestrates the regulation of energy pathways, has been demonstrated to be rapidly activated during ischemia, as part of an innate survival cardiac mechanism(Eltzschig *et*

al., 2011). The cardioprotective effects of DT1 were associated with significant increases in phosphorylation of proteins involved in cytoprotection like AKT and PDK1, an immediate upstream kinase necessary for AKT activation, in DT1-treated hearts compared to I/R hearts. In agreement with these data, an increase in the expression of anti-apoptotic proteins of the Bcl-2 family and reduction of the effector pro-apoptotic protein caspase-3 were evidenced. Activation of AMPK was also observed in DT1-treated hearts.

Involvement of these molecular mechanisms was later confirmed when we moved to a rat MI model induced by LAD artery occlusion. Interestingly, pretreatment with an AKT inhibitor suppressed most of the cardioprotective effects of the diterpene, including caspase-3 inhibition, reduction of apoptosis and activation of protective cell-survival signaling pathways. These results strongly suggest that AKT plays a key role in the cytoprotection provided by DT1 and that approximately two thirds of this protection is dependent on the AKT pathway. In addition to this, the existence of complementary pathways converging in cardioprotection is evidenced by the fact that inhibition of AKT is unable to restore a full injury phenotype in the presence of the diterpene.

I/R is also associated with a strong inflammatory response (Entman *et al.*, 1991; Frank *et al.*, 2012). Previous studies have indicated that NF-κB plays a key role in inflammatory responses during myocardial I/R injury and activation of this transcription factor is found in post-ischemic reperfusion tissue (Kis *et al.*, 2003). Indeed, blockade of NF-κB improves cardiac function and survival after myocardial infarction(Kawano *et al.*, 2006). Data from our previous studies indicated that these labdane diterpenes are inhibitors of NF-κB (Giron *et al.*, 2008). In addition, some gene products that are regulated by NF-κB are expressed in support of cell survival, principally by preventing apoptosis, like Bcl-2. Therefore, the protective effects of DT1 may also be due, in part, to the suppression of the inflammatory response via inhibition of NF-κB activation. Interestingly, we also observed that DT1 induced HIF-1α levels in an AKT-dependent manner. This transcription factor has been reported as a therapeutic target for cardioprotection, as it activates an array of genes required for the adaptation to hypoxia (Ong *et al.*, 2012). Therefore, increased HIF-1α protein

levels may be part of the cardioprotective response activated by DT1 through AKT.

In summary, the diterpene-induced cardioprotection at reperfusion mainly occurs through regulation of different pathways involved in cytoprotection like AKT. The protection exerted by diterpene treatment when administered at reperfusion opens a new area of therapeutic strategies to control cardiac reperfusion injury that could be translated to clinical settings.

Acknowledgments

We are grateful to Julio and Fernando Asensio for technical assistance. This study was supported in part by Grants BFU2011-24760 from Ministerio de Economía y Competitividad, S2010/BMD-2378 from Comunidad de Madrid, and Fondo de Investigación Sanitaria-Red Cardiovascular (RIC) Grant RD12/0042/0019. RIC and Centro de Investigación Biomédica en Red de Enfermedades Hepáticas y Digestivas are funded by the Instituto de Salud Carlos III. IC was recipient of a short-term FEBS fellowship and MVGG was funded by an Intraeuropean Marie Curie fellowship (EIF 275885). This work was also supported by Grants PR6/13-18857 from Santander-UCM to B. de las Heras.

Conflict of interest

None declared

References

Barrere-Lemaire S, Nargeot J, Piot C (2012). Delayed postconditioning: not too late? Trends Cardiovasc Med 227**:** 173-179.

Castrillo A, de Las Heras B, Hortelano S, Rodriguez B, Villar A, Bosca L (2001). Inhibition of the nuclear factor kappa B (NF-kappa B) pathway by tetracyclic kaurene diterpenes in macrophages. Specific effects on NF-kappa B-inducing kinase activity and on the coordinate activation of ERK and p38 MAPK. J Biol Chem 27619**:** 15854-15860.

Cuadrado I, Cidre F, Herranz S, Estevez-Braun A, de las Heras B, Hortelano S (2012). Labdanolic acid methyl ester (LAME) exerts anti-inflammatory effects through inhibition of TAK-1 activation. Toxicol Appl Pharmacol 2581**:** 109-117.

Cuadrado I, Fernandez-Velasco M, Bosca L, de Las Heras B (2011). Labdane diterpenes protect against anoxia/reperfusion injury in cardiomyocytes: involvement of AKT activation. Cell Death Dis 2**:** e229.

Chinou I (2005). Labdanes of natural origin-biological activities (1981-2004). Curr Med Chem 1211**:** 1295-1317.

de las Heras B, Hortelano S (2009). Molecular basis of the anti-inflammatory effects of terpenoids. Inflamm Allergy Drug Targets 81**:** 28-39.

de las Heras B, Navarro A, Diaz-Guerra MJ, Bermejo P, Castrillo A, Bosca L*, et al.* (1999). Inhibition of NOS-2 expression in macrophages through the inactivation of NF-kappaB by andalusol. Br J Pharmacol 1283**:** 605-612.

de las Heras B, Rodriguez B, Bosca L, Villar AM (2003). Terpenoids: sources, structure elucidation and therapeutic potential in inflammation. Curr Top Med Chem 32**:** 171-185.

Eltzschig HK, Eckle T (2011). Ischemia and reperfusion--from mechanism to translation. Nat Med 1711**:** 1391-1401.

Entman ML, Michael L, Rossen RD, Dreyer WJ, Anderson DC, Taylor AA*, et al.* (1991). Inflammation in the course of early myocardial ischemia. FASEB J 511**:** 2529-2537.

Frank A, Bonney M, Bonney S, Weitzel L, Koeppen M, Eckle T (2012). Myocardial ischemia reperfusion injury: from basic science to clinical bedside. Semin Cardiothorac Vasc Anesth 163**:** 123-132.

Fu Y, Rubin CS (2011). Protein kinase D: coupling extracellular stimuli to the regulation of cell physiology. EMBO Rep 128**:** 785-796.

García-Álvarez M, Pérez-Sirvent, L, Rodriguez, B (1981). Transformaciones de hispanolona I. Síntesis parcial del diterpenoide furolabdánico galeopsina. Anales Quím77**:** 316-319.

Giron N, Traves PG, Rodriguez B, Lopez-Fontal R, Bosca L, Hortelano S*, et al.* (2008). Suppression of inflammatory responses by labdane-type diterpenoids. Toxicol Appl Pharmacol 2282**:** 179-189.

Go AS, Mozaffarian D, Roger VL, Benjamin EJ, Berry JD, Borden WB*, et al.* (2013). Heart disease and stroke statistics--2013 update: a report from the American Heart Association. Circulation 1271**:** e6-e245.
Hausenloy DJ, Boston-Griffiths EA, Yellon DM (2011). Cyclosporin A and cardioprotection: from investigative tool to therapeutic agent. Br J Pharmacol 1655**:** 1235-1245.

Hausenloy DJ, Tsang A, Yellon DM (2005). The reperfusion injury salvage kinase pathway: a common target for both ischemic preconditioning and postconditioning. Trends Cardiovasc Med 152**:** 69-75.

Hausenloy DJ, Yellon DM (2013). Myocardial ischemia-reperfusion injury: a neglected therapeutic target. J Clin Invest 1231**:** 92-100.

Heusch G (2013). Cardioprotection: chances and challenges of its translation to the clinic. Lancet 3819861**:** 166-175.

Hueso-Falcon I, Cuadrado I, Cidre F, Amaro-Luis JM, Ravelo AG, Estevez-Braun A*, et al.* (2011). Synthesis and anti-inflammatory activity of ent-kaurene derivatives. Eur J Med Chem 464**:** 1291-1305.

Kawano S, Kubota T, Monden Y, Tsutsumi T, Inoue T, Kawamura N*, et al.* (2006). Blockade of NF-kappaB improves cardiac function and survival after myocardial infarction. Am J Physiol Heart Circ Physiol 2913**:** H1337-1344.

Kis A, Yellon DM, Baxter GF (2003). Role of nuclear factor-kappa B activation in acute ischaemia-reperfusion injury in myocardium. Br J Pharmacol 1385**:** 894-900.

Ma XH, Shi Z, Tan C, Jiang Y, Go ML, Low BC*, et al.* (2010). In-silico approaches to multi-target drug discovery : computer aided multi-target drug design, multi-target virtual screening. Pharm Res 275**:** 739-749.

Matsui T, Nagoshi T, Rosenzweig A (2003). Akt and PI 3-kinase signaling in cardiomyocyte hypertrophy and survival. Cell Cycle 23**:** 220-223.

Matsui T, Tao J, del Monte F, Lee KH, Li L, Picard M*, et al.* (2001). Akt activation preserves cardiac function and prevents injury after transient cardiac ischemia in vivo. Circulation 1043**:** 330-335.

Matsui Y, Takagi H, Qu X, Abdellatif M, Sakoda H, Asano T*, et al.* (2007). Distinct roles of autophagy in the heart during ischemia and reperfusion: roles of AMP-activated protein kinase and Beclin 1 in mediating autophagy. Circ Res 1006**:** 914-922.

Mozaffari MS, Liu JY, Schaffer SW (2010). Effect of pressure overload on cardioprotection via PI3K-Akt: comparison of postconditioning, insulin, and pressure unloading. Am J Hypertens 236**:** 668-674.

Ong SG, Hausenloy DJ (2012). Hypoxia-inducible factor as a therapeutic target for cardioprotection. Pharmacol Ther 1361**:** 69-81.

Pérez-Sirvent L, García-Álvarez, MC, Balestrieri, MA, Rodríguez, B (1981a). Transformaciones de hispanolona III. Reacciones del anillo B y degradación a di-homo-drimanos. Anales Quím77**:** 330-334.

Pérez-Sirvent L, García-Álvarez, MC, Rodríguez, B (1981b). Transformaciones de hispanolona II. Reacción retroaldólica de hispanolona y condensación aldólica de δ-dicetonas diterpénicas. Anales Quím77**:** 324-329.

Rogiers V (2003). Ecopa: actual status and plans. Toxicol In Vitro 175-6**:** 779-784.

Rohilla A, Rohilla S, Kushnoor A (2011). Myocardial postconditioning: next step to cardioprotection. Arch Pharm Res 349**:** 1409-1415.

Schwartz Longacre L, Kloner RA, Arai AE, Baines CP, Bolli R, Braunwald E*, et al.* (2011). New horizons in cardioprotection: recommendations from the 2010 National Heart, Lung, and Blood Institute Workshop. Circulation 12410**:** 1172-1179.

Shao Z, Bhattacharya K, Hsich E, Park L, Walters B, Germann U*, et al.* (2006). c-Jun N-terminal kinases mediate reactivation of Akt and cardiomyocyte survival after hypoxic injury in vitro and in vivo. Circ Res 981**:** 111-118.
Singh SS, Kang PM (2011). Mechanisms and Inhibitors of Apoptosis in Cardiovascular Diseases. Curr Pharm Des 1718**:** 1783-1793.

Takagawa J, Zhang Y, Wong ML, Sievers RE, Kapasi NK, Wang Y*, et al.* (2007). Myocardial infarct size measurement in the mouse chronic infarction model: comparison of area- and length-based approaches. J Appl Physiol 1026**:** 2104-2111.

Takagi H, Matsui Y, Sadoshima J (2007). The role of autophagy in mediating cell survival and death during ischemia and reperfusion in the heart. Antioxid Redox Signal 99**:** 1373-1381.

Tsutsumi YM, Tsutsumi R, Mawatari K, Nakaya Y, Kinoshita M, Tanaka K*, et al.* (2011). Compound K, a metabolite of ginsenosides, induces cardiac protection mediated nitric oxide via Akt/PI3K pathway. Life Sci 8815-16**:** 725-729.

Turer AT, Hill JA (2010). Pathogenesis of myocardial ischemia-reperfusion injury and rationale for therapy. Am J Cardiol 1063**:** 360-368.

Waldman M, Hochhauser E, Fishbein M, Aravot D, Shainberg A, Sarne Y (2013). An ultra-low dose of tetrahydrocannabinol provides cardioprotection. Biochem Pharmacol 8511**:** 1626-1633.

Xia YF, Ye BQ, Li YD, Wang JG, He XJ, Lin X*, et al.* (2004). Andrographolide attenuates inflammation by inhibition of NF-kappa B activation through covalent modification of reduced cysteine 62 of p50. J Immunol 1736**:** 4207-4217.

Xu D, Li Y, Wang J, Davey AK, Zhang S, Evans AM (2007). The cardioprotective effect of isosteviol on rats with heart ischemia-reperfusion injury. Life Sci 804**:** 269-274.

Figures

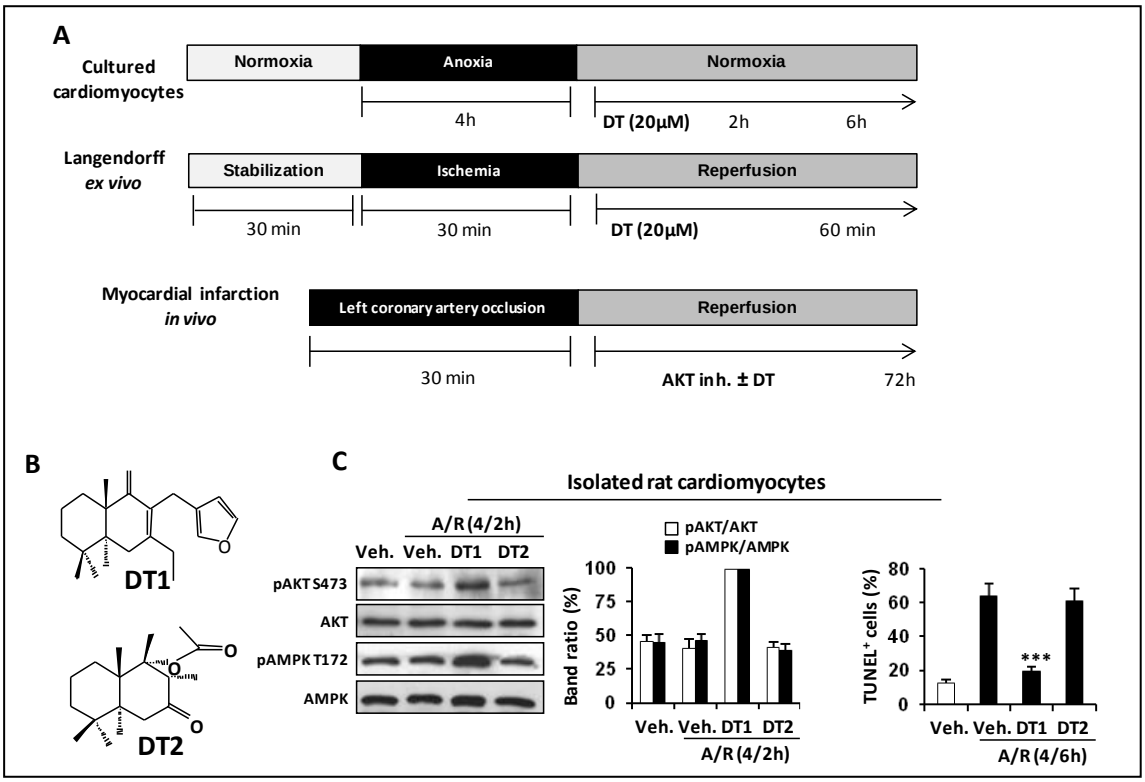

Figure 1. Experimental design, chemical structure of the labdane diterpenes (DTs) and effects on isolated rat cardiomyocytes. Experimental groups and protocols for isolated cultured rat cardiomyocytes, global I/R in Langendorff isolated perfused rat hearts and myocardial infarction by left anterior descending coronary artery (LAD) occlusion (A). Chemical structures of the labdane diterpenes derived from hispanolone. DT1 exerted cytoprotective effects *in vitro* whereas DT2 was a structurally-related labdane lacking most of these properties (Cuadrado *et al.*, 2011) (B). DT1, but not DT2 increased the levels of the survival proteins pAKT and pAMPK after anoxia (4h) and reperfusion (A/R) (2h; *left panel*) and apoptosis (6h; *right panel*) in isolated cultured rat cardiomyocytes (C). ***P<0.001 *vs.* the A/R condition in the presence of vehicle.

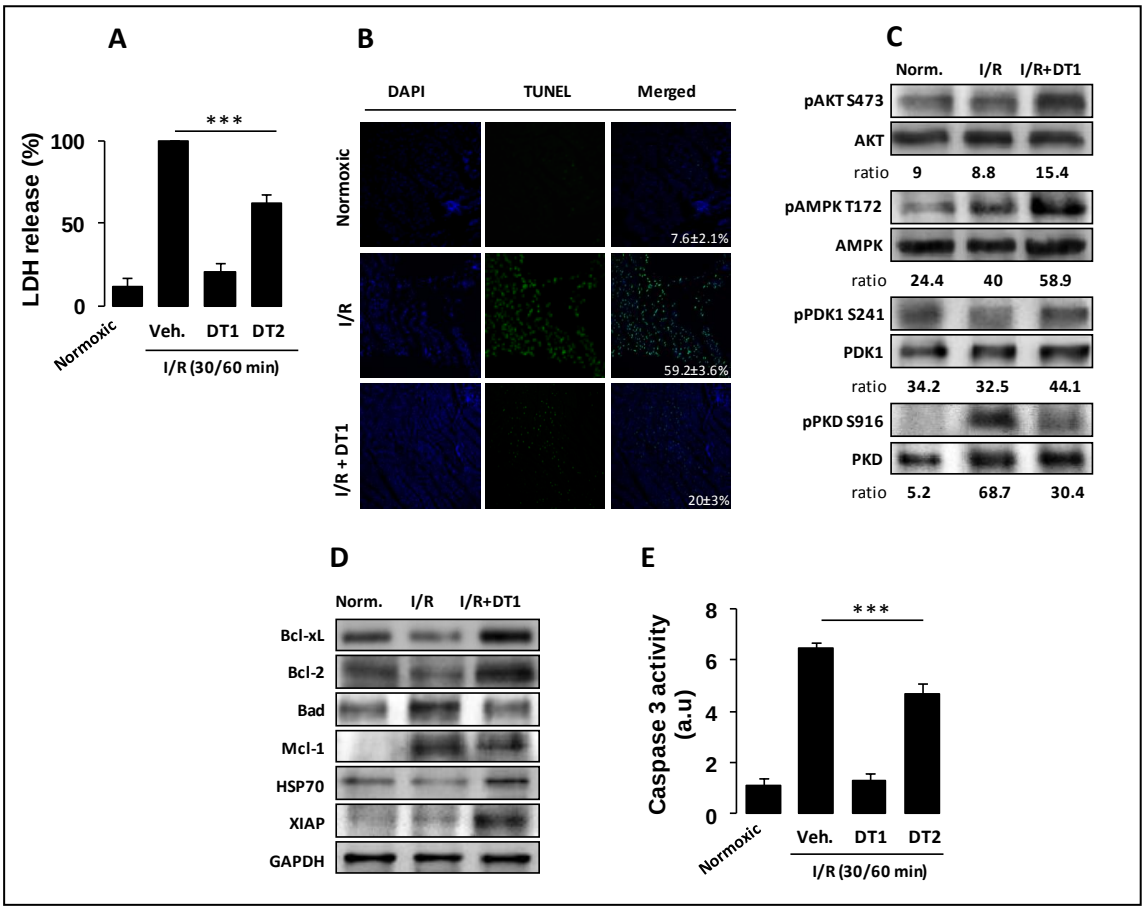

Figure 2. DT1 treatment activates survival pathways and attenuates myocardial apoptosis and necrosis **after I/R in isolated rat hearts.** LDH release to the perfusate in hearts after normoxia and I/R (30/60 min each) ± DTs (20 µM each) (A). Representative images and quantitative results from isolated perfused hearts after I/R in the presence of 20 µM DT1 following reoxygenation. TUNEL-positive nuclei are in green and total nuclei staining with DAPI are in blue (B). TUNEL-positive cells are expressed as percentage of total cells in the sections (*inset*, B). Representative immunoblots for pAKT(S473), total AKT, pAMPK(T172), total AMPK, pPDK1(S241), total PDK1, pPKD(S916) and total PKD expression in whole heart. The ratio of phospho/total protein levels is showed for each respective blot pair (mean; n=4) (C). Levels of apoptosis-related proteins were determined in total extracts from hearts after I/R-injury treated as depicted in Figure 1A (D). Caspase-3 activity was also determined in these extracts (E). Results show the mean±SD of 4 hearts per condition or a representative section (B) or blots (C,D). ****P*<0.001 *vs.* the I/R condition in the presence of vehicle.

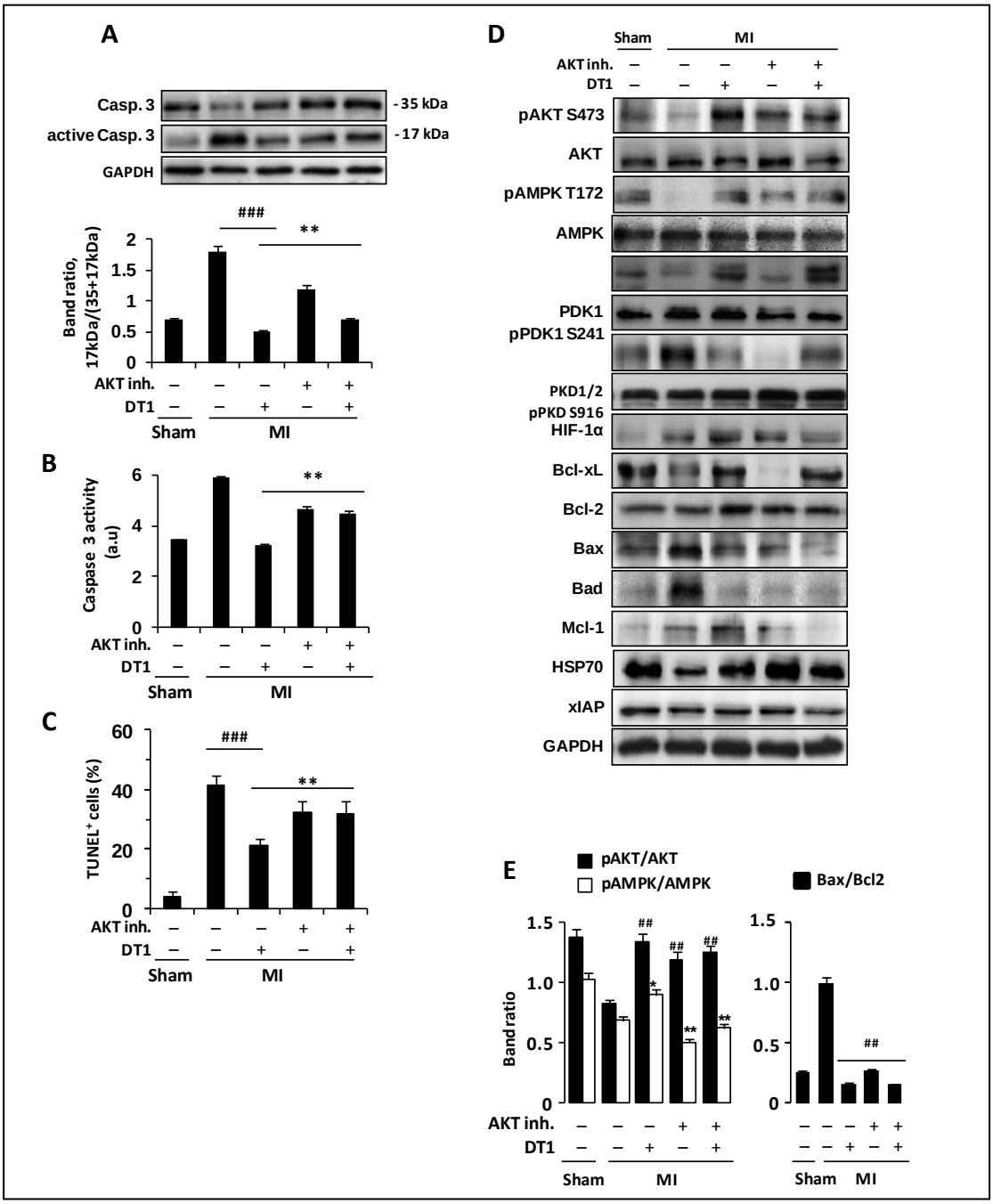

Figure 3. Attenuation of apoptotic death and enhancement of survival pathways by DT1 after rat myocardial infarction (MI). Pro-caspase-3 (35 kDa) and active caspase-3 (17 kDa) protein levels (A) and activity (B) in total extracts from whole heart of sham, MI, MI+DT1 and MI+AKT inh.±DT1 rat groups as described in Figure 1A. DT1 (5 mg/kg) was i.v. injected at reperfusion. Quantification of TUNEL staining in the area at risk in the different animal groups (C). Western blots analyses of survival- and apoptosis-related proteins from total extracts of hearts after MI in the presence or absence of DT1 and AKT inh. at 72h after reoxygenation (D). The ratios of pAKT/AKT, pAMPK/AMPK and Bax/Bcl2 are shown (E). In all blots, protein loading was normalized with GADPH. Results show the mean±SD of n=10 animals per condition or a representative blot. $^{###}P<0.001$, $^{##}P<0.01$ *versus* non-treated MI animals. **p<0.05 *vs.* the same condition in the presence of DT1.

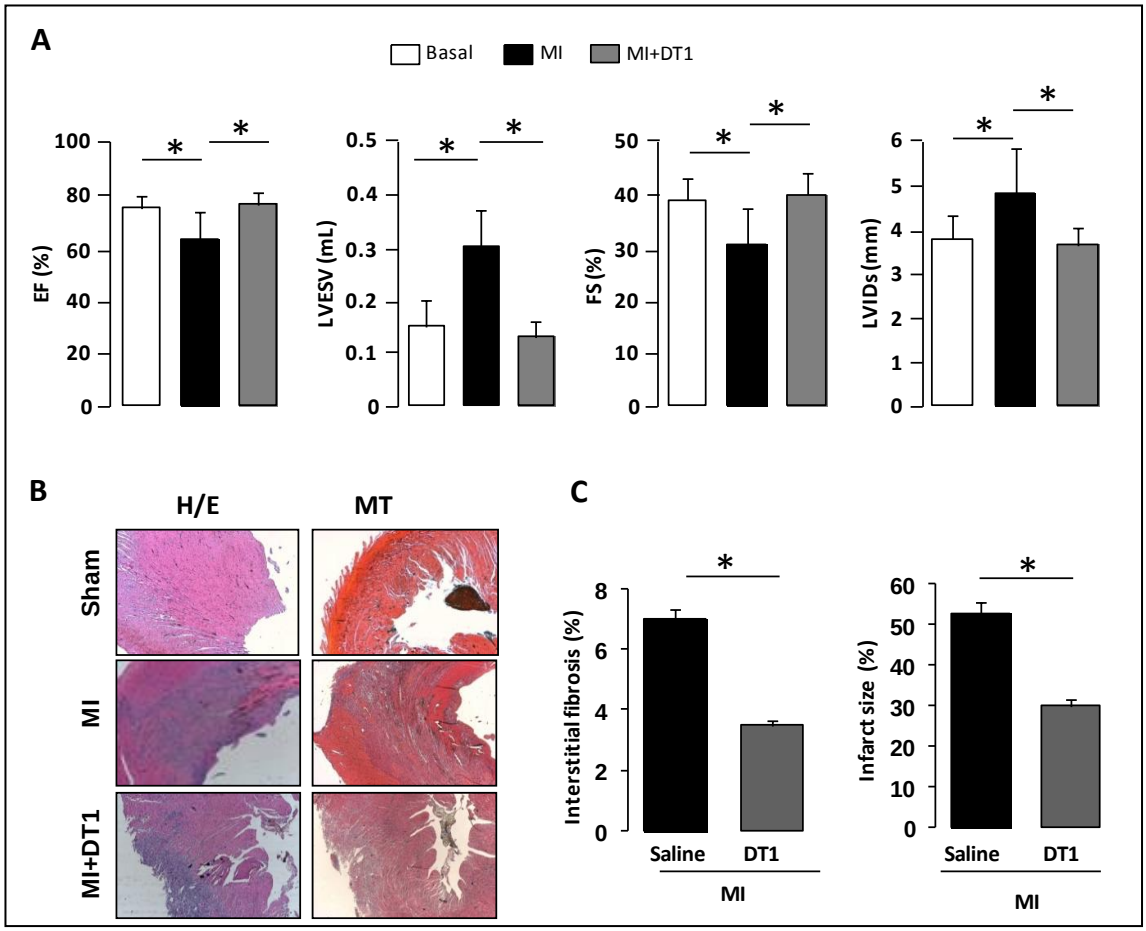

Figure 4. DT1 improves cardiac function after MI. Rats underwent occlusion of the left anterior coronary artery (LAD) for 30 min followed by reperfusion as depicted in Figure 1A and Figure 3 and DT1 (5 mg/kg) was i.v. injected at the onset of reperfusion. Echocardiography parameters evaluating Ejection Fraction (EF, in %), Left Ventricular End Systolic Volume (LVESV, in ml), Fraction Shortening (FS, in %)) and Left Ventricular Internal Dimension in systole (LVIDs, in mm) were measured in the three experimental groups (A). Recordings were performed before (basal) and 72h after the operation. Rats were sacrificed 72h post-MI and hearts were excised off and fixed. Histological analysis was carried out using hematoxilin/eosin (H/E; *left panels*) and Masson Trichrome (MT; *right panels*) (B). The scar lenght was measured using the midline method and expressed as the percentage of the left ventricle circumference length in which the scar occupies at least 50% of the ventricular wall thickness. For interstitial fibrosis, results are expressed as mean percentage of collagen over the entire tissue in the section. In both cases ImageJ analysis was used (C). Results show the mean± SD of n=10 animals per condition (A, C) or a representative staining (B). *P<0.05 MI *vs.* basal or MI.

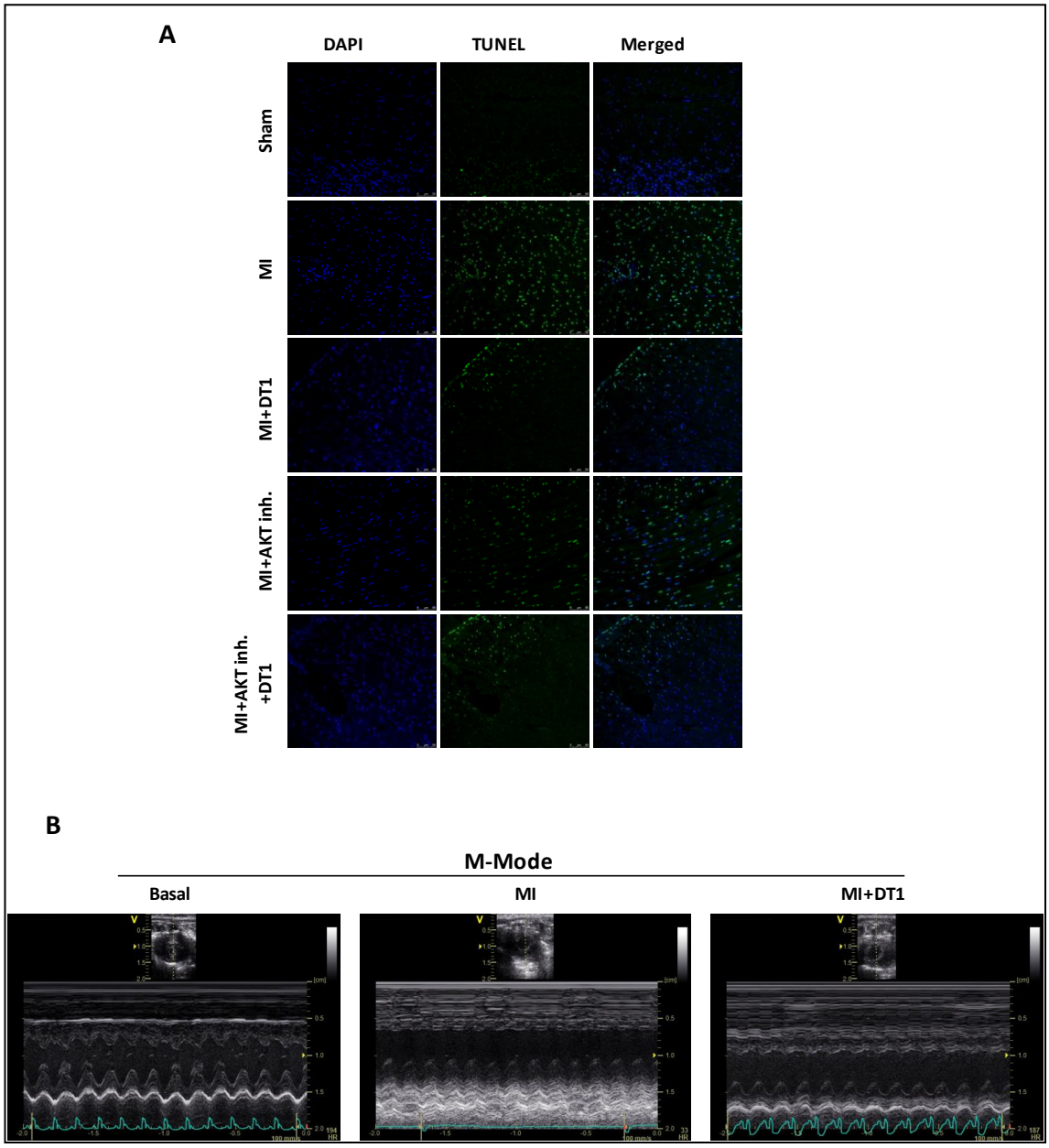

Figure S1. **Protective effects of DT1 in the MI rat model**. Representative images of TUNEL-positive sections of hearts from sham, MI, MI+DT1 and MI+AKT inh.±DT1 rat groups. TUNEL-positive nuclei are visualized in green and total nuclei were stained with DAPI in blue. Results show the mean±SD of 4 hearts per condition or a representative section (A). DT1 (5 mg/kg) was i.v. injected at reperfusion. Cardiac function was analyzed by echocardiography in M-mode 72h after operation. Representative images of M-Mode echocardiographic images of the left ventricle are shown.

DISCUSIÓN

Discusión

La búsqueda de nuevos fármacos a partir de productos naturales, entre los que se incluyen aquellos obtenidos de las plantas y sus derivados bioactivos, ha llevado al desarrollo de numerosos compuestos farmacológicamente activos con utilidad en el tratamiento y prevención de numerosas enfermedades, particularmente en las áreas como el cáncer, la inflamación, enfermedades infecciosas, enfermedades cardiovasculares, entre otras (Newman *et al.*, 2012). Los nuevos avances en el conocimiento de dianas moleculares y métodos de screening farmacológico, han permitido avanzar en la identificación de nuevas estructuras de origen natural que puedan servir como "cabezas de serie" para el diseño de nuevos compuestos (Chin *et al.*, 2006; Harvey *et al.*, 2010).

El trabajo experimental presentado en esta Tesis se encuadra dentro de una línea de investigación orientada al screening de nuevos productos bioactivos. Este estudio proporciona nuevos datos sobre la actividad de diterpenos labdanos y kauranos, analizando sus efectos como agentes antiinflamatorios y cardioprotectores, identificándose las dianas moleculares de actuación de los mismos.

Los diterpenos son compuestos con gran potencial farmacológico habiéndose descrito sus propiedades antiinflamatorias, antitumorales, antiinfecciosas, antivirales, entre otras (Chinou, 2005; de las Heras *et al.*, 2009; de las Heras *et al.*, 2003; Salminen *et al.*, 2008). Estudios previos han descrito la actividad antiinflamatoria de diterpenos con estructuras diversas como es el caso de los labdanos andalusol, derivados de hispanolona, andrografólido, (Giron *et al.*, 2008; Navarro *et al.*, 1997; Singh *et al.*, 1999), kauranos como es la kamebakaurina, oridonina (Castrillo *et al.*, 2001) o los derivados de tipo clerodano y pimarano (Demetzos *et al.*, 2001; Lam *et al.*, 2003; Lee *et al.*, 2005; Suh *et al.*, 2004; Traves *et al.*, 2007).

En la primera parte de la Tesis Doctoral se analizaron los efectos de dos series de diterpenos de tipo labdano y kaurano en vías de señalización implicadas en la regulación del proceso inflamatorio.

La inflamación es una respuesta biológica de defensa frente a un patógeno o agente nocivo, participando en la destrucción del mismo y contribuyendo así a la reparación del tejido dañado. Existen evidencias científicas que apoyan la

presencia de un componente inflamatorio en distintas patologías como las enfermedades neurodegenerativas o cardiovasculares (Marchant *et al.*, 2012).

Los macrófagos participan activamente en el inicio de la inflamación y sirven como una interfaz esencial entre la inmunidad innata y adaptativa en la activación del sistema inmune. Se encuentran en todos los tejidos y presentan gran diversidad funcional ya que, además de participar en la inmunidad, desarrollan un papel muy importante en el mantenimiento de la homeostasis y reparación tisular. Varias vías de señalización temprana han sido identificadas cuando los macrófagos son activados a través de los receptores de membrana TLRs y otros receptores por citoquinas proinflamatorias o por moléculas tipo PAMPs, como es el caso de moléculas de origen bacteriano como el LPS. Por ello, la regulación de la activación de los macrófagos se ha convertido en una diana terapéutica importante para el tratamiento de un gran número de enfermedades (Wynn *et al.*, 2013), concretamente la modulación de la señalización de los TLR4 tras ser inducidos por LPS, así como la regulación de la producción de citoquinas constituye una estrategia terapéutica en muchas enfermedades inflamatorias.

Una primera aproximación para el estudio de la actividad antiinflamatoria de los diterpenos es la determinación de mediadores proinflamatorios como NO y PGE_2. Los resultados obtenidos mostraron que, de la serie de 63 diterpenos kaurano evaluada (Capítulo 1), tres compuestos (**28**, **55** y **62)** provocaban una disminución significativa de la liberación de NO en macrófagos estimulados con LPS. Así mismo, el diterpeno **LAME** de la serie de diterpenos labdánicos (Capítulo 2), inhibió la liberación de NO y PGE_2. Se confirmó que la inhibición de la liberación de estos mediadores por los diterpenos estaba mediada por la inhibición a nivel transcripcional de la expresión de las enzimas NOS-2 y COX-2, responsables de la síntesis de NO y PGE_2 respectivamente.

Es ampliamente conocido que NF-κB desempeña un papel fundamental en el control de la respuesta inmune, la inflamación y otros procesos como la apoptosis, la diferenciación y supervivencia celular (Baeuerle, 1998; Bonizzi *et al.*, 2004). La unión del LPS al receptor TLR4 en el macrófago activa al factor de transcripción nuclear NF-κB, responsable de la expresión de enzimas inflamatorias como NOS-2 y COX-2, así como de la expresión de genes que

codifican para citoquinas proinflamatorias (TNF-α, IL-1β, IL-6 o MCP-1) o de moléculas de adhesión como la E-selectina.

En las células no estimuladas el factor NF-κB se encuentra retenido en el citoplasma asociado a las proteínas inhibitorias IκBs. Sin embargo, en respuesta a una señal extracelular (mitógenos, estrés oxidativo o moléculas de origen bacteriano como LPS) las proteínas IκB son fosforiladas en residuos específicos de serina, por las proteínas quinasas de IκB (IKK) (Hacker *et al.*, 2006). La fosforilación de IκB seguido de su poliubiquitinización, conduce a su degradación permitiendo que NF-κB se transloque al núcleo donde se une a la región promotora de distintos genes (Perkins, 2006). Por ello, la inhibición de la activación de NF-κB ha constituido una estrategia terapéutica en la búsqueda de nuevos agentes antiinflamatorios (Bremner *et al.*, 2002; Gupta *et al.*, 2010; Karin *et al.*, 2005; Nam, 2006). La inhibición de la activación de este factor de transcripción puede ocurrir por distintos mecanismos: la inhibición de la activación del complejo IKK, modulando la degradación proteosomal de las proteínas IκBs o interfiriendo en la translocación de NF-κB al núcleo. De todos estos mecanismos, la inhibición de la actividad quinasa de IKK constituiría el enfoque más selectivo y eficaz (Bremner *et al.*, 2002; Karin *et al.*, 2004; Uwe, 2008). En este contexto, distintos diterpenos labdano y kaurano tales como el andalusol, los derivados de hispanolona o la oridinina han sido descritos como inhibidores específicos de NF-κB por inhibir, alguno de ellos, la actividad quinasa IKK (Castrillo *et al.*, 2001; Chao *et al.*, 2005; de las Heras *et al.*, 2009; de las Heras *et al.*, 1999; Giron *et al.*, 2008).

Dado que NF-κB es una diana de actuación de compuestos diterpénicos, quisimos evaluar el efecto de los diterpenos objeto de estudio en la vía de activación de este factor. El tratamiento de los macrófagos con los diterpenos redujo la degradación de los niveles citosólicos de la proteína inhibidora IκBα. Como se ha descrito previamente que varios diterpenos de tipo kaurano como el foliol y linearol, eran capaces de inhibir la actividad IKK, reduciendo así la fosforilación de las proteínas IκBs (Castrillo, 2001), no se puede descartar que el mecanismo de actuación de los diterpenos **28**, **55** y **62** sea semejante. Además, en el caso de LAME comprobamos que también estaba inhibida la

traslocación al núcleo de la subunidad p65. Por ello la inhibición de NF-κB es un mecanismo común para los diterpenos kaurano y el labdano LAME.

Por otra parte, la activación de los macrófagos también produce la liberación citoquinas proinflamatorias y quimioquinas. La inhibición de la síntesis de estos mediadores, así como el bloqueo de sus receptores es una diana en la búsqueda de fármacos activos en diversas patologías inflamatorias como la enfermedad de Crohn, la artritis reumatoide o la aterosclerosis (Smolen *et al.*, 2013; Thomson *et al.*, 2012) (Smolen, 2013, Thomson, 2012), donde los niveles de las citoquinas IL-1, IP-10, IL-6 o TNF-α están muy elevados. Además, se ha descrito la actividad proinflamatoria de citoquinas como TNF-α e IL-6 tanto *in vitro* como *in vivo*. Así mismo, TNF-α está implicado en procesos como el shock endotóxico, la caquexia, apoptosis o la inflamación, siendo esta citoquina esencial para la inducción de la síntesis de NO en macrófagos estimulados con IFN-γ y/o LPS. Además, la IL-6 es un mediador endógeno que en respuesta a LPS puede producir fiebre.

Los datos obtenidos mostraron que tanto los diterpenos kauranos como el labdano LAME eran capaces de inhibir significativamente la liberación de citoquinas (IP-10, IL-6, IL-1α, TNF-α e IFN-γ). En la literatura se han descrito compuestos con actividad inhibidora de IKK, que bloqueaban a su vez la producción de TNF-α tras la estimulación con LPS en modelos murinos (Uwe, 2008).

El efecto inhibitorio de los diterpenos observado sobre la liberación de citoquinas fue más marcado en el caso de IL-6. Existen varios sitios de unión en la región 5’ del gen de IL-6 para distintos factores de transcripción, entre los que se incluye NF-κB, CREB, NF-IL-6 y AP-1. Por tanto los datos obtenidos indican la activación de NF-κB como único factor de transcripción implicado en la liberación de IL-6. Nuestros resultados están de acuerdo con otros estudios recientes sobre el promotor de IL-6 donde se demuestra la inducción de IL-6 por numerosos factores de transcripción (Chen *et al.*, 2006a).

Además de la activación de NF-κB la estimulación de TLR4 por el LPS desencadena la activación de la vía de las MAPKs, que en última instancia resulta en la activación de las proteínas p38, ERK y JNK. Se confirmó que en

presencia del diterpeno LAME se inhibía la fosforilación de ERK y JNK lo que sugería que la actividad antiinflamatoria está mediada también por esta vía.

La inhibición mostrada en las cascadas de NF-κB y MAPKs hacía pensar que LAME podría estar actuando en una diana previa a la activación de estas vías. Numerosos estudios destacan el papel regulador de la proteína quinasa TAK-1 en estas vías de señalización (Cuevas *et al.*, 2007; Chen *et al.*, 2006b). Por lo tanto, TAK-1 representaría una nueva estrategia para la intervención farmacológica en numerosos procesos inflamatorios. Observamos que el tratamiento de los macrófagos con LAME inhibió la fosforilación de TAK-1 inducida por el LPS.

Hasta el momento, el compuesto LAME mostraba efectos antiinflamatorios en macrófagos. Sin embargo, en la evaluación del potencial antiinflamatorio de las moléculas de interés terapéutico, los ensayos *in vitro* han de ser completados con ensayo de actividad antiinflamatoria en modelos experimentales *in vivo*. Por ello se evaluó la actividad del nuestro compuesto activo en un modelo de sepsis inducida por LPS en ratón. En este modelo se confirmó que el tratamiento de los animales con LAME, provocaba una reducción de los niveles circulantes de las citoquinas IL-6 y TNF-α, aumentando la supervivencia de los animales con endotoxemia. Otros diterpenos como los derivados del labdano andrografólido o la Tanshinona IIA, también habían mostrado un efecto protector de endotoxemia en modelos animales (Guo *et al.*, 2012; Zhang *et al.*, 2010).

Finalmente, intentamos establecer la relación entre la estructura química y la actividad farmacológica de la serie de los diterpenos kauranos evaluados con objeto de identificar grupos funcionales que pudieran ser los responsables de la actividad mostrada por los compuestos activos **28**, **55** y **62**. Los tres diterpenos comparten en su estructura un ácido carboxílico (C-19) que parece estar implicado en la actividad antiinflamatoria mostrada. La combinación de grupos funcionales, en la combinación de un grupo éster metílico en el C-19 junto con un grupo hidroxilo en el C-15 o bien de un ácido carboxílico en C-19 con uno carbonilo en C-15 conlleva a un incremento en la actividad antiinflamatoria (Figura 9).

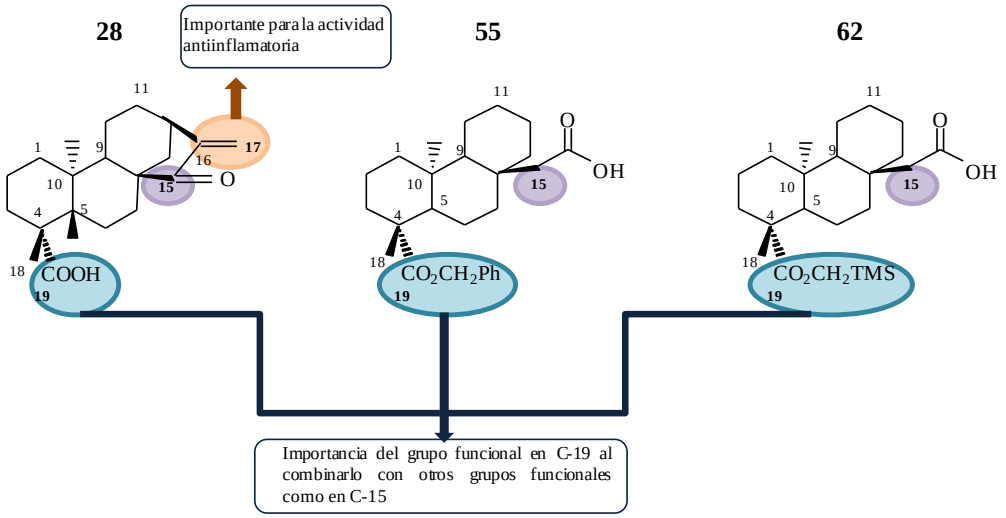

Figura 9: Relación estructura-actividad de los diterpenos kaurano 28, 55 y 62.

En resumen, los datos obtenidos demuestran que tres diterpenos de tipo kaurano de la serie evaluada, **28**, **55** y **62**, y el labdano **LAME** poseen actividad antiinflamatoria en macrófagos. Esta actividad podría deberse en parte a la actividad inhibitoria del factor de transcripción NF-κB. Los diterpenos también inhiben la expresión génica de las enzimas NOS-2 y COX-2, así como la secreción de distintas citoquinas implicadas en la respuesta inflamatoria. En el caso de LAME, se puede concluir que sus efectos están mediados por la inhibición de la fosforilación de TAK-1. Por último, la baja toxicidad de LAME y la eficacia mostrada *in vivo*, indican que LAME podría tener potencial terapéutico como agente antiinflamatorio.

Cada vez existen más evidencias científicas que apoyan la implicación de la inflamación como un componente destacado de enfermedades cardiovasculares, entre ellas, el daño por isquemia/reperfusión (I/R), habiéndose descrito la liberación de diversos mediadores inflamatorios que aumentan el daño miocárdico (Marchant *et al.*, 2012). En la actualidad continúa la búsqueda de nuevos tratamientos dirigidos a proteger al corazón frente un daño por I/R. La isquemia del miocardio producida por el bloqueo del flujo sanguíneo hacia el corazón conlleva cambios en el balance energético como disminución de ATP. Sin embargo, los cardiomiocitos responden ante este cambio al inhibir la oxidación de ácidos grasos (Hausenloy *et al.*, 2009;

Hausenloy *et al.*, 2011b; Turer *et al.*, 2010; Wang, 2007). A pesar de que la caída de ATP durante el periodo de isquemia provoca la inhibición de varios procesos básicos en el interior de la célula, como es la alteración de la Na+/K+-ATPasa de la membrana, la reperfusión que se produce en el miocardio conduce a un incremento rápido del Ca^{2+} intracelular, que favorece la apertura del poro de transición de permeabilidad mitocondrial. Este evento conlleva a la muerte celular por necrosis o apoptosis debido a la liberación de factores clave en la disfunción cardiaca, como son los mediadores proapoptóticos y los ROS (Carreira *et al.*, 2011).

Una aproximación terapéutica en el tratamiento de la I/R es la búsqueda de agentes cardioprotectores que pudieran ser administrados en el momento de la reperfusión, para atenuar el daño miocárdico. Distintos fármacos (agonistas de receptores de adenosina, de bradiquinina y de opioides y la ciclosporina A) han demostrado potencial cardioprotector en modelos animales, siendo los resultados con ciclosporina, los más prometedores (Hausenloy *et al.*, 2011a; Schwartz Longacre *et al.*, 2011). Datos preclínicos confirman que la administración de ciclosporina en el momento de la reperfusión conlleva a una reducción del tamaño del infarto. Sin embargo, hasta el momento estos resultados no se han podido trasaladar a la aplicación clínica en pacientes. Por ello es necesario desarrollar estrategias farmacológicas adicionales que mimeticen, sinergizen o aumenten la protección ejercida por los protocolos habituales en la reperfusión. Actualmente, continúa siendo un área de intensa investigación el conocimiento de nuevas dianas y vías de señalización implicadas en la cardioprotección (Downey *et al.*, 2009; Frohlich *et al.*, 2013; Sanz-Rosa *et al.*, 2012).

Como se comentó anteriormente, los productos naturales, en particular los diterpenos de tipo labdano han sido descritos como moléculas con potente actividad antiinflamatoria, mostrando además propiedades citoprotectoras (Chinou, 2005; Giron *et al.*, 2008; Navarro *et al.*, 1997). En la literatura, un reducido número de productos naturales han sido evaluados como agentes cardioprotectores. Se incluyen compuestos de diversa naturaleza química como polifenoles con propiedades antioxidante (Thomas *et al.*, 2011; Townsend *et al.*, 2004; Zhao *et al.*, 2010)), la curcumina, rapamicina, (Duan *et*

al., 2012), saponinas triterpénicas, como los ginsenósidos (Li *et al.*, 2010; Tsutsumi *et al.*, 2011), o más recientemente los derivados del cannabinol (Waldman *et al.*, 2013). Hasta el momento no existen datos científicos sobre el potencial cardioprotector de los diterpenos labdano.

En la segunda parte de esta Tesis Doctoral pretendimos evaluar la potencial actividad cardioprotectora de tres diterpenos labdanos derivados de hispanolona (**T1**: dehidrohispanolona, **T2**: 8,9-dehidrohispanolona 15,16-lactol y **T3**: 14,15,16-trisnor-13,9α-hispanolida) en el proceso de I/R, con el estudio de los mecanismos moleculares implicados (Capítulo 3 y 4). Dos de los diterpenos objeto de estudio (T1 y T2) habían mostrado propiedades antiinflamatorias y citoprotectoras en estudios previos.

Se ha descrito ampliamente que la muerte de los cardiomiocitos tras un periodo de isquemia se produce por procesos de apoptosis, necrosis y autofagia, contribuyendo los tres a la recuperación de la función celular. De hecho, la prevención de la apoptosis inducida por la anoxia o la isquemia sería una estrategia para minimizar la lesión cardiaca. Inicialmente se demostró en cardiomiocitos que estos diterpenos ejercían efecto protector en las etapas iniciales de la apoptosis, al provocar una reducción de los niveles de la proteína proapoptótica Bax y un incremento significativo de las proteínas antiapoptóticas (xIAP, Bcl-2, Bcl-xL). El perfil antiapoptótico de T1 y T2 se corroboró por la reducción de la actividad caspasa-3.

El efecto protector mostrado nos llevó a evaluar el efecto de estos compuestos en vías de señalización de supervivencia descritas en cardioprotección, como la vía PI3K/AKT, incluida en la vía RISK (Hausenloy *et al.*, 2004; Matsui *et al.*, 2001). Al analizar los niveles de p-AKT se observó que en condiciones de normoxia se producía la fosforilación de AKT y que esta activación fue incluso mayor bajo las condiciones de anoxia y reoxigenación (A/R). Es importante destacar que la inhibición selectiva de PI3K o AKT tenía como consecuencia la pérdida del efecto protector de T1 como se deduce del aumento de los niveles de Bax y de caspasa-3, con una disminución marcada de la viabilidad de los cardiomiocitos.

Otra vía implicada en la cardioprotección es la vía de las proteínas MAP quinasas (MAPKs), que incluyen las proteínas ERK 1/2, JNK y p38.

Observamos que los diterpenos activos aumentaban la fosforilación de ERK 1/2 en cardiomiocitos sometidos a un daño por A/R, desempeñando un papel antiapoptótico en los primeros minutos de la reoxigenación. No se observaron cambios significativos en la expresión de las proteínas quinasas p38 y JNK en presencia de los diterpenos. De hecho, la activación en el corazón de JNK parece dar lugar a efectos proinflamatorios ya que favorece el reclutamiento de células del sistema inmune (Qi *et al.*, 2009).

Por otra parte, se ha descrito la función cardioprotectora de la proteína AMPK en los cardiomiocitos que tras una I(A)/R se enfrentan a una insuficiencia metabólica (Eltzschig *et al.*, 2011; Takagi *et al.*, 2007a; Wang, 2007; Wang *et al.*, 2009). Nuestros datos mostraron una activación significativa de la AMPK tras un daño por A/R tanto en la línea celular de cardiomiocitos como en cardiomiocitos primarios de rata. Aunque el mecanismo de acción de T1 en este proceso está aún en estudio, los datos apuntan a que se trata de un proceso activado tras la anoxia y reoxigenación, lo cual es interesante desde el punto de vista farmacológico. De acuerdo con estos resultados, existen datos de modelos de ratones transgénicos que expresan una forma inactiva de AMPK y sometidos a un proceso de I/R mostraron disminución significativa de la absorción de glucosa, la glucolisis y la absorción de ácidos grasos (Russell *et al.*, 2004).

En todos estos estudios el diterpeno T1 mostraba un efecto protector superior a T2 en cardiomiocitos, por lo que fue evaluado posteriormente en modelos experimentales en animales. Para ello se seleccionaron los modelos *ex vivo* de corazón aislado y perfundido de Langendorff (Chaudhary *et al.*, 2013; Skrzypiec-Spring *et al.*, 2007; Yan *et al.*, 2012), y un modelo *in vivo* de daño agudo en el miocardio por la ligadura temporal de la arteria coronaria descendente izquierda (oclusión LAD), de modo que la isquemia se consigue bloqueando el flujo sanguíneo temporalmente para después reperfundirlo. Ambos modelos son ampliamente utilizados en la literatura (Das *et al.*, 2012; Quintieri *et al.*, 2012; Yao *et al.*, 2013).

Inicialmente nos centramos en la vía apoptótica mitocondrial con el fin de corroborar el efecto protector de T1 observado en cardiomiocitos. En ambos modelos animales este diterpeno fue capaz de reducir la actividad caspasa-3 y

aumentar la expresión de los miembros antiapoptóticos de la familia Bcl-2 (como Bcl-xL o Bcl-2), confirmándose su perfil antiapoptótico. Así mismo observamos una disminución de la muerte de los cardiomiocitos mediante TUNEL.

Así mismo se confirmó de nuevo la activación de vías de supervivencia como PI3K/AKT, sugiriéndose la activación de AKT como mecanismo de acción principal del diterpeno T1. Los efectos protectores del diterpeno se asocian con un aumento en la fosforilación de distintas proteínas implicadas en la supervivencia cardiaca, como AKT y PDK1 (una quinasa de activación previa en la vía PI3K/AKT). Es interesante destacar que el tratamiento previo de los animales con un inhibidor de AKT conllevaba la supresión de la mayor parte de los efectos cardioprotectores del diterpeno, incluyendo la inhibición de la expresión y actividad caspasa-3, reducción de la apoptosis y activación de las vías de supervivencia. Estos datos demuestran el papel destacado de AKT en la protección de los cardiomiocitos proporcionada por T1. Además, se sugiere la participación de otros mecanismos que confieren cardioprotección puesto que la inhibición de AKT no fue capaz de restaurar completamente el fenotipo isquémico, en presencia del diterpeno activo.

En ambos modelos experimentales, en el grupo de animales tratados con el diterpeno T1 también se observó activación de AMPK como parte de la supervivencia innata que poseen los cardiomiocitos.

Como se comentó anteriormente, la inflamación es un componente fundamental en el proceso de I/R (Entman *et al.*, 1991; Frank *et al.*, 2012), habiéndose descrito la participación del factor de transcripción NF-κB en la respuesta inflamatoria durante el daño miocárdico por I/R ya que se activa en los periodos postisquémicos (Kis *et al.*, 2003). Por ello, se ha descrito que el bloqueo de NF-κB contribuiría a mejorar la función cardiaca y la supervivencia (Kawano *et al.*, 2006). Estudios previos del grupo de investigación indicaron que el diterpeno activo era capaz de inhibir la activación de NF-κB (Giron *et al.*, 2008), lo cual sugiere que T1 puede ejercer, en parte, su efecto protector y antiapoptótico (modulando la familia de proteínas Bcl-2) a través de la supresión de la respuesta inflamatoria a través de la inhibición de la activación de este factor.

Los resultados de este trabajo experimental muestran que los diterpenos labdanos actúan a nivel de las vías de supervivencia AKT y ERK 1/2 protegiendo a los cardiomiocitos de la muerte celular tras un periodo de I/R. Además, los datos ecocardiográficos de los animales tratados, confirmaron el efecto protector del diterpeno al mejorar la función cardiaca y reduciendo el tamaño del infarto, en ratas con oclusión de la arteria coronaria descendente. La protección ejercida por T1 cuando se administra en el inicio de la reperfusión abre un área novedosa de estrategias terapéuticas para el control del daño por reperfusión. Un esquema representativo del mecanismo de acción de T1 se muestra en la figura 10.

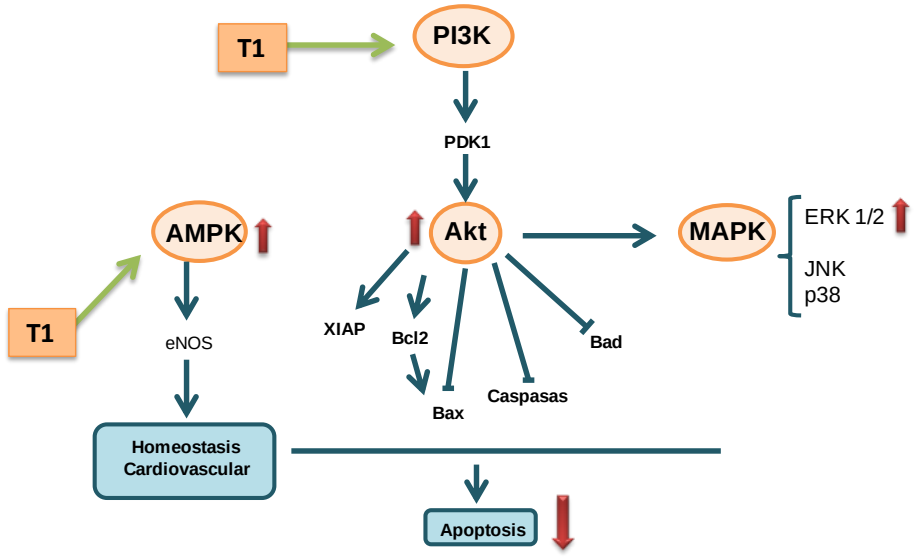

Figura 10. Mecanismo de cardioprotección propuesto para el diterpeno labdano T1

Este estudio aporta nuevas perspectivas sobre el potencial terapéutico de los compuestos diterpénicos. En primer lugar, se ha contribuido a la generación/obtención de moléculas activas en inflamación y cardioprotección que puedan servir como “cabezas de serie” (*leads*) para la síntesis de nuevas moléculas a partir de ellas, con identificación de las modificaciones estructurales que derivan en una mayor actividad biológica. Al tratarse de un estudio integrado, esta Tesis ha permitido validar la actividad de estas

moléculas en modelos celulares y de órgano aislado, para finalmente corroborar sus efectos en modelos animales. Por otra parte, los datos aportados pueden constituir un punto de partida para la valoración de los diterpenos en otras cardiopatías, como la miocarditis bacteriana o viral. Finalmente, estas moléculas podrían constituir una estrategia terapéutica debido a su efecto citoprotector en terapias con fármacos con toxicidad cardiaca utilizados en el tratamiento del cáncer. Ejemplos representativos de fármacos cardiotóxicos son las antraciclinas, fluorouracilo o transtuzumab, entre otros, con amplio uso clínico.

CONCLUSIONES

Conclusiones

1. Los diterpenos de tipo kaurano y labdano mostraron efectos antiinflamatorios en macrófagos. Estos compuestos son capaces de inhibir la activación de NF-κB y en consecuencia, la expresión de los genes inflamatorios clásicos regulados por este factor de transcripción. Los diterpenos kauranos **28**, **55** y **62** y el diterpeno de tipo labdano éster metílico del ácido labdanólico (**LAME),** destacaron por su mayor actividad antiinflamatoria.

2. El diterpeno LAME mantuvo su actividad antiinflamatoria en un modelo experimental de sepsis inducida por LPS en ratón, aumentando la supervivencia y reduciendo los niveles séricos de las citoquinas TNF-α e IL-6, en los animales tratados.

3. Los diterpenos labdanos derivados de la hispanolona (**T1 y T2**) ejercieron efectos citoprotectores en cardiomiocitos sometidos a un daño por anoxia/reperfusión. Estos compuestos muestran un perfil antiapoptótico además de incrementar los niveles de proteínas implicadas en supervivencia celular.

4. El diterpeno T1 presentó actividad cardioprotectora en modelos animales de isquemia/reperfusión (I/R) cuando se administra al inicio de la reperfusión, activando vías de supevivencia específicas (PI3K/AKT). Así mismo, este compuesto es capaz de mejorar la función cardiaca y reducir el tamaño del infarto en un modelo de infarto miocárdico en ratas.

5. Los diterpenos de tipo labdanos tendrían potencial uso en patologías de base inflamatoria.

REFERENCIAS BIBLIOGRÁFICAS

Auffray C, Sieweke MH, Geissmann F (2009). Blood monocytes: development, heterogeneity, and relationship with dendritic cells. Annu Rev Immunol 27**:** 669-692.

Awang K, Abdullah NH, Hadi AH, Fong YS (2012). Cardiovascular activity of labdane diterpenes from Andrographis paniculata in isolated rat hearts. J Biomed Biotechnol 2012**:** 876458.

Baeuerle PA (1998). Pro-inflammatory signaling: last pieces in the NF-kappaB puzzle? Curr Biol 81**:** R19-22.

Barrabes JA, Mirabet M, Agullo L, Figueras J, Pizcueta P, Garcia-Dorado D (2007). Platelet deposition in remote cardiac regions after coronary occlusion. Eur J Clin Invest 3712**:** 939-946.

Barreiro O, Martin P, Gonzalez-Amaro R, Sanchez-Madrid F (2010). Molecular cues guiding inflammatory responses. Cardiovasc Res 862**:** 174-182.

Barrere-Lemaire S, Nargeot J, Piot C (2012). Delayed postconditioning: not too late? Trends Cardiovasc Med 227**:** 173-179.

Beinke S, Ley SC (2004). Functions of NF-kappaB1 and NF-kappaB2 in immune cell biology. Biochem J 382Pt 2**:** 393-409.

Bonizzi G, Karin M (2004). The two NF-kappaB activation pathways and their role in innate and adaptive immunity. Trends Immunol 256**:** 280-288.

Bopassa JC, Ferrera R, Gateau-Roesch O, Couture-Lepetit E, Ovize M (2006). PI 3-kinase regulates the mitochondrial transition pore in controlled reperfusion and postconditioning. Cardiovasc Res 691**:** 178-185.

Bratton SB, Salvesen GS (2010). Regulation of the Apaf-1-caspase-9 apoptosome. J Cell Sci 123Pt 19**:** 3209-3214.

Bremner P, Heinrich M (2002). Natural products as targeted modulators of the nuclear factor-kappaB pathway. J Pharm Pharmacol 544**:** 453-472.

Broskova Z, Knezl V (2011). Protective effect of novel pyridoindole derivatives on ischemia/reperfusion injury of the isolated rat heart. Pharmacol Rep 634**:** 967-974.

Brown GC, Neher JJ (2012). Eaten alive! Cell death by primary phagocytosis: 'phagoptosis'. Trends Biochem Sci 378**:** 325-332.

Calzado MA, Bacher S, Schmitz ML (2007). NF-kappaB inhibitors for the treatment of inflammatory diseases and cancer. Curr Med Chem 143**:** 367-376.

Carmody RJ, Chen YH (2007). Nuclear factor-kappaB: activation and regulation during toll-like receptor signaling. Cell Mol Immunol 41**:** 31-41.

Carreira RS, Lee P, Gottlieb RA (2011). Mitochondrial therapeutics for cardioprotection. Curr Pharm Des 1720**:** 2017-2035.

Castrillo A, de Las Heras B, Hortelano S, Rodriguez B, Villar A, Bosca L (2001). Inhibition of the nuclear factor kappa B (NF-kappa B) pathway by tetracyclic kaurene diterpenes in macrophages. Specific effects on NF-kappa B-inducing kinase activity and on the coordinate activation of ERK and p38 MAPK. J Biol Chem 27619**:** 15854-15860.

Classen A, Lloberas J, Celada A (2009). Macrophage activation: classical versus alternative. Methods Mol Biol 531**:** 29-43.

Croft M, Benedict CA, Ware CF (2013). Clinical targeting of the TNF and TNFR superfamilies. Nat Rev Drug Discov 122**:** 147-168.

Croft M, Duan W, Choi H, Eun SY, Madireddi S, Mehta A (2012). TNF superfamily in inflammatory disease: translating basic insights. Trends Immunol 333**:** 144-152.

Cuadrado I, Cidre F, Herranz S, Estevez-Braun A, de las Heras B, Hortelano S (2012). Labdanolic acid methyl ester (LAME) exerts anti-inflammatory effects through inhibition of TAK-1 activation. Toxicol Appl Pharmacol 2581**:** 109-117.

Cuadrado I, Fernandez-Velasco M, Bosca L, de Las Heras B (2011). Labdane diterpenes protect against anoxia/reperfusion injury in cardiomyocytes: involvement of AKT activation. Cell Death Dis 2**:** e229.

Cuevas BD, Abell AN, Johnson GL (2007). Role of mitogen-activated protein kinase kinase kinases in signal integration. Oncogene 2622**:** 3159-3171.

Chao TH, Lam T, Vong BG, Traves PG, Hortelano S, Chowdhury C*, et al.* (2005). A new family of synthetic diterpenes that regulates cytokine synthesis by inhibiting IkappaBalpha phosphorylation. Chembiochem 61**:** 133-144.

Chao W (2009). Toll-like receptor signaling: a critical modulator of cell survival and ischemic injury in the heart. Am J Physiol Heart Circ Physiol 2961**:** H1-12.

Chaudhary KR, Cho WJ, Yang F, Samokhvalov V, El-Sikhry HE, Daniel EE*, et al.* (2013). Effect of ischemia reperfusion injury and epoxyeicosatrienoic acids on caveolin expression in mouse myocardium. J Cardiovasc Pharmacol 613**:** 258-263.

Chen BC, Liao CC, Hsu MJ, Liao YT, Lin CC, Sheu JR*, et al.* (2006a). Peptidoglycan-induced IL-6 production in RAW 264.7 macrophages is mediated by cyclooxygenase-2, PGE2/PGE4 receptors, protein kinase A, I kappa B kinase, and NF-kappa B. J Immunol 1771**:** 681-693.

Chen ZJ, Bhoj V, Seth RB (2006b). Ubiquitin, TAK1 and IKK: is there a connection? Cell Death Differ 135**:** 687-692.

Chin YW, Balunas MJ, Chai HB, Kinghorn AD (2006). Drug discovery from natural sources. AAPS J 82**:** E239-253.

Chinou I (2005). Labdanes of natural origin-biological activities (1981-2004). Curr Med Chem 1211**:** 1295-1317.

Chiong M, Wang ZV, Pedrozo Z, Cao DJ, Troncoso R, Ibacache M*, et al.* (2011). Cardiomyocyte death: mechanisms and translational implications. Cell Death Dis 2**:** e244.

Chouchani ET, Methner C, Nadtochiy SM, Logan A, Pell VR, Ding S*, et al.* (2013). Cardioprotection by S-nitrosation of a cysteine switch on mitochondrial complex I. Nat Med 196**:** 753-759.

Chu WM (2013). Tumor necrosis factor. Cancer Lett 3282**:** 222-225.

Das A, Salloum FN, Durrant D, Ockaili R, Kukreja RC (2012). Rapamycin protects against myocardial ischemia-reperfusion injury through JAK2-STAT3 signaling pathway. J Mol Cell Cardiol 536**:** 858-869.

Datta K, Bellacosa A, Chan TO, Tsichlis PN (1996). Akt is a direct target of the phosphatidylinositol 3-kinase. Activation by growth factors, v-src and v-Ha-ras, in Sf9 and mammalian cells. J Biol Chem 27148**:** 30835-30839.

de las Heras B, Hortelano S (2009). Molecular basis of the anti-inflammatory effects of terpenoids. Inflamm Allergy Drug Targets 81**:** 28-39.

de las Heras B, Navarro A, Diaz-Guerra MJ, Bermejo P, Castrillo A, Bosca L*, et al.* (1999). Inhibition of NOS-2 expression in macrophages through the inactivation of NF-kappaB by andalusol. Br J Pharmacol 1283**:** 605-612.

de las Heras B, Rodriguez B, Bosca L, Villar AM (2003). Terpenoids: sources, structure elucidation and therapeutic potential in inflammation. Curr Top Med Chem 32**:** 171-185.

Demetzos C, Dimas K, Hatziantoniou S, Anastasaki T, Angelopoulou D (2001). Cytotoxic and anti-inflammatory activity of labdane and cis-clerodane type diterpenes. Planta Med 677**:** 614-618.

Dinarello CA (2011). Blocking interleukin-1beta in acute and chronic autoinflammatory diseases. J Intern Med 2691**:** 16-28.

Dinarello CA (2000). Proinflammatory cytokines. Chest 1182**:** 503-508.

Dong Y, Morris-Natschke SL, Lee KH (2011). Biosynthesis, total syntheses, and antitumor activity of tanshinones and their analogs as potential therapeutic agents. Nat Prod Rep 283**:** 529-542.

Downey JM, Cohen MV (2009). Why do we still not have cardioprotective drugs? Circ J 737**:** 1171-1177.

Duan W, Yang Y, Yan J, Yu S, Liu J, Zhou J*, et al.* (2012). The effects of curcumin post-treatment against myocardial ischemia and reperfusion by activation of the JAK2/STAT3 signaling pathway. Basic Res Cardiol 1073**:** 263.

Eltzschig HK, Eckle T (2011). Ischemia and reperfusion--from mechanism to translation. Nat Med 1711**:** 1391-1401.

Entman ML, Michael L, Rossen RD, Dreyer WJ, Anderson DC, Taylor AA*, et al.* (1991). Inflammation in the course of early myocardial ischemia. FASEB J 511**:** 2529-2537.

Fekonja O, Avbelj M, Jerala R (2012). Suppression of TLR signaling by targeting TIR domain-containing proteins. Curr Protein Pept Sci 138**:** 776-788.

Feng Y, Chao W (2011). Toll-like receptors and myocardial inflammation. Int J Inflam 2011**:** 170352.

Ferdinandy P, Schulz R, Baxter GF (2007). Interaction of cardiovascular risk factors with myocardial ischemia/reperfusion injury, preconditioning, and postconditioning. Pharmacol Rev 594**:** 418-458.

Frank A, Bonney M, Bonney S, Weitzel L, Koeppen M, Eckle T (2012). Myocardial ischemia reperfusion injury: from basic science to clinical bedside. Semin Cardiothorac Vasc Anesth 163**:** 123-132.

Frohlich GM, Meier P, White SK, Yellon DM, Hausenloy DJ (2013). Myocardial reperfusion injury: looking beyond primary PCI. Eur Heart J.

Fu Y, Rubin CS (2011). Protein kinase D: coupling extracellular stimuli to the regulation of cell physiology. EMBO Rep 128**:** 785-796.

Fujiwara N, Kobayashi K (2005). Macrophages in inflammation. Curr Drug Targets Inflamm Allergy 43**:** 281-286.

García-Álvarez M, Pérez-Sirvent, L, Rodriguez, B (1981). Transformaciones de hispanolona I. Síntesis parcial del diterpenoide furolabdánico galeopsina. Anales Quím77**:** 316-319.

Gilani AH, Rahman AU (2005). Trends in ethnopharmocology. J Ethnopharmacol 1001-2**:** 43-49.

Giron N, Traves PG, Rodriguez B, Lopez-Fontal R, Bosca L, Hortelano S*, et al.* (2008). Suppression of inflammatory responses by labdane-type diterpenoids. Toxicol Appl Pharmacol 2282**:** 179-189.

Go AS, Mozaffarian D, Roger VL, Benjamin EJ, Berry JD, Borden WB*, et al.* (2013). Heart disease and stroke statistics--2013 update: a report from the American Heart Association. Circulation 1271**:** e6-e245.

Gonzalez-Burgos E, Carretero ME, Gomez-Serranillos MP (2013). Involvement of Nrf2 signaling pathway in the neuroprotective activity of natural kaurane diterpenes. Neuroscience 231**:** 400-412.

Gordon S, Martinez FO (2010). Alternative activation of macrophages: mechanism and functions. Immunity 325**:** 593-604.

Gordon S, Taylor PR (2005). Monocyte and macrophage heterogeneity. Nat Rev Immunol 512**:** 953-964.

Gottlieb RA (2011). Cell death pathways in acute ischemia/reperfusion injury. J Cardiovasc Pharmacol Ther 163-4**:** 233-238.

Green DR (2000). Apoptotic pathways: paper wraps stone blunts scissors. Cell 1021**:** 1-4.

Gross GJ, Hsu A, Pfeiffer AW, Nithipatikom K (2013). Roles of endothelial nitric oxide synthase (eNOS) and mitochondrial permeability transition pore (MPTP) in

epoxyeicosatrienoic acid (EET)-induced cardioprotection against infarction in intact rat hearts. J Mol Cell Cardiol 59**:** 20-29.

Guo W, Liu W, Chen G, Hong S, Qian C, Xie N*, et al.* (2012). Water-soluble andrographolide sulfonate exerts anti-sepsis action in mice through down-regulating p38 MAPK, STAT3 and NF-kappaB pathways. Int Immunopharmacol 144**:** 613-619.

Gupta SC, Sundaram C, Reuter S, Aggarwal BB (2010). Inhibiting NF-kappaB activation by small molecules as a therapeutic strategy. Biochim Biophys Acta 179910-12**:** 775-787.

Gustafsson AB, Gottlieb RA (2009). Autophagy in ischemic heart disease. Circ Res 1042**:** 150-158.

Hacker H, Karin M (2006). Regulation and function of IKK and IKK-related kinases. Sci STKE 2006357**:** re13.

Halliwell B (2013). The antioxidant paradox: less paradoxical now? Br J Clin Pharmacol 753**:** 637-644.

Hamacher-Brady A, Brady NR, Gottlieb RA (2006). Enhancing macroautophagy protects against ischemia/reperfusion injury in cardiac myocytes. J Biol Chem 28140**:** 29776-29787.

Harvey AL (2008). Natural products in drug discovery. Drug Discov Today 1319-20**:** 894-901.

Harvey AL, Clark RL, Mackay SP, Johnston BF (2010). Current strategies for drug discovery through natural products. Expert Opin Drug Discov 56**:** 559-568.

Hasko G, Pacher P (2012). Regulation of macrophage function by adenosine. Arterioscler Thromb Vasc Biol 324**:** 865-869.

Hausenloy DJ, Boston-Griffiths EA, Yellon DM (2011a). Cyclosporin A and cardioprotection: from investigative tool to therapeutic agent. Br J Pharmacol 1655**:** 1235-1245.

Hausenloy DJ, Erik Botker H, Condorelli G, Ferdinandy P, Garcia-Dorado D, Heusch G*, et al.* (2013a). Translating cardioprotection for patient benefit: position paper from the Working Group of Cellular Biology of the Heart of the European Society of Cardiology. Cardiovasc Res 981**:** 7-27.

Hausenloy DJ, Tsang A, Yellon DM (2005). The reperfusion injury salvage kinase pathway: a common target for both ischemic preconditioning and postconditioning. Trends Cardiovasc Med 152**:** 69-75.

Hausenloy DJ, Yellon DM (2013b). Myocardial ischemia-reperfusion injury: a neglected therapeutic target. J Clin Invest 1231**:** 92-100.

Hausenloy DJ, Yellon DM (2004). New directions for protecting the heart against ischaemia-reperfusion injury: targeting the Reperfusion Injury Salvage Kinase (RISK)-pathway. Cardiovasc Res 613**:** 448-460.

Hausenloy DJ, Yellon DM (2009). Preconditioning and postconditioning: underlying mechanisms and clinical application. Atherosclerosis 2042**:** 334-341.

Hausenloy DJ, Yellon DM (2011b). The therapeutic potential of ischemic conditioning: an update. Nat Rev Cardiol 811**:** 619-629.

Hayden MS, Ghosh S (2012). NF-kappaB, the first quarter-century: remarkable progress and outstanding questions. Genes Dev 263**:** 203-234.

Heusch G (2013). Cardioprotection: chances and challenges of its translation to the clinic. Lancet 3819861**:** 166-175.

Heusch G (2009). No risk, no ... cardioprotection? A critical perspective. Cardiovasc Res 842**:** 173-175.

Hirano T (2010). Interleukin 6 in autoimmune and inflammatory diseases: a personal memoir. Proc Jpn Acad Ser B Phys Biol Sci 867**:** 717-730.

Hishikari K, Suzuki J, Ogawa M, Isobe K, Takahashi T, Onishi M*, et al.* (2009). Pharmacological activation of the prostaglandin E2 receptor EP4 improves cardiac function after myocardial ischaemia/reperfusion injury. Cardiovasc Res 811**:** 123-132.

Hoffmann J, Akira S (2013). Innate immunity. Curr Opin Immunol 251**:** 1-3.

Hoffmann JA (2003). The immune response of Drosophila. Nature 4266962**:** 33-38.

Hofmann U, Ertl G, Frantz S (2011). Toll-like receptors as potential therapeutic targets in cardiac dysfunction. Expert Opin Ther Targets 156**:** 753-765.

Hong SS, Lee SA, Han XH, Hwang JS, Lee C, Lee D*, et al.* (2008). ent-Kaurane diterpenoids from Isodon japonicus. J Nat Prod 716**:** 1055-1058.

Hristodorov D, Mladenov R, Huhn M, Barth S, Thepen T (2012). Macrophage-targeted therapy: CD64-based immunotoxins for treatment of chronic inflammatory diseases. Toxins (Basel) 49**:** 676-694.

Huang M, Lu JJ, Huang MQ, Bao JL, Chen XP, Wang YT (2012). Terpenoids: natural products for cancer therapy. Expert Opin Investig Drugs 2112**:** 1801-1818.

Hueso-Falcon I, Cuadrado I, Cidre F, Amaro-Luis JM, Ravelo AG, Estevez-Braun A*, et al.* (2011). Synthesis and anti-inflammatory activity of ent-kaurene derivatives. Eur J Med Chem 464**:** 1291-1305.

Iyer SS, Cheng G (2012). Role of interleukin 10 transcriptional regulation in inflammation and autoimmune disease. Crit Rev Immunol 321**:** 23-63.

Jayakumar T, Hsieh CY, Lee JJ, Sheu JR (2013). Experimental and Clinical Pharmacology of Andrographis paniculata and Its Major Bioactive Phytoconstituent Andrographolide. Evid Based Complement Alternat Med 2013**:** 846740.

Jenkins CM, Cedars A, Gross RW (2009). Eicosanoid signalling pathways in the heart. Cardiovasc Res 822**:** 240-249.

Karin M, Greten FR (2005). NF-kappaB: linking inflammation and immunity to cancer development and progression. Nat Rev Immunol 510**:** 749-759.

Karin M, Yamamoto Y, Wang QM (2004). The IKK NF-kappa B system: a treasure trove for drug development. Nat Rev Drug Discov 31**:** 17-26.

Kawabata A (2011). Prostaglandin E2 and pain--an update. Biol Pharm Bull 348**:** 1170-1173.

Kawai T, Akira S (2006). TLR signaling. Cell Death Differ 135**:** 816-825.

Kawano S, Kubota T, Monden Y, Tsutsumi T, Inoue T, Kawamura N*, et al.* (2006). Blockade of NF-kappaB improves cardiac function and survival after myocardial infarction. Am J Physiol Heart Circ Physiol 2913**:** H1337-1344.

Keating SE, Maloney GM, Moran EM, Bowie AG (2007). IRAK-2 participates in multiple toll-like receptor signaling pathways to NFkappaB via activation of TRAF6 ubiquitination. J Biol Chem 28246**:** 33435-33443.

Kim SF (2011). The role of nitric oxide in prostaglandin biology; update. Nitric Oxide 253**:** 255-264.

Kin H, Zatta AJ, Lofye MT, Amerson BS, Halkos ME, Kerendi F*, et al.* (2005). Postconditioning reduces infarct size via adenosine receptor activation by endogenous adenosine. Cardiovasc Res 671**:** 124-133.

Kis A, Yellon DM, Baxter GF (2003). Role of nuclear factor-kappa B activation in acute ischaemia-reperfusion injury in myocardium. Br J Pharmacol 1385**:** 894-900.

Kishimoto T (2010). IL-6: from its discovery to clinical applications. Int Immunol 225**:** 347-352.

Kloner RA (2011). No-reflow phenomenon: maintaining vascular integrity. J Cardiovasc Pharmacol Ther 163-4**:** 244-250.

Kloner RA, Ganote CE, Jennings RB (1974). The "no-reflow" phenomenon after temporary coronary occlusion in the dog. J Clin Invest 546**:** 1496-1508.

Knowles RG, Moncada S (1994). Nitric oxide synthases in mammals. Biochem J 298 (Pt 2)**:** 249-258.

Kohli P, Levy BD (2009). Resolvins and protectins: mediating solutions to inflammation. Br J Pharmacol 1584**:** 960-971.

Kubota T, McTiernan CF, Frye CS, Slawson SE, Lemster BH, Koretsky AP*, et al.* (1997). Dilated cardiomyopathy in transgenic mice with cardiac-specific overexpression of tumor necrosis factor-alpha. Circ Res 814**:** 627-635.

Kuo PC, Yang ML, Hwang TL, Lai YY, Li YC, Thang TD*, et al.* (2013). Anti-inflammatory diterpenoids from Croton tonkinensis. J Nat Prod 762**:** 230-236.

Lacerda L, Somers S, Opie LH, Lecour S (2009). Ischaemic postconditioning protects against reperfusion injury via the SAFE pathway. Cardiovasc Res 842**:** 201-208.

Lage R, Dieguez C, Vidal-Puig A, Lopez M (2008). AMPK: a metabolic gauge regulating whole-body energy homeostasis. Trends Mol Med 1412**:** 539-549.

Lam T, Ling T, Chowdhury C, Chao TH, Bahjat FR, Lloyd GK*, et al.* (2003). Synthesis of a novel family of diterpenes and their evaluation as anti-inflammatory agents. Bioorg Med Chem Lett 1319**:** 3217-3221.

Laskin DL, Laskin JD (2001). Role of macrophages and inflammatory mediators in chemically induced toxicity. Toxicology 1601-3**:** 111-118.

Lecour S (2009). Activation of the protective Survivor Activating Factor Enhancement (SAFE) pathway against reperfusion injury: Does it go beyond the RISK pathway? J Mol Cell Cardiol 471**:** 32-40.

Lee HN, Surh YJ (2012). Therapeutic potential of resolvins in the prevention and treatment of inflammatory disorders. Biochem Pharmacol 8410**:** 1340-1350.

Lee KC, Chang HH, Chung YH, Lee TY (2011). Andrographolide acts as an anti-inflammatory agent in LPS-stimulated RAW264.7 macrophages by inhibiting STAT3-mediated suppression of the NF-kappaB pathway. J Ethnopharmacol 1353**:** 678-684.

Lee KO, Min KH, Suh YG (2005). Synthesis of C4-modified acanthoic acid analogs and their biological evaluation as nitric oxide inhibitors. Arch Pharm Res 286**:** 648-651.

Li C, Tian J, Li G, Jiang W, Xing Y, Hou J*, et al.* (2010). Asperosaponin VI protects cardiac myocytes from hypoxia-induced apoptosis via activation of the PI3K/Akt and CREB pathways. Eur J Pharmacol 6491-3**:** 100-107.

Li Q, Verma IM (2002). NF-kappaB regulation in the immune system. Nat Rev Immunol 210**:** 725-734.

Lim JC, Chan TK, Ng DS, Sagineedu SR, Stanslas J, Wong WS (2012). Andrographolide and its analogues: versatile bioactive molecules for combating inflammation and cancer. Clin Exp Pharmacol Physiol 393**:** 300-310.

Lourenco AM, Ferreira LM, Branco PS (2012). Molecules of natural origin, semi-synthesis and synthesis with anti-inflammatory and anticancer utilities. Curr Pharm Des 1826**:** 3979-4046.

Ma XH, Shi Z, Tan C, Jiang Y, Go ML, Low BC*, et al.* (2010). In-silico approaches to multi-target drug discovery : computer aided multi-target drug design, multi-target virtual screening. Pharm Res 275**:** 739-749.

Mancuso DJ, Abendschein DR, Jenkins CM, Han X, Saffitz JE, Schuessler RB*, et al.* (2003). Cardiac ischemia activates calcium-independent phospholipase A2beta, precipitating ventricular tachyarrhythmias in transgenic mice: rescue of the lethal electrophysiologic phenotype by mechanism-based inhibition. J Biol Chem 27825**:** 22231-22236.

Mann DL (2011). The emerging role of innate immunity in the heart and vascular system: for whom the cell tolls. Circ Res 1089**:** 1133-1145.

Mantovani A, Sica A, Sozzani S, Allavena P, Vecchi A, Locati M (2004). The chemokine system in diverse forms of macrophage activation and polarization. Trends Immunol 2512**:** 677-686.

Marco JA (2006) Terpenos. In: *Química de los productos naturales*, pp 172-227: Síntesis S.A.

Marchant DJ, Boyd JH, Lin DC, Granville DJ, Garmaroudi FS, McManus BM (2012). Inflammation in myocardial diseases. Circ Res 1101**:** 126-144.

Matsui T, Nagoshi T, Rosenzweig A (2003). Akt and PI 3-kinase signaling in cardiomyocyte hypertrophy and survival. Cell Cycle 23**:** 220-223.

Matsui T, Tao J, del Monte F, Lee KH, Li L, Picard M*, et al.* (2001). Akt activation preserves cardiac function and prevents injury after transient cardiac ischemia in vivo. Circulation 1043**:** 330-335.

Matsui Y, Takagi H, Qu X, Abdellatif M, Sakoda H, Asano T*, et al.* (2007). Distinct roles of autophagy in the heart during ischemia and reperfusion: roles of AMP-activated protein kinase and Beclin 1 in mediating autophagy. Circ Res 1006**:** 914-922.

Mills CD (2001). Macrophage arginine metabolism to ornithine/urea or nitric oxide/citrulline: a life or death issue. Crit Rev Immunol 215**:** 399-425.

Minamino T (2012). Cardioprotection from ischemia/reperfusion injury: basic and translational research. Circ J 765**:** 1074-1082.

Mishra BB, Tiwari VK (2011). Natural products: an evolving role in future drug discovery. Eur J Med Chem 4610**:** 4769-4807.

Moreu-Burgos J, Macaya-Miguel C (2007). **Fisiopatología del miocardio isquémico. Importancia de la frecuencia cardiaca**. Rev Esp Cardiol Supl 7**:** 19-25.

Morrison A, Li J (2011). PPAR-gamma and AMPK--advantageous targets for myocardial ischemia/reperfusion therapy. Biochem Pharmacol 823**:** 195-200.

Moser B, Willimann K (2004). Chemokines: role in inflammation and immune surveillance. Ann Rheum Dis 63 Suppl 2**:** ii84-ii89.

Mosser DM, Edwards JP (2008). Exploring the full spectrum of macrophage activation. Nat Rev Immunol 812**:** 958-969.

Mozaffari MS, Liu JY, Schaffer SW (2010). Effect of pressure overload on cardioprotection via PI3K-Akt: comparison of postconditioning, insulin, and pressure unloading. Am J Hypertens 236**:** 668-674.

Murphy E (2004). Primary and secondary signaling pathways in early preconditioning that converge on the mitochondria to produce cardioprotection. Circ Res 941**:** 7-16.

Nagata M (2005). Inflammatory cells and oxygen radicals. Curr Drug Targets Inflamm Allergy 44**:** 503-504.

Nam NH (2006). Naturally occurring NF-kappaB inhibitors. Mini Rev Med Chem 68**:** 945-951.

Nathan C (2008). Metchnikoff's Legacy in 2008. Nat Immunol 97**:** 695-698.

Nathan C (2002). Points of control in inflammation. Nature 4206917**:** 846-852.

Navarro A, de las Heras B, Villar AM (1997). Andalusol, a diterpenoid with anti-inflammatory activity from Siderits foetens Clemen. Z Naturforsch C 5211-12**:** 844-849.

Newman DJ, Cragg GM (2012). Natural products as sources of new drugs over the 30 years from 1981 to 2010. J Nat Prod 753**:** 311-335.

Ojha SK, Bharti S, Joshi S, Kumari S, Arya DS (2012). Protective effect of hydroalcoholic extract of Andrographis paniculata on ischaemia-reperfusion induced myocardial injury in rats. Indian J Med Res 135**:** 414-421.

Ojima I, Zuniga ES, Berger WT, Seitz JD (2012). Tumor-targeting drug delivery of new-generation taxoids. Future Med Chem 41**:** 33-50.

Ong SG, Hausenloy DJ (2012). Hypoxia-inducible factor as a therapeutic target for cardioprotection. Pharmacol Ther 1361**:** 69-81.

Oyama J, Blais C, Jr., Liu X, Pu M, Kobzik L, Kelly RA*, et al.* (2004). Reduced myocardial ischemia-reperfusion injury in toll-like receptor 4-deficient mice. Circulation 1096**:** 784-789.

Pérez-Sirvent L, García-Álvarez, MC, Balestrieri, MA, Rodríguez, B (1981a). Transformaciones de hispanolona III. Reacciones del anillo B y degradación a di-homo-drimanos. Anales Quím77**:** 330-334.

Pérez-Sirvent L, García-Álvarez, MC, Rodríguez, B (1981b). Transformaciones de hispanolona II. Reacción retroaldólica de hispanolona y condensación aldólica de δ-dicetonas diterpénicas. Anales Quím77**:** 324-329.

Perkins ND (2006). Post-translational modifications regulating the activity and function of the nuclear factor kappa B pathway. Oncogene 2551**:** 6717-6730.

Peters RJ (2010). Two rings in them all: the labdane-related diterpenoids. Nat Prod Rep 2711**:** 1521-1530.

Piper HM, Garcia-Dorado D (2009). Cardiac protection takes off. Cardiovasc Res 832**:** 163-164.

Portt L, Norman G, Clapp C, Greenwood M, Greenwood MT (2011). Anti-apoptosis and cell survival: a review. Biochim Biophys Acta 18131**:** 238-259.

Qi D, Hu X, Wu X, Merk M, Leng L, Bucala R*, et al.* (2009). Cardiac macrophage migration inhibitory factor inhibits JNK pathway activation and injury during ischemia/reperfusion. J Clin Invest 11912**:** 3807-3816.

Quintieri AM, Baldino N, Filice E, Seta L, Vitetti A, Tota B*, et al.* (2012). Malvidin, a red wine polyphenol, modulates mammalian myocardial and coronary performance and protects the heart against ischemia/reperfusion injury. J Nutr Biochem 247**:** 1221-1231.

Raes G, De Baetselier P, Noel W, Beschin A, Brombacher F, Hassanzadeh Gh G (2002a). Differential expression of FIZZ1 and Ym1 in alternatively versus classically activated macrophages. J Leukoc Biol 714**:** 597-602.

Raes G, Noel W, Beschin A, Brys L, de Baetselier P, Hassanzadeh GH (2002b). FIZZ1 and Ym as tools to discriminate between differentially activated macrophages. Dev Immunol 93**:** 151-159.

Ravingerova T, Barancik M, Strniskova M (2003). Mitogen-activated protein kinases: a new therapeutic target in cardiac pathology. Mol Cell Biochem 2471-2**:** 127-138.

Rogiers V (2003). Ecopa: actual status and plans. Toxicol In Vitro 175-6**:** 779-784.

Rohilla A, Rohilla S, Kushnoor A (2011). Myocardial postconditioning: next step to cardioprotection. Arch Pharm Res 349**:** 1409-1415.

Roman-Blas JA, Jimenez SA (2006). NF-kappaB as a potential therapeutic target in osteoarthritis and rheumatoid arthritis. Osteoarthritis Cartilage 149**:** 839-848.

Ruiz-Meana M, Garcia-Dorado D (2009). Translational cardiovascular medicine (II). Pathophysiology of ischemia-reperfusion injury: new therapeutic options for acute myocardial infarction. Rev Esp Cardiol 622**:** 199-209.

Ruiz PG (2002) Terpenos. In: *Productos naturales*, Navarra, UPd (ed), pp 116-141.

Russell RR, 3rd, Li J, Coven DL, Pypaert M, Zechner C, Palmeri M*, et al.* (2004). AMP-activated protein kinase mediates ischemic glucose uptake and prevents postischemic cardiac dysfunction, apoptosis, and injury. J Clin Invest 1144**:** 495-503.

Salminen A, Lehtonen M, Suuronen T, Kaarniranta K, Huuskonen J (2008). Terpenoids: natural inhibitors of NF-kappaB signaling with anti-inflammatory and anticancer potential. Cell Mol Life Sci 6519**:** 2979-2999.

Salvemini D, Kim SF, Mollace V (2013). Reciprocal regulation of the nitric oxide and cyclooxygenase pathway in pathophysiology: relevance and clinical implications. Am J Physiol Regul Integr Comp Physiol 3047**:** R473-487.

Sanz-Rosa D, Garcia-Prieto J, Ibanez B (2012). The future: therapy of myocardial protection. Ann N Y Acad Sci 1254**:** 90-98.

Scarabelli TM, Knight R, Stephanou A, Townsend P, Chen-Scarabelli C, Lawrence K*, et al.* (2006). Clinical implications of apoptosis in ischemic myocardium. Curr Probl Cardiol 313**:** 181-264.

Schnare M, Barton GM, Holt AC, Takeda K, Akira S, Medzhitov R (2001). Toll-like receptors control activation of adaptive immune responses. Nat Immunol 210**:** 947-950.

Schwab JM, Chiang N, Arita M, Serhan CN (2007). Resolvin E1 and protectin D1 activate inflammation-resolution programmes. Nature 4477146**:** 869-874.

Schwab JM, Serhan CN (2006). Lipoxins and new lipid mediators in the resolution of inflammation. Curr Opin Pharmacol 64**:** 414-420.

Schwartz Longacre L, Kloner RA, Arai AE, Baines CP, Bolli R, Braunwald E*, et al.* (2011). New horizons in cardioprotection: recommendations from the 2010 National Heart, Lung, and Blood Institute Workshop. Circulation 12410**:** 1172-1179.

Serhan CN, Chiang N, Van Dyke TE (2008). Resolving inflammation: dual anti-inflammatory and pro-resolution lipid mediators. Nat Rev Immunol 85**:** 349-361.

Shao Z, Bhattacharya K, Hsich E, Park L, Walters B, Germann U*, et al.* (2006). c-Jun N-terminal kinases mediate reactivation of Akt and cardiomyocyte survival after hypoxic injury in vitro and in vivo. Circ Res 981**:** 111-118.

Sherwood ER, Toliver-Kinsky T (2004). Mechanisms of the inflammatory response. Best Pract Res Clin Anaesthesiol 183**:** 385-405.

Shimamoto A, Chong AJ, Yada M, Shomura S, Takayama H, Fleisig AJ*, et al.* (2006). Inhibition of Toll-like receptor 4 with eritoran attenuates myocardial ischemia-reperfusion injury. Circulation 1141 Suppl**:** I270-274.

Silva MT (2010). Secondary necrosis: the natural outcome of the complete apoptotic program. FEBS Lett 58422**:** 4491-4499.

Simon LS (1999). Role and regulation of cyclooxygenase-2 during inflammation. Am J Med 1065B**:** 37S-42S.

Singh M, Pal M, Sharma RP (1999). Biological activity of the labdane diterpenes. Planta Med 651**:** 2-8.

Singh SS, Kang PM (2011). Mechanisms and Inhibitors of Apoptosis in Cardiovascular Diseases. Curr Pharm Des 1718**:** 1783-1793.

Skrzypiec-Spring M, Grotthus B, Szelag A, Schulz R (2007). Isolated heart perfusion according to Langendorff---still viable in the new millennium. J Pharmacol Toxicol Methods 552**:** 113-126.

Smith WL, Urade Y, Jakobsson PJ (2011). Enzymes of the cyclooxygenase pathways of prostanoid biosynthesis. Chem Rev 11110**:** 5821-5865.

Smolen JS, Schoels MM, Nishimoto N, Breedveld FC, Burmester GR, Dougados M*, et al.* (2013). Consensus statement on blocking the effects of interleukin-6 and in particular by interleukin-6 receptor inhibition in rheumatoid arthritis and other inflammatory conditions. Ann Rheum Dis 724**:** 482-492.

Stiles BL (2009). PI-3-K and AKT: Onto the mitochondria. Adv Drug Deliv Rev 6114**:** 1276-1282.

Suh YG, Lee KO, Moon SH, Seo SY, Lee YS, Kim SH*, et al.* (2004). Synthesis and anti-inflammatory effects of novel pimarane diterpenoid analogs. Bioorg Med Chem Lett 1413**:** 3487-3490.

Suzuki J, Ogawa M, Watanabe R, Takayama K, Hirata Y, Nagai R*, et al.* (2011). Roles of prostaglandin E2 in cardiovascular diseases. Int Heart J 525**:** 266-269.

Takagawa J, Zhang Y, Wong ML, Sievers RE, Kapasi NK, Wang Y*, et al.* (2007). Myocardial infarct size measurement in the mouse chronic infarction model: comparison of area- and length-based approaches. J Appl Physiol 1026**:** 2104-2111.

Takagi H, Matsui Y, Hirotani S, Sakoda H, Asano T, Sadoshima J (2007a). AMPK mediates autophagy during myocardial ischemia in vivo. Autophagy 34**:** 405-407.

Takagi H, Matsui Y, Sadoshima J (2007b). The role of autophagy in mediating cell survival and death during ischemia and reperfusion in the heart. Antioxid Redox Signal 99**:** 1373-1381.

Takeda K, Akira S (2001). Roles of Toll-like receptors in innate immune responses. Genes Cells 69**:** 733-742.

Takeda K, Akira S (2004). TLR signaling pathways. Semin Immunol 161**:** 3-9.

Taylor EL, Megson IL, Haslett C, Rossi AG (2003). Nitric oxide: a key regulator of myeloid inflammatory cell apoptosis. Cell Death Differ 104**:** 418-430.

Thomas CJ, Ng DC, Patsikatheodorou N, Limengka Y, Lee MW, Darby IA*, et al.* (2011). Cardioprotection from ischaemia-reperfusion injury by a novel flavonol that reduces activation of p38 MAPK. Eur J Pharmacol 6582-3**:** 160-167.

Thomson AB, Gupta M, Freeman HJ (2012). Use of the tumor necrosis factor-blockers for Crohn's disease. World J Gastroenterol 1835**:** 4823-4854.

Thygesen K, Alpert JS, Jaffe AS, Simoons ML, Chaitman BR, White HD*, et al.* (2012). Third universal definition of myocardial infarction. Circulation 12616**:** 2020-2035.

Tian W, Chen SY (2013). Recent advances in the molecular basis of anti-neoplastic mechanisms of oridonin. Chin J Integr Med 194**:** 315-320.

Townsend PA, Scarabelli TM, Pasini E, Gitti G, Menegazzi M, Suzuki H*, et al.* (2004). Epigallocatechin-3-gallate inhibits STAT-1 activation and protects cardiac myocytes from ischemia/reperfusion-induced apoptosis. FASEB J 1813**:** 1621-1623.

Traves PG, Hortelano S, Zeini M, Chao TH, Lam T, Neuteboom ST*, et al.* (2007). Selective activation of liver X receptors by acanthoic acid-related diterpenes. Mol Pharmacol 716**:** 1545-1553.

Traves PG, Lopez-Fontal R, Cuadrado I, Luque A, Bosca L, de las Heras B*, et al.* (2012a). Critical role of the death receptor pathway in the antitumoral effects induced by hispanolone derivatives. Oncogene 322**:** 259-268.

Traves PG, Luque A, Hortelano S (2012b). Macrophages, inflammation, and tumor suppressors: ARF, a new player in the game. Mediators Inflamm 2012**:** 568783.

Tsutsumi YM, Tsutsumi R, Mawatari K, Nakaya Y, Kinoshita M, Tanaka K*, et al.* (2011). Compound K, a metabolite of ginsenosides, induces cardiac protection mediated nitric oxide via Akt/PI3K pathway. Life Sci 8815-16**:** 725-729.

Turer AT, Hill JA (2010). Pathogenesis of myocardial ischemia-reperfusion injury and rationale for therapy. Am J Cardiol 1063**:** 360-368.

Uwe S (2008). Anti-inflammatory interventions of NF-kappaB signaling: potential applications and risks. Biochem Pharmacol 758**:** 1567-1579.

Vallabhapurapu S, Karin M (2009). Regulation and function of NF-kappaB transcription factors in the immune system. Annu Rev Immunol 27**:** 693-733.

Vandenbon A, Teraguchi S, Akira S, Takeda K, Standley DM (2012). Systems biology approaches to toll-like receptor signaling. Wiley Interdiscip Rev Syst Biol Med 45**:** 497-507.

Vasanthi HR, ShriShriMal N, Das DK (2012). Phytochemicals from plants to combat cardiovascular disease. Curr Med Chem 1914**:** 2242-2251.

Venkatachalam K, Prabhu SD, Reddy VS, Boylston WH, Valente AJ, Chandrasekar B (2009). Neutralization of interleukin-18 ameliorates ischemia/reperfusion-induced myocardial injury. J Biol Chem 28412**:** 7853-7865.

Vezzani A, Maroso M, Balosso S, Sanchez MA, Bartfai T (2011). IL-1 receptor/Toll-like receptor signaling in infection, inflammation, stress and neurodegeneration couples hyperexcitability and seizures. Brain Behav Immun 257**:** 1281-1289.

Wagner KH, Elmadfa I (2003). Biological relevance of terpenoids. Overview focusing on mono-, di- and tetraterpenes. Ann Nutr Metab 473-4**:** 95-106.

Waldman M, Hochhauser E, Fishbein M, Aravot D, Shainberg A, Sarne Y (2013). An ultra-low dose of tetrahydrocannabinol provides cardioprotection. Biochem Pharmacol 8511**:** 1626-1633.

Wang K, Zhang J, Liu J, Tian J, Wu Y, Wang X*, et al.* (2012). Variations in the protein level of Omi/HtrA2 in the heart of aged rats may contribute to the increased susceptibility of cardiomyocytes to ischemia/reperfusion injury and cell death : Omi/HtrA2 and aged heart injury. Age (Dordr) 353**:** 733-746.

Wang Y (2007). Mitogen-activated protein kinases in heart development and diseases. Circulation 11612**:** 1413-1423.

Wang Y, Gao E, Tao L, Lau WB, Yuan Y, Goldstein BJ*, et al.* (2009). AMP-activated protein kinase deficiency enhances myocardial ischemia/reperfusion injury but has minimal effect on the antioxidant/antinitrative protection of adiponectin. Circulation 1196**:** 835-844.

Wei C, Li H, Han L, Zhang L, Yang X (2013). Activation of autophagy in ischemic postconditioning contributes to cardioprotective effects against ischemia/reperfusion injury in rat hearts. J Cardiovasc Pharmacol 615**:** 416-422.

Wells TN (2011). Natural products as starting points for future anti-malarial therapies: going back to our roots? Malar J 10 Suppl 1**:** S3.

Weylandt KH, Chiu CY, Gomolka B, Waechter SF, Wiedenmann B (2012). Omega-3 fatty acids and their lipid mediators: towards an understanding of resolvin and protectin formation. Prostaglandins Other Lipid Mediat 973-4**:** 73-82.

Whelan RS, Kaplinskiy V, Kitsis RN (2010). Cell death in the pathogenesis of heart disease: mechanisms and significance. Annu Rev Physiol 72**:** 19-44.

Wymann MP, Marone R (2005). Phosphoinositide 3-kinase in disease: timing, location, and scaffolding. Curr Opin Cell Biol 172**:** 141-149.

Wynn TA, Chawla A, Pollard JW (2013). Macrophage biology in development, homeostasis and disease. Nature 4967446**:** 445-455.

Xia YF, Ye BQ, Li YD, Wang JG, He XJ, Lin X*, et al.* (2004). Andrographolide attenuates inflammation by inhibition of NF-kappa B activation through covalent modification of reduced cysteine 62 of p50. J Immunol 1736**:** 4207-4217.

Xie QW, Kashiwabara Y, Nathan C (1994). Role of transcription factor NF-kappa B/Rel in induction of nitric oxide synthase. J Biol Chem 2697**:** 4705-4708.

Xu D, Li Y, Wang J, Davey AK, Zhang S, Evans AM (2007). The cardioprotective effect of isosteviol on rats with heart ischemia-reperfusion injury. Life Sci 804**:** 269-274.

Yan XF, Zhang ZM, Yao HY, Guan Y, Zhu JP, Zhang LH*, et al.* (2012). Cardiovascular Protection and Antioxidant Activity of the Extracts from the Mycelia of Cordyceps Sinensis Act Partially Via Adenosine Receptors. Phytother Res.

Yao YY, Zhu MH, Zhang FJ, Wen CY, Ma LL, Wang WN*, et al.* (2013). Activation of Akt and cardioprotection against reperfusion injury are maximal with only five minutes of sevoflurane postconditioning in isolated rat hearts. J Zhejiang Univ Sci B 146**:** 511-517.

Yeh CC, Malhotra D, Yang YL, Xu Y, Fan Y, Li H*, et al.* (2013). MEK1-induced physiological hypertrophy inhibits chronic post-myocardial infarction remodeling in mice. J Cell Biochem 1141**:** 47-55.

Zaha VG, Young LH (2012). AMP-activated protein kinase regulation and biological actions in the heart. Circ Res 1116**:** 800-814.

Zatta AJ, Kin H, Yoshishige D, Jiang R, Wang N, Reeves JG*, et al.* (2008). Evidence that cardioprotection by postconditioning involves preservation of myocardial opioid content and selective opioid receptor activation. Am J Physiol Heart Circ Physiol 2943**:** H1444-1451.

Zhang Y, Zhang L, Chu W, Wang B, Zhang J, Zhao M*, et al.* (2010). Tanshinone IIA inhibits miR-1 expression through p38 MAPK signal pathway in post-infarction rat cardiomyocytes. Cell Physiol Biochem 266**:** 991-998.

Zhao Y, Zhao B (2010). Protective effect of natural antioxidants on heart against ischemia-reperfusion damage. Curr Pharm Biotechnol 118**:** 868-874.

Zhao ZQ, Corvera JS, Halkos ME, Kerendi F, Wang NP, Guyton RA*, et al.* (2003). Inhibition of myocardial injury by ischemic postconditioning during reperfusion: comparison with ischemic preconditioning. Am J Physiol Heart Circ Physiol 2852**:** H579-588.

Zhu T, Wang DX, Zhang W, Liao XQ, Guan X, Bo H*, et al.* (2013). Andrographolide protects against LPS-induced acute lung injury by inactivation of NF-kappaB. PLoS One 82**:** e56407.

ANEXO

Oncogene (2012) 1 – 10

www.nature.com/onc

ORIGINAL ARTICLE

Critical role of the death receptor pathway in the antitumoral effects induced by hispanolone derivatives

PG Través[1,6], R López-Fontal[2,6], I Cuadrado[3], A Luque[4], L Boscá[1], B de las Heras[3] and S Hortelano[5]

Labdane diterpenoids have a broad spectrum of biological activities including antibacterial, antiviral and anti-inflammatory properties. However, little is known about their possible role in the apoptotic cell death machinery. Here, we report that hispanolone derivatives, a group of labdane diterpenoids, induce apoptosis in different tumor cell lines by activating caspase-8 with subsequent participation of mitochondrial signaling. Activation of caspase-8 by hispanolone derivatives was followed by a decrease in mitochondrial membrane potential, the release of apoptotic factors from mitochondria to the cytosol, and activation of caspases-9 and 3. Hispanolone derivatives also led to a time-dependent cleavage of Bid. Inhibition of caspase-8 abrogated these processes, suggesting that the death receptor pathway has a critical role in the apoptotic events induced by hispanolone derivatives. In addition, silencing death receptors with small interfering RNA s or pretreating cells with neutralizing antibodies to Fas ligand, tumor necrosis factor receptor 1 (TNF-R1), and TNF-α receptor 2 (TRAIL) inhibited diterpenoid-induced apoptosis, revealing it to be dependent on these death receptors. Interestingly, hispanolone derivatives had no effect on non-tumor cells. Consistently, *in vivo* bioluminescence imaging corroborates this antineoplasic effect, as hispanolone derivatives significantly decrease cancer growth in tumor xenograft assays. These data demostrate the antitumoral effects of hispanolone derivatives and provide relevant preclinical validation for the use of these compounds as potent therapeutic agents in cancer treatment.

Oncogene advance online publication, 6 February 2012; doi:10.1038/onc.2012.23

Keywords: hispanolone derivatives; apoptosis; death receptors; TRAIL; caspase-8

INTRODUCTION

Terpenoids are the largest and most abundant class of natural compounds. They are extracted from higher plants, mosses, liverworts, algae and lichens, and are also present in insects, microbes or marine organisms. Labdanes, which are bicyclic diterpenoids, have a broad spectrum of biological activities including antibacterial, antiviral and anti-inflammatory actions.[1] We recently reported that hispanolone derivatives, a group of labdane diterpenoids, exert anti-inflammatory effects by inhibiting the activation of nuclear factor-κB (NF-κB);[2] however, to date there have been no reports characterizing the possible interaction of hispanolone derivatives with the apoptotic cell death machinery.

Apoptosis is an evolutionarily conserved program cell death process that is essential for normal tissue homeostasis and participates in the elimination of potentially dangerous cells, including the precursors of tumor cells.[3] Two main activation pathways have been identified, termed the extrinsic and intrinsic pathways.[4] The extrinsic pathway is initiated at the plasma membrane by activation of cell surface death receptors such as Fas/CD95, tumor necrosis factor receptor 1 (TNF-R1) and TNF-α receptor 2 (TRAIL). Ligand-activated death receptors recruit the adaptor molecule Fas-associated death domain protein, which in turn recruits and activates an initiator enzyme, usually caspase-8, in the death-inducing signaling complex.[5] Processed caspase-8 activates downstream apoptotic effectors such as caspases 3, 6 and 7.[6] The intrinsic pathway is mediated by mitochondria, and involves the release of proapoptotic factors such as cytochrome c from the intramembrane space to the cytosol. Once released, cytochrome c and dATP bind to apoptotic proteinase-activating factor-1. This complex, together with adenine nucleotides, promotes the autoactivation of procaspase-9 to caspase-9 followed by the activation of the effector caspases 2, 3, 6, 8 and 10.[7] Release of apoptosis-related proteins from mitochondria is controlled by proapoptotic members of the Bcl-2 family such as Bid. Caspase-8 can process Bid to generate the active truncated form, providing a link between the extrinsic and intrinsic pathways.[8]

In this study, we have evaluated the proapoptotic potential of the natural labdane diterpenoids hispanolone (T1)[9] and galeopsin (T9),[10] together with a series of nine synthetic hispanolone derivatives (T2–T8, T10 and T11). Our results reveal that two of these compounds, T2 and T6, promote apoptosis through the death receptor pathway. The caspase-8 inhibitor Ac-IETD-CHO dramatically reduced apoptosis, demonstrating that caspase-8 is the upstream initiator enzyme. The mitochondrial pathway was subsequently activated, with loss of $\Delta\Psi m$,

[1]Instituto de Investigaciones Biomédicas Alberto Sols (CSIC-UAM), Madrid, Spain; [2]Centro Nacional de Investigaciones Cardiovasculares (CNIC), Madrid, Spain; [3]Departamento de Farmacología. Facultad de Farmacia, Universidad Complutense de Madrid (UCM), Madrid, Spain; [4]Oncohematología y Trasplante. FIB Hospital Universitario Niño Jesús and IIS Hospital La Princesa, Madrid, Spain and [5]Unidad de Inflamación y Cáncer, Área de Biología Celular y Desarrollo, Centro Nacional de Microbiología, Instituto de Salud Carlos III, Madrid, Spain; [6]These authors contributed equally to this work. Correspondence: Dr S Hortelano, Unidad de Inflamación y Cáncer, Área de Biología Celular y del Desarrollo, Centro Nacional de Microbiología, Instituto de Salud Carlos III, Ctra Majadahonda-Pozuelo, Km 2,200. 28220 Majadahonda, Madrid, Spain. E-mail: shortelano@isciii.es and B de las Heras, Departamento de Farmacología. Facultad de Farmacia, Plaza Ramón y Cajal s/n, Universidad Complutense de Madrid (UCM), 28040 Madrid. Spain.
E-mail: lasheras@farm.ucm.es
Received 24 July 2011; revised 19 December 2011; accepted 6 January 2012

cytochrome *c* release and activation of caspases 9 and 3. Moreover, neutralizing antibodies against TRAIL-R2, TNF-R1 and Fas ligand and gene silencing of these receptors also effectively inhibited cell death. Relevantly for clinical application, treatment with hispanolone derivatives significantly inhibited the tumor growth induced by B16F10 and ID8 cells implanted in NOD SCID mice. Thus, our finding shows that hispanolone derivatives may offer a new promising therapeutic agent for cancer.

RESULTS

Induction of apoptosis by labdane diterpenoids

The terpenoids selected for this study have been previously described;[2] and are the natural labdane diterpenoids hispanolone (T1) and galeopsin (T9) and a series of nine hispanolone derivatives (T2–T8, T10 and T11). To investigate the apoptotic potential of these compounds, RAW 264.7 (mouse leukemic macrophagic cell line), Jurkat (human acute T-cell leukemia) and THP-1 (human acute monocytic leukemia cell line) cells were treated for 24 h with 50 μM of each compound (Figure 1a). T2 and T6 were the most effective terpenoids, reaching the levels of apoptosis around 88.2 and 92.8% in RAW 264.7 cells, 83.3 and 89.17% in Jurkat cells, 76.6 and 91.7% in THP-1 cells, respectively. To further analyze the apoptotic effect of T2 and T6, a panel of human and mouse tumor cell lines (RAW 264.7, Jurkat, THP-1, HT-29, B16F10 and ID8 cells) were exposed to a range of concentrations from 1 to 100 μM (Figure 1b). Both compounds increased apoptosis levels in a concentration-dependent manner in all cell lines tested, although RAW 264.7, THP-1, Jurkat and HT-29 cells showed a higher sensibility to the treatment, reaching IC_{50} values in the range of 1–15 μM (Supplementary Table 1). Given their stronger apoptotic action, T2 and T6 were the principal compounds tested in subsequent experiments. When indicated, T7 was used as an internal negative control.

To discard possible induction of necrosis, we measured LDH release from RAW 264.7 cells treated with T6 or T7. Despite that T6 treatment reduced the number of viable cells, as measured by flow cytometry, this terpenoid did not induce necrosis over the concentration range studied (Supplementary Figure 1). Compound T7 used as control did not alter cell viability in this assay.

Expression of apoptosis-related genes in cells treated with hispanolone derivatives

To identify genes differentially expressed in response to hispanolone derivatives, cells were incubated with T6 (25 μM for 2, 4 and 8 h, respectively), and RNA isolated from treated and control cells was hybridized to a RT^2 Profiler PCR Array. Genes that exhibited at least 2-fold difference in expression were considered T6-responsive. Employing this criterion, we identified 45 genes similarly expressed in control and treated cells (data not shown), four genes downregulated and 35 genes upregulated (Supplementary Table 2). Upregulated events included a group of signal transduction genes involved in the induction of apoptosis such as the death receptors TNF-R1, TRAIL-R2 and Fas, as well as the proapoptotic members of the Bcl-2 family, Bak, Bid and Bax. In contrast, antiapoptotic molecules like Bcl-2 were downregulated. In order to validate the data obtained in the RT^2 Profiler PCR Array, we performed quantitative PCR showing similar ratio of the gene expression (Figure 1c).

Diterpenoids activate caspase-8 and the mitochondrial pathway

Given the finding that T6 upregulates the death receptors expression, we next investigated its ability to modify other key events in apoptosis signaling, such as caspase activation and mitochondrial signaling. Treatment of RAW 264.7 and Jurkat cells with T6 induced caspase-8 activation, as determined fluorometrically using Ac-IETD-AMC (Figure 2a).

Active caspase-8 can trigger the mitochondrial apoptotic pathway by cleaving Bid, originating the truncated form that induces the release of cytochrome c from mitochondria. Treatment of RAW 264.7 and Jurkat cells with T6 (25 μM) induced cleavage of Bid in a time-dependent manner, as shown by western blot in the Figure 2b. Moreover, protein analysis confirmed the reduction in the expression of the anti-apoptotic protein Bcl-2 (Figure 2b). T6-induced Bid activation was accompanied by increment in cytosolic cytochrome c (Figure 2b). To determine whether truncated Bid alters mitochondrial signaling, we monitored $\Delta\Psi_m$ by flow cytometry using TMRM labeling, as measurement of the permeability of the organelle. As shown in Figure 2c, RAW 264.7 and Jurkat cells treated with T6 induced a collapse in $\Delta\Psi_m$. T7 was used as control. T6-induced Bid processing and mitochondrial membrane depolarization were accompanied by upregulation in the enzymatic activities of caspases 9 and 3 (Figures 2d and e). These data thus demonstrate that the selected hispanolone derivative induces apoptosis via the activation of caspase-8, which activates the extrinsic pathway, and induction of mitochondrial apoptotic events through the action of truncated Bid.

Inhibition of caspase-8 prevents hispanolone derivative-induced apoptosis

To confirm the primary role of caspase-8 activity in diterpenoid-induced apoptosis, we tested the ability of the caspase-8 inhibitor IETD-CHO to block this effect. Pretreatment of cells with IETD-CHO completely inhibited T6-induced caspase-8 activation and apoptosis (Figure 3a). Moreover, IETD-CHO also inhibited the mitochondrial apoptotic pathway. The caspase-8 inhibitor impaired Bid cleavage, the reduction in the expression of Bcl-2 and Bcl-xl, and the release of cytochrome *c* from mitochondria (Figure 3b), and prevented the collapse of $\Delta\Psi_m$ (Figure 3c). Consistently, there was a corresponding blockade of the activation of the downstream effectors caspase-9 and 3 (Figure 3d). Similar results were obtained in Jurkat cells (data not shown).

Blockage of death receptors abrogates apoptosis induced by hispanolone derivatives

As T6 increases the mRNA expression of Fas, TNF-R1 and TRAIL-R2, next we examined the regulation at the protein level of these receptors. A time-course experiment determined that addition of 25 μM T6 to Jurkat cells progressively increased Fas, TNF-R1 and TRAIL-R2 levels up to 24 h (Figure 4a). Accordingly, flow cytometry analysis also showed an enhanced surface expression of these receptors after T6 treatment (Supplementary Figure 2).

Next, we used neutralizing antibodies to determine the biological significance of the upregulated death receptors signaling in the T6-induced apoptosis. Pre-treatment with neutralizing antibodies to Fas ligand, TRAIL-R2 and TNF-R1 inhibited T6-induced apoptosis by 66.35, 60.28 and 43.45% in RAW264.7 cells and 47.2, 56.4 and 39.8% in Jurkat cells, respectively. Moreover, a combination of all three antibodies completely prevented diterpenoid-induced apoptosis (Figure 4b). Light microscopy corroborated this result revealing inhibition of the typical apoptotic morphological changes (Figure 4d). The neutralizing antibodies also inhibited caspase-8 activity (Figure 4c), as well as Bid cleavage and the reduction in Bcl-2 levels (Figure 4e), confirming that diterpenoid-induced apoptosis is initiated via activation of death receptor pathways. To further confirm the critical role of these receptors on T6-induced apoptosis, RNA interference technology was applied. Jurkat cells were transfected with small interfering RNAs (siRNAs) against Fas, TRAIL-R2 and TNF-R1, and 24 h after transfection cells were treated with T6. siRNAs efficiency was evaluated by western blot (Figure 4f). Suppression of Fas, TRAIL-R2 and TNF-R1 significantly blocked the apoptosis induced by T6 (43.01%, 67.03% and 40.93%,

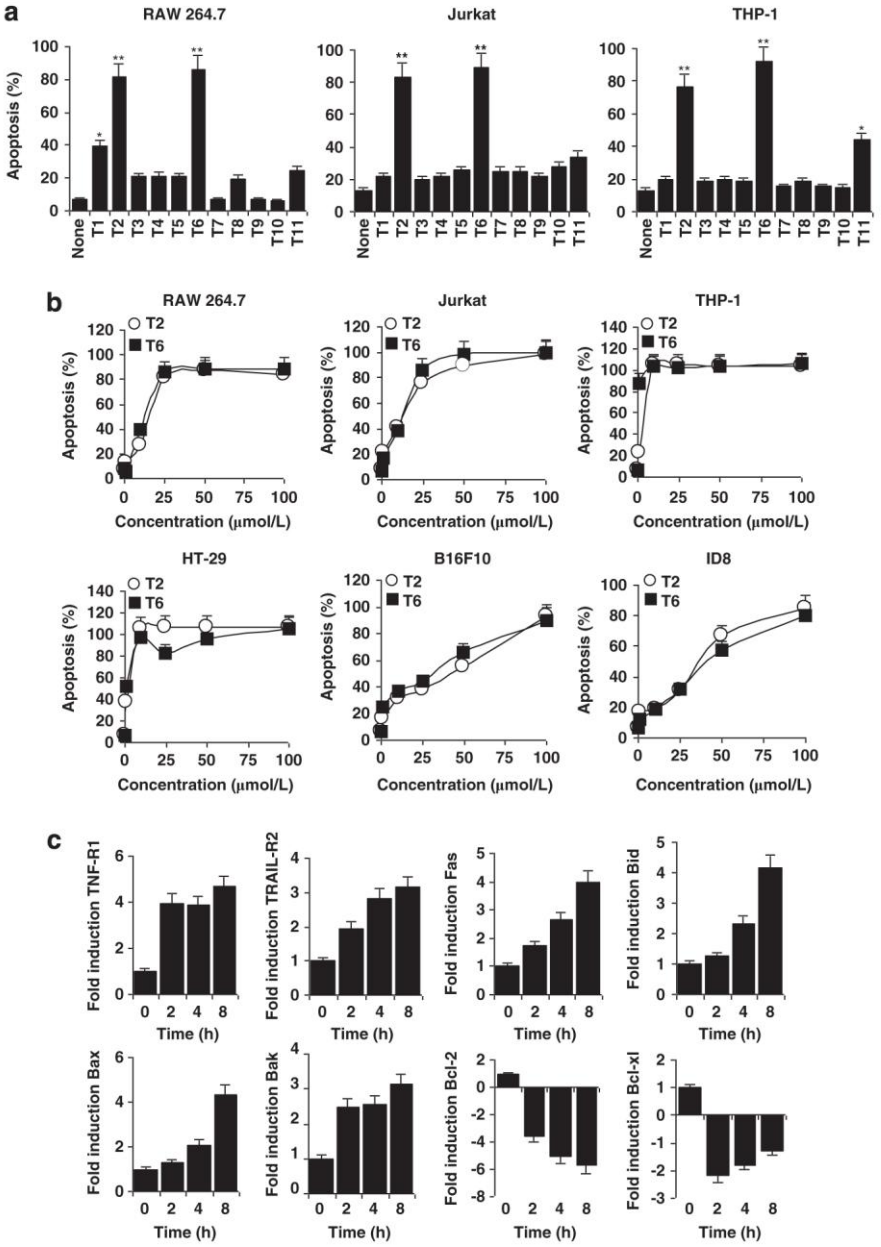

Figure 1. Induction of apoptosis by labdane diterpenoids. (**a**) RAW 264.7, Jurkat and THP-1 cells were incubated with 50 μM of the different diterpenoids for 24 h. The percentage of apoptotic cells was determined by flow cytometry after staining with PI and annexin-V. (**b**) RAW 264.7, Jurkat, THP-1, HT-29, B16F10 and ID8 cells were incubated with the indicated concentrations of T2 and T6 for 24 h. The percentage of apoptotic cells was determined by flow cytometry after staining with PI and annexin-V. **(c)** Expression profile of apoptosis-related genes**.** RAW 264.7 cells were incubated for 2, 4 and 8 h with 25 μM T6**,** and expression of apoptosis-related genes was analyzed by quantitative PCR. Graphs show the relative expression levels of selected genes. Data are the means ± s.d. of three independent experiments carried out in triplicate. $^{*}P<0.05$, $^{**}P<0.01$ with respect to the control condition.

respectively) (Figure 4g). Similar results were obtained with RAW 264.7 cells (data not shown). These results collectively indicate that upregulation of death receptors is important for T6-induced apoptosis.

Non-tumor cells are more resistant to T6-induced apoptosis

To examine the effects of T6 on non-tumor cells, we used primary cultures of peritoneal macrophages obtained from thioglycolate-injected mice. Peritoneal macrophages or RAW 264.7 cells were stimulated for 24 h with a range of concentrations of T6 or T7, and apoptosis and caspase activation were determined (Figure 5a). T6 (50 μM) induced apoptosis and activated caspase-8, 9 and 3 in RAW 264.7 cells. However, even at this high dose, apoptosis was slightly induced in peritoneal macrophages (34.77%) compared with RAW 264.7 cells (95.8%). Moreover, the IC_{50} of T6 in RAW 264.7 cells did not induce apoptosis in peritoneal macrophages.

To further examine the effect of T6 on normal cells, we compared the cytotoxicity of T6 on leukemic cells and freshly isolated peripheral blood lymphocytes (PBLs). As shown in Figure 5b, the percentage of apoptosis of Jurkat and REH cells was much higher than that on PBLs after T6 treatment. In addition, we also found that percentage of caspase-3 activity in PBLs was much lower comparing with leukemic cells (Figure 5b). These data

thus suggest that transformed cells are more susceptible to apoptosis elicited by T6 than normal cells, providing evidence for the potential use of the selected hispanolone derivatives as antitumor agents.

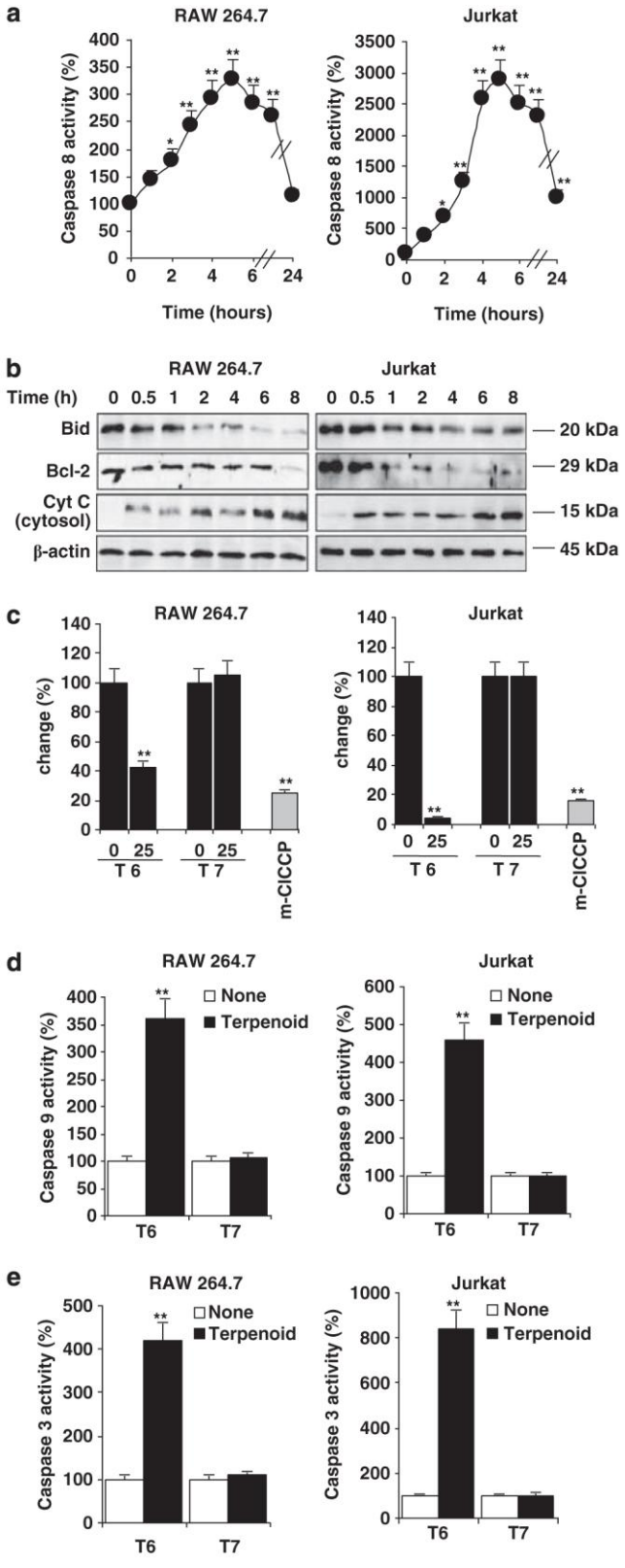

T2 and T6 exert greater cytotoxic effect than andrographolide

Andrographolide is the main labdane diterpenoid present in *Andrographis paniculata*, and induces apoptosis in several tumor cell lines.[11–13] To compare the antitumor potential of andrographolide vs T2 and T6, we treated different tumor cell lines with the three compounds over a range of concentrations. As shown in Figure 5c, T2 and T6 induced higher apoptosis rates than andrographolide in all tested lines. Thus, IC_{50} values of andrographolide were 100 μM, 75 μM, 80 μM and 90 μM for RAW 264.7, Jurkat, B16F10 and ID8 cells, respectively, whereas T2 and T6 showed IC_{50} values in a range of 15 μM for RAW 264.7 and Jurkat cells, and 40 μM for B16F10 and ID8 cells.

Toxicity studies of T6 in mice

We examined the toxicity profile of T6 in C57BL/6 mice. To this end, 30 8-week-old mice were treated with a daily intraperitoneally (i.p.) dose of T6 at 30 mg/kg/day for 1 week. Control mice ($n = 10$) were treated with vehicle alone. All T6-treated mice remained healthy and gained weight throughout the 30-day observation period with no evidence of morbidity (Supplementary Figure 3b). Blood tests done on days 7, 15 and 30 did not suggest any significant systemic toxicity. In particular, T6 did not cause: (i) anemia, neutropenia, lymphopenia, or thrombocytopenia suggestive of hematologic toxicity (Supplementary Figure 3c); (ii) elevations of creatinine suggestive of renal toxicity (Supplementary Figure 3d); or (iii) elevations of alanine aminotransferase and aspartate aminotransferase suggestive of hepatotoxicity (Supplementary Figure 3d). Moreover, no toxicity was found in any of the organs from 20 T6-treated mice (or 10 vehicle-treated control mice) killed at 15 days (data not shown) or 30 days (Supplementary Figure 3e). Thus, T6 treatment was nontoxic and was not associated with any subclinical systemic toxicity.

Evaluation of T6 as anticancer therapy in animal models

In an effort to determine whether T6 could inhibit *in vivo* tumor growth, luc-B16F10 cells were treated for 15 min *in vitro* with T6 (25 μM) or dimethyl sulfoxide (DMSO) (vehicle) and subsequently transplanted into the subcutaneously (s.c.) space of NOD SCID mice. T6-treated cells (left flank) significantly retarded tumor growth compared with non-treated cells (right flank) as shown whole mount analysis of the dissected tumor, cancer mass weight and luciferase activity (Figure 6a). Additionally, luc-B16F10 cells were injectd s.c. into the flanks of mice. After 24 h, T6 or equivalent

Figure 2. Caspase-8 activation and mitochondrial signaling after treatment with T6. **(a)** RAW 264.7 and Jurkat cells were treated with T6 (25 μM) for the indicated periods. Caspase-8 activity was determined in cell extracts by fluorometry, using Ac-IETD-AMC as the fluorigenic substrate. (**b**) RAW 264.7 and Jurkat cells were incubated with T6 (25 μM) and the expression of the apoptosis-related proteins Bid, Bcl-2 and cytochrome c was determined at the indicated times by western blot in cytosolic extracts. Protein loading was normalized to the expression of β-actin. A representative experiment is shown to be performed thrice. (**c**) RAW 264.7 and Jurkat cells were incubated with T6 or T7 (25 μM) for 6 h, labeled with TMRM, and $\Delta\Psi$m determined by flow cytometry of TMRM fluorescence; the uncoupling agent mClCCP (10 μM) was used as a positive control. (**d**) RAW 264.7 and Jurkat cells were stimulated with T6 or T7 (25 μM) for 6 h. Caspase-9 activity was determined in cell extracts by fluorometry, using Ac-LEHD-AMC as the fluorigenic substrate. (**e**) RAW 264.7 and Jurkat cells were stimulated with T6 or T7 (25 μM) for 6 h. Caspase-3 activity was determined in cell extracts by fluorometry, using Ac-DEVD-AMC as the fluorigenic substrate. Data are the means ± s.d. of three independent experiments carried out in triplicate. $^{*}P < 0.05$ and $^{**}P < 0.01$ with respect to the control condition (**a, c, d** and **e**).

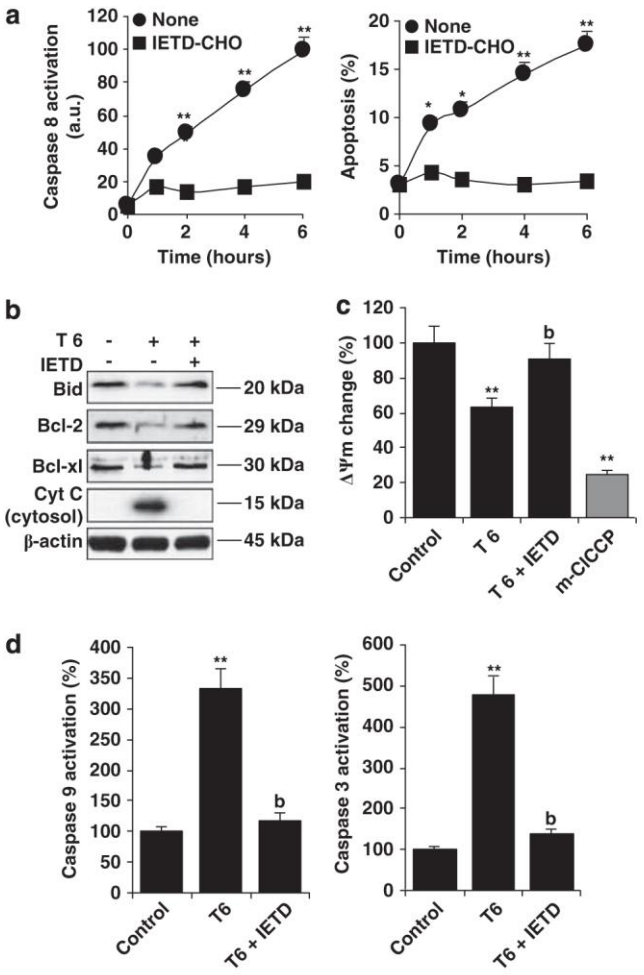

Figure 3. Inhibition of caspase-8 prevents diterpenoid-induced apoptosis. **(a)** RAW 264.7 cells were pretreated with 100 μM Ac-IETD-CHO for 1 h before treatment with T6 (25 μM) for the indicated periods. Cells were loaded with the selective caspase-8 substrate CaspGLOW Fluorescein caspase-8, and caspase-8 activity was determined in live cells by flow cytometry. The percentage of apoptotic cells was determined by flow cytometry after labeling with PI and annexin-V. (**b**) RAW 264.7 cells were pretreated with Ac-IETD-CHO, treated with 25 μM T6 for 6 h, and the expression levels of Bid, Bcl-2, Bcl-xl and cytochrome *c* determined by western blot of cytosolic extracts. β-actin was used as loading control. A representative experiment is shown to be performed thrice. (**c**) RAW 264.7 cells were incubated as in **b**, labeled with TMRM, and ΔΨm determined by flow cytometry; mClCCP (10 μM) was used as a positive control. (**d**) RAW 264.7 cells were incubated as in **c**, and caspase-9 and 3 activities in cell extracts were determined by fluorometry. Data are mean ± s.d. of three independent experiments carried out in triplicate. $^{*}P<0.05$, $^{**}P<0.01$ with respect to the control condition (**a, c, d**); b, $P<0.01$ vs T6 (**c, d**).

volume of vehicle alone were administered as described in material and methods. Again, tumor growth was inhibited in T6-treated mice with 52% reduction in tumor growth, and 49% reduction in luciferase activity compared with the control group (Figure 6b). Finally, luc-ID8 cells were i.p. injected to NOD SCID mice and T6 or vehicle was administered. *In vivo* luciferase analysis of the tumor cells corroborates the T6-mediated antitumoral activity (Figure 6c). In order to determine whether the inhibition of tumor growth is mediated by T6-induced apoptosis, we evaluated caspase-3 activity in extracts obtained from B16F10 and ID8-induced tumors. Caspase-3 activity was increased in cancer tissues from T6-treated animals, whereas no activity was observed in DMSO-injected animals (Figures 6b and c). Thus, tumor weight measurements and luciferase activity evaluation indicate that T6 inhibits tumor progression. Collectively, all these results propose diterpenoid T6 as a new drug for cancer therapy.

DISCUSSION

Terpenoids are present in all organisms but are especially abundant in plants, with >30 000 compounds identified. So far several terpenoids, including diterpenes, triterpenes and sesquiterpenes, have been found to have excellent anti-inflammatory and antineoplastic potential.[2,14–17] Although the mechanisms of action of these compounds have not been fully characterized, their ability to suppress tumor proliferation and to induce apoptosis may represent an important means of chemoprevention.

Apoptosis, or programmed cell death, is a highly organized physiological process that functions to eliminate damaged or abnormal cells. In the present study, we have described the pro-apoptotic action of hispanolone derivatives in tumor cells. To recapitulate the essence of our findings, selected hispanolone derivatives T2 and T6 induce: (1) apoptosis in a panel of human and mouse tumor cell lines; (2) caspase-8 activation; (3) processing of the proapoptotic Bcl-2-related protein Bid; (4) activation of the mitochondrial apoptotic pathway with a significant decrease in $\Delta\Psi_m$; (5) release of cytochrome c to the cytosol and (6) activation of caspase-9 and 3. The observed effects of hispanolone derivatives were abrogated completely by the specific caspase-8 inhibitor Ac-IETD-CHO, demonstrating that caspase-8 is the upstream initiator enzyme. With regard to mechanisms, hispanolone derivatives were found to trigger marked mRNA and protein expression of the death receptors Fas, TNF-R1 and TRAIL. Interestingly, blockage of death receptor pathway with neutralizing antibodies or gene silencing effectively inhibited cell death.

Taken together, these observations illustrate the involvement of the death receptor pathway in hispanolone derivatives-induced apoptosis and suggest the possible clinical use of these derivatives to selectively induce apoptosis in tumor cells. Other natural products have been shown to induce apoptosis via this pathway, highlighting death receptors like one of the most attractive targets for the treatment of cancer.[12,18,19] For example, TRAIL receptors represent a promising candidate for cancer treatment because of their ability to be toxic to human tumor cells *in vitro* and *in vivo,* whereas they have a more limited effect on normal cells.[20,21] Of particular interest in this regard is our finding that the labdane diterpenoid T6 present a stronger proapoptotic action on tumor cells than on primary cell cultures or freshly isolated PBLs. This selective T2-, T6-apoptosis for transformed cells requires further study, but might indicate a greater resistance of normal cells to apoptosis than tumor cells, and suggests a promising future for these compounds as therapeutic agents. In addition, T6 was very well tolerated *in vivo* without any obvious toxicity. Thus, nor mortality was observed in T6-injected mice and neither significant changes in body weight, hematological and biochemical parameters and histopathological analyses were found.

Natural products have been investigated as potential sources of novel anticancer drugs for decades.[22] However, the genetic complexity of human cancers calls for refocused efforts to develop new multifunctional, rather than monofunctional, drugs to be used either for prevention or treatment. In this regard, synthetic oleanane triterpenoids have recently been shown to have profound effects on inflammation and tissue redox state, as well as being potent anti-proliferative and pro-apoptotic agents.[17] Other studies have shown that inhibition of NF-κB potentiates the efficacy of the antitumor effects of ionizing radiation and some chemotherapeutic compounds.[23,24] NF-κB is a transcription factor whose activity is required for the induction of >150 genes involved in cell growth, differentiation and apoptosis. Recent data indicate that some terpenoids, including labdane diterpenes,

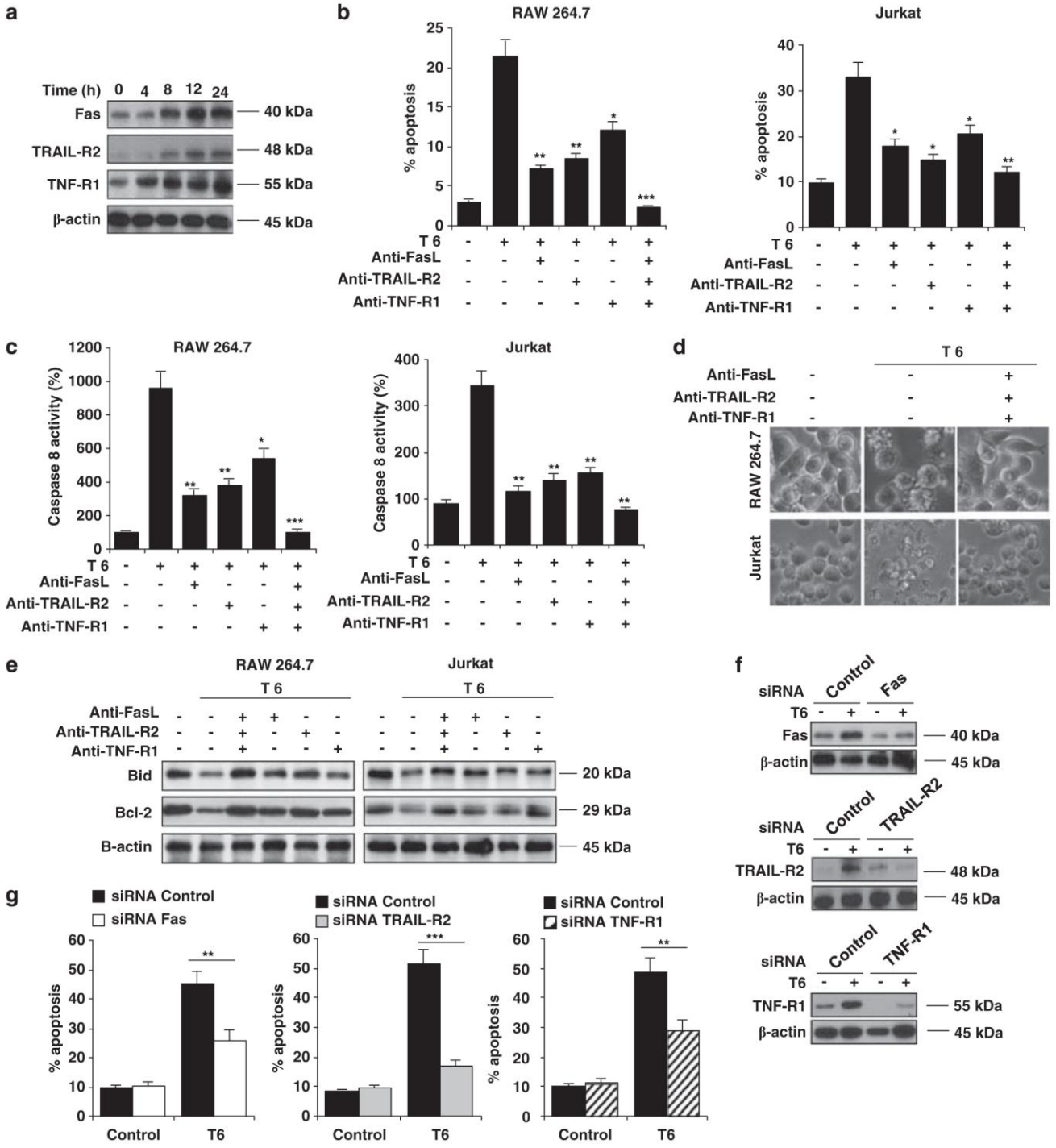

Figure 4. Blockage of death receptors inhibits diterpenoid-induced apoptosis. **(a)** Jurkat cells were treated with T6 25 μM for the indicated times and levels of Fas, TRAIL-R2 and TNF-R1 were determined by western blot. (**b**) RAW 264.7 or Jurkat cells were pretreated (1 h) with neutralizing antibodies (20 μg/ml) to Fas ligand and the death receptors TNFR1 and TRAIL-R2, either alone or in combination. Cells were then stimulated with T6 (25 μM, 6 h) and tested for apoptosis-related events. The percentage of apoptotic cells was determined by flow cytometry after labeling with PI and annexin-V. (**c**) Cells were treated as in **b**, and caspase-8 activity was determined fluorometrically in cell extracts. (**d**) Cells were treated as in **b**. Light micrographs show morphological alterations in response to T6 treatment with or without neutralizing antibodies. Pictures are from a representative experiment of three performed. (**e**) Cells were treated as in **b**. Levels of Bid and Bcl-2 were determined in cytosolic extracts by western blot. β-actin was used as a loading control. (**f**) Jurkat cells were transfected with Fas, TRAIL-R2, TNF-R1 or control scrambled siRNA duplex oligonucleotides. Twenty-four hours after transfection, cells were stimulated with T6 (25 μM, 6 h) and lysates obtained from siRNA-treated cells were immunoblotted with antibodies to the indicated molecules to determine the knockdown efficacy. (**g**) Jurkat cells were treated with the indicated siRNA oligonucleotides, after which they were treated with T6 (25 μM, 6 h) and tested for apoptosis-related events. The percentage of apoptotic cells was determined by flow cytometry after labeling with PI and annexin-V. A representative experiment is shown in **a, d, e** and **f** of three performed. Data in **b, c** and **g** are the mean ± s.d. of three independent experiments carried out in triplicate. $^{*}P<0.05$, $^{**}P<0.01$, $^{***}P<0.001$ with respect to the T6 alone in **b** and **c**. $^{**}P<0.01$, $^{***}P<0.001$ with respect to the cells transfected with siRNA control in the presence of T6 in **g**.

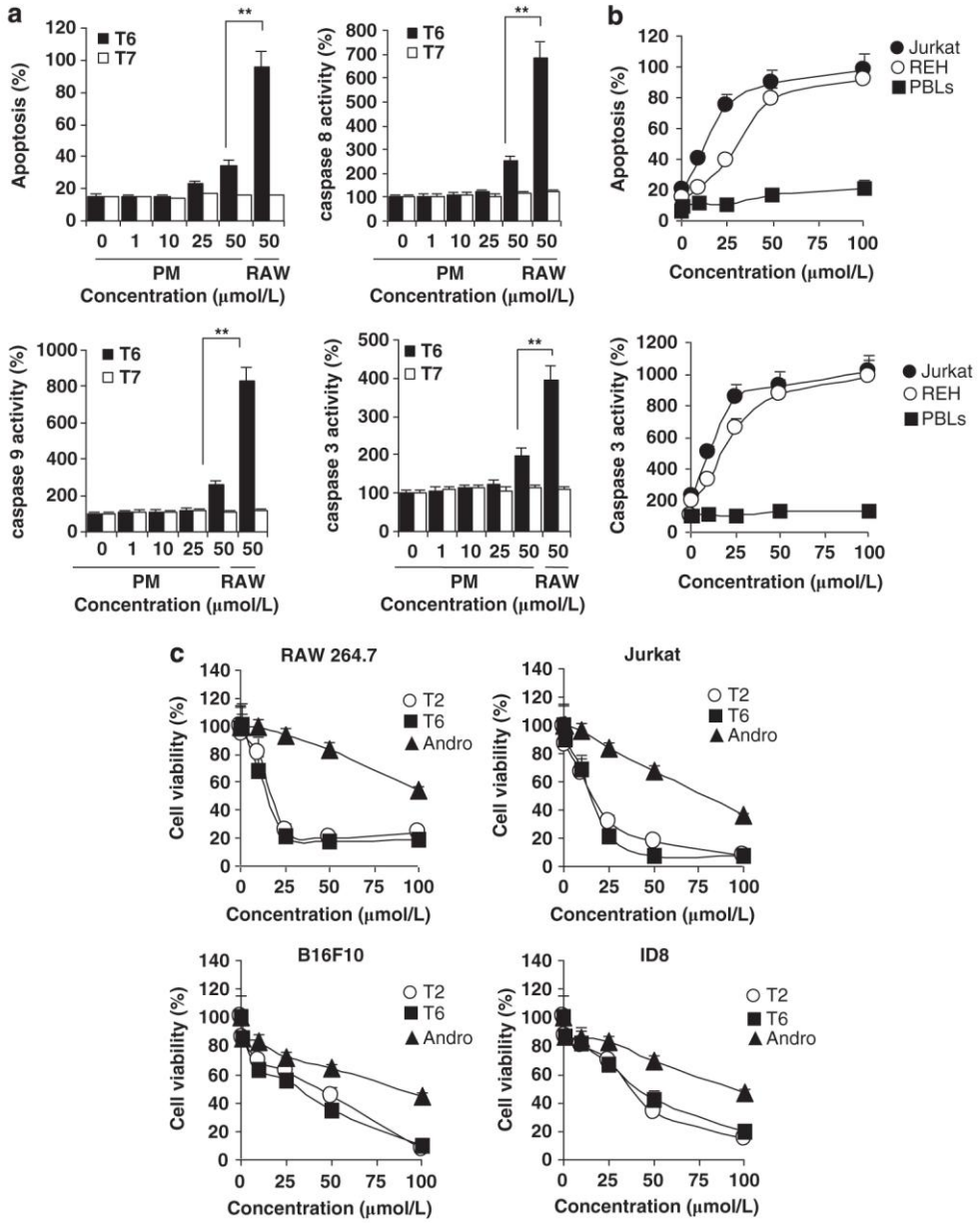

Figure 5. Hispanolone derivatives selectively induce apoptosis in tumor cells and are more cytotoxic than andrographolide. (**a**) Peritoneal macrophages (PM) isolated from thioglycolate-injected mice were treated with the indicated concentrations of diterpenoids T6 or T7 for 24 h, and RAW 264.7 cells were incubated with 50 μM T6 or T7. The percentage of apoptotic cells was determined by flow cytometry after staining with PI and annexin-V, and caspase activities were determined fluorometrically in cell extracts. (**b**) Leukemic cells (Jurkat and REH) and PBLs were treated with the indicated concentrations of diterpenoid T6 for 24 h. The percentage of apoptotic cells was determined by flow cytometry after staining with PI and annexin-V, and caspase-3 activity was determined fluorometrically in cell extracts. (**c**) RAW 264.7, Jurkat, B16F10 and ID8 cells were treated with the indicated concentrations of T2, T6 and andrographolide. The percentage of live cells was determined by flow cytometry after staining with PI and annexin-V. Data are the means ± s.d. of three independent experiments carried out in duplicate. $^{**}P<0.01$ with respect to the T6 condition.

kaurane diterpenes and sesquiterpenes, inhibit NF-κB signaling.[11,25–28] Among them, andrographolide, a labdane diterpenoid isolated from a traditional herbal medicine *Andrographis paniculata*, not only possess potent anti-inflammatory activity but also has been described to induce apoptosis in human cancer cells via activation of caspase-8.[12] These effects are similar to those described for the selected hispanolone derivatives T2 and T6. Indeed, we have recently reported that hispanolone derivatives inhibit NF-κB signaling in macrophages, by directly binding to and inhibiting its kinase activator IKKβ.[2] The mechanism is thought to involve the ability of α,β-unsaturated carbonyl groups in labdane diterpenoids to react with cysteine sulfhydryl groups in IKK through Michael-type addition.[2] This inhibition of NF-êB activation by hispanolone derivatives, through the resulting downregulation of antiapoptotic genes, may augment their activation of caspase-8. Interestingly, when we have compared the effects of hispanolone derivatives with andrographolide, T2 and T6 were both more potent inducers of apoptosis than andrographolide, suggesting that hispanolone derivatives could be promising anticancer agents.

Further support for this notion comes from *in vivo* experiments. Hispanolone derivative T6 was well tolerated and induced a growth inhibition in tumor xenografts. Moreover, an increase in

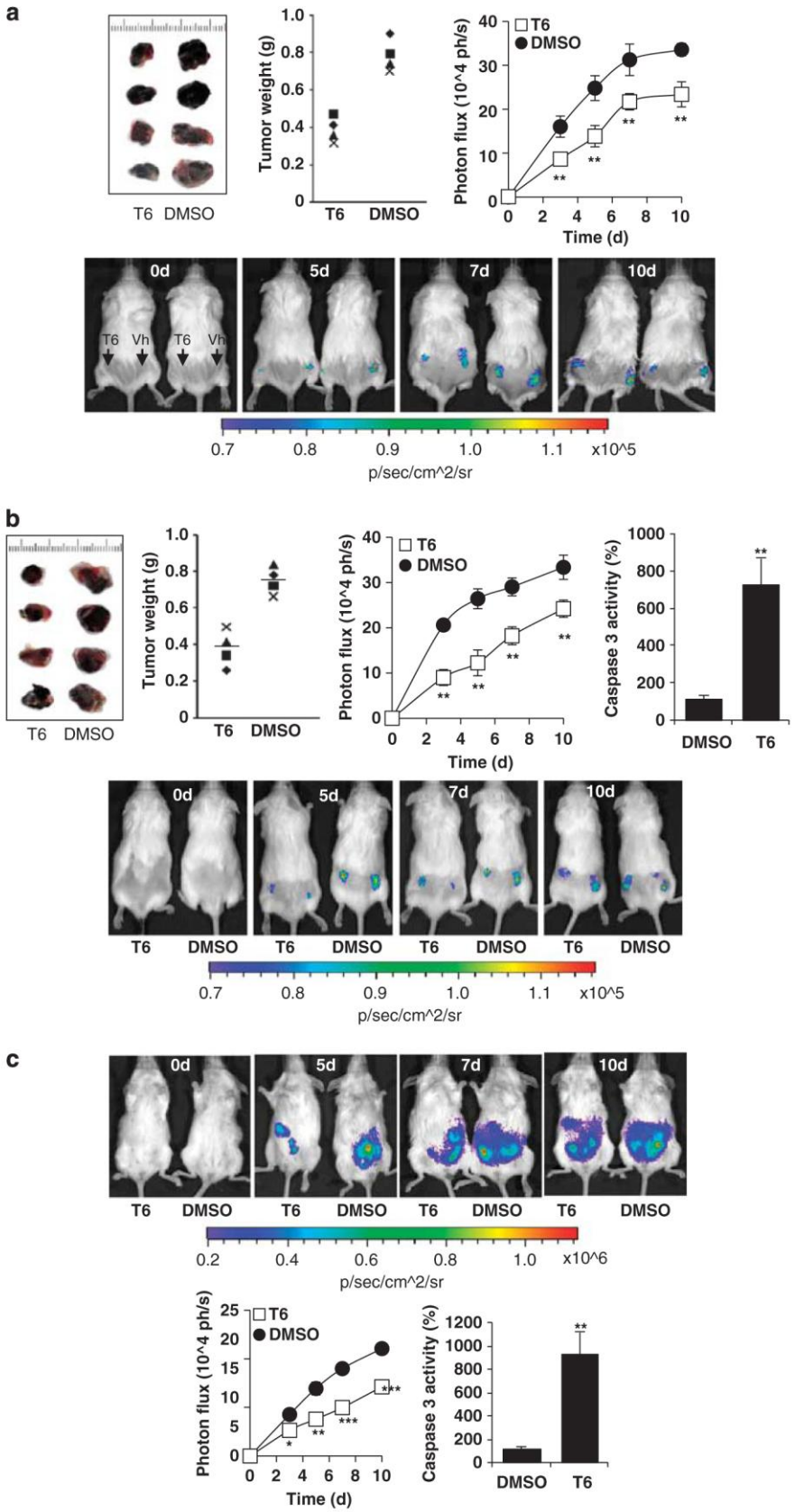

Figure 6. T6 inhibits the growth of B16F10 and ID8 tumors in NOD SCID mice. (**a**) T6-treated or vehicle-treated cells (25 μM, 15 min) were s.c. injected in both flanks of NOD SCID mice and the change in tumor weight and luciferase activity was determined for each animal. (**b**) B16F10 tumor-bearing mice were daily injected i.p. with 20 mg/kg T6. The change in tumor weight and luciferase activity was determined for each animal. Caspase-3 activity was determined fluorometrically in B16F10 tumor extracts (**c**) ID8 tumor-bearing mice were daily injected i.p. with 20 mg/kg. Luciferase activity was determined for each animal. Caspase-3 activity was determined fluorometrically in ID8 tumor extracts. Data are the mean ± s.d. $^{*}P<0.05$, $^{**}P<0.01$, $^{***}P<0.001$ with respect to the DMSO treatment.

caspase-3 activity was observed in tumors treated with T6. These promising results also emphasize the potential therapeutic value of hispanolone derivatives in human cancer treatment.

In summary, hispanolone derivatives T2 and T6 are able to induce tumor apoptosis by activating the death receptor pathway; moreover, although most chemotherapeutic agents are limited to proapoptotic effects, hispanolone derivatives also inhibit the NF-κB pathway. Thus, the novel proapoptotic biological activity of hispanolone derivatives provides valuable knowledge for further investigation, and an excellent base from which to develop new chemotherapeutic drugs.

MATERIALS AND METHODS

Materials

Terpenoids (T1–T11) were obtained as previously described.[2,9,10] Western blot reagents were from GE Healthcare (Pittsburgh, PA, USA). Antibodies were from Santa Cruz Biotechnology (Santa Cruz, CA, USA), Abcam (Cambridge, MA, USA), BD Biosciences (San Jose, CA, USA), Cell Signaling (Danvers, MA, USA), and R&D Systems (Abingdon, UK). Fluorescent probes for caspase activity were from BD Biosciences (San Jose, CA, USA), and CaspGlow was from BioVision (Milpitas, CA, USA). Culture media were from Lonza (Basel, Switzerland). Ligand stocks, including terpenoids, were dissolved in DMSO and subsequently diluted in PBS before use. siRNAs were purchased from Santa Cruz Biotechnology. The RT^2 Profiler PCR Array was from SuperArray Bioscience (Frederick, MD, USA).

Cell culture conditions

RAW 264.7, Jurkat, HT-29, REH and THP-1 cells were purchased from American Type Culture Collection (ATCC, Rockville, MD, USA). B16F10 cells were a gift from Dr S Alemany and ID8 cells were a gift from Dr K Roby. For culture, RAW 264.7, Jurkat, REH and THP-1 were maintained in RPMI 1640 medium supplemented with 10% fetal bovine serum (FBS), L-glutamine and antibiotics. HT-29 and B16F10 cells were maintained in DMEM supplemented with 10% FBS, L-glutamine and antibiotics. ID8 cells were maintained in DMEM supplemented with 4% FBS and antibiotics, insulin (5 μg/ml) transferring (5 μg/ml) and sodium selenite (5 ng/ml). All cell lines were mycoplasma tested and kept frozen under liquid nitrogen until resuscitated for use.

Preparation of elicited peritoneal macrophages

Pathogen-free C57BL/6 mice were injected i.p. with 1 ml sterile 10% (w/v) thioglycollate broth. After 4 days, peritoneal macrophages were prepared as previously described.[29]

Isolation of PBLs

PBLs were isolated from healthy volunteers by Ficoll–Hypaque gradient. The cells were washed with PBS twice and then suspended in complete RPMI 1640 with 10% FBS. The viability of the isolated lymphocytes was measured by trypan blue exclusion assay and found to be about 99%.

Flow cytometry analysis of apoptosis and necrosis

After treatment with the appropriate stimuli, cells were stained with 0.005% (w/v) propidium iodide (PI) and annexin V-FITC as recommended by the manufacturer (BD Biosciences), being immediately analyzed in a FACSCanto II flow cytometer (Becton Dickinson Biosciences, San Jose, CA, USA). 10 000 events were counted by flow cytometry and an increase in the percentage of annexin-V-positive cells indicates increased apoptosis.

Cytosolic extracts and western blot

Cytosolic extracts were prepared as previously described.[30] Protein content was estimated by the Bio-Rad protein assay. Protein extracts were subjected to SDS–PAGE (10–15% gels) and blotted onto polyvinylidene difluoride membranes, which were incubated with the following antibodies: anti-β-actin, anti-Bid, anti Bcl-xl, anti-Bcl-2 (all from Santa Cruz Biotechnology), anti-TNF-R1, anti-Fas (R&D systems), anti-TRAIL-R2 (Abcam) and anti-cytochrome c (BD Biosciences). After incubation with HRP-conjugated secondary antibody, protein bands were revealed with an enhanced chemiluminescence kit (GE Healthcare). β-actin was used as a loading control.

Assessment of mitochondrial depolarization

To detect changes in $\Delta\Psi m$, diterpenoid-stimulated cells were harvested and stained (30 min, 37 °C) with tetramethylrhodamine ethyl ester (TMRE; Molecular Probes, Carlsbad, CA, USA), a lipophilic cationic fluorochrome that selectively stains mitochondria that have an intact electrochemical gradient. Cells were analyzed for TMRE fluorescence on a FACSCanto II flow cytometer.

Caspase assays

The activities of caspase-3, 8 and 9 were determined fluorimetrically in cytosolic protein extracts, using the substrates Ac-DEVD-AMC, Ac-IETD-AMC and Ac-LEHD-AMC, respectively, according to the supplier's instructions (BD Biosciences). Alternatively, caspase-8 activity was measured by flow cytometry of living cells, using the CaspGLOW Fluorescein caspase-8 kit according to the supplier's instructions (BioVision).

Gene expression profile

Total RNA was extracted from diterpenoid-treated cells with Trizol reagent (Invitrogen). Expression of apoptotic genes was evaluated with the mouse RT^2*Profiler* PCR Apoptosis Array (SuperArray Bioscience). Briefly, 2 μg of RNA were used for cDNA synthesis with RT^2 First Standard kit (SuperArray Bioscience). The mouse apoptosis PCR array was performed according to the manufacturer's protocol, using the Profiler PCR Array System and the SYBR Green/Fluorescein qPCR master mix (SuperArray Bioscience) on an ABI7900 sequence detector (Applied Biosystems). Gene expression was compared with the web-based software package for the PCR Array System (http://pcrdataanalysis.sabiosciences.com/pcr/arrayanalysis.php); this software automatically performs all ΔΔCt-based fold-change calculations from the specific uploaded raw threshold cycle data.

RNA analysis and quantitative PCR

Total RNA was isolated from cells and mouse tissues with Trizol reagent (Invitrogen). Quantitative PCR (SYBRgreen) analysis was performed with an ABI7900 sequence analyzer as described.[29] Each sample was run in duplicate, and all samples were analyzed in parallel for the expression of the housekeeping gene 36B4 (acidic ribosomal phosphoprotein P0), which was used as an endogenous control for normalization of the expression level of target genes. Fold induction was determined from mean replicate values. Primer sequences are available on request.

Treatment of cells with neutralizing antibodies to death receptors

Cells were pretreated with 20 μg/ml of neutralizing antibodies raised against Fas ligand, TNF-R1, or the extracellular domains of TRAIL-R2 (R&D Systems), either separately or in combination, for 1 h before stimulation for 6 h with 25 μM of the selected diterpenoid.

Small interfering RNA

Scrambled (sc-44230) and specific short interfering RNAs (siRNA) to either Fas (sc-29311), TNF-R1 (sc-29507) or TRAIL-R2 (DR5 sc-40237) were from Santa Cruz Biotechnology. Jurkat cells were transfected with siRNA oligos by electroporation (AMAXA, Walkersville, MD, USA). Jurkat cells were transfected with 50 nM Fas siRNA, 50 nM TNF-R1 siRNA, 50 nM TRAIL-R2 siRNA and 100 nM scrambled sequence, which served as a control. The depletion of the respective death receptors was determined by western blot analysis.

In vivo tumor progression in immunodeficient mice and bioluminescence imaging

Procedures were performed with approved protocols, in accordance with the Ethics Committee for Animal Experimentation' of the Instituto de Salud Carlos III (ISCIII), EU commission regulations for laboratory animals' care.

In vivo tumor progression was examined using the noninvasive bioimaging system IVIS (Xenogen, Caliper Life Sciences, Hopkinton, MA, USA). Luciferase-expressing B16F10 (luc-B16F10) melanoma cells and murine ovarian cancer ID8 (luc-ID8) cells were used to visualize the fate of tumor progression *in vivo*. Three different approaches were performed. First, luc-B16F10 cells (1×10^6) were treated for 15 min *in vitro* with T6 (25 μM) or DMSO (vehicle) and were s.c. implanted in NOD SCID mice. Cells treated with T6 were implanted in the left flank and cells treated with the vehicle were implanted in the right flank of the animal. Tumors were allowed to grow for 10 days. Second, luc-B16F10 cells (1×10^6) were s.c. implanted in both flanks of NOD SCID mice, and tumors were allowed to grow for 24 h. They were then separated into two groups ($n = 4$), and each group received daily intraperitoneal injections of either 20 mg/kg of T6 (dissolved in 50 μl DMSO; treated) or 50 μl DMSO (control). Finally, luc-ID8 cells (5×10^6) were i.p. injected to NOD SCID mice and tumors were allowed to grow for 24 h. They were then separated into two groups ($n = 4$), and each group received daily intraperitoneal injections of either 20 mg/kg of T6 (dissolved in 50 μl DMSO; treated) or 50 μl DMSO (control).

In all experiments, tumor-implanted mice were anesthetized with isoflurane, and D-luciferin (potassium salt; BioGold, St Louis, MO, USA) was injected into the peritoneal cavity at 3 mg per body, immediately followed by measurement of the luciferase activity. The same sequence of bioluminescence imaging was repeated at different time points (0, 3, 5 and 10 days) of tumor implantation. The signal from tumors was quantified as photons flux in units of photons/sec/cm^2/steradian. Additionally, melanoma tumor growth at the skin was monitored by measurement of the two maximum perpendicular tumor diameters. At day 10, animals were killed and the weight and photographs of tumors were taken. Tumor tissue samples obtained from control and T6-treated mice were minced and incubated on ice for 30 min in 0.5 ml of ice-cold lysate buffer (20 mmol/l Tris-HCl (pH 7.4), containing 10% NP40, 5 mol/L NaCl, 1 mol/l HEPES, 0.5 mol/l EDTA, 0.1 mol/l phenylmethylsulfonyl fluoride, 0.2 mol/l sodium orthovanadate, 1 mol/l NaF, 2 μg/ml aprotinin, and 2 μg/ml leupeptin). The minced tissue was homogenized using a Dounce homogenizer and centrifuged at $16\,000 \times g$ at 4 °C for 10 min. The activity of caspase-3 was determined fluorimetrically in protein extracts, using the substrate Ac-DEVD-AMC according to the supplier's instructions (BD Biosciences).

Statistical analysis

The data presented are shown as means ± s.d. of three independent experiments. Statistical significance was estimated by Student's *t* test for unpaired observations, with $P < 0.05$ considered significant. For western blots, a linear correlation was observed between increasing amounts of input protein and signal intensity.

CONFLICT OF INTEREST

RL-F, B de las H, BR and SH are inventors on a Spanish patent application on labdane diterpenoids as antitumoral agents. The other authors declared no conflict of interest.

ACKNOWLEDGEMENTS

This study was supported by grant PI08.0070 from the FIS and MPY 1410/09 from ISCIII to SH, and by a Santander-Complutense grant to SH and B de las H. We thank Gemma Benito for excellent technical assistance and Simon Bartlett for critical reading of the manuscript. We thank Dr S Alemany and Dr K Roby for kindly provide luc-B16F10 and ID8 cells, respectively.

REFERENCES

1 Chinou I. Labdanes of natural origin-biological activities (1981–2004). *Curr Med Chem* 2005; **12**: 1295–1317.
2 Girón N, Traves PG, Rodriguez B, Lopez-Fontal R, Bosca L, Hortelano S *et al.* Supression of inflammatory responses by labdane-type diterpenoids. *Toxicol Appl Pharmacol* 2007; **228**: 179–189.
3 Song Z, Steller H. Death by design: mechanism and control of apoptosis. *Trends Cell Biol* 1999; **9**: M49–M52.
4 Nicholson DW. Caspase structure, proteolytic substrates, and function during apoptotic cell death. *Cell Death Differ* 1999; **6**: 1028–1042.
5 Peter ME, Krammer PH. Mechanisms of CD95 (APO-1/Fas)-mediated apoptosis. *Curr Opin Immunol* 1998; **10**: 545–551.
6 Enari M, Talanian RV, Wong WW, Nagata S. Sequential activation of ICE-like and CPP32-like proteases during Fas-mediated apoptosis. *Nature* 1996; **380**: 723–726.
7 Slee EA, Adrain C, Martin SJ. Serial killers: ordering caspase activation events in apoptosis. *Cell Death Differ* 1999; **6**: 1067–1074.
8 Li H, Zhu H, Xu CJ, Yuan J. Cleavage of BID by caspase 8 mediates the mitochondrial damage in the Fas pathway of apoptosis. *Cell* 1998; **94**: 491–501.
9 Savona G, Piozzi F, Rodriguez B. Hispanolone, a new furanoditerpene. *Heterocycles* 1978; **9**: 257–261.
10 Rodriguez B, Savona G. Diterpenoids from *Galeopsis Angustifolia*. *Phytochemistry* 1980; **19**: 1805–1807.
11 Xia YF, Ye BQ, Li YD, Wang JG, He XJ, Lin X *et al.* Andrographolide Attenuates Inflammation by Inhibition of NF-κB Activation through Covalent Modification of Reduced Cysteine 62 of p50. *J Immunol* 2004; **173**: 4207–4217.
12 Zhou J, Zhang S, Ong CN, Shen HM. Critical role of pro-apoptotic Bcl-2 family members in andrographolide-induced apoptosis in human cancer cells. *Biochem Pharmacol* 2006; **72**: 132–144.
13 Zhou J, Lu GD, Ong CS, Ong CN, Shen HM. Andrographolide sensitizes cancer cells to TRAIL-induced apoptosis via p53-mediated death receptor 4 up-regulation. *Mol Cancer Ther* 2008; **7**: 2170–2180.
14 de Las Heras B, Abad MJ, Silvan AM, Pascual R, Bermejo P, Rodriguez B *et al.* Effects of six diterpenes on macrophage eicosanoid biosynthesis. *Life Sci* 2001; **70**: 269–278.
15 Hwang BY, Lee JH, Koo TH, Kim HS, Hong YS, Ro JS *et al.* Kaurane diterpenes from Isodon japonicus inhibit nitric oxide and prostaglandin E2 production and NF-kappaB activation in LPS-stimulated macrophage RAW264.7 cells. *Planta Med* 2001; **67**: 406–410.
16 Nagashima F, Kasai W, Kondoh M, Fujii M, Watanabe Y, Braggins JE *et al.* New ent-kaurene-type diterpenoids possessing cytotoxicity from the New Zealand liverwort Jungermannia species. *Chem Pharm Bull (Tokyo)* 2003; **51**: 1189–1192.
17 Liby KT, Yore MM, Sporn MB. Triterpenoids and rexinoids as multifunctional agents for the prevention and treatment of cancer. *Nat Rev Cancer* 2007; **7**: 357–369.
18 Dirsch VM, Antlsperger DS, Hentze H, Vollmar AM. Ajoene, an experimental anti-leukemic drug: mechanism of cell death. *Leukemia* 2002; **16**: 74–83.
19 Kuo PL, Hsu YL, Lin TC, Lin LT, Lin CC. Induction of apoptosis in human breast adenocarcinoma MCF-7 cells by prodelphinidin B-2 3,3′-di-O-gallate from Myrica rubra via Fas-mediated pathway. *J Pharm Pharmacol* 2004; **56**: 1399–1406.
20 Kelley SK, Ashkenazi A. Targeting death receptors in cancer with Apo2L/TRAIL. *Curr Opin Pharmacol* 2004; **4**: 333–339.
21 Wajant H. CD95L/FasL and TRAIL in tumour surveillance and cancer therapy. *Cancer Treat Res* 2006; **130**: 141–165.
22 Mann J. Natural products in cancer chemotherapy: past, present and future. *Nat Rev Cancer* 2002; **2**: 143–148.
23 Wang CY, Cusack Jr JC, Liu R, Baldwin Jr AS. Control of inducible chemoresistance: enhanced anti-tumor therapy through increased apoptosis by inhibition of NF-kappaB. *Nat Med* 1999; **5**: 412–417.
24 Wang CY, Mayo MW, Baldwin Jr AS. TNF- and cancer therapy-induced apoptosis: potentiation by inhibition of NF-kappaB. *Science* 1996; **274**: 784–787.
25 Castrillo A, de Las Heras B, Hortelano S, Rodriguez B, Villar A, Bosca L. Inhibition of the nuclear factor kappa B (NF-kappa B) pathway by tetracyclic kaurene diterpenes in macrophages. Specific effects on NF-kappa B-inducing kinase activity and on the coordinate activation of ERK and p38 MAPK. *J Biol Chem* 2001; **276**: 15854–15860.
26 Lee JH, Koo TH, Yoon H, Jung HS, Jin HZ, Lee K *et al.* Inhibition of NF-kappa B activation through targeting I kappa B kinase by celastrol, a quinone methide triterpenoid. *Biochem Pharmacol* 2006; **72**: 1311–1321.
27 Lee JH, Koo TH, Hwang BY, Lee JJ. Kaurane diterpene, kamebakaurin, inhibits NF-kappa B by directly targeting the DNA-binding activity of p50 and blocks the expression of antiapoptotic NF-kappa B target genes. *J Biol Chem* 2002; **277**: 18411–18420.
28 Lyss G, Knorre A, Schmidt TJ, Pahl HL, Merfort I. The anti-inflammatory sesquiterpene lactone helenalin inhibits the transcription factor NF-kappaB by directly targeting p65. *J Biol Chem* 1998; **273**: 33508–33516.
29 Zeini M, Traves PG, Lopez-Fontal R, Pantoja C, Matheu A, Serrano M *et al.* Specific contribution of p19(ARF) to nitric oxide-dependent apoptosis. *J Immunol* 2006; **177**: 3327–3336.
30 Hueso-Falcon I, Cuadrado I, Cidre F, Amaro-Luis JM, Ravelo AG, Estevez-Braun A *et al.* Synthesis and anti-inflammatory activity of ent-kaurene derivatives. *Eur J Med Chem* 2011; **46**: 1291–1305.

Supplementary Information accompanies the paper on the Oncogene website (http://www.nature.com/onc)

Bioorganic & Medicinal Chemistry 21 (2013) 2471–2477

Contents lists available at SciVerse ScienceDirect

Bioorganic & Medicinal Chemistry

journal homepage: www.elsevier.com/locate/bmc

Synthesis and cytotoxic activity of metallic complexes of lawsone

Sandra Oramas-Royo [a,b,†], Concepción Torrejón [c,†], Irene Cuadrado [c], Rita Hernández-Molina [d], Sonsoles Hortelano [e,*], Ana Estévez-Braun [a,b,*], Beatriz de las Heras [c,*]

[a] Instituto Universitario de Bio-Orgánica 'Antonio González', Departamento de Química Orgánica, Universidad de La Laguna, Avda. Astrofísico Fco. Sánchez 2, 38206 La Laguna, Tenerife, Spain
[b] Instituto Canario de Investigaciones del Cáncer (ICIC), Spain
[c] Departamento de Farmacología, Facultad de Farmacia, Universidad Complutense, Plaza Ramón y Cajal s/n, 28040 Madrid, Spain
[d] Departamento de Química Inorgánica, Facultad de Farmacia, Universidad de La Laguna, Tenerife, Spain
[e] Unidad de Inflamación y Cáncer. Centro Nacional de Microbiología, Instituto de Salud Carlos III, Madrid, Spain

ARTICLE INFO

Article history:
Received 8 October 2012
Revised 1 February 2013
Accepted 2 March 2013
Available online 14 March 2013

Keywords:
HepG2
Apoptosis
Lawsone
Metallic complexes
Cytotoxicity

ABSTRACT

In the present study, a series of metallic complexes of the 1,4-naphthoquinone lawsone (**2–6**) were synthesized and evaluated for potential cytotoxicity in a mouse leukemic macrophagic RAW 264.7 cell line. Cell viability was determined by the MTT assay. Significant growth inhibition was observed for the copper complex **(4)** with an IC_{50} value of 2.5 μM. This compound was selected for further evaluation of cytotoxic activity on several human cancer cells including HT-29 (human colorectal adenocarcinoma), HepG2 (human hepatocellular carcinoma) and HeLa, (human cervical adenocarcinoma cells). Significant cell viability decrease was also observed in HepG2 cells. The apoptotic potential of this complex was evaluated in these cells. Compound **4** induced apoptosis by a mechanism that involves the activation of caspases 3, 8 and 9 and modulation of apoptotic-related proteins such as Bax, Bad, and p53. These results indicate that metal complexes of lawsone derivatives, in particular compound **4**, might be used for the design of new antitumoral agents.

1. Introduction

The quinonic moiety is considered by the National Cancer Institute (NCI) as an important biologically validated scaffold for the development of new bioactive compounds with good levels of cytotoxicity.[1,2] Indeed, many clinically important antitumoral drugs containing a quinone moiety such as anthracyclines, mitoxantrones and saintopin, show excellent anticancer properties.[3] A representative group of quinonoid compounds are 1,4-naphthoquinones which are widely distributed in nature and have been recognized to possess a wide range of biological activities such as antibacterial, anti-inflammatory, antifungal, antiviral.[4–7] Some illustrative examples of antitumoral naphthoquinones are plumbagin,[8] juglone,[9] β-lapachol[10] and rhinacanthone.[11]

Furthermore, transition metal-based drugs are increasing their importance in the therapy of cancer and other diseases. The best example of these metal-based drugs is cisplatin, one of the most used anticancer drugs.[12] Interestingly, metals can play an important role in modifying the pharmacological properties of known drugs.[13]

Quinones can bind potentially to metal ions in three different oxidations states: (i) quinone, (ii) its one electron reduced form semiquinone, (iii) catechol the two electrons reduced form. The binding ability of quinones in different oxidations states allows them to play an important role in biological systems.

There are only a few examples of metal complexes of 1,4-naphthoquinones. In this sense, Chen et al.[14] have recently published the synthesis, characterization and preliminary cytotoxicity evaluation of five lanthanide(III)–plumbagin complexes. Hernández-Molina et al.[15] reported the preparation of complexes of Co(II), Ni(II) and Cu(II) with the naturally occurring hydroxynaphthoquinone lapachol, and the Co(II) complex showed activity against the trophozoite stage of *Acanthamoeba castellanii* Neff.[16] Bustamante et al.[17] reported the isomerism and nuclearity control in bis(lawsonato)zinc(II) complexes. Some iron(II) complexes of *ortho*-functionalized *p*-naphthoquinones and the characterization by X-ray of a copper(II) complex of 2-hydroxy-1,4-naphthoquinone have also been described.[18]

In this paper we describe the preparation of five metal complexes of lawsone (**2–6**) and their cytotoxicity in human cancer

Abbreviations: MTT, 3-[4,5-dimethylthiazol-2-yl]-2,5-diphenyl tetrazolium bromide; DMSO, dimethylsulphoxide; TLCK, N_α-Tosyl-L-lysine chloromethyl ketone hydrochloride.

* Corresponding authors. Tel.: +34 913942276; fax: +34 913941726.
E-mail addresses: shortelano@isciii.es (S. Hortelano), aestebra@ull.es (A. Estévez-Braun), lasheras@farm.ucm.es (B. de las Heras).
URL: http://www.icic.es.
† These authors contributed equally to this work.

0968-0896/$ - see front matter © 2013 Elsevier Ltd. All rights reserved.
http://dx.doi.org/10.1016/j.bmc.2013.03.002

cells. The copper complex (**4**) was the most active compound of this series and the results presented here show that **4** significantly induced apoptosis in HepG2 human cancer cells by a mechanism that involves activation of caspases and modulation of apoptotic-related proteins.

2. Chemistry

2.1. Synthesis and structures of the metallic complexes of lawsone

Complexes **2**–**6** were synthesized by mixing ethanolic solutions of lawsone (**1**) and the corresponding metallic salts in the molar ratio ligand/metal 2:1 to afford the complexes as red solids (Fig. 1). Since the metallic salts used were acetates, it was not necessary the addition of a base to deprotonate lawsone. The reaction is driven to completion by the chelate effect and low solubility of the final products in ethanol. The lawsone–Metal(II) complexes $[Zn(Lw)_2(H_2O)_2]\cdot 2H_2O$ (**2**), $[Co(Lw)_2(H_2O)_2]$ (**3**), $[Cu(Lw)_2(H_2O)_2]$ (**4**), $[Ni(Lw)_2(H_2O)_2]$ (**5**), $[Mn(Lw)_2(H_2O)_2]$ (**6**) were characterized by elemental analyses and FT-IR spectroscopy. $[Zn(Lw)_2(H_2O)_2]\cdot 2H_2O$ (**2**) and $[Co(Lw)_2(H_2O)_2]$ (**3**) were furthermore characterized by diffraction of X-ray of suitable crystals grown from slow evaporation of the ethanolic solution (Fig. 2, Table S1 in Supplementary data contents), and in the case of the complex (**2**) by ^{1}H NMR spectrum.

The bis(lawsonato)copper(II) complex was prepared using $Cu(OAc)_2$ as metal source instead of $CuCl_2$ in the presence of Et_3N to ensure the full deprotonation of the hydroxyl group of the ligand as previously reported by Salunke-Gawali et al.[19] Recently, Bustamante et al.[17] have reported the structures of different isomers of bis(lawsonato)zinc complexes. These complexes have been prepared using zinc(II) acetate and triethylamine to increase the pH. The formation of the *cis* and the *trans* isomers depends on the order of the addition of the reagents being the *cis* isomer obtained when a methanolic solution of lawsone was added into a solution of zinc(II) acetate in water followed by the addition of NEt_3. The sequence of addition of the reagents for the formation of the *trans* isomer is just the opposite and zinc(II) acetate dissolved in water was slowly added to a solution of lawsone and triethylamine. In our case the *cis* isomer was obtained by addition of an ethanolic solution of zinc(II) acetate to an ethanolic solution of lawsone (1:2 ratio).

The lawsone–Co(II) complex is hexacoordinated and centrosymmetric with two bidentate ONQ ligands and two water molecules. The Co(II) environment is approximately octahedral. The basal plane of the complex is occupied by the quinone carbonyl oxygen atoms O(1) and O(1′) at 2.136(2) Å and the phenoxy oxygens O(3) and O(3′) of ONQ at 2.032(7) Å. The apical position are occupied by the two oxygen atoms of water O(1w) and O(1w) at a distance of 2.092(12) Å in *trans* position. The structure with the water in *trans* position is also found for the bis(lawsonato)copper(II)[19] complexes and for the *trans* isomer of the Zn(II) bis(lawsonato) complex[17] and the bond distances for the Zn–O apical in the *trans* isomer complex is 2.141(3) Å and the corresponding to the copper(II) complex is 2.007(3) Å. The binding angle of the ligand for the two groups O(1)-Co-O(3) are and 78.91(8)° and 101.09(8)°, respectively, while the bond angle between O1w–Co–O3 is 89.40(8)° and 90.60(8)° which are quite close to the right angle for an octahedral geometry. Selected bond distances and angles are given in Table S2 in Supplementary data contents.

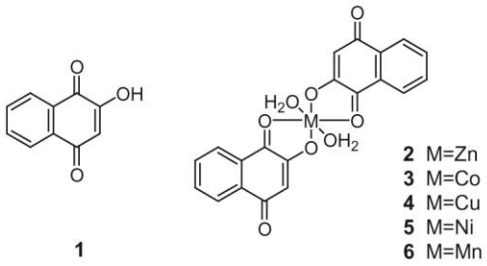

Figure 1. Structure of lawsone (**1**) and general structure of the metallic complexes of lawsone (**2**–**6**).

Supramolecular assemblies via H-bonding formed between one of the hydrogen of the water ligand and the phenoxy oxygen of a nearby molecule and between the second hydrogen of the water ligand and oxygen of the uncoordinated carbonyl group of a quinone ring of the next molecule is an interesting part of the molecular structure (See Fig. S1, Supplementary data contents). A table showing the distances of the hydrogen bonding for the cobalt(II)–lawsonato is provided (Table S4, Supplementary data Contents). Lawsone with its *ortho*-hydroxy group is known to exhibit keto/enol tautomerism. In the present compound the shorter bond distance of C(7)–O(1) (1.230(5) Å) compared to the bond distances C(10)–O(2) and C(8)–O(3) of 1.239(5) Å and 1.287(3) Å, respectively, alongside with the increase in the bond distance of C(7)–C(8) (1.515(7) Å) is indicative of a carbonyl character for the former bond. For this complex C(1)–O(1) and the C(8)–O(3) bond distances Å are shorter than the typical carbonyl bonds of semiquinonate (1.27–1.30 Å) and catecholate (1.30–1.36 Å)[20] forms of the ligand implying that the two lawsonate anions are coordinated to the Co(II) cation in their fully oxidized form.

One striking difference of the Zn–Lw complex prepared in this work with respect to that of cobalt complex is that the water molecules are situated in *cis* position contrarily to the Co–Lw complex, where the water molecules are *trans* to each other. However, in a recent paper on isomerism and nuclearity control in bis(lawsonato)zin(II) complexes, the isomers *cis* and *trans* were isolated and their structures determined by X-ray. The addition sequence of the reagents during the reaction seems to play a crucial role in the isolation of the *cis* or the *trans* isomers. When the reaction mixture was allowed to stand for a long period both isomers *cis* and *trans* were obtained, which can be identified and separated by the different form of the crystals.[17] The zinc(II) structure consists of a distorted octahedron with one water molecule occupying an equatorial position alongside three phenoxy oxygens and the other water molecule occupying the apical position. The Zn–Ow distance is of 2.044(3) Å for the water axial and 2.106(3) Å for the water equatorial. The Zn–O distances of the phenoxy groups are Zn–O(1) 2.180(3) Å, Zn–O(3) 2.050(3) Å, Zn–O(4) 2.311(3) Å and Zn–O(6) 1.992(3) Å. The O(1)–C(7) and the O(3)–C(8) distances are 1.229(5) and 1.281(4) Å. The hydroxyl groups and the water ligands are involved in an extensive hydrogen bonding network. These structural features are in good agreement with those reported for the Zn(II) *cis* isomer.

The complexes show a broad hydroxyl absorption band centered around 3400 cm^{-1}, indicative of the water molecules present in the complexes. The bands occurring at 1680–1700 cm^{-1} are typical of 1,2-quinone carbonyl group.

3. Results and discussion

3.1. Compound 4 decreases cell viability in a dose-dependent manner

To establish the pharmacological potential of the lawsone metal complexes synthesized (Fig. 1), the compounds were initially tested for cytotoxicity in a mouse leukemic macrophagic RAW

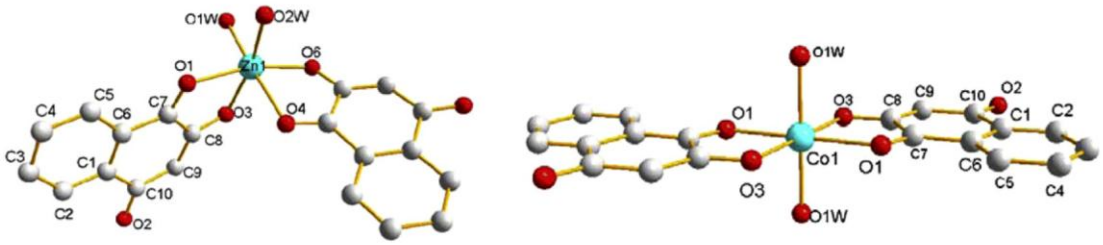

Figure 2. X-ray structures of $[Zn(Lw)_2(H_2O)_2]\cdot 2H_2O$ (**2**) and $[Co(Lw)_2(H_2O)_2]$ (**3**).

264.7 cell line. The cytotoxic activities, expressed as IC_{50} values, were determined by the MTT assay. As shown in Table 1, compound **4** was the most active compound (IC_{50} = 2.5 μM) inhibiting cell growth in a dose-dependent manner (Fig. 3A). In contrast, cell viability was not significantly affected by treatment with compounds **1**, **2**, **3**, **5** and **6**. From these results we can see the influence of the nature of the metal on the activity, since only the copper complex was active, inclusive compared to lawsone (**1**). To discard that the cytotoxic activity exhibited by compound **4** was not due to the Cu(II) ion, we treated the cells with increasing concentrations of $Cu(OAc)_2$. As shown in Fig. 3B, cell viability was not significantly affected by $Cu(OAc)_2$ treatment, even at concentrations as high as 200 μM. According to our results, reported data in the literature have been shown that $Cu(OAc)_2$ is not toxic up to 708 μM in HeLa cells.[21] Thus, compound **4** was selected for further experiments. When indicated, the parent compound **1** (lawsone) was used as negative control.

3.2. Compound 4 induces caspase activation in RAW 264.7 cells

Apoptosis plays a key role in the pathogenesis of cancers and genes relating to this process are focus of interest in the studies of cancer onset and progression. Anti-cancer drugs showing apoptotic effects provide new promising therapeutic strategies.[22,23] Apoptosis is primarily executed by a family of proteases known as the caspases.[22] Caspase activity may be required to induce the biochemical and morphological changes specific of apoptotic cells. Two main signalling pathways initiate apoptosis in mammalian cells: the extrinsic and intrinsic pathways. Caspase 8 is the main executer of the extrinsic pathway initiated at the plasma membrane by activation of cell surface death receptors, whereas caspase 9 is activated in the intrinsic pathway mediated by mitochondria. In addition, both caspases activate downstream apoptotic effectors such as caspase 3.

To gain insight into the mechanisms of compound **4** cytotoxicity, we explored its ability to induce caspase activation. Cells were treated with compounds **1** and **4** (10 μM) for 6 h and 24 h and caspases activities were measured using specific fluorogenic peptide substrates for caspase 3, caspase 8 and caspase 9. Treatment of cells with compound **4** significantly increased activity of caspase 3, 8 and 9, whereas no effects were observed after treatment with compound **1** (Fig. 4A and B). Additionally, we confirmed caspase 3 activation by Western blot. As we can observe in Fig. 4C, stimulation with compound **4** (10 μM) significantly decreased levels of pro-caspase 3, and increased activated caspase 3. As expected, compound **1** had no effects on caspase 3 activation.

Table 1
Cell viability (%) and IC_{50} values[a] (μM) of compounds **1**–**6**

Compound	Cell viability (%) (10 μM)	IC_{50}
1	98.82	>100
2	96.45	>100
3	96.91	75 ± 2.4*
4	38.23	2.5 ± 0.3**
5	93.55	75 ± 1.9*
6	100	>100

[a] IC_{50} values refer to the concentration needed to inhibit 50% of cell viability in the presence of the compounds. RAW 264.7 cells were treated with different concentrations of derivatives (1–100 μM) for 24 h. The effects on cell viability of the compounds are reported as IC_{50} values (μM) determined using the MTT assay. *P <0.05 and **P <0.01 with respect to non-treated cells.

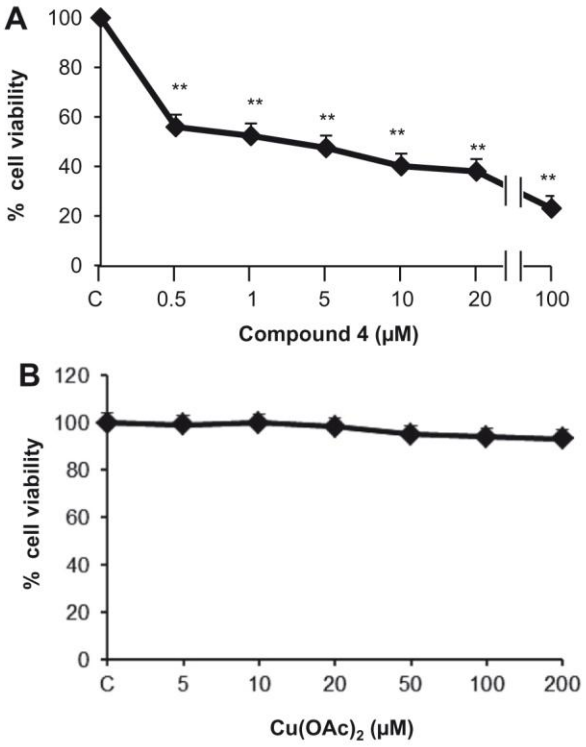

Figure 3. Effects on cell viability. RAW 264.7 cells were treated with increasing concentrations of compound **4** (0.5–100 μM) for 24 h (A) or Cu $(OAc)_2$ (0–200 μM). (B) Cell viability was determined by MTT assay, and results are reported as mean of cell viability (%) of at least three independent experiments ± SD. **P <0.01 with respect to the non-treated cells.

3.3. Compound 4 modulates expression of pro-apoptotic proteins

Activation of caspases might be also modulated by protein members of the Bcl-2 family.[22] This family comprises two functionally distinct groups, apoptotic inhibitors such as Bcl-2 and Bcl-xl, and pro-apoptotic proteins including Bax and Bad. In order to evaluate levels of Bax and Bad, cells were exposed to 10 μM of compounds **1** and **4**. Expression of Bax and Bad notably increased after compound **4** treatment, with no changes observed after compound **1** stimulation (Fig. 5).

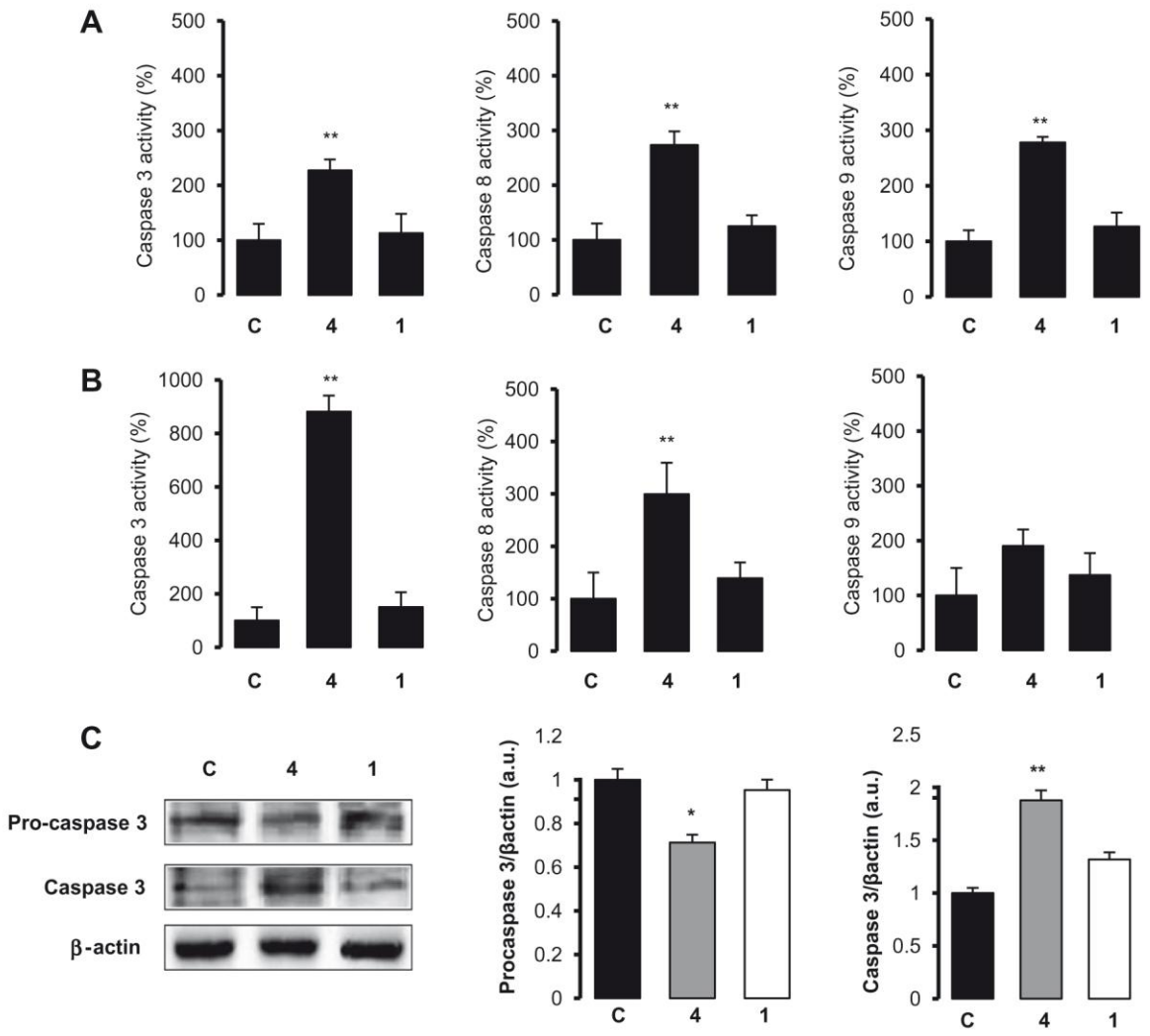

Figure 4. Compound **4** induces caspase activation. Caspase activities were fluorimetrically determined in cell extracts after treatment of cells with compounds **1** and **4** (10 μM) for 6 h (panel A) or 24 h (panel B). Data are expressed as means ± SD of three independent experiments carried out in triplicate. RAW 264.7 cells were incubated with compounds **1** and **4** (10 μM) and the expression of the caspase 3 was determined by Western blot (panel C). A representative experiment is shown of three performed. Densitometric analysis of Western blot is shown ($n = 3$). Results were normalized by arbitrarily setting the densitometry of control cells to 1.0. $^{*}P < 0.05$, $^{**}P < 0.01$ with respect to the control condition.

Apoptosis induced by p53 is firmly established as a central mechanism of tumor suppression. To further explore the signals induced by compound **4** treatment, we analysed p53 levels by Western blot. The results shown in Figure 5 indicate that compound **4** significantly induced p53 levels.

3.4. Effect of compound 4 on human tumor cells

In order to verify the potential of compound **4** as antitumoral agent, we examined its effects on different human cancer cells (HeLa, HT-29 and HepG2). Significant cytotoxic effects were observed in HeLa and HepG2 cells (Fig. 6). Moreover, some markers of apoptosis were also analysed in HepG2 cells. As shown in Figure 7A, treatment with compound **4** induces a significant activation of caspases 8 and 9, whereas the parent compound lawsone (**1**) had not effect (data not shown). Additionally, we determined by Western blot the protein levels of Bax, Bcl-2, Bcl-xL and procaspase-3. Expression of Bax significantly increased in cells treated with compound **4**, whereas levels of antiapoptotic proteins such Bcl-xL, Bcl-2 and procaspase-3 were decreased (Fig. 7B). These data confirm the apoptotic activity of this compound.

4. Conclusion

The present study shows the synthesis and cytotoxic evaluation of a series of metal complexes prepared from lawsone. The in vitro cytotoxic activity of all the metal complexes synthesized was evaluated in cancer cell lines, with the highest cytotoxic activity being observed for the copper complex of lawsone (compound **4**). This compound induces apoptosis in human cancer cells by a mechanism which involves caspase activation and modulation of several apoptosis markers. The presence of copper in the structure might be a critical factor for cell survival. In summary, these findings provide strong evidences of the apoptotic effect of 1,4-naphthoquinones, in particular lawsone derivatives and suggest a useful starting point for the rational design of new antitumor agents.

5. Experimental protocols

5.1. Chemistry

All solvents and reagents were used as supplied from commercial sources. ^{1}H NMR spectra were recorded in ($(CD_3)_2SO$) at

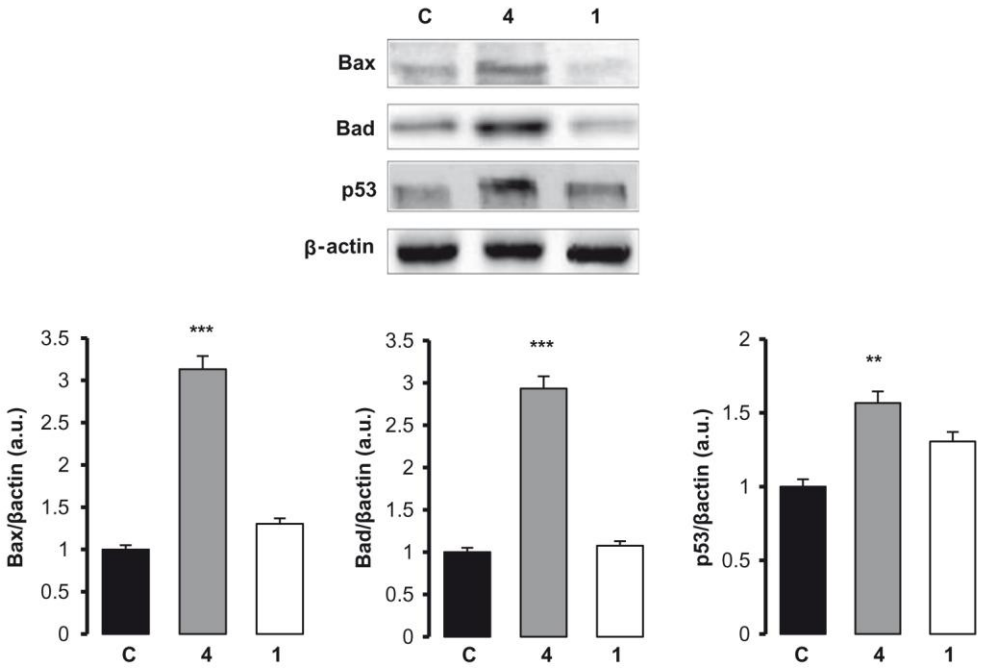

Figure 5. Immunoblot analysis of the expression of Bax, Bad and p53. RAW 264.7 cells were incubated with compounds **1** and **4** (10 μM) and the expression of the apoptosis-related proteins was determined by Western blot. Protein loading was normalized to the expression of β-actin. A representative experiment is shown of three performed. Densitometric analysis of Western blot is shown ($n = 3$). Results were normalized by arbitrarily setting the densitometry of control cells to 1.0. $^{**}P$ <0.01, $^{***}P$ <0.001 versus control cells.

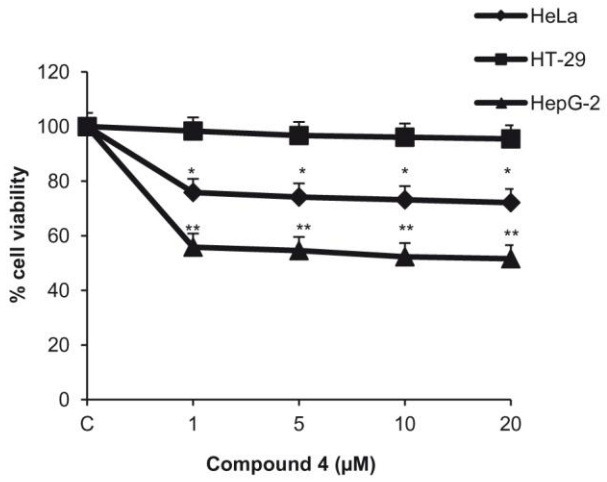

Figure 6. Cytotoxic effects of compound **4** on human cancer cells. Hela, HT-29 and HepG2 cells were treated with different concentrations of compound **4** (1–20 μM) for 24 h. Cell viability was determined by MTT assay. Experiments were carried out in triplicate and the results are the means ± SD of three different experiments. $^{*}P$ <0.05, $^{**}P$ <0.01. Results are normalized to cell viability of non-treated cells at 24 h.

400 MHz, using a Bruker AMX400 instrument. Chemical shifts are given in parts per million (ppm) and are referenced to the residual solvent peak. The following abbreviations are used: s, singlet; t, triplet. Coupling constants (J) are given in hertz (Hz). IR spectra were recorded as a thin film on NaCl plates with a Bruker IFS28/55 spectrophotometer. Elemental analyses were done in a EA 1108 CHNS–O microanalytical analyzer. Diffraction data were collected at room temperature using a Bruker-Nonius Kappa CCD diffractometer with graphite monochromated Mo Kα radiation ($\lambda = 0.71073$ Å). Frames were collected with the COLLECT program,[24] indexed and processed using Denzo SMN and the files scaled together using the HKL2000 program.[25] The structure solution was obtained by direct methods, using the SIR2004[26] and refined with the SHELXL-97.[27,28] Crystallographic parameters are given in Table S1 in Supplementary data contents.

5.1.1. Preparation of $[Zn(Lw)_2(H_2O)_2]\cdot 2H_2O$ (2)

This compound has been prepared by a modification of a previously reported method.[17] A solution of $Zn(CH_3COO)_2\cdot 2H_2O$ (63.1 mg, 0.29 mmol) in 150 mL of ethanol is added to a solution of lawsone (100 mg, 0.58 mmol) in 90 mL of ethanol, giving immediately a bright-red solution. The solution was left at room temperature and the product appeared as red needles. Then the complex was washed with diethyl ether and dried with an IR lamp, affording 93.9 mg (68%) of **2**. The product is moderately soluble in methanol and ethanol, and soluble in diethyl ether. Anal. Calcd for $ZnC_{20}H_{18}O_{10}$: C, 49, 65; H, 3.75. Found: C, 50.55; H, 3.16. ^{1}H NMR (400 MHz, $(CD_3)_2SO$) δ: 7.87 (4H, t, J = 9.6 Hz), 7.78 (2H, t, J = 10 Hz), 7.62 (2H, t, J = 9.6 Hz), 5.71 (2H, s). IR (film) ν_{max}: 3445, 2927, 1645, 1586, 1559, 1455, 1378, 1339, 1274, 1158, 1121, 992, 848 cm^{-1}. For crystallographic data see Table S1 in Supplementary data contents.

5.1.2. Preparation of $[Co(Lw)_2(H_2O)_2]$ (3)

This compound was prepared in a similar way as the zinc complex by mixing 28.62 mg (0.12 mmol) of $Co(CH_3COO)_2\cdot 4H_2O$ in 40 mL of ethanol and 40 mg (0.23 mmol) of lawsone in 60 mL of ethanol, yielding 41.7 mg (82%) of **3** as a red, crystalline solid. Anal. Calcd for $CoC_{20}H_{14}O_8$: C, 54.44; H, 3.20. Found: C, 54.24; H, 2.94. IR ν_{max} (film): 3319, 2926, 1584, 1557, 1375, 1340, 1276, 1121, 993, 842 cm^{-1}. For crystallographic data see Table S1 in Supplementary Data Contents.

5.1.3. Preparation of $[Cu(Lw)_2(H_2O)_2]$ (4)

A modified method of that reported in the literature[19] was used to prepare this complex. 59.3 mg of $Cu(CH_3COO)_2\cdot H_2O$ (0.29 mmol)

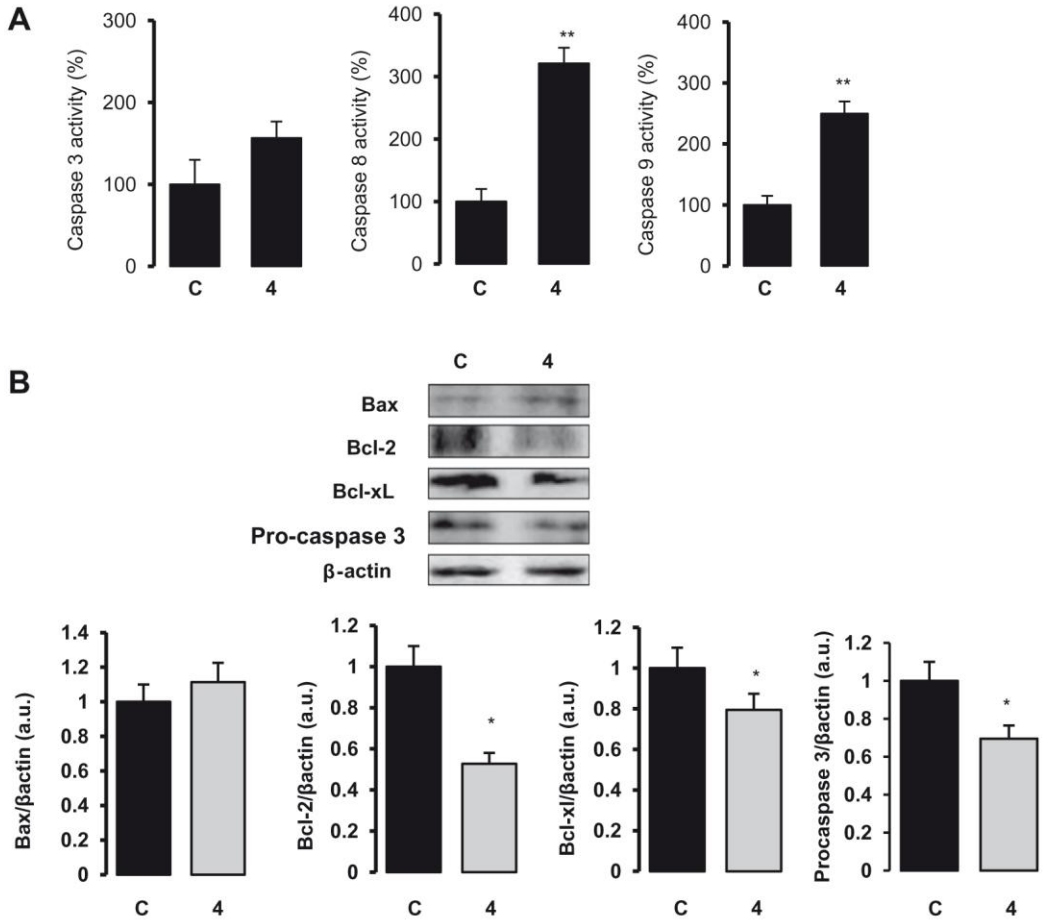

Figure 7. Compound **4** induces apoptosis in HepG2 cells. (A) Caspase 3, 8 and 9 activities were fluorimetrically determined in total cell extracts after cell treatment with compound **4** (10 μM) for 6 h. (B) Levels of apoptotic-related proteins in HepG2 cells. Cells were incubated with compound **4** (10 μM) for 24 h and the expression of Bax, Bcl-2, Bcl-xl and procaspase-3 was determined by Western blot in total extracts. Protein was normalized with β-actin as a loading control. A representative experiment is shown of three performed. Densitometric analysis of Western blot is shown ($n = 3$). Results were normalized by arbitrarily setting the densitometry of control cells to 1.0. $^{*}P < 0.05$, $^{**}P < 0.01$ with respect to the control condition.

were dissolved in 150 mL of ethanol and then added to lawsone (100 mg, 0.58 mmol) in 90 mL of ethanol following the same procedure described above. The copper complex was obtained as a red solid (124.9 mg, 98%). Anal. Calcd for $CuC_{20}H_{14}O_8$: C, 53.88; H, 3.16. Found: C, 53.80; H, 2.42. IR ν_{max} (film): 2924, 1557, 1396, 1339, 1270, 671 cm^{-1}.

5.1.4. Preparation of $[Ni(Lw)_2(H_2O)_2]$ (5)

This complex was obtained following the same procedure described for **2**. 71.5 mg (0.29 mmol) of $Ni(CH_3COO)_2{\cdot}4H_2O$ were dissolved in 150 ml of ethanol and then added to the solution of lawsone (100 mg, 0.58 mmol) in 90 mL of ethanol to yield 111.2 mg (88%) of compound **5**. Anal. Calcd for $NiC_{20}H_{14}O_8$: C, 54.47; H, 3.20. Found: C, 54.17; H, 3.01. IR ν_{max} (film): 3319, 2926, 1584, 1557, 1375, 1340, 1276, 1121, 993, 842 cm^{-1}.

5.1.5. Preparation of $[Mn(Lw)_2(H_2O)_2]$ (6)

Following the same procedure described for 2 the ethanolic solutions of $Mn(CH_3COO)_2{\cdot}4H_2O$ (70.5 mg, 0.29 mmol) and lawsone (100 mg, 0.58 mmol) were mixed, affording 83 mg (66%) of the manganese complex of lawsone. Anal. Calcd for $MnC_{20}H_{14}O_8$: C, 54.94; H, 3.23. Found: C, 55.13; H, 3.05. IR ν_{max} (film): 3319, 2926, 1584, 1557, 1375, 1340, 1276, 1121, 993, 842 cm^{-1}.

5.2. Cell culture conditions

RAW 264.7, mouse leukemic macrophagic cells were maintained in RPMI 1640 medium supplemented with 10% FBS (fetal bovine serum), L-arginine (1 mM), penicillin/streptomycin (100 IU/mL/100 μg/mL) and gentamycin (40 μg/mL) and maintained in 5% CO_2 at 37 °C, as previously described.[29] For experiments, cells were maintained in RPMI plus 2% FBS.

HT-29, human colorectal adenocarcinoma; HepG2, human hepatocellular carcinoma and HeLa, human cervical adenocarcinoma cells were maintained in Dulbecco's Modified Eagle's Medium (DMEM) supplemented with 10% FBS, penicillin/streptomycin (100 IU/mL/100 μg/mL) and gentamycin (40 μg/mL). For experiments cells were maintained in DMEM plus 2% FBS.

5.3. MTT assay for cell viability

Cells were incubated in the presence of different concentrations of derivatives for 24 h, before they were then reacted with MTT (2 mg/mL) (3-[4,5-dimethylthiazol-2-yl]-2,5-diphenyl tetrazolium bromide) at 37 °C for 4 h. The reaction product, formazan, was extracted with dimethyl sulphoxide (DMSO) and the absorbance was read at 540 nm as previously described.[30] Assays were performed in triplicate, and results are expressed as the percent reduction

in cell viability compared to untreated control cultures for at least three independent experiments. IC_{50} values refer to the concentration needed to inhibit 50% of cell viability in the presence of the compounds.

5.4. Preparation of total extracts

To prepare total cell extracts in RAW 264.7 and HepG2, both types of cells were seeded at 10^6 cells/mL and washed with ice-cold buffer (0,5% CHAPS, 10 mM Tris, pH 7.5, 1 mM $MgCl_2$, 1 mM EGTA, 10% glicerol, 5 mM β-mercaptoetanol y 0.1 mM of protein inhibitor cocktail). After centrifugation (8000*g*, 15 min, 4 °C), the supernatant was stored. Protein content was assayed with the Bio-Rad protein reagent.

5.5. Western blot analysis

Protein extracts were subjected to SDS-PAGE (10-15% gels). The gels were blotted onto a Hybond™-PVDF membrane, which were incubated with the following antibodies: anti-p53, anti-Bax, anti-Bcl-xl and anti-Bcl-2 (all from Santa Cruz Biotechnology), anti-Bad and anti-caspase 3 (from Cell Signalling). After incubation with a secondary antibody, protein bands were revealed by ECL according to the manufacturer's instructions (Amersham Pharmacia Biotech, GE Healthcare). β-actin (Sigma) was used as a loading control.[31]

5.6. Caspase assays

The activities of caspases were determined in total cell extracts, using the fluorogenic substrates Ac-DEVD-AMC for caspase 3 (λ_{exc} = 360 nm; λ_{em} = 460 nm), Ac-IETD-AFC for caspasa 8 (λ_{exc} = 360 nm; λ_{em} = 528 nm) and Ac-LEHD-AFC for caspase 9 (λ_{exc} = 360 nm; λ_{em} = 528 nm), according to the supplier's instructions (BD Biosciences).

5.7. Statistical analysis

Data are expressed as mean ± standard deviations (SD) of three independent experiments. The statistical significance of differences between the means were determined with SPSS 19 software (SPSS Inc., Chicago, IL, USA) for Windows using a one-way analysis of variance (ANOVA) followed by Dunnet's *t* test, as appropriate. $P < 0.05$ was considered significant.

Acknowledgments

We thank the financial support from the Spanish MICINN (SAF2009-13296-C02-01) and ICIC (Instituto Canario de Investigación del Cáncer) to A.E.B. SOR thanks ACIISI and FSE for the predoctoral grant. R.H.M. is grateful to the Spanish Ministerio de Ciencia e Innovación for the financial support through the Project CTQ2009-14443-C02-02. This study was also supported by grant PI11.0036 from the FIS and MPY 1410/09 from ISCIII to S.H. We are also grateful to the Servicios Generales de Apoyo a la Investigación for providing the X-ray facilities and to Javier Gonzalez-Platas and Pavel Abramov for his help.

Supplementary data

Supplementary data associated with this article can be found, in the online version, at http://dx.doi.org/10.1016/j.bmc.2013.03.002.

References and notes

1. Driscoll, J. S.; Hazard, G. F., Jr.; Wood, H. B., Jr.; Goldin, A. *Cancer Chemother. Rep. 2* **1974**, *4*, 1.
2. Liu, K. K.; Li, J.; Sakya, S. *Mini-Rev. Med. Chem.* **2004**, *4*, 1105.
3. Avendaño, C.; Menéndez, J. C. *Medicinal Chemistry of Anticancer Drugs*; Elsevier: Oxford, 2008.
4. de Castro, S. L.; Batista, D. G.; Batista, M. M.; Batista, W.; Daliry, A.; de Souza, E. M.; Menna-Barreto, R. F.; Oliveira, G. M.; Salomao, K.; Silva, C. F.; Silva, P. B.; SoeiroMde, N. *Mol. Biol. Int.* **2011**, 306928.
5. Verma, R. P. *Anticancer Agents Med. Chem.* **2006**, *6*, 489.
6. Kim, B. H.; Yoo, J.; Park, S. H.; Jung, J. K.; Cho, H.; Chung, Y. *Arch. Pharm. Res.* **2006**, *29*, 123.
7. Kuete, V.; Wabo, H. K.; Eyong, K. O.; Feussi, M. T.; Wiench, B.; Krusche, B.; Tane, P.; Folefoc, G. N.; Efferth, T. *PLoS ONE* **2011**, *6*, e21762.
8. Tiwari, S. B.; Pai, R. M.; Udupa, N. *J. Drug Target.* **2002**, *10*, 585.
9. Polonik, S. G.; Prokof'eva, N. G.; Agafonova, I. G.; Uvarova, N. I. *Pharm. Chem. J.* **2003**, *37*, 397.
10. Ravelo, A. G.; Estevez-Braun, A.; Chavez-Orellana, H.; Perez-Sacau, E.; Mesa-Siverio, D. *Curr. Top. Med. Chem.* **2004**, *4*, 241.
11. Thirumurugan, R. S.; Kavimani, S.; Srivastava, R. S. *Biol. Pharm. Bull.* **2000**, *23*, 1438.
12. Kelland, L. *Nat. Rev. Cancer* **2007**, *7*, 573.
13. Gokhale, N.; Padhye, S.; Newton, C.; Pritchard, R. *Met. Based. Drugs* **2000**, *7*, 121.
14. Chen, Z. F.; Tan, M. X.; Liu, Y. C.; Peng, Y.; Wang, H. H.; Liu, H. G.; Liang, H. *J. Inorg. Biochem.* **2011**, *105*, 426.
15. Hernández-Molina, R.; Kalinina, I.; Esparza, P.; Sokolov, M.; Gonzalez-Platas, J.; Estevez-Braun, A.; Perez-Sacau, E. *Polyhedron* **2007**, *26*, 4860.
16. Martin-Navarro, C. M.; Lopez-Arencibia, A.; Lorenzo-Morales, J.; Oramas-Royo, S.; Hernandez-Molina, R.; Estevez-Braun, A.; Ravelo, A. G.; Valladares, B.; Pinero, J. E. *Exp. Parasitol.* **2010**, *126*, 106.
17. Bustamante, F. L. S.; Silva, M. M. P.; Alves, W. A.; Pinheiro, C. B.; Resende, J. A. L. C.; Lanznaster, M. *Polyhedron* **2012**, *42*, 43.
18. Garge, P.; Chikate, R.; Padhye, S.; Savariault, J. M.; De Loth, P.; Tuchagues, J. P. *Inorg. Chem.* **1990**, *29*, 3315.
19. Salunke-Gawali, S.; Rane, S. Y.; Puranik, V. G.; Gyard-Duhayon, C.; Varret, F. *Polyhedron* **2004**, *23*, 2541.
20. Allen, F. H. *Acta Crystallogr. Struct. Sci.* **2002**, *B58*, 407.
21. Qiao, X.; Ma, Z. Y.; Xie, C. Z.; Xue, F.; Zhang, Y. W.; Xu, J. Y.; Qiang, Z. Y.; Lou, J. S.; Chen, G. J.; Yan, S. P. *J. Inorg. Biochem.* **2011**, *105*, 728.
22. Plati, J.; Bucur, O.; Khosravi-Far, R. *Integr. Biol. (Camb.)* **2011**, *3*, 279.
23. Pavet, V.; Portal, M. M.; Moulin, J. C.; Herbrecht, R.; Gronemeyer, H. *Oncogene* **2011**, *30*, 1.
24. Bruker-Nonius. The Netherlands, 1997–2000.
25. Otwinowski, Z.; Minor, W.; Academic Press: New York, 1997; Vol. 276, 307 Pt. A.
26. Spek, A. L. *Acta Crystallogr.* **1990**, A46.
27. Sheldrick, G. M. SHELXL-*97, Programm for the Refinement of Crystal Structures*; University of Göttingen: Germany, 1997.
28. Burla, M. C.; Caliandro, R.; Camalli, M.; Carrozzini, B.; Cascarazo, G. L.; Caro, L. D.; Giacovazzo, C.; Polidori, G.; Spagna, R. *J. Appl. Crystallogr.* **2005**, *38*, 381.
29. Giron, N.; Traves, P. G.; Rodriguez, B.; Lopez-Fontal, R.; Bosca, L.; Hortelano, S.; De las Heras, B. *Toxicol. Appl. Pharmacol.* **2008**, *228*, 179.
30. Cuadrado, I.; Cidre, F.; Herranz, S.; Estevez-Braun, A.; de las Heras, B.; Hortelano, S. *Toxicol. Appl. Pharmacol.* **2012**, *258*, 109.
31. Zeini, M.; Traves, P. G.; Lopez-Fontal, R.; Pantoja, C.; Matheu, A.; Serrano, M.; Bosca, L.; Hortelano, S. *J. Immunol.* **2006**, *177*, 3327.